

**THE EFFECT OF INJECTION
MOULD SURFACE FINISH ON THE
EJECTION OF PLASTICS PRODUCT**

MOHD. A

PhD 2014

THE EFFECT OF INJECTION MOULD SURFACE FINISH ON THE EJECTION OF PLASTICS PRODUCT

ALIAS BIN MOHD

**A thesis submitted in partial fulfillment of the requirements of
Edinburgh Napier University, for the award of Doctor of Philosophy**

September 2014

DECLARATION

I hereby declare that the work presented in this thesis was solely carried out by myself at Edinburgh Napier University, Edinburgh and TATI University College, Kemaman, Terengganu, Malaysia, except where acknowledgement is made, and that is has not been submitted for any other degree.

A handwritten signature in black ink, appearing to read 'Alias Mohd', is centered within a light gray rectangular box.

Alias Mohd (candidate)

Date: 25 September 2014

ABSTRACT

The development and fabrication injection of moulding tools is complex and demands highly skilled personal. The research aim is to study the effect of surface roughness on mould filling and the ejection of parts for amorphous and semi-crystalline polymers. This study is to simulate and analyse polymers used and investigates the ejection force needed for different selected polymer resins for a series of cavity and core inserts with different surface roughnesses. Mould filling and comparison studies for polymers used also were carried out. Three common thermoplastics polymers were used for the cylindrical part: two amorphous thermoplastics: high impact polystyrene and an acrylonitrile butadiene styrene and a semi-crystalline polyamide. These three thermoplastics were selected due to these polymers are engineering materials being widely used in automotive parts, in the casing of household products and in gears. Apart from that there are different processing conditions for an amorphous and crystalline thermoplastic in terms of melting temperature, injection pressure, packing pressure and cooling times which are considered in this study. A two-cavity prototype tool for cylindrically shaped components was fabricated with variations in wall thickness by using a series of core inserts each with a different surface roughness. The part was constructed using CAD software and simulated in Autodesk Moldflow Insight 2010-R2 (AMI 2010-R2) in order to carry out the simulation works to obtain the required processing parameters for the injection moulding process. The application of simulation software packages for mould design and injection moulding process are vital in order to optimise the part quality and satisfy the market needs. For amorphous thermoplastics there is no melting point in terms of physical properties and having a high toughness due to butadiene chain present, in this case both for high impact polystyrene and an acrylonitrile butadiene styrene. Since polyamide has a viscosity lower than these two amorphous thermoplastics, the processing conditions and pressure will be different which can be identified through the melt flow rate of the resin. Polyamide also has a higher density which is 1.14 g/cm^3 compared with high impact polystyrene and an acrylonitrile butadiene styrene which were 1.04 g/cm^3 and 1.04 g/cm^3 respectively. The study concludes that polyamide resin requires a shorter cavity filling time and less pressure compared with an acrylonitrile butadiene styrene resin. Polyamide also requires high ejection forces due to surface texture generated as compared with high

impact polystyrene and an acrylonitrile butadiene styrene. The mathematical model results for the ejection force closely agree with the experimental data for the three materials used.

ACKNOWLEDGEMENT

I am grateful and would like to express my sincere gratitude to my supervisors Dr. Colin Hindle and Dr. Mike Barker for their full support and advice throughout my research work. I would also like to thank Dr. Erry and Dr. Wan Ahmad from the Department of Manufacturing and Material Engineering at International Islamic University Malaysia (IIUM), Kuala Lumpur, Malaysia for their support of allowing me to use all of the facilities and the equipments available at IIUM.

I would like to express very special thanks to Dr. Saiful Bahri from University of Sultan Zainal Abidin, Kuala Terengganu and Dr. Ruzlaini Abd Ghoni for their suggestions and cooperation throughout the study. I also would like to express sincere gratitude and thanks to Mr. Rohan Haksar from Edinburgh, Scotland for the time spent proofreading my thesis.

I also would like to express my gratitude and appreciation to all of those that have contributed directly and indirectly toward the accomplishment of my research work whether from Edinburgh Napier University or TATI University College.

I acknowledge my sincere indebtedness and gratitude to my wife, Norkiah and my children (Mimi, Syakir and Naq) for their patience, support and encouragement throughout the period in completing my thesis. I can not find the appropriate words that could properly describe my appreciation for their devotion, support and faith in my ability to attain my goal.

TABLE OF CONTENTS

	Page
ABSTRACT	iv
ACKNOWLEDGEMENT	vi
TABLE OF CONTENTS	vii
LIST OF FIGURES	xiii
LIST OF TABLES	xvii
LIST OF ABBREVIATIONS	xx
LIST OF SYMBOLS	xxii
CHAPTER 1 – INTRODUCTION	
1.1 Overview	1
1.2 Problem statement	2
1.3 Aim and objectives of the research	3
1.4 Scope of study	4
1.5 Outline of the thesis	4
CHAPTER 2 – LITERATURE REVIEW	
2.1 Overview	6
2.2 Polymer	7
2.3 Polymerization Process	7
2.4 Structure of Polymers	8

2.5	Classification of Polymers	9
2.5.1	Thermoplastics	10
2.5.2	Thermoset plastics	11
2.6	Different between Thermoplastics	13
2.6.1	Amorphous materials	13
2.6.2	Crystalline and semi-crystalline materials	13
2.7	Tool design and construction in injection moulding processes	16
2.7.1	Injection moulding machine	16
2.7.2	Tool Basic Construction	19
2.8	Surface roughness of the mould inserts	23
2.8.1	Method of producing the surface roughness	24
2.9	Mould/cavity filling	25
2.10	Injection Pressure	33
2.11	The simulation packages software	35
2.12	Pressure and force	36
2.13	Ejection Force	37
2.14	Tool venting	39
2.15	Tool cooling	40
2.15.1	Tool cooling design consideration	42
2.15.2	Design of cooling channel	43
2.16	Summary	43

CHAPTER 3 – METHODOLOGY

3.1	Overview	44
3.2	Tool Design	46

3.2.1	Design procedure	46
3.2.2	Rationale design of the part and modeling	47
3.3	Simulation in Autodesk Moldflow Insight 2010-R2 (AMI 2010-R2)	49
3.3.1	Moldflow Simulation Analysis	49
3.3.2	Modeling and Analysis Methodology	51
3.3.3	Simulation process	52
3.4	Fabricating the tool	53
3.4.1	Machine Tool and Equipment	53
3.4.2	Mould base	53
3.4.3	Core and cavity inserts	54
3.4.5	Runner, Gating and Ejection System	55
3.4.6	Venting Design System	57
3.4.7	Mould Cooling System Design	59
3.4.8	Surface Roughness	63
3.4.9	Measurement of surface roughness	65
3.4.10	The matrix combination for core insert	68
3.4.11	Process of Obtaining Microscopic Core Insert	69
3.5	Tooling Construction	71
3.6	Experimental work	72
3.6.1	Material	72
3.6.2	Equipment and machine set-up	73
3.6.3	Instrument Set-up	74
3.6.4	Force link 9331B	75
3.6.5	Experimental Design	77
3.6.5.1	Taguchi Design of Experiment	77

3.6.5.2 Orthogonal Arrays (OA)	79
3.6.5.3 Order of running the experiments	81
3.7 Summary	89

CHAPTER 4 – MOLDFLOW ANALYSIS

4.1 Overview	90
4.2 Moldflow Analysis Result	91
4.2.1 Gate Location Analysis Result	92
4.2.2 Mould Filling Analysis Result	93
4.2.2.1 Flow Analysis	93
4.2.2.2 Fill Time Result	94
4.2.2.3 Pressure Result	95
4.2.2.4 Shear Stress at Wall Result	98
4.2.2.5 Air Traps Result	98
4.2.2.6 Weld lines result	99
4.2.2.7 Clamp force result	100
4.2.2.8 Volumetric Shrinkage Result	101
4.2.2.9 Polymer Fill region	101
4.2.2.10 Time to Freeze Result	101
4.3 Conclusion	104
4.4 Summary	105

CHAPTER 5 – RESULT AND DISCUSSION

5.1 Overview	106
--------------	-----

5.2	Ejection Force Experiment Results	107
5.2.1	Surface roughness of the core inserts	107
5.2.2	Surface roughness of part	108
5.2.3	Mechanical bonding and van der Waal effect of the ejection force	110
5.2.4	The effect of ejection forces on the surface roughness	112
5.2.5	Ejection Force Experiment Data	123
5.2.6	Validation of Melting Temperature, Injection Pressure, Packing Pressure and Cooling Times against Ejection Force	131
5.2.7	Model graph and surface contour plot	139
5.3	Effect of Control Factors	146
5.3.1	Analysis of Variance (ANOVA)	146
5.3.2	ANOVA and regression analysis	147
5.4	Analysis Method	157
5.5	Effect of machining parameter on ejection force, F_e	157
5.6	Mathematical Models	170
5.7	Summary	173

CHAPTER 6 – CONCLUSIONS AND RECOMMENDATIONS

6.1	Conclusion	174
6.2	Contribution to knowledge	176
6.3	Recommendation for Further Work	177

REFERENCES	179
-------------------	-----

BILBLIOGRAPHY	184
----------------------	-----

APPENDICES

Appendix A	Tool Drawings	187
Appendix B	Surface Roughness	212
Appendix C	Tooling Fabricating	215
Appendix D	Resin Specification	219
Appendix E	Injection Moulding Specification	225
Appendix F	Force Link and Signal Processing Conditioning Specification	227
Appendix G	Moldflow Analysis Log	247
Appendix H	Moldflow Analysis Results	282
Appendix I	Surface Roughness Value	289
Appendix J	Sample Graph for Injection Force Dry-Run and with Moulding	298
Appendix K	Tabulated Data for L ₈₁ Orthogonal Array	300

LIST OF PUBLICATIONS	307
-----------------------------	------------

LIST OF FIGURES

	Page
Figure 2.1 Polymer family: the formation of plastics and the polymerisation process	8
Figure 2.2 Types of molecular structures in polymers	9
Figure 2.3 Classification of polymers	10
Figure 2.4 Structure of thermoplastics	11
Figure 2.5 Structure of thermoset	12
Figure 2.6 Microstructure of various plastic	15
Figure 2.7 The construction of Injection moulding machine	17
Figure 2.8 Mould Component	23
Figure 2.9 The principle of EDM process	25
Figure 2.10 Method of venting thermoplastic injection mould	39
Figure 2.11 Proper and efficient cooling improves part quality and productivity	40
Figure 2.12 Laminar and turbulent flow	42
Figure 3.1 Overview of the work flow for research work	45
Figure 3.2 (a) A hollow cup modeled in Autodesk Inventor. (b) Part drawing was developed in AutoCAD 2005	48
Figure 3.3 Steps in preparation of Finite Element Model for Moldflow Analysis	50
Figure 3.4 Component properties pre-processing model	51
Figure 3.5 The geometric and FE model of hollow cup (a) Single. (b) Two cavities (multiple)	51
Figure 3.6 Simulation process outlines	52
Figure 3.7 (a) DF3 tool steel for inserts (b) Copper for EDM machining	54
Figure 3.8 Process producing electrode by using CNC lathe	55
Figure 3.9 Half round runner and rectangular gate system	56
Figure 3.10 Air vent on cavity insert and cavity plate	58
Figure 3.11 Air vent on core insert	58

Figure 3.12	Copper plates is used for baffle cooling system design at core inserts	62
Figure 3.13	A series of cooling system for cavity plate	62
Figure 3.14	A baffle of cooling system for core insert	63
Figure 3.15	Sampling length with individual peak height	64
Figure 3.16	Process of producing surface roughness for the mould inserts	66
Figure 3.17	The position of (green marked) for surface roughness checking	67
Figure 3.18	The equipment set-up for checking the surface roughness for core inserts	67
Figure 3.19	The process of measuring the surface roughness	67
Figure 3.20	Process obtaining microscopic core inserts by using optical microscope	70
Figure 3.21	The 3D solid modelling test mould for plastic injection moulding	71
Figure 3.22	Test mould ready for trial out	71
Figure 3.23	An Engel injection moulding machine (HLV-125)	73
Figure 3.24	Kistler's instrumentation set-up	75
Figure 3.25	Force link 9331B	76
Figure 3.26	Ejector rod and Kistler's force transducer assembly with the ejector rod of the injection moulding machine	76
Figure 3.27	Kistler's force link position	77
Figure 4.1	Suggested gating suitability for the moulding	93
Figure 4.2	Fill time. (a) HIPS. (b) ABS. (c) PA6	96
Figure 4.3	Pressure at the end of fill. (a) HIPS. (b) ABS. (c) PA6	97
Figure 4.4	(a) Air entrapment marked with circle. (b) HIPS. (c) PA6. (d) ABS	99
Figure 4.5	(a) Weld lines position with circle marked. (b) HIPS. (c) ABS. (d) PA6	100
Figure 4.6	Volumetric shrinkage (a) HIPS. (b) ABS. (c) PA6	102
Figure 4.7	Polymer Fill region (a) HIPS. (b) ABS. (c) PA6	103
Figure 5.1	Microscopic for core insert surface roughness x100 (a) Polished insert, and (b, c) Sparked insert	107
Figure 5.2	Moulding Sample of HIPS	108

Figure 5.3	SEM image for mouldings at different level of surface roughness for different types of thermoplastic (a) (d) (e) HIPS. (b) (e) (h) ABS. (c) (f) (i) PA6 resin	109
Figure 5.4	The combination of surface roughness and ejection force for HIPS	114
Figure 5.5	The error of the ejection force for different combination surface for HIPS	116
Figure 5.6	The combination of surface roughness and ejection force for ABS.	119
Figure 5.7	The error of the ejection force for different combination surface for ABS	119
Figure 5.8	The combination of surface roughness and ejection force for PA6	122
Figure 5.9	The error of the ejection force for different combination surface for PA6	122
Figure 5.10	Comparison between the observed to predicted values in ejection force for the HIPS material	132
Figure 5.11	Comparison between the observed to predicted values in ejection force for the ABS material	132
Figure 5.12	Comparison between the observed to predicted values in ejection force for the PA6 material	133
Figure 5.13	Surface plot of surface roughness and melting temperature against ejection force for HIPS	140
Figure 5.14	Surface plot of surface roughness and melting temperature against ejection force for ABS	140
Figure 5.15	Surface plot of surface roughness and melting temperature against ejection force for PA6	141
Figure 5.16	Surface plot of surface roughness and injection pressure against ejection force for HIPS	141
Figure 5.17	Surface plot of surface roughness and injection pressure against ejection force for ABS	142
Figure 5.18	Surface plot of surface roughness and injection pressure against ejection force for PA6	142
Figure 5.19	Surface plot of surface roughness and packing pressure against ejection force for HIPS	143

Figure 5.20	Surface plot of surface roughness and packing pressure against ejection force for ABS	143
Figure 5.21	Surface plot of surface roughness and packing pressure against ejection force for PA6	144
Figure 5.22	Surface plot of surface roughness and cooling time against ejection force for HIPS	144
Figure 5.23	Surface plot of surface roughness and cooling time against ejection force for ABS	145
Figure 5.24	Surface plot of surface roughness and cooling time against ejection force for PA6	145
Figure 5.25	(a) HIPS, (b) ABS and (c) PA6. Ejection force versus injection pressure for surface roughness $S1x + S1y$	162
Figure 5.26	(a) HIPS, (b) ABS and (c) PA6. Ejection force versus packing pressure for surface roughness $S1x + S1y$	163
Figure 5.27	(a) HIPS, (b) ABS and (c) PA6. Ejection force versus injection pressure for surface roughness $S2x + S2y$	164
Figure 5.28	(a) HIPS, (b) ABS and (c) PA6. Ejection force versus packing pressure for surface roughness $S2x + S2y$	165
Figure 5.29	(a) HIPS, (b) ABS and (c) PA6. Ejection force versus injection pressure for surface roughness $S3x + S3y$	166
Figure 5.30	(a) HIPS, (b) ABS and (c) PA6. Ejection force versus packing pressure for surface roughness $S3x + S3y$	167
Figure 5.31	Average S/N ratio by control factor and their levels for HIPS	168
Figure 5.32	Average S/N ratio by control factor and their levels for ABS	169
Figure 5.32	Average S/N ratio by control factor and their levels for PA6	169
Figure 5.34	Normal probability plot of ejection force for HIPS	172
Figure 5.35	Normal probability plot of ejection force for ABS	172
Figure 5.36	Normal probability plot of ejection force for PA6	173

LIST OF TABLES

	Page
Table 2.1 Structures and properties of thermoplastics and thermosets	15
Table 3.1 Chemical composition for Assab DF-3 tool steel for inserts	54
Table 3.2 Standard gate size	56
Table 3.3 Kinematics Viscosity	61
Table 3.4 Matrix combination for core and cavity inserts	68
Table 3.5 The combination of core surface roughness	68
Table 3.6 Typical properties of polymer resin used	72
Table 3.7 The parameters of moulding conditions for the experiment for the resins	74
Table 3.8 The parameter for three levels of selected factors for HIPS	80
Table 3.9 The parameter for three levels of selected factors for ABS	80
Table 3.10 The parameter for three levels of selected factors for PA6	80
Table 3.11 L ₈₁ Taguchi orthogonal array for the experiment of HIPS resin	82
Table 3.12 L ₈₁ Taguchi orthogonal array for the experiment of ABS resin	84
Table 3.13 L ₈₁ Taguchi orthogonal array for the experiment of PA6 resin	86

Table 4.1	Process condition for HIPS, PA6 and ABS	94
Table 4.2	Flow analysis results	95
Table 5.1	Average ejection force for HIPS	113
Table 5.2	The parameter setting for HIPS for the experiment	114
Table 5.3	The parameter setting for ABS for the experiment	116
Table 5.4	Average ejection force for ABS	118
Table 5.5	Average ejection force and standard error for PA6	120
Table 5.6	The parameter setting for PA6 for the experiment	121
Table 5.7	Table of result from ejection force experiment for HIPS	124
Table 5.8	Table of result from ejection force experiment for ABS	126
Table 5.9	Table of result from ejection force experiment for PA6	128
Table 5.10	Effect estimate table of ejection force for HIPS	135
Table 5.11	Effect estimate table of ejection force for ABS	136
Table 5.12	Effect estimate table of ejection force for PA6	137
Table 5.13	ANOVA table of ejection force for HIPS	149
Table 5.14	ANOVA table of ejection force for ABS	150

Table 5.15	ANOVA table of ejection force for PA6	152
Table 5.16	Regression coefficient table of ejection force for HIPS	153
Table 5.17	Regression coefficient table of ejection force for ABS	154
Table 5.18	Regression coefficient table of ejection force for PA6	155
Table 5.19	Ejection force for injection pressure and melting temperature for S1 _x +S1 _y surface roughness combinations	159
Table 5.20	Ejection force for melting temperature and packing pressure for S1 _x +S1 _y surface roughness combinations	159
Table 5.21	Ejection force for injection pressure and melting temperature for S2 _x +S2 _y surface roughness combinations	160
Table 5.22	Ejection force for packing pressure and melting temperature for S2 _x +S2 _y surface roughness combinations	160
Table 5.23	Ejection force for Injection pressure and melting temperature for S3 _x +S3 _y surface roughness combinations	161
Table 5.24	Ejection force for packing pressure and melting temperature for S3 _x +S3 _y surface roughness combinations	161

LIST OF ABBREVIATIONS

EDM	Electric discharge machine
AISI	American Iron and Steel Institute
AFM	Atomic force microscopy
MRR	material removal rate
ABS	Acrylonitrile Butadiene Styrene
MPA 7.3	MoldFlow Plastic Advisers 7.3
PMMA	Poly (methyl methacrylate)
LDPE	Low density polyethylene
HDPE	High density polyethylene
PS	Polystyrene
HIPS	High Impact Polystyrene
PP	Polypropylene
PVC	Polyvinyl Chloride
MAC	Marker and Cell
PET	Polyethylene terephthalate
PA6	Polyamide 6
SEM	Scanning electron microscope
SPC	Simplified Predictive Control
MFL	Melt flow length
DC	Direct Current
F_e	Ejection force
AMI	Autodesk Moldflow Plastic Insight
PPS	Poly (p-phenylene sulphide)

PC	Polycarbonate
CAD	Computer aided drafting
CNC	Computer numerical control
MFR	Melt mass flow
SPC	Signal conditioning platform
DOF	Degree of freedom
OA	Orthogonal array
DoE	Design of experiment
ANOVA	Analysis of variance
DAQ	Data acquisition

LIST OF SYMBOLS

		Unit
T_g	Glass Temperature	$^{\circ}\text{C}$
T_m	Melting Temperature	$^{\circ}\text{C}$
Adj- R^2	Adjusted coefficient of determination	-
Kg	Kilogramme	-
MPa	Mega pascal	-
s	Second	-
K^{-1}	Thermal expansion coefficient	-
V	Fluid velocity	m/s
D	Diameter of passage	m
n	Kinematics viscosity	m^2/s
Q	Flow rate	m^3/s
gym	Gram per minute	-

Greek Symbols

β_0	Constant
β_i	The first order or linear effect coefficients
β_{ii}	The second order or quadratic effect coefficients
β_{ij}	The interaction effect coefficients

CHAPTER 1

INTRODUCTION

1.1 Overview

Integrated knowledge, of mould design and the injection of moulding process and materials, is essential to meet the part's quality requirement. Injection moulding is one of the most versatile and robust operations for processing thermoplastics from a simple to a very complicated product with excellent dimensional tolerance at a relatively low cost. One should have a good understanding of the flow behaviour of molten plastic in the mould cavity as well as the process parameters of the injection moulding machine.

The ejection of the moulding from the core is a paramount factor in this research to maintain the part quality and smoothness of the operation of the tool especially when it comes to the actual production (bulk quantity). Ideally speaking, an injection moulding process will involve friction forces where the tendency of the part is to shrink onto the core insert which then causes part defects if not properly controlled. For long usage and mass production, the inserts tend to wear due to the polymers rubbing the surface of the tool.

The research therefore is concerned on the ejection force generated to eject the part by using different types of surface roughness/texture for the cavity and core inserts. The thermoplastic materials used are: high-impact Polystyrene (HIPS), acrylonitrile butadiene styrene (ABS) and polyamide (PA6). The materials have different thermal expansion coefficient compared to steel ($0.6 - 1.4 \times 10^{-4}$ and $12 \times 10^{-6} \text{K}^{-1}$, respectively A.S. Pouzada et al., 2006) which is the important element of this research in order to establish the ejection force model for each polymer used.

1.2 Problem Statement

The tool is expensive to fabricate and so requires good planning in the fabrication stage as any mistake during this stage will lead to severe losses and time delay. So it is a must to use a certain method which is capable of resolving the potential problems which might arise before the actual production takes place. The surface roughness of the inserts plays an important role in determining the quality of part and the ejection force required. It is a necessity to develop and model the ejection force for amorphous and crystalline resin which can later help people in moulding industries in planning and undertaking jobs and also improving easy manufacture of the plastic parts. It is essential and a main objective of the present work to develop a mathematical model to predict the ejection forces for amorphous and crystalline thermoplastic resins. It is, therefore, imperative that the ejection forces be balanced and adequate so as to reduce the probability of part deformation.

1.3 Aim and Objectives of the research

The aim of this research was to study the effect of surface roughness for HIPS, ABS and PA6 with the different processing conditions (melting temperature, injection pressure, packing pressure and cooling times). These polymers are selected because they are engineering material which widely used for engineering application such casing for air conditioning, automotive parts and internal part (gear). The processing conditions and pressure can be indentified through melt flow rate of the resin. PA6 is higher density which is 1.14 g/cm^3 comparing with HIPS and ABS which were 1.04 g/cm^3 and 1.04 g/cm^3 respectively. These characteristics definitely will influence the processing conditions and the ejection force for polymer used.

The objectives of the research are as follows:

- a. To simulate and analyze the different types of thermoplastics material with Autodesk Moldflow Plastic Insight (AMI) software.
- b. To analyse the effect of different types of surface roughness for both core and cavity: mirror-polished and spark erosion by EDM (Electro discharge machining).
- c. To analyze the mould filling and process parameters for HIPS, ABS and PA6 on the actual tool.
- d. To develop the ejection force for HIPS, ABS and PA6 by using such instrumentation.
- e. To optimize value of process parameter and correlation among HIPS, ABS and PA6.

1.4 Scope of study

In this study, the effectiveness and accuracy of simulation result using AMI 2010-R2 software were compared with the actual injection moulding process parameters. It is essential to find the correlations and optimum ejection force for different types of polymer resin. Thus the experimental data were further studied by using statistical tool (Statistica Release 7), to analyse the optimum conditions for the processing parameters of injection moulding machine. This was followed by prediction and model development for ejecting the part.

1.5 Outline of the thesis

This thesis consists of six chapters. A brief introduction on the injection moulding process and the ejection of moulding part is outlined in Chapter 1 (Introduction). This is followed by problem statement in order to provide some basis (ideas and suggestion) to determine the research's direction. Based on the defined problem statement, research aim and objectives and scope of the study were elucidated clearly.

The technology and application of various machining process with emphasis given are to describe the process parameters which influence the quality of the moulding which were revealed in Chapter 2. The following sections of the chapter include the mould design concept, the adoption of simulation software package and also the working condition requirement for the polymer resins.

Chapter 3 discusses the methodology used in the study and experimental procedures. These procedures include instrumentation set-up and materials preparation. It also involves design and tool fabrication as a platform to run the study based on the researcher's knowledge and experience. The facilities available at TATI University College and the supports from Edinburgh Napier University were employed to enhance the study works.

Meanwhile, Chapter 4 focuses on the Moldflow analysis and computational method in examining the associated problems which may arise during filling, packing and curing during the cycle time of the moulding. The information gathered from the analysis log will be used as guidance during the experimental work.

In Chapter 5, the optimum ejection force based on the setting parameters and conditions and model building for predicting response function were developed. The essential parameters include surface roughness of cavity inserts, injection pressure, melt temperature, packing pressure and cooling time which were considered in developing the mathematical model.

Findings from these studies were summarised in Chapter 6 (Conclusions and Recommendations for Future Direction). Conclusions are drawn based on the results throughout the study on mould filling and ejection of part for HIPS, ABS and PA6. Some of the possibilities for extending for the future work were suggested based on the obtained result and observations.

CHAPTER 2

LITERATURE REVIEW

2.1 Overview

The development and manufacture of tooling for injection moulding are complex tasks involving the knowledge of the injection moulding process parameters and the material changes induced by processing. Thus, in the tool design stage, the aspects associated with the ejection system will require special consideration especially for parts with deep cavities; quite often the ejection phase of the moulding cycle is critical. Hence, the prediction of the ejection force will contribute to optimizing the tool design and to guarantee the integrity of the parts. If there are any errors happened involving complicated machining and related process by tool making industries, they may suffered a big loss. Nevertheless, it is without any doubt that, the input towards the knowledge in this field is very vital and fruitful for the tool maker and also the machine operator. Each and every one of the aspects stated above will lead to a better production of good product quality. The links between injection moulding parameters such as melting temperature, injection pressure, cooling time and packing pressure integrated with technology used and current research carried out were also elaborated.

Generally speaking, an injection moulding process involves four different stages which are filling, packing, cooling and ejection. The robustness of the injection moulding process enables various shape and complex geometry which can be moulded at relatively low cost (B. H. Min, 2002). Four important aspects of mould filling and ejection of part will be discussed, which are related to the research are: surface finish and EDM process, melting temperature, injection pressure and ejection force.

2.2 Polymer

Polymer can be defined as a substance (natural or synthetic), molecules of which consist of numerous repeated chemical units (monomers) linked to each other in a regular pattern.

2.3 Polymerization Process

Plastics are one group of polymers built up from relatively simple units called monomer (or mers) through a chemical polymerisation process as shown in Figure 2.1. For processing polymers into end product will involves physical phase change such as melting and solidification (for thermoplastics) or a chemical reaction (for thermosets).

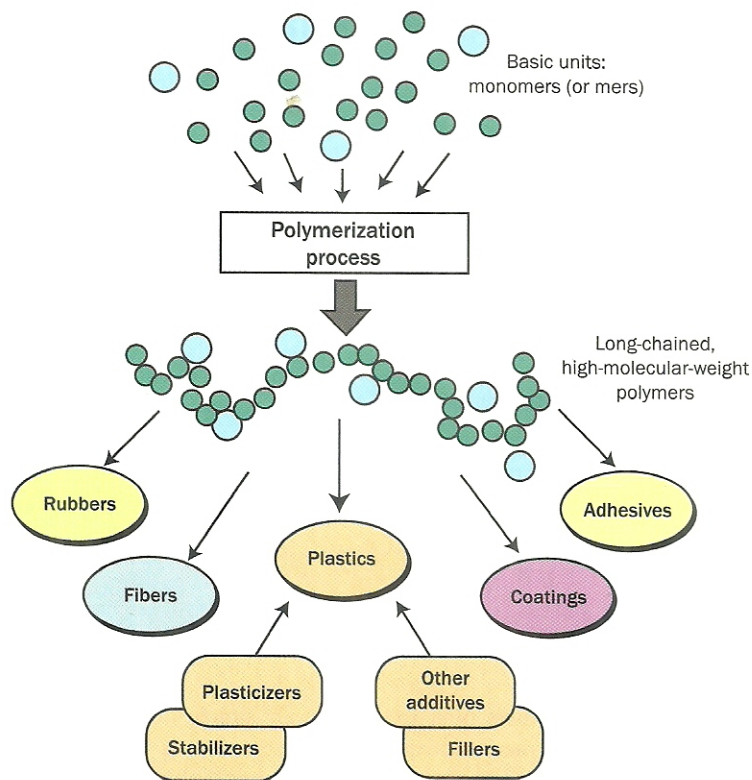


Figure 2.1: Polymer family: the formation of plastics and the polymerisation process (Jay Shoemaker, 2006)

2.4 Structure of Polymers

The structure of polymer may form of a long chain of repeating units in the shape of branched molecules, in the form of giant three dimensional networks, in the form of linear molecules with regular lateral connections to form “ladder-type” polymers, in the form of two-dimensional networks or platelets, and so forth, depending on how many connections or bonds can exist between the mono-disperse monomer molecules that were used to form the polymer and between sites on the forming or already formed polymer molecules as shown in Figure 2.2. Thus, many

different structures are possible with plastics-and each will affect the basic properties of the polymer.

Plastics generally represent polymeric compounds that are formulated with plasticisers, stabilisers, fillers and other additives for the purpose of processibility and performance.

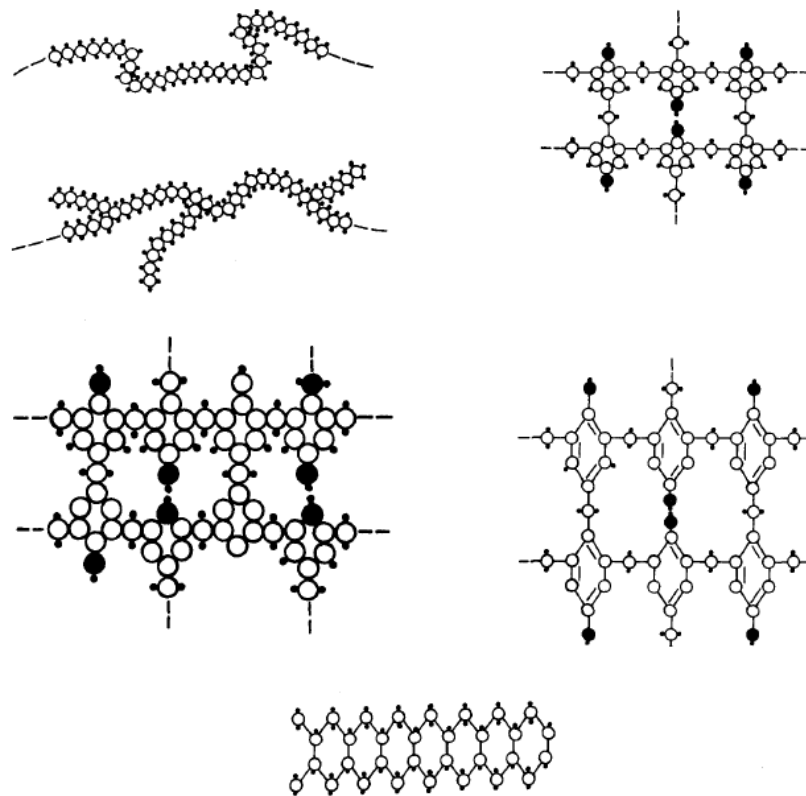


Figure 2.2: Types of molecular structures in polymers (Michael L. Berins, 2000)

2.5 Classification of Polymers

Polymer builds up from numerous smaller molecules or monomers through the polymerisation process. There are many types of polymers with the different properties and applications. In general polymers can be categorised into three main

groups namely as thermoplastics, thermoset and elastomers is illustrated in Figure 2.3.

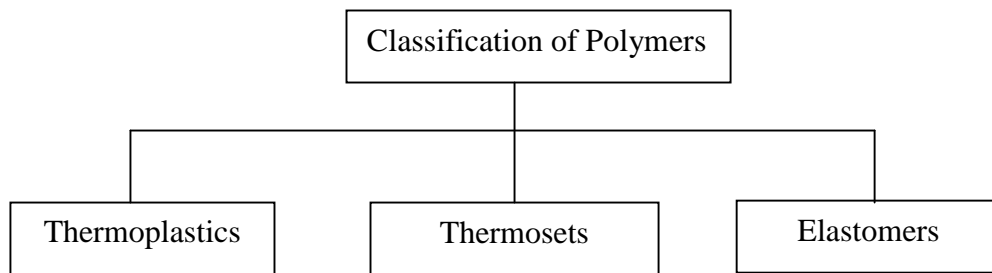


Figure 2.3: Classification of polymers (Belofsky, 1995 and Callister, 2005)

Chain structure of polymers consists of branch, linear and cross link. Branch polymers have long chain polymers could have similar type a monomer, different types of AB monomers block AABB or graft linear ABBBABAA. Polymers with similar of monomer known as homopolymer and polymer with different types of monomers or repeating units identified as copolymer.

2.5.1 Thermoplastics

Thermoplastic polymers are plastics in which, unlike elastomers and thermoset plastics, the molecular chains are not cross linked. They consequently demonstrate plastic elastic behaviour and are thermoformable (melttable and weldable) which melt when heated, and resolidify when cooled for examples polyamides (PA), polypropylene (PE), and PVC. They are various types of polyamides, but they tend to have similar physical properties. These include high impact strength, toughness, flexibility, and abrasion resistance due to the linear molecular chain structure (Crawford, 1990) as shown in Figure 2.4.

This formability is reversible, in other words can be repeated as often as required as long as the material is not thermally damaged by overheating.

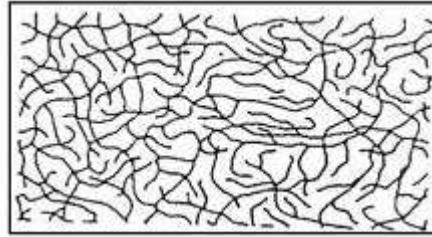


Figure 2.4: Structure of thermoplastics

(Source: <http://www.ensinger-online.com/en/materials/basics-of-plastics/plastics-classification/> Visited: 22/02/14)

Thermoplastics may experience high molecular weights due to high degree polymerisation. The long molecular chain whether has side chains or not or group which are not attached to other polymer molecules. As the end result, thermoplastics can be softened constantly with only an increase of temperature which makes it reversible.

The material of thermoplastics will maintain its original hardness when heated as well as its strength when it is being cooled. Often, thermoplastic materials are purchased as either pellets or granules. It is the process in which they are melted by heat under pressure into a relatively viscously fluid and then can be shaped into any desirable product.

2.5.2 Thermoset plastics

Thermoset is a group of plastics that is permanently hardened by cooling. If heated after it has been initially cooled, the thermoset will char or burn. The individual molecular chains of thermoset polymers are characterized by three-dimensional

closely-meshed cross linking of covalent chemical bonding for example melamine and epoxy. This property means that they can no longer be shaped after hardening. They also cannot be melted. However, because of their strong cross linking, thermoset polymers do offer good chemical resistance and a high level of thermal stability, as well as being hard and brittle.

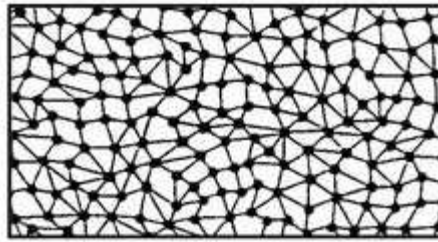


Figure 2.5: Structure of thermoset

(Source: <http://www.ensinger-online.com/en/materials/basics-of-plastics/plastics-classification/> Visited: 22/02/14)

The process happens when the thermosets polymerise with the activation of heat or chemical reaction in a cross-linked microstructure. Once the process is completed, the cross-link are bonded together in order to create a three-dimensional network. This network (cross bond) which is positioned in the thermosets plastic, excludes the slippage of the individual molecular as shown in Figure 2.5. Thus, as a result, the thermosets becomes an infusible solid and cannot be re-softened even though with the application of heat without degrading linkage. The fact is that, the process is irreversible. Thermosets plastics exhibit greater mechanical strength, higher working temperature, more ductility and greater dimensional stability than thermoplastics. Elastomers refer to cross link chain structure for example rubber.

2.6 Difference between Thermoplastics

As plastic materials are heated, they also go through changes in structure. The temperatures that these changes occur at are called transition points. Plastic materials can be divided into two broad categories according to their structure. These are amorphous materials and crystalline materials.

2.6.1 Amorphous materials

Amorphous materials have their molecular chains in a random tangle. As heat is applied to amorphous material, it becomes gradually softer. An amorphous material will show a gradual transition as it is transformed from a solid to a rubbery material. The temperature at which this occurs is called the material's Glass Transition Temperature (T_g). As the material is heated further, it will become softer, allowing it to be moulded. Amorphous material does not show sharp changes in properties as it is heated and typically has a broad processing range. For amorphous polymers ΔT is usually greater than 100°C . For example ABS: melt temp. 250°C - solidification temperature $110^\circ\text{C} = \Delta T$ 140°C and PC: melt temperature 300°C - solidification temperature $150^\circ\text{C} = \Delta T$ 150°C .

2.6.2 Crystalline and semi-crystalline materials

Crystalline materials are in fact semi-crystalline; they have small regions of crystalline material, surrounded by amorphous material. In the crystalline regions, the polymer chains have taken up a tight, orderly,

arranged structure. As a crystalline material is heated up, a change in the mechanical properties will be witnessed as the amorphous regions encounter a glass transition phase. The crystalline regions remain intact, preventing the material from flowing. Considerably more heat must be applied before the crystalline regions break apart. This is a sharp transition point, occurring at a specific temperature for that material. This temperature is called the Melting Temperature (T_m). Below the T_m , the material is a solid. Above the T_m , the material is a melt, and can be processed. The behaviour of crystalline material can be compared to that of ice and water, having a sharp transition between being solid and being liquid. Crystalline polymers are characterized by (ΔT) less than 50°C . For example PA 66: melt temperature 285°C - solidification temperature 255°C = ΔT 30°C and POM: melt temperature 200°C - solidification temperature 180°C = ΔT 20°C .

The major difference of thermoplastics and thermosetting is, it is primarily depends on the molecular structure as shown above. The microstructure of various plastic is shown in Figure 2.6. Table 2.1 is a summary of the relevant structure and properties of thermoplastic and thermosets.

Table 2.1: Structures and properties of thermoplastics and thermosets
(Jay Shoemaker 2006)

Material	Thermoplastics	Thermosets
Microstructure	Linear or branch molecules No chemical changes generally take place during forming	Cross-linking network with chemical bonds between molecules after the chemical reaction
Reaction to heat	Can be re-softened (physical phase change)	Cannot be re-softened after cross-linking without degradation
General properties	Higher impact strength Easier processing Better adaptability to complex shapes	Greater mechanical strength Greater dimensional stability Better heat and moisture resistance

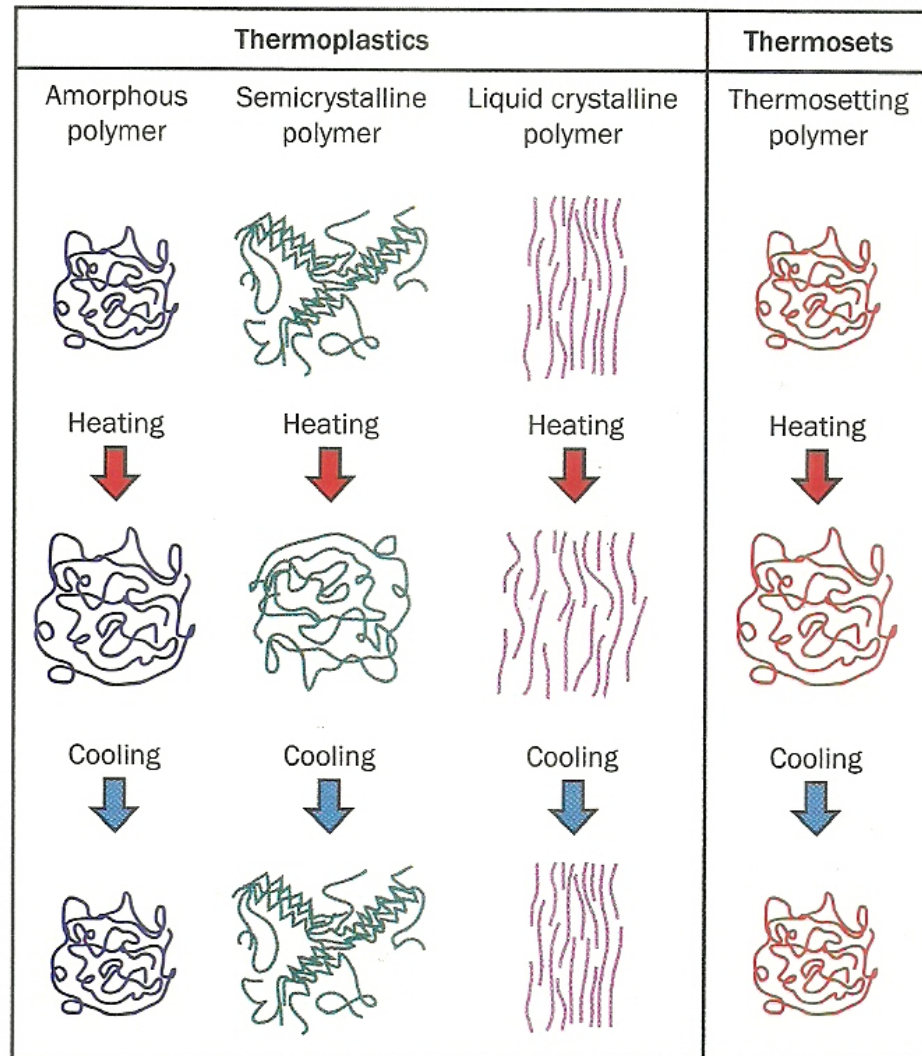


Figure 2.6: Microstructure of various plastic (Jay Shoemaker, 2006)

2.7 Tool design and construction in injection moulding processes

The design and construction of the tool is essential for a high quality moulded component or product. A tool may consist of two or more parts in which the shape of the part has been cut. Where large quantities of a product are required (long production run) a hard wearing, durable mould material is required (steel). However, the injection moulding operations can be more challenging to tool designer and tool maker which target fewer defects such as warpage, shrinkage, weld lines and air traps.

2.7.1 Injection moulding machine

Injection moulding machines are of two types which include vertical and horizontal configuration. Both of these types of injection moulding machine have their own functions and benefits. Meanwhile, the horizontal injection moulding is usually used for different varieties in industries.

Basically, there are four types of horizontal injection moulding machine which are used in today's industries. The four types are as follows:

i. Conventional injection moulding machine

In this process, the plastic granules or pellets are poured into a machine hopper and feed into the chamber of the heating cylinder. A plunger then compresses the material, forcing it through progressively hotter zones of the heating cylinder, where it is spread thin by a torpedo. The torpedo is an unflighted cylindrical portion of the screw,

usually located at the discharge end that provides additional shear heating capabilities during melting action. Also the torpedo can be installed in the centre of the cylinder in order to accelerate the heating of the centre of the plastic mass. The torpedo may also be heated so that the plastic is heated from the inside as well as from the outside.

The material is delivered from the heating cylinder through a nozzle into the mould. The nozzle is the end of cylinder and form seal with tool in which it is used to prevent leakage of material, which is caused by the pressure used within it. The conventional plunger machine is the only type of machine that can produce multi-colour part. The other types of injection moulding machines combine the plastic material thoroughly that only one colour is produced. Figure 2.7 shows the construction of injection-moulding machine.

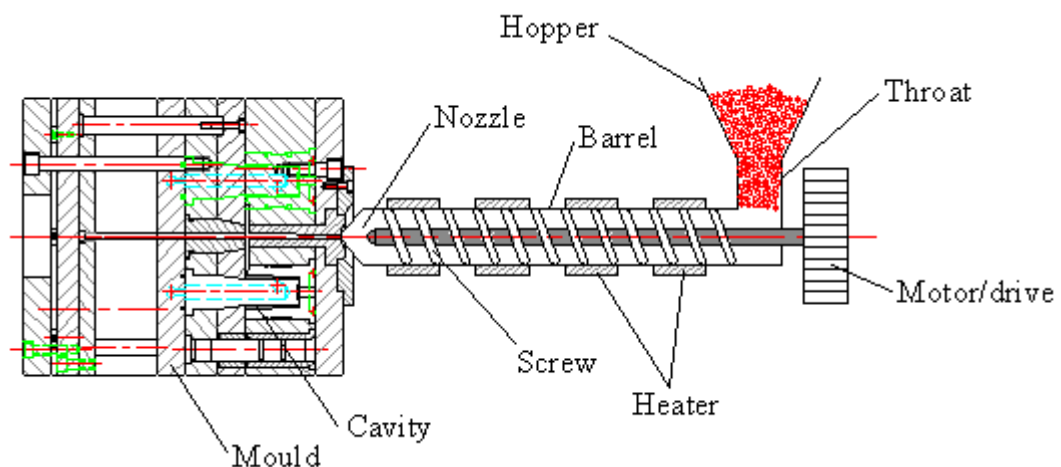


Figure 2.7: The construction of Injection moulding machine (Author's design)

ii. Piston type pre-plastifying machine

This machine employs a torpedo ram heater to pre-plastify the plastic granules. After the melt stage, the fluid plastic is pushed into a holding chamber until it is ready to be forced into the die. This type of machine produces pieces faster than a conventional machine, because the moulding chamber is filled to shot capacity during the cooling time of the part. Due to the fact that the injection plunger is acting on fluid material, no pressure loss is encountered in compacting the granules. This allows for larger parts with more projected area. The remaining features of a piston-type pre-plastifying machine are identical to the conventional single-plunger injection machine.

iii. Screw type pre-plastifying machine

In this injection-moulding machine, an extruder is used to plasticize the plastic material. The turning screw feeds the pellets forward to the heated interior surface of the extruder barrel. The molten, plasticized material moves from the extruder into a holding chamber, and from there is forced into the die by the injection plunger. The use of a screw gives the following advantages:

- Better mixing and shear action of the plastic melt.
- A broader range of stiffer flow and heat sensitive.
- Materials can be run.
- Colour changes can be handled in a shorter time.
- Fewer stresses are obtained in the moulded part.

iv. Reciprocating screw injection machine

This type of injection moulding machine employs a horizontal extruder in place of the heating chamber. The plastic material is moved forward through the extruder barrel by the rotation of a screw. As the material progresses through the heated barrel with the screw, it is changing from the granular condition to the plastic molten state. In the reciprocating screw, the heat delivered to the moulding compound is caused by both friction and conduction between the screw and the walls of the barrel of the extruder. As the material moves forward, the screw backs up to a limit switch that determines the volume of material in the front of the extruder barrel. It is at this point that the resemblance to a typical extruder ends. On the injection of the material into the die, the screw moves forward to displace the material in the barrel. In this machine, the screw performs as a ram as well as a screw. After the gate sections, in the mould have frozen to prevent backflow, the screw begins to rotate and moves backward for the next cycle.

2.7.2 Tool Basic Construction

In making plastic injection moulding tool, there are certain procedures that need to be followed. The tool is considered as the most vital part of the injection moulding process because it controls the shape and the surface finish of the moulded part. The tool consists of two parts which include the stationary part (plastic is

injected here), as well as the moving part for closing or ejector side. The division line between them is called the parting line.

The tool determines the size, shape, dimension, physical properties and the surface finished of the ejected product. Usually, a melted plastic is forced to be fed by using a channel called sprue to the cavity of the mould. There are five (5) major areas that should be taken into consideration when making the tools which are listed below. Figure 2.8 showed the location of these tool components.

i. Mould form

The mould form consists of cavity, core plate and also air ventilation system. Mould form controls the properties of the injected product. The injection mould is an assembly of part containing within it an impression into which plastic material is injected and cooled. It is the impression which gives the moulding its form. The impression may, therefore, be defined as that part of the mould which imparts shape to the moulding

The impression is formed by two mould members:

- The cavity, which is the female portion of the mould, gives the moulding its external form.
- The core, which is the male portion of the mould, form the internal shape of the moulding

ii. Feed system

This system includes gate, runner and sprue systems which control the material flow to the mould. During the injection process plastic material is delivered to the nozzle of the machine as melt; it is then transferred to the impression through a passage. The material in this passage is termed the sprue, and the bush is called a sprue bush. The materials may be directly injected into the impression through the sprue bush or for mould containing several impressions (multi-impression mould) it may pass from the sprue bush hole through a runner and gate system before entering the impression.

iii. Ejection

Ejection system consists of the Ejector plate and Ejector pins. When ejecting the component it is important not to distort or otherwise damage the component. This can be avoided by appropriate location of ejector pins to insure the ejection forces are evenly distributed and applied to the more rigid areas of the moulded component. An alternative to edge ejection is to use a stripper plate mould. Stripper plate moulds remove the component from the core by moving an entire mould plate to 'strip' the part from the core.

iv. Cooling System

Cooling system is the system in which it controls the mould temperature. There are two types of cooling system which include serial and parallel cooling system. Temperature control is an essential part of the moulds operation. It is essential to remove heat from the mould as quickly as possible so that it will be sufficiently cool and rigid to be ejected without

damage. The shorter the cooling times the shorter the cycle time and the more parts can be produced.

Chilled water is most often the cooling agent of choice because it's low-cost, has excellent thermal transfer properties, and is readily available. Process water temperature is different for every tool creates, and it's determined by a large number of variables. The wall thickness of the part, dimensional requirements, the type of resin used, and size factors in the tool design all affect process water temperature.

Convection heating with water or oil through single or multiple heat/cool circuits in the tool. Hot dry air or steam is also used which can be turned on and off during injection/cooling.

Induction by means of an inductor that generates an alternating electromagnetic field. Inductors can be integrated into the tool or built in a “cage” surrounding the tool.

v. Mould Mounting

Mould mounting consists of the guide pillar, guide bush and slot, which are then used for mounting the mould to the injection moulding machine. To mould an even-walled article it is necessary to ensure that cavity and core are kept in alignment. This is done by incorporating guide pillars on one mould plate which then enter corresponding guide bushes in the other mould plate as the mould closes. The size of guide pillar should be

such that they maintain alignment irrespective of the applied moulding force;
this they are normally able to do.

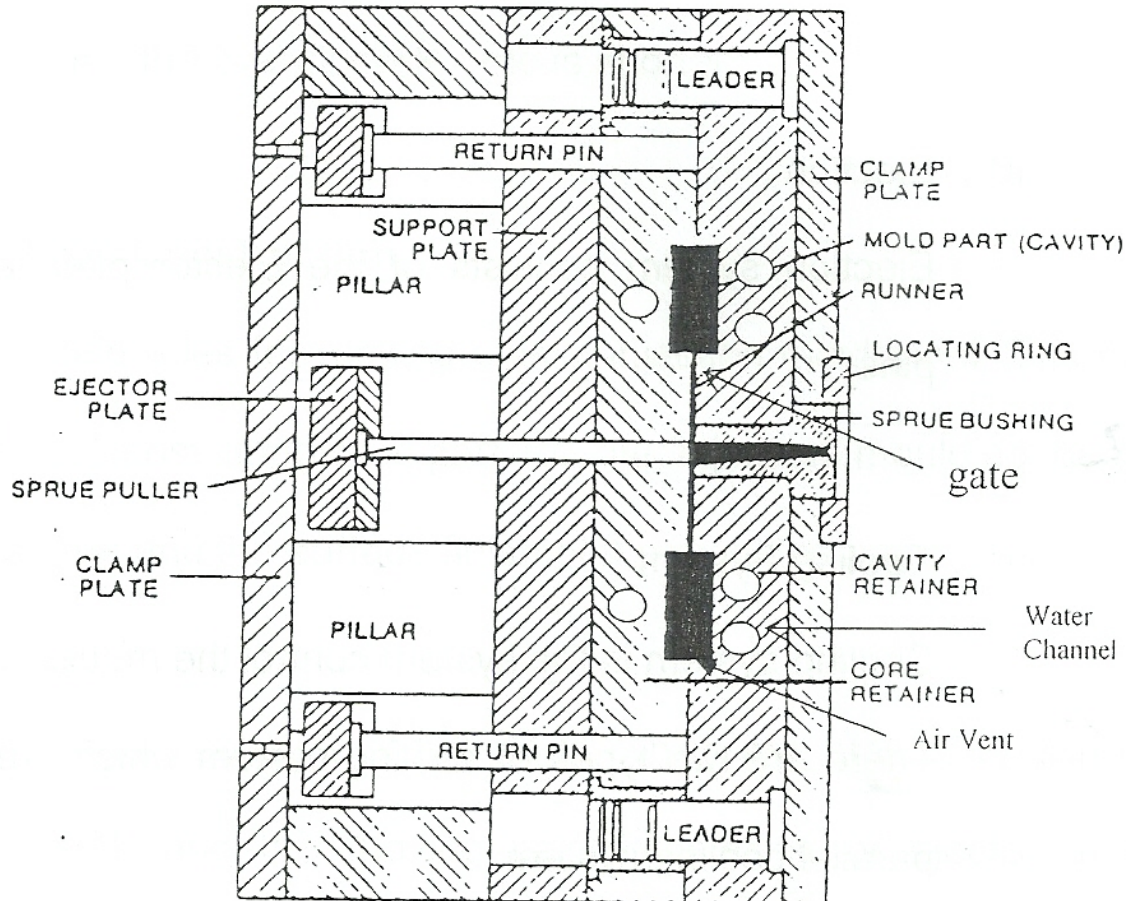


Figure 2.8: Mould component (Rosato Dominick V. *et al.*, 2000)

2.8 Surface roughness of the mould inserts

The surface roughness of cavity and core plays very important role in determining the quality of moulding. The surface roughness of the insert can be produced by using EDM process or manually polishing.

2.8.1 Method of producing the surface roughness

Electrical discharge machining (EDM) has been proved effectively on the machining for hard, high strength and temperature resistant materials by means of rapid removing and repetition spark discharged between the gaps of electrode and work piece. Figure 2.9 shows the principle of EDM operation. The process is widely adopted in mould making industries to produce critical and complicated parts for aerospace, electronics and medical. On statistics, ninety percent of the EDM is used in mould making, stamping dies, forging dies, tool fixtures and gauges in the United State (Harry, 2000).

The EDM process is used especially to intricate complex shape component. The correlation between EDM parameter (current) with the machining factors (material removal rate and electrode wear rate) is the paramount factor in determining highest material removal rate and lowest wear rate of the electrode (Che Haron et al., 2001; Guu, 2004; Amorim and Weingaertner, 2005). The electrode material made from copper offered a good surface finish and low electrode wear rate compared to copper tungsten, brass and aluminium (Singh et al., 2003).

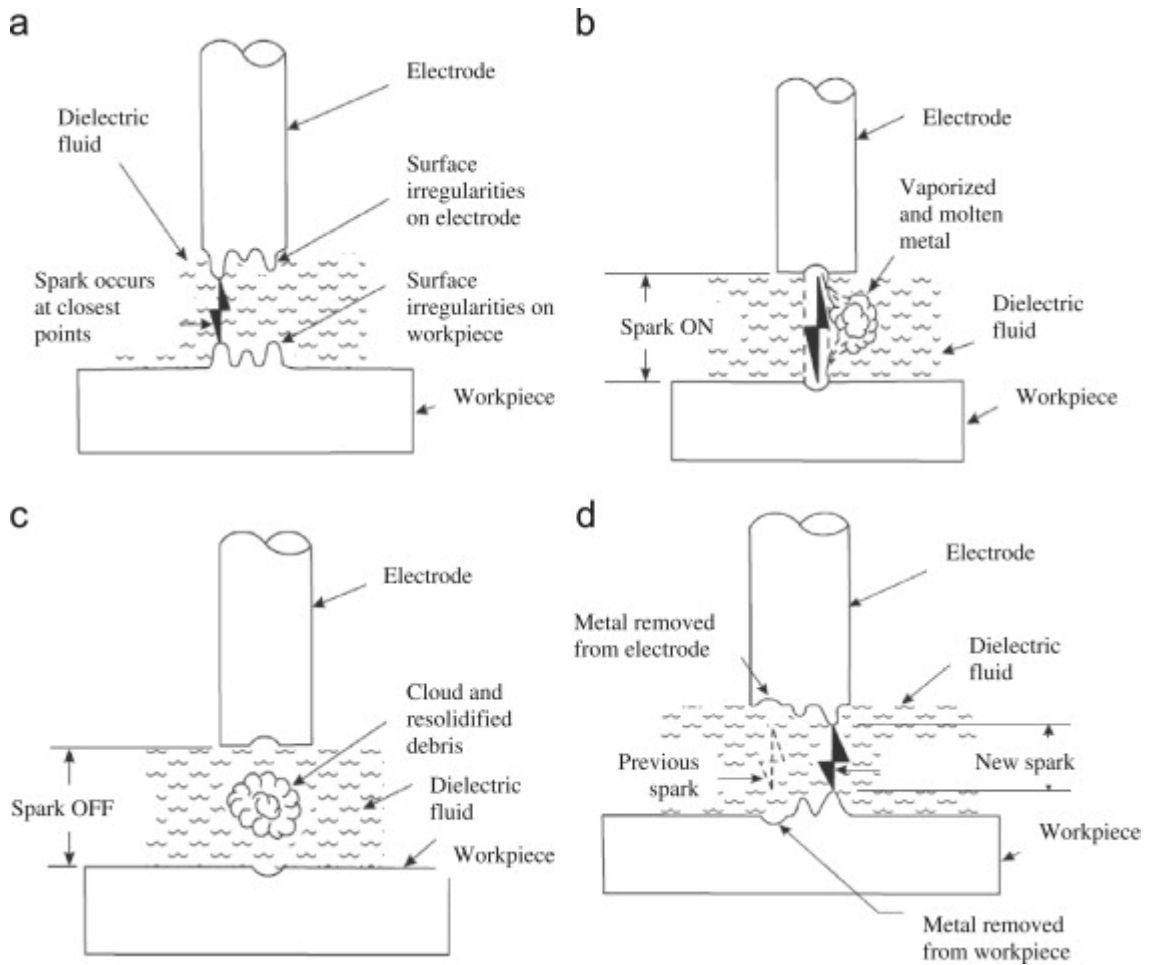


Figure 2.9: The principle of EDM process (<http://ars.els-cdn.com>)

2.9 Mould/cavity filling

This research work deals with two-cavity. Since it is in multi-cavity, the possibility of variation of mechanical properties in different region might possibly happen.

The fountain flow's behaviour of polymers during cavity filling by using several of techniques such as finite element and numerical integration scheme were carried out by numerous researchers (A. Özdemir et al., 2004; H. Yokoi et al., 2002;

B. S. Chen and W. H. Liu, 1994; C. G. Gogos and C. F. Huang, 1986). In the finite element method, a body to be analyzed is divided into a number of small subdivisions, or finite elements. The elements are defined by a number of nodal points, which for the elements considered are their corner points. The finite element analysis approach is useful to simulate and solve the flow characteristics for parameters such as the flow problem, velocity, pressure, temperature and shear stress distributions in nonisothermal and isothermal filling process in determining quality of moulding which is closely related to mould design and processing condition (Kumar et al., 2001; Ho, 1997; Chen and Liu 1994; Soh and Chang, 1986). So, the finite element and numerical integration are widely used in polymer processing in order to understand the interaction between the material properties and the process. A numerical simulation of nonisothermal filling process in the thickness direction gets together with free-surface boundary condition and relevant governing equations. Result showed that as the melt front advances, the free surface becomes flatter. The finite element analysis approach is useful to simulate the flow characteristic of Styron 678 (Ho, 1997).

This research does not employ finite element method while dealing with these parameters. Somehow, the information given above can be used when dealing with the fountain flow of thermoplastics.

During the design stage, the moulding with varieties of wall thickness is thoroughly studied. Then some calculations were done before the mould drawings are produced. The type of runner system, ejection system and the size of all mould

elements are being put in appropriate sizes to overcome deflection of plate as well as to facilitate the experiment.

A 3D finite element model is utilized to predict the velocity, pressure, temperature field and the flow front (Hétu *et al.*, 1998). They have used Stokes equation to solve the velocity and pressure fields and Carreau Law and Arrhenius constitutive models to predict fluid behaviour. Meanwhile for the flow front is modelled by using a pseudo-concentration method. The 3D approach used by these authors was able to predict weld line, air entrapment, and pressure and temperature distribution at the end of filling. Instead of using a 3D finite element, this research has utilised the simulation software MPA 7.3 which is able to simulate and predict possible associated problems with the moulding like weld line and air entrapment. Somehow, the approach used by these authors is very effective to simulate very complex three-dimensional cavities during the filling stage such as car handle.

Mould filling for cylindrical part is investigated under isothermal and non-isothermal conditions by using LDPE material (A. Kumar *et al.*, 2001). They have used the finite-difference method to solve the governing differential equation for the work. They have looked into two cases: isothermal filling at constant flow rate and non-isothermal filling at constant flow rate. The result for non-isothermal filling shows physically realistic trend and there is a strong agreement between analytical solution and numerical method. The experimental work by the authors is also concerned about the quality of moulding which is closely related to mould design and processing condition. So, the processing conditions such as melt temperature, mould temperature and filling time as emphasized by the authors will be used in this

research. These processing conditions definitely affected the melt viscosity which are resulting the quality of moulding. Since this research will employ three types of thermoplastics: PS, PP and PVC, the processing condition may vary. So therefore, a very close attention during cavity filling for this research is profound to be essential.

The simulation of cavity filling by using the Marker-and-Cell (MAC) numerical technique to investigate the fountain flow effect (Gogos and Huang, 1986). Therefore an assumption has been made: the flow is isothermal and the fluid is incompressible. The fountain flow effect is caused by the non-slip condition of moulding wall where the material is forced to flow outward of mould surface. The fountain flow in the front of region during mould filling by using MAC was accomplished satisfactorily. This research will also look at the fountain effect while dealing with different types of thermoplastics. It will determine the filling time and pressure and affects part orientation in that region.

A numerical simulation is used to study the post filling stage for PP and PS materials (B. S. Chen and W. H. Liu, 1994). A modified Cross Model was used to describe the viscosity under nonisothermal conditions. The melt (Hele-Shaw flow) is considered to obey either a double-domain Tait or single-domain Spencer Gilmore equation of state. Hele-Shaw Model is the flow of a real fluid (viscous Newtonian liquid) between two closely spaced parallel plates in which the fluid flow is generated by a pressure gradient applied across the ends of the plates, and the spacing, d is sufficiently small to ensure that the viscous forces. For modelling the viscosity of the resin, a modified Cross model was used with a double-domain Tait equation of state being employed in describing the compressibility of the resin during

moulding. The energy balance equation, including latent-heat dissipation semi-crystalline and amorphous materials, was solved in order to predict the solidified layer and temperature profile in detail. The result indicates a good agreement between the present simulation and experimental work. Since the materials used by the authors are of the same with this research, it gives more information concerned at the post filling stage. The approach used by the authors about nonisothermal conditions was relevant because the melt temperature for amorphous materials lies between the glass transition, T_g or T_m for semi-crystalline polymers which provides significant information towards this research.

A system is developed to measure the dynamic flow front position (Yokoi *et al.*, 2002). The result indicated that, at high velocities filling, an asymmetric fountain flow may occur and no flow mark caused. The flow behaviour of polymers during the filling stage and the causes of moulding defects will be considered in this research while using difference type of polymers. Most of the defects occurred during this critical filling where the melt resin flows inside the cavity. The melt temperature for the thermoplastics used for this research will be closely monitored.

The reliability of mould filling simulation is investigated for part design (Reifschneider, 2001). The simulation program is used to predict the filling pattern when there is a gradual change in part thickness. The process conditions are simulated from short shot mouldings to completely full parts. This will provide a better understanding towards this research where the simulation works are done prior to experimental work.

A governing equation is derived with a power-law fluid for thin cavities (S.K. Soh and C. J. Chang, 1986). The interactions between delivery channel flows with cavity flow have been reported. Their experiment was observed on three conditions: melt front location from isothermal, Newtonian filling of a constant gap rectangular cavity and bi-gap rectangular cavity. Thus, they concluded with a new field equation for variable gap, the melts front equilibrates with dissipation density when the pressure drop in the cavity exceeds the upstream delivery channel and the proposed equilibration principle satisfies with the experiment for isothermal filling of a Newtonian fluid. The concepts used by the authors provide more understanding towards this research parallel to the apprehension of isothermal filling studied.

A numerical simulation by using different rheological models was proposed by using power law, moldflow second order, cross and carreau models in processing polymer (PE-HD) (Koszkul and Nabialek, 2004). Only filling stage is considered. They concluded that only proper viscosity model will produce reliable result, the computer analysis will influence the accuracy of the plastic properties and the technical development in computer hardware will result towards more complex calculation of viscosity models. The rheological models used by the authors gave a good comparison result where the viscosity requirement models were discussed. By combining the inputs given by the authors and the application of AMI 2010 R-2 in this research, the behaviour of polymer melt can be thoroughly studied especially during cavity filling.

The injection velocity is to get uniformity of mould filling. (Chen and Gao, 2006). They have investigated the profiling method for mould filling to get the

uniform melt front velocity. They have used a neural network model to estimate the melt flow length (MFL) from online for variables of measurable process. Based on their results, the neural network model is proven effective to ensure a uniform mould filling. This experiment and works done by the authors gave significant values for this research in determining the uniformity of mould filling at constant melt front velocity.

A simplified predictive control (SPC) is developed to control the injection velocity during the filling phase (B. Prajumati *et al.*, 2005). A simplified predictive control approach is a systematic handling of constraints through Linear Programming (LP) without requiring large computational effort (Yash P. Gupta, 1993). The performance and robustness of the proposed approach are compared with the general approach on process models exhibiting interactions, time-delays, and inverse response, through computer simulations.

The experiments were conducted on the DC motor for control simulation process to obtain the required tuning parameter D (distance). They concluded that SPC provides good control performance for multi-set point position profiles in order to minimise injection time and maintaining a uniform melt flow front. In this research, the filling stage will be regulated by controlling the injection velocity of the screw. In addition, a suitable injection velocity and time will be used whilst maintaining a uniform melt flow to get a better moulding.

Flow length is the capability of a melt polymer to flow while filling the cavity. The physical properties of injection-moulded parts are affected mainly by a

specified set of processing conditions: temperature, pressure, velocity, resin properties and mould geometry (Qin Sheng *et al.*, 1999; X. Chen *et al.*, 2004). Based on the development of microstructure in the injection moulding process, polymer materials can be classified into three categories according to their crystallisation behaviours (M. R. Kamal, 1979): rapidly crystallising polymers such as polystyrene and polypropylene; slowly crystallising polymers such as poly (p-phenylene sulfide) (PPS) and poly (ether ether ketone); non-crystallising polymers such as polystyrene and polymethylmethacrylate.

A model associated with numerical and followed by the simulation program to investigate polymer flow length for amorphous Styron 484-27 polystyrene and a semi crystalline 6401 polyethylene is investigated (Buchmann *et al.*, 1997). The result indicated a good combination between these two. Since the component for this research is a cylindrical shape with 30mm in diameter and 48mm in height, it is very important to understand the polymer behaviour used for this research. The method used by the authors was similar with this research where the model was developed and simulated before being placed into the experiment. Later result will be compared and established between the different types of polymers used.

The relationship between the filling and flow behaviour in the mould cavity was studied by A. Özdemir *et al.*, 2004. HDPE and PP materials were used at five different injection pressure and six different injection velocities. The experimentally result is then compared with the injection moulding analysis software (Moldflow 5.0). This research will also monitor the injection pressure and velocity. But the method is slightly different where experimental work will look into the surface

roughness of core and cavity then compared with MPA 7.3. Somehow, the approach used by these authors can be implemented in this research especially when using different injection pressure and velocity.

2.10 Injection Pressure

The pressure and force are the paramount factors in determining the ease and good quality of moulding. The cavity pressure is closely monitored by transducer and used to control the moulding operation (Kazmer *et al.*, 2005). They have surveyed that the pressure and temperature sensors are commercially available and widely used. They have listed out common pressure sensors, melt pressure sensors and temperature sensors. The geometry and performance of common transducers were discussed. But in this research the force sensor with $\pm 20\text{kN}$ will use to monitor the force during ejecting the moulding. In addition, the requirements and benefits of adapting the sensor also were discussed by the authors who will be benefited towards this research as guidance.

How to monitor the cavity pressure by using direct and indirect measurements is explained by Collins (1999). He has demonstrated on how to fix the transducers in cavity. His idea was based on the Kistler's product. The concept of implementing the position of sensor by the author gave an idea towards this research. In this research, I intended to use indirect measurement where the sensor will fix the hydraulic cylinder (movable platen). Since there is only one transducer which will be used in this research, the position mentioned is suitable to monitor the ejecting element (stripper plate) of the mould while pushing out the moulding.

PP (ICI 'Propathene' GXM 43) and low-density polyethylene, PE (ICI 'Alkathene' XRM 21) were used to study the pressure losses in the packing stage (Darlington *et al.*, 1986). The experiments have been done on cold mould and hot mould. The results confirmed that the cavity pressure is lower than nozzle pressure during the packing stage. In this research, it is important to make sure that the nozzle pressure is higher than cavity pressure to avoid gate freezing which might cause shot short problem. Hence the melt temperature of the thermoplastics has to be followed accordingly.

The experimental work associated with theoretical aspects was found better result in determining the effect of the holding pressure and prediction of the ejection force (Pontes *et al.*, 2004; Pontes *et al.*, 2005). The results are closely matched with the three common polymers been used: PP, PS and PC. Since there are lots of similarities in the experiment carried out by the authors, this research will greatly benefited. For the experimental work were discussed four processing parameters such as surface temperature, mould temperature, injection temperature and holding pressure (Pontes *et al.*, 2005). These parameters are very useful for this research. Theoretical aspects were discussed where some assumptions have been established (Pontes *et al.*, 2004). This research has absolutely gained a lot of input while dealing with the research activities.

The increasing screw speed and back pressure was demonstrated which may increase the melt temperatures 44°C greater than the barrel temperature results from viscous dissipation: plastication and adiabatic compression (Dontula *et al.*, 1991). Hence they were affected by the cavity pressure profile. The experimental works

done by the authors have given a significant value for this research and can be adapted in the experimental work since there is no mechanism to control the cavity pressure especially with the preparation before the actual experiment.

An Open loop test for several step inputs to a hydraulic servo-valve is conducted to measure the cavity pressure and injection speed (Dubay, 2001). Through his experiments, a predictive control has been developed and implemented to control the cavity pressure during filling phase. He concluded that the controlled performance is suitable for high-speed, medium and slow cavity pressure rates. By using multi-cavity pressure, control system has improved the quality of moulding and the process capability. The concept introduced by the authors has helped this research prior to experiment in terms of processing parameter.

2.11 The simulation packages software

The simulation software package like MPA is able to simulate and predict the associated problems with the moulding like weld line and air entrapment together with 3D finite element to predict the velocity, pressure, temperature field and the flow front (Hétu et al., 1998). The software is also able to predict the cavity filling and flow pattern behaviour (Özdemir et al., 2004; Reifschneider, 2001). This will provide a better understanding towards this research where the simulation works are done prior to experimental work. A numerical simulation by using different rheological models at filling stage to get the uniform melt front velocity is proven effective to ensuring uniform mould filling (Chen and Gao, 2006; Koszkuł and Nabialek, 2004).

2.12 Pressure and force

The pressure and force are the paramount factor in determining the ease and good quality of moulding. The cavity pressure can be monitored by transducer whether directly or indirectly (Kazmer et al., 2005; Collins, 1999).

The pressure losses in the packing stage were studied to the effect of moulding (Darlington et al., 1986). The experiments have been done on cold mould and hot mould. The results confirmed that the cavity pressure is lower than nozzle pressure during the packing stage. It is important to make sure that the nozzle pressure is higher than the cavity pressure so that to avoid gate freezing which might cause shot short problem. The experimental work associated with theoretical aspects carried out by Pontes et al., [Pontes et al., 2005; Pontes et al., 2004] were found better result in determining the effect of the holding pressure and prediction of the ejection force. The results are closely agreed with three common polymers used: PP, PS and PC. For the experimental work [Pontes et al., 2004], the authors had discussed four processing parameters such as surface temperature, mould temperature, injection temperature and holding pressure. Theoretical aspects were discussed by the authors [Pontes et al., 2005] where some assumptions have been established. Dontula et al., [Dontula et al., 1991] demonstrated that increasing screw speed and back pressure can increase the melt temperature 44°C greater than the barrel temperature results from viscous dissipation: plastication and adiabatic compression. Hence they were affected with the cavity pressure profile. Meanwhile Dubay [R. Dubay, 2001] has also conducted an open loop test for several step inputs to a hydraulic servo-valve to measure the cavity pressure and injection speed. A

predictive control has been developed and implemented to control the cavity pressure during filling phase. He concluded that the control performance is suitable for high-speed, medium and slow cavity pressure rates. Through the usage of multi-cavity pressure control system has improved the quality of moulding and its process capability.

Basically there are two groups which affected the ejection force: independent factor from mould (type of material and process condition) and related factor to the mould (part geometry, draft angle and surface roughness) [Pontes et al., 2002]. The experimental work by Sazaki et al., [Sazaki et al., 2000] has been established to show the relationship between the core surface roughnesses with the ejection forces. Three materials used: PP, PMMA and PET. Their experiment confirmed that for the ejection force for a certain surface roughness increases as the surface roughness decreases. The core surface roughness at $0.212\mu\text{mRa}$, PP and PET showed a minimum ejection force. For PMMA, the minimum ejection force obtained when the value reached near $0.092\mu\text{mRa}$.

2.13 Ejection Force

The ejection of part from the core is a paramount factor in this research in order to maintain the part quality and smooth operation of the mould especially when it comes to the actual production (bulk quantity). Ideally speaking, in injection moulding process, it will involve friction force where the tendency of moulding shrinks onto the core insert which causes the moulding to defect. For long usage and

mass production, the inserts tend to wear due to polymers rubbing the surface of the mould.

There are two groups which have affected the ejection force: independent factor from mould (type of material and process condition) and related factor to the mould (part geometry, draft angle and surface roughness) (Pontes *et al.*, 2002). Since the ejection force is paramount of this research, an independent factor and its related factors will be observed carefully. All aspects discussed by the authors will be considered for all of the thermoplastics used for this research. The properties and processing parameters of thermoplastics used should be strictly followed for this research.

The experimental work has been done to show the relationship between the core surface roughnesses with the ejection forces by (Sazaki *et al.*, 2000). Three materials used: PP, PMMA and PET. Their experiment has confirmed that for the ejection force for a certain surface roughness increases as the surface roughness decreases. The core surface roughness at 0.212 μ mRa, PP and PET showed minimum ejection force. For PMMA, the minimum ejection force obtained when the value reached near 0.092 μ mRa. To produce the surface roughness of core and cavity in this research, EDM process and ordinary polishing method will be used. Somehow, the comparison will be made for the same surface roughness but with different type of thermoplastics. Hence the correlation between surface roughness and materials used will be established.

2.14 Tool Venting

Generally, every tool contains air which must be removed as the tool is being filled with a plastic material. The presence of air in the mould cavity must be allowed to escape freely during injection. During high injection speeds, deficient mould venting may produce a considerable amount of air compression, with consequent slow mould filling, premature plastic pressure built up and in some extreme cases, burning of the plastic-brown streak on the moulding may happen. Hence, it is a must for the ventilation of air as it is generally needed so that the defect of the product can be best avoided.

Venting is done by making small gaps or vent provided in the mould parting line, or by small channel in the mould. Vent should be provided at the end of flow path. This will ensure that the air is forced to the end of the mould cavity during the filling phase. Figure 2.10 illustrates a method of venting.

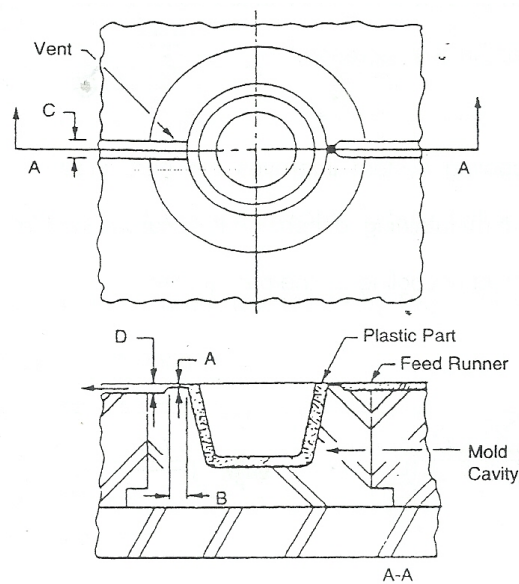


Figure 2.10: Method of venting thermoplastic injection mould
(Rosato Dominick V. *et al.*, 2000)

2.15 Tool cooling

One of the most important aspects of mould design that has to be observed is the provision of suitable and adequate cooling arrangements. If a mould had no means of cooling and was insulated to prevent any escape of heat by conduction, convection or radiation, it will quickly reach the temperature of the material being moulded and would no longer have its functions. The cooling system is a vital mould feature, requiring a special attention in mould design.

A good cooling circuit design reduces the cooling time, in which at the end, increases the overall productivity. This cost cutting is possible because injection moulding of thermoplastic requires additional time on cooling time rather than injection time. It normally takes about (2/3) of the cycle time. Hence, it means that, the production time is decreased.

A uniform cooling system improves the part's quality by reducing residual stresses and maintaining dimensional accuracy and stability. Figure 2.11 shows the effect of cooling on the part's quality.

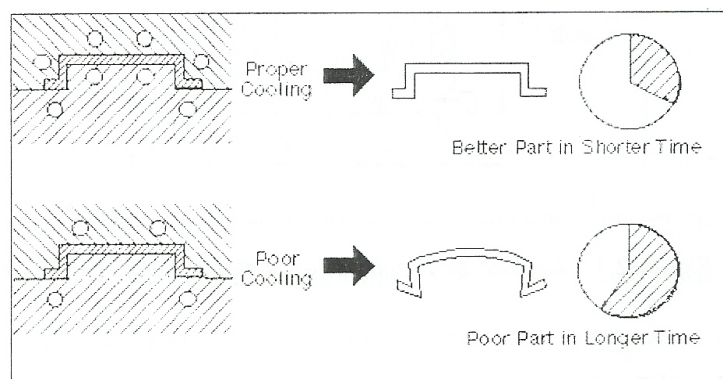


Figure 2.11: Proper and efficient cooling improves part quality and productivity ([www. Crms.engr.uk.edu//pages/cmold/](http://www.Crms.engr.uk.edu/pages/cmold/))

Fluid passages for effective mould and part cooling should be placed to cover most of the moulding surfaces and to be closed to the mould cavity. The distance between the mould cavity and fluid passage opening has to be wide enough to resist the distortion of the metal under injection pressures. Commonly, turbulent flow is recommended and used because it enables heat to be transferred more efficiently whereas it is of three times as many BTU's (Heat) as laminar flow.

The physical different between laminar and turbulent flow is that laminar flow of a fluid when each particle of the fluid follows a smooth path and never interfere with one another. One result of laminar flow is that the velocity of the fluid is constant at any point in the fluid. Meanwhile in turbulent flow an irregular flow that is characterized by tiny whirlpool regions. The velocity of this fluid is definitely not constant at every point as shown in Figure 2.12. Laminar flows are much less viscous, or resistant to flow, than turbulent flows. When using forced air or water applications, for instance, it is much easier to pump the fluids at lower speeds that produce laminar flows. Turbulent flows require more energy to push because much of that energy is diverted into the secondary currents from the turbulence.

Reynolds number is used to check whether the flow is laminar or turbulent. It is denoted by Re . This number got by comparing inertial force with viscous force as shown below.

$$Re = \frac{\text{Inertial forces}}{\text{viscous forces}} \quad (2.1)$$

Reynolds number formula is given by

$$Re = \frac{\rho V L}{\mu} \quad (2.2)$$

where ρ is the density of the fluid,

V is the velocity of the fluid,

ρ is the density of fluid,

μ is the viscosity of fluid,

L is the length or diameter of the fluid.

The kind of flow depends on value of Re

- If $Re < 2000$ the flow is Laminar
- If $Re > 4000$ the flow is turbulent

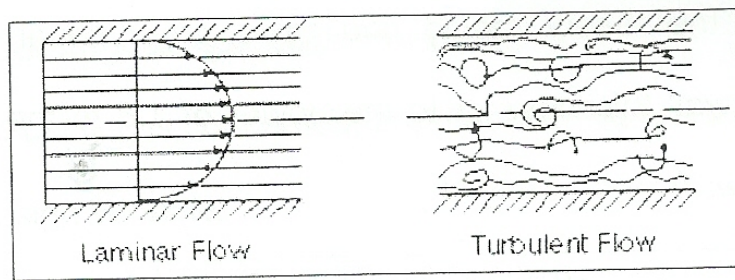


Figure 2.12: Laminar and turbulent flow

2.15.1 Tool cooling design consideration

The mould designer needs to determine the following design variables:

- i. Location of cooling channel
- ii. Size of cooling channel
- iii. Type of cooling channel
- iv. Layout and connection of cooling channels
- v. Length of cooling channel circuit
- vi. Flow rate of coolant

2.15.2 Design of cooling channel

Standard and optimum sizes of cooling channels are encouraged to be used in the design because they are easy to use with standard machine tools, standard fittings and quick disconnection. In order to sustain an economically acceptable cooling time, the excessive part of the wall thickness should be avoided. But, the thickness of the part should also be remained as consistent as possible.

The temperature difference on the opposite sides of the part should be kept to a minimum and should not exceed 10 °C for parts that require high tolerance. For steel mould, the surface of cooling channels (i.e. depth) is one to two channel diameters from the cavity or core. The pitch (distance between cooling channels' centre) should be three to five times the channels diameter. A typical cooling channel diameter ranges from 10 to 14 mm.

2.16 Summary

This chapter presents the types of polymers used in moulding industries including the technology and application of various machining process with emphasis are given to describe the process parameters which influence the quality of the moulding include the mould design concept, tool design, the adoption of simulation software package and also the working condition requirement for the polymer resins. The ejection force of the part and mould cavity filling are also highlighted and discussed.

CHAPTER 3

METHODOLOGY

3.1 Overview

This chapter presents the method that has been used to accomplish the objectives of the research. This chapter consists of research design, simulation works, mould fabrications and research procedures. The simulation process in Section 3.3 and the experimental work in Section 3.6 and will be discussed with details respectively. It also covers the process of designing the test tool, fabrication of tool, simulation work by using the appropriate software, experimental work and data collection.

The work flow of the process was summarised as shown in Figure 3.1. The initial stage of the research modelled the part design which was done in CAD software drawing package i.e. AutoCAD 2005 for 2D drawing. The model then was transformed into 3D by employing Autodesk Inventor Release 7.0 for simulation purpose in Autodesk Moldflow Insight 2010-R2 (AMI 2010-R2). The details of simulation and experimental methods will be elaborated in the next section.

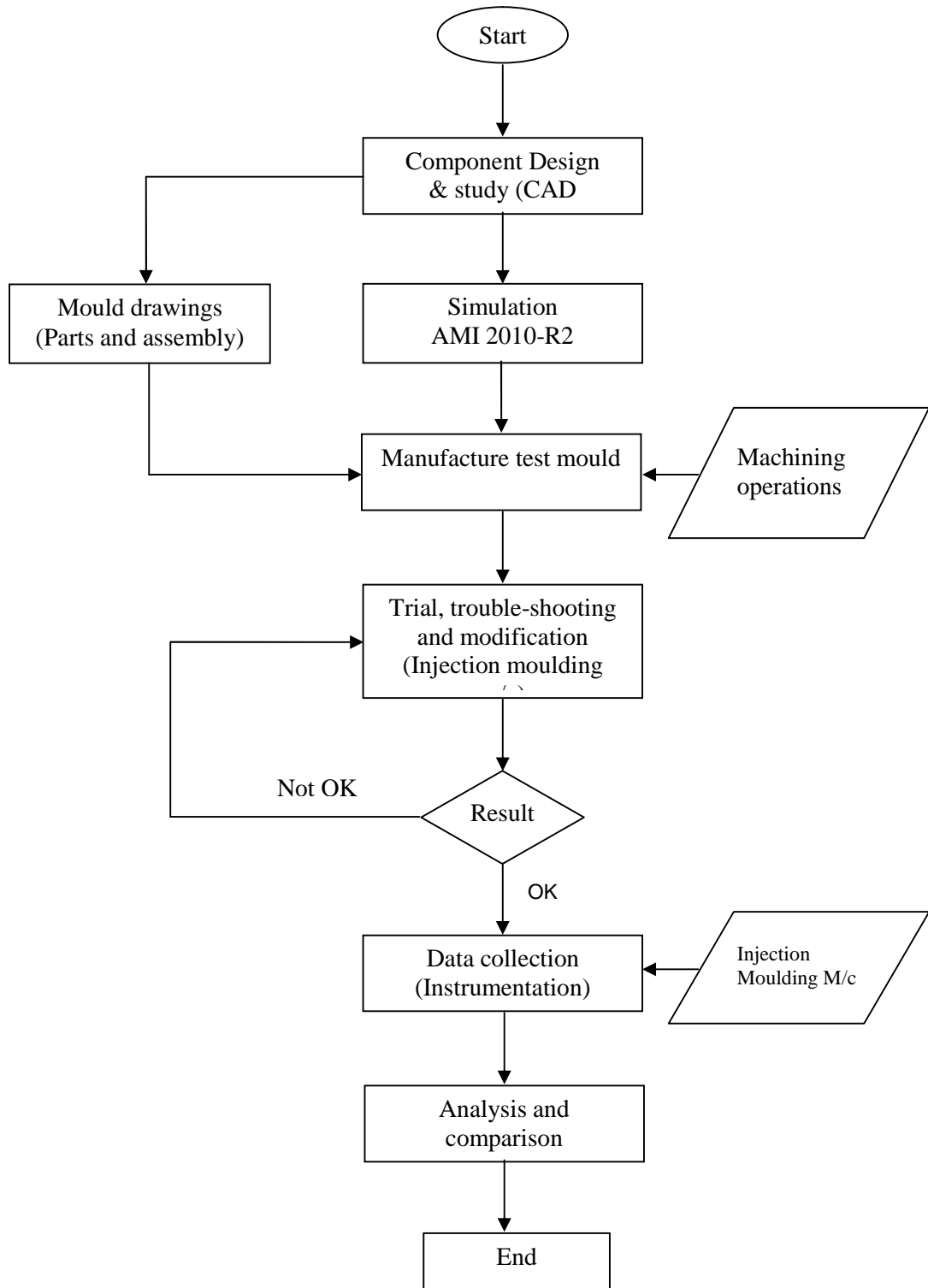


Figure 3.1: Overview of the work flow for research work

3.2 Tool design

Before the tool is produced, component weight and the elements related to the machines selection are required to be calculated. Since the process of manufacturing mould is time consuming and expensive, it is recommended by tool's designer to take some initial stages such as calculations, materials and machines availability etc.

3.2.1 Design procedure

Before the tool is manufactured, few numbers of stages should be done accordingly. The process of mould design and construction for this research are typically complex tool. The tools are expected to be more efficient and reliable in operation, cost and time. To design this tool, the following aspects have to be considered:

- The moulding or component drawing study.
- Part drawings development.
- Layout of the mould (including the number of cavity).
- Runner and gating system
- Shrinkage.
- Ejection system.
- Assembly drawing.
- Cavity and core insert drawing development.
- Identify the using of standard parts.
- Machining operation

- Trial/trouble-shooting
- Other matters related to designing process and operation.

3.2.2 Rationale design of the part and modelling

A component of a cylinder shape of 48 mm in height and Ø 25 mm with variation of wall thickness was designed in Autodesk Inventor 7.0. Figure 3.2 (a) and (b) shows the solid model for a hollow cup and part drawing that has been developed by using Autodesk Inventor 7.0 and two-cavity test mould's drawing for the component was designed by using AutoCAD 2005 including the assembly and part drawing.

An important consideration in this design of plastic injection moulded part is the wall thickness. A wall section that is too thin can lead to structural failure or poor insulation characteristics. A wall section that is too thick can result in appearance defects and an overweight or over-engineered part. With the latter point it is also worth remembering that wall thickness governs the moulding cycle time – the thicker the section the longer the cycle time and therefore the more expensive the part becomes. In this case, the top portion of the part is having 2mm in thickness and at the bottom is 1mm in thickness together with the sloping design at the middle. This is to facilitate of ease filling and flow of the resins used which among of the parameters studies (injection pressure) together with ejection process.

Furthermore, plastics shrink during cooling which in thick sections can result either in the surface of the part forming a sink mark or an internal void. Another

parameter include in this study was cooling time. However, this does depend on the design and function of the part concerned.

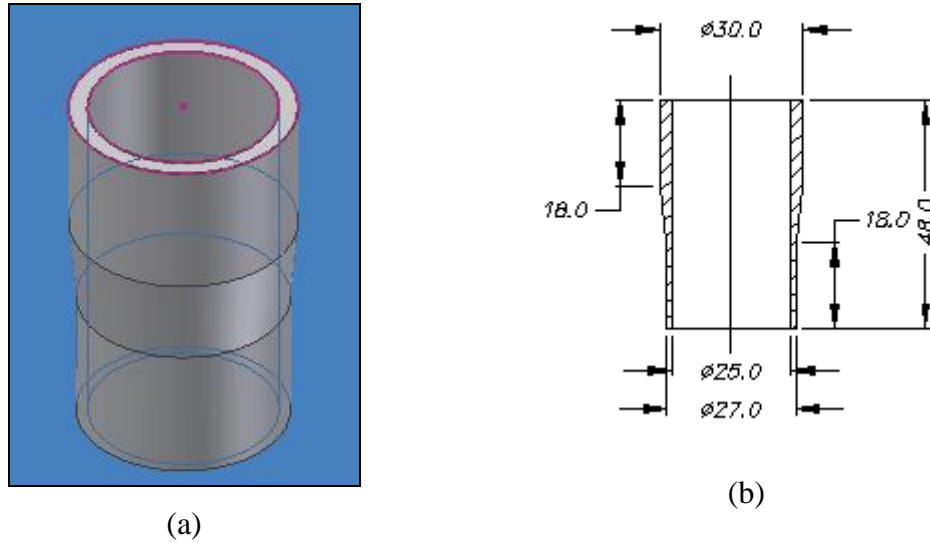


Figure 3.2: (a) A hollow cup modelled in Autodesk Inventor. (b) Part drawing was developed in AutoCAD 2005

Conversion of the component model to STL data format is essential which is companionable with AMI 2010-R2, and ready for a pre-processing stage. Figure 3.3 illustrates the procedure in preparing a finite element model for Moldflow Analysis. The mesh density then can be set locally or uniformly depending on the shape and feature of complexity. There are three types of meshing available; fusion mesh, midplane mesh and 3D mesh. In this research, a 3D mesh was used since it creates a true 3D representation of the part.

The next pre-processing step is to define the part material. Figure 3.4 shows the properties of component such as mass, area and the volume of the component. From the pre-processing model, the mass of the part is 8 gram excluding the feeding

system. The volume of material for filling the part is 8.17 mm^3 . This value can be used as a comparison with the actual experimental work.

3.3 Simulation in Autodesk Moldflow Insight 2010-R2 (AMI 2010-R2)

The 3D model was modelled in Autodesk Inventor Professional 10 and transformed to the *.stl file. The simulation was carried out by using the simulation software package AMI 2010-R2 to rectify any associated problem with the component.

3.3.1 Moldflow Simulation Analysis

Flow simulation analysis was carried out to investigate the most optimum mould filling and processing parameters in order to mould the moulding designated as hollow cup. A stereo lithography file (*.stl) from a CAD software (Autodesk Inventor Release 9.0) for the moulding was exported to AMI 2010-R2. The moulding is to be moulded with semi-round runner and rectangular gating using HIPS, ABS and PA6.

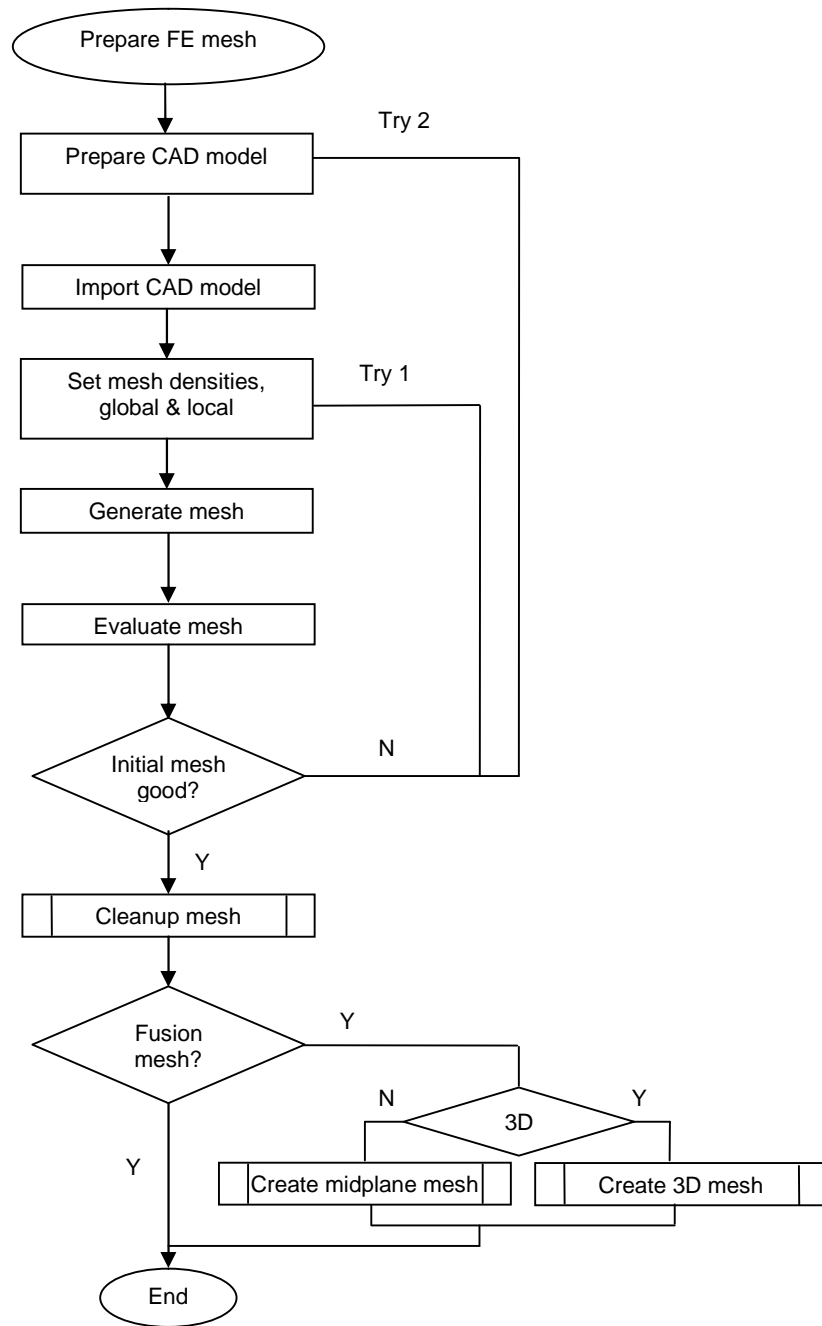


Figure 3.3: Steps in preparation of Finite Element Model for Moldflow Analysis

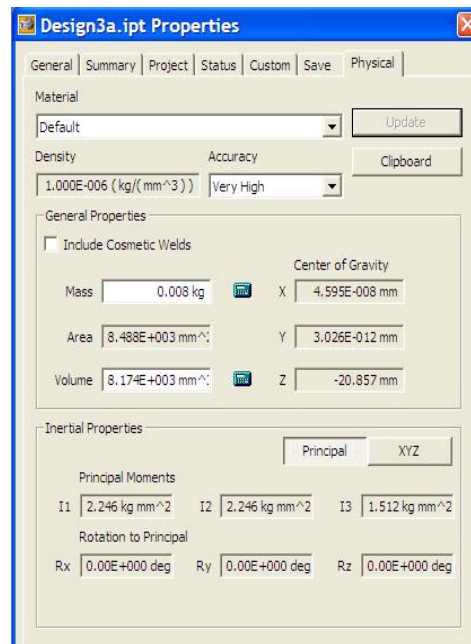


Figure 3.4: Component properties pre-processing model

3.3.2 Modeling and Analysis Methodology

AMI 2010-R2 was used in the analysis. The *.stl file was first transformed into moldflow model (*.mpi). Mending of the *.stl transformed model was required as the defective surfaces were found after the translation process. The meshed model of the moulding is as shown in Figure 3.5 and the simulation process is described in Figure 3.6.

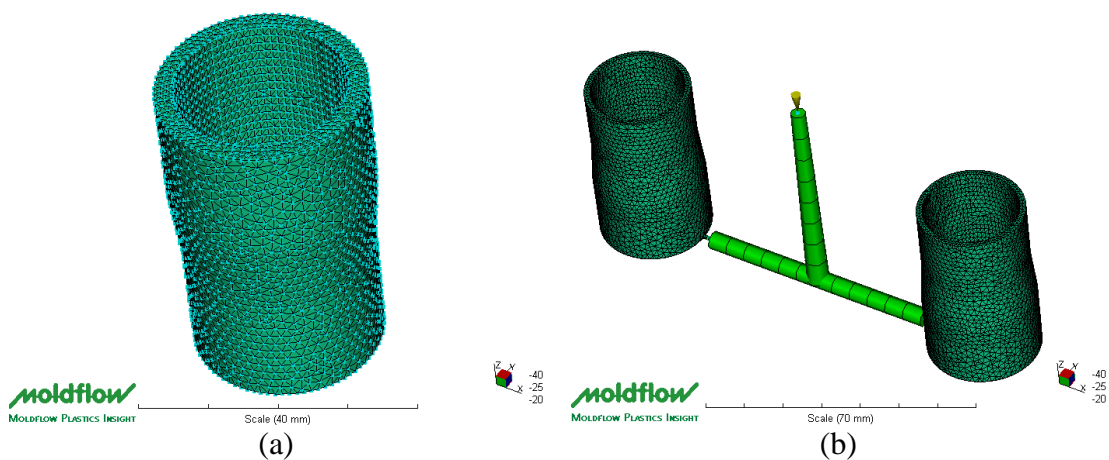


Figure 3.5: The geometric and FE model of hollow cup (a) Single. (b) Two cavities (multiple)

The process parameters used for setting the MoldFlow analysis are type of material used, injection point for the part, melting temperature, the screw diameter for the injection moulding (in this case the diameter of screw is 45 mm for Engel injection moulding machine) and clamping force which is kept constant throughout the analysis for all the material which is 330 kN. Once the analysis is run, the MoldFlow will suggest the injection pressure, packing pressure and cooling time for HIPS, ABS and PA6. These processing parameters will be put into the machine for running the experiment.

3.3.3 Simulation process

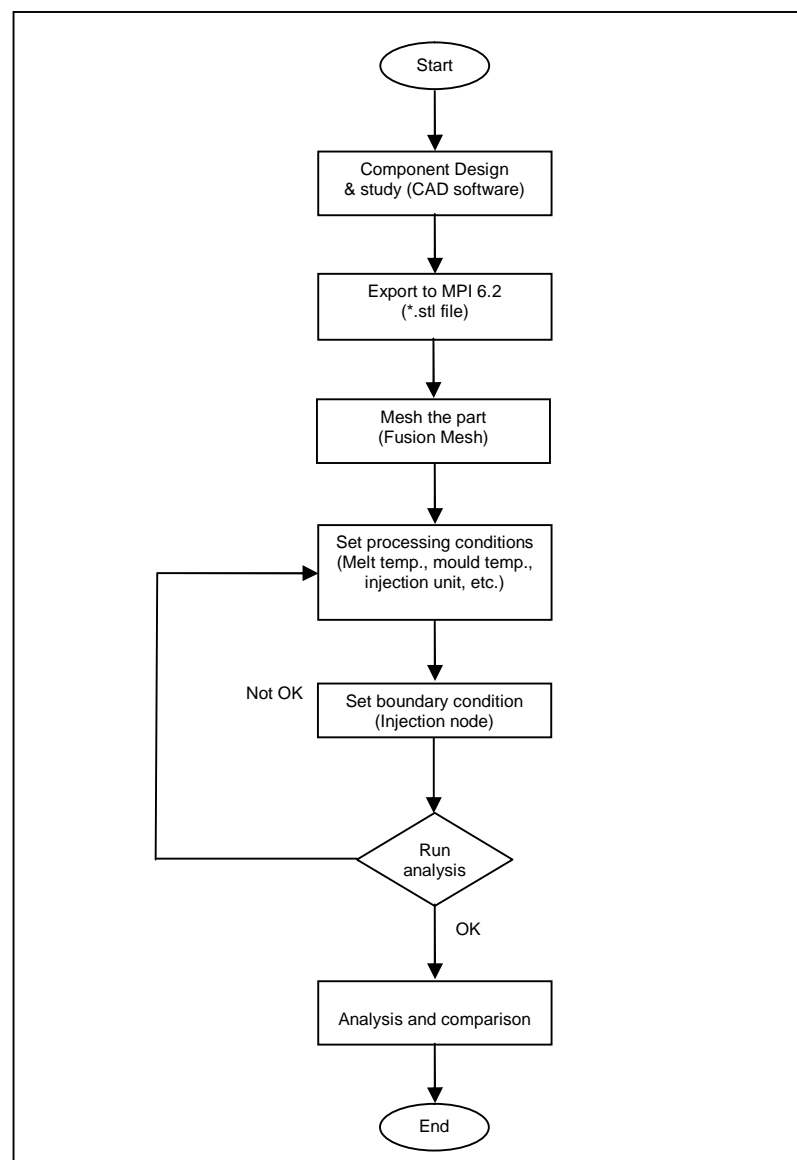


Figure 3.6: Simulation process outlines

3.4 Fabricating the tool

3.4.1 Machine Tool and Equipment

All the machining operations were conducted to manufacture the mould components in injecting hollow cup plastic components according to the drawing specifications as shown in Appendix A. The fabrication tool processes undergo both the traditional machine such as lathe, milling, grinding and drilling machines and non-traditional machine such as CNC milling, CNC lathe and Electrode Discharge Machining (EDM).

CNC milling machine is used for machining the pocket for fitting the core and cavity insert. Meanwhile CNC lathe is used to produce the core inserts (pre-dimensioning size) before the inserts (2 sets) are sparked by using EDM machine and mirror polished (1 set) according to the shape and the required surface roughness.

3.4.2 Mould base

A standard mould base will be used for time saving and perfect matching while assembling. A Lee Kum Mung (LKM) mould base standard was selected for this research after confirming the size of tool needed to be used.

3.4.3 Core and cavity inserts

The material used for core insert and cavity insert are high quality tool steel (DF-3) from Assab Steels (Malaysia) Sdn. Bhd. The material is oil harden tool steel with good wear resistance and durability as shown in Figure 3.7(a). Table 3.1 shows the chemical composition for the material. Figure 3.7 (b) shows the copper material used to obtain the required surface roughness by using EDM machining process. The copper then are machined according to the shape of the moulding. The shapes of cavity inserts are produced according to the shape of copper as shown in Figure 3.8.

Table 3.1: Chemical composition for Assab DF-3 tool steel for inserts

Grade	Chemical composition %							Hardness supplied approx HB
Assab DF-3	C	Mn	Cr	Mo	V	W	others	
	0.95	1.1	0.6	-	0.1	0.6	-	190



(a)



(b)

Figure 3.7: (a) DF3 tool steel for inserts (b) Copper for EDM machining

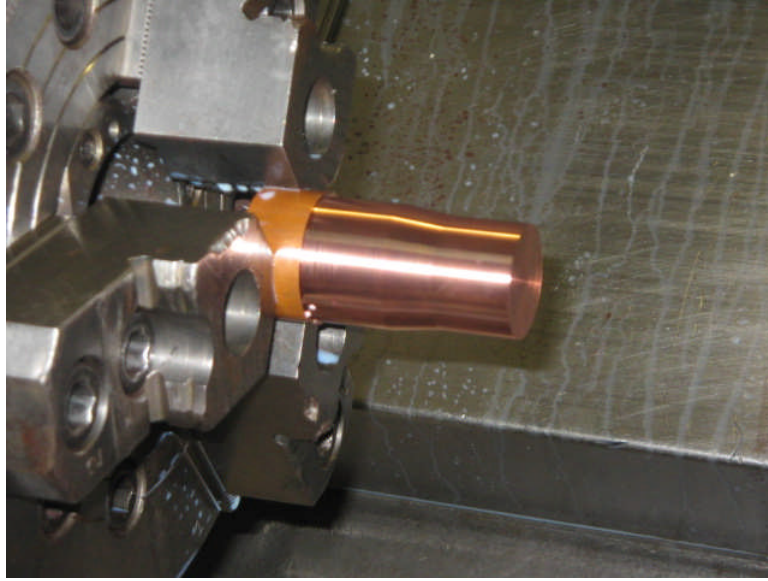


Figure 3.8: Process producing electrode by using CNC lathe

3.4.5 Runner, Gating and Ejection System

The designer is supposed to calculate the runner and gate size that are needed for the resin flow inside the cavity. In this case the gate size is 2 mm x 2mm (L. Sors and I. Balazs, 1988) which was selected as shown in Table 3.2. Meanwhile the half round runner with diameter 5 mm was also selected. Figure 3.9 showed the layout of gating and runner system on the cavity plate.

The stripper plate ejection system was employed due to the product design itself which is in cylindrical shape. The ejection system also provides a stability of stripper plate to eject the moulding. This is very important for this research in measuring the ejection force generated.

Table 3.2: Standard gate size (L. Sors and I. Balazs, 1989)

Mass of part (g)	Conical beam sprue (direct gate)	Needle gate (pinpoint or tunnel)	Rectangular gate
To 10	2.5 – 3.5	0.8	1.0 x 2.0 – 2.0 x 2.0
11 – 20	3.5 – 4.5	0.8	1.5 x 2.5 – 2.5 x 3.5
21 – 40	4.0 – 5.0	1.0 – 1.2	2.0 x 3.0 – 2.5 x 3.5
41 – 150	4.5 – 6.0	1.5 – 2.5	2.5 x 3.5 – 3.5 x 4.5
151 – 300	4.5 – 7.5	1.5 – 2.8	2.5 x 3.5 – 3.5 x 4.5
301 – 500	6.0 – 8.0	1.8 – 3.5	–
501 – 1000	8.0 – 10.0	–	–
10001 – 5000	10.0 – 15.0	–	–

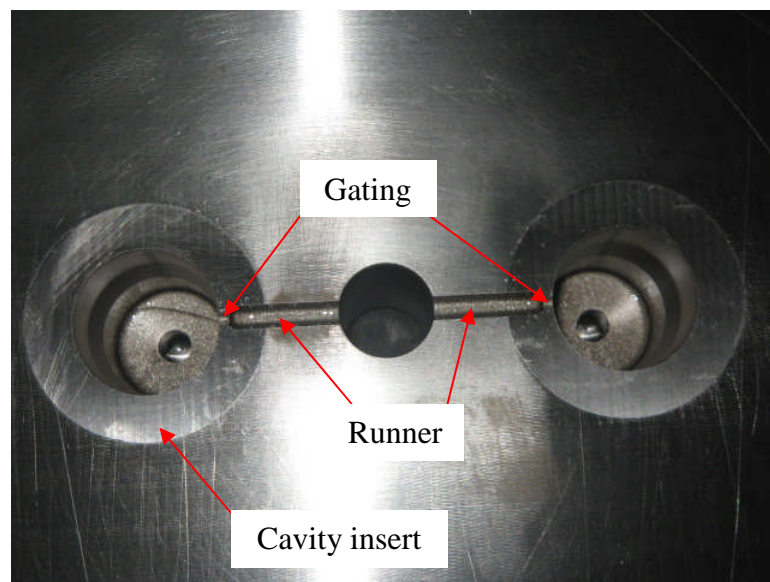


Figure 3.9: Half round runner and rectangular gate system

3.4.6 Venting Design System

In order to avoid the air entrapment which might cause a short-shot problem or blemishing, air need to be evacuated from the cavity. Based on the simulation result in Figure 4.5 in Chapter 4, the air-bubbles are generated both on top and the bottom of the moulding. For ABS resins indicate more air-bubble compared to HIPS and PA6 whereas HIPS shows less air-bubble.

The recommended size of venting for the design is 4 mm wide and 0.025 mm in depth (Liu et al., 2000 and Gao et al., 1998). It is recommended for low viscosity material, the depth of venting should be 0.015 mm and for high viscosity material should be 0.03 mm (Moldflow plastic Insight Manual, 2006). To be more effective, the venting system should be provided both on the core and the cavity plate where parting line meets the mould. For some reason in the research, the ventilation has been provided both on the core inserts and the cavity inserts. Figure 3.10 and 3.11 showed the air ventilation design system for core insert and cavity insert. Surface grinding machine has been used to produce the air-vent both on core and cavity inserts.

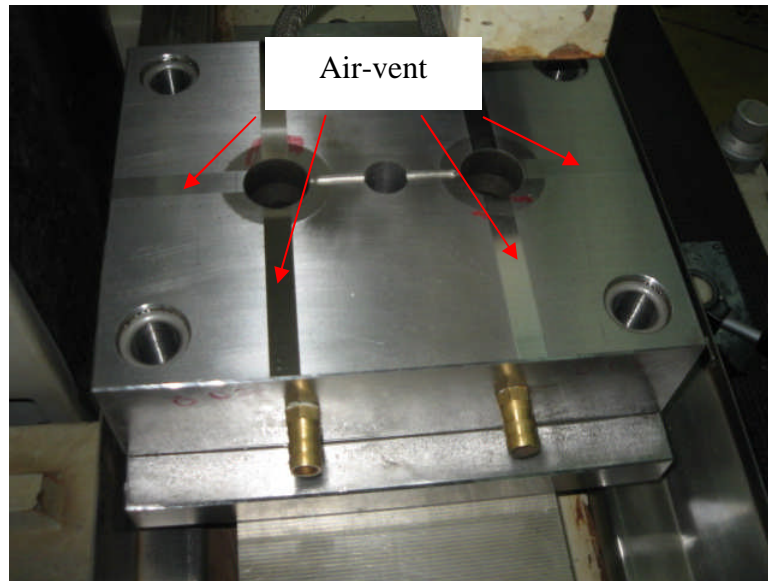


Figure 3.10: Air vent on cavity insert and cavity plate

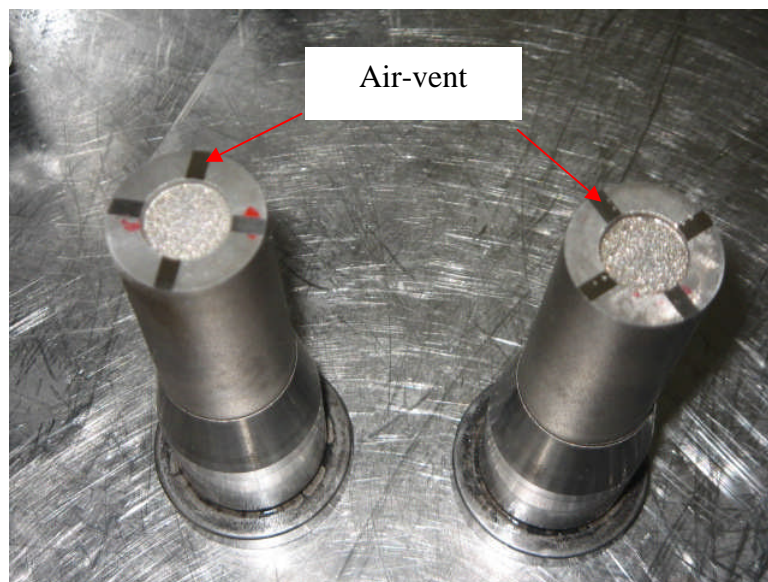


Figure 3.11: Air vent on core insert

3.4.7 Mould Cooling System Design

Mould cooling system is related to the heat dissipation theory. The designer has to understand the heat introduced by the plastic resin inside the cavity. The design of cooling system mainly depends on the moulding shape. The following criteria also need to be considered while designing the mould cooling system.

- ❖ Logically, the hottest area is the cavities of the cavity plate where the melt of resin is filled. It means that few cooling channels are needed at this area compared to the core plate. Therefore, in order to obtain a similar temperature between these two plates, the designer has to provide an effective cooling channel for both on core and cavity plates.
- ❖ On the cavity plate the series layout is used where one turns round the water flow and encircled in the middle.
- ❖ For the core plate, a baffle cooling layout is used. This is due to the depth of the core insert and needs of a balanced cooling system along the core.

Figure 3.12 shows the copper plate which was used to design the baffle cooling system for the core insert. Figure 3.13 and 3.14 show diagrams for cooling system design of the cavity and core plate. The cooling method can be figured from the formulas and related information which can be found in each heat transfer condition. In order to determine the minimum mass flow rate required for turbulent flow and heat conducted to the equation is as shown below.

$$R = \frac{7740VD}{n} \text{ or } \frac{3160Q}{Dn} \quad (3.1)$$

Where, R = Reynolds number
 V = fluid velocity, m/s
 D = Diameter of passage, m
 ν = kinematics viscosity, m²/s
 Q = flow rate, m³/s

Source of formula: Injection Moulding Handbook, 3rd. Edition by Rosato et al., 2000.

A Reynolds number of 2000 or less yields laminar flow and turbulence sets in at values 3500 to 5500 or even higher (Rosato et al., 2000). The calculation is based on the water entrance temperature of 10 °C, and diameter of cooling passage is 9 mm.

From table 3.3, kinematics viscosity, $\nu = 1.3 \times 10^{-6}$ for 10 °C.

Hence, the minimum flow rate required for turbulent flow will be

$$R = 3500 = \frac{3160 Q}{D \nu}$$

$$Q_{\min} = \frac{3500 \times 0.009 \times 1.3 \times 10^{-6}}{3160}$$

$$Q_{\min} = 1.3 \times 10^{-8} \text{ m}^3/\text{s}$$

For a Reynolds number of 5500, we will have an average flow rate of

$$Q_{\text{avg}} = \frac{5500 \times 0.009 \times 1.3 \times 10^{-6}}{3160}$$

$$Q_{\text{avg}} = 2 \times 10^{-8} \text{ m}^3/\text{s}$$

The design of cooling channel according to literature research and the rules (Rosato et al., 2000), the cooling channel is 9 mm diameter, the distance between

moulding surface and cooling is 29.5 mm and 8 mm, the pitch between cooling channel is 89 mm and 100 mm for cavity and core plate respectively.

Also, for an efficient cooling, a turbulent flow is used rather than the laminar flow. From the calculation, the turbulent flow can be achieved by having a minimal flow of 9 mm cooling channel size with a flow rate of $1.3 \times 10^{-8} \text{ m}^3/\text{s}$ and average a flow rate of $2 \times 10^{-8} \text{ m}^3/\text{s}$.

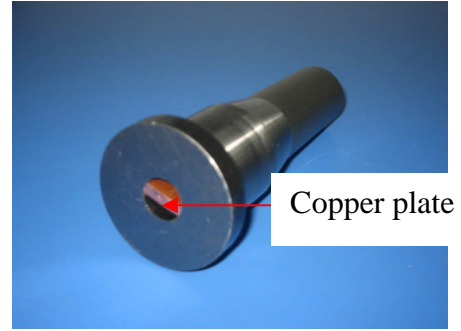
Table 3.3: Kinematics Viscosity

Water temperature, t (°C)	Viscosity, $\nu \text{ (m}^2/\text{s) } \times 10^{-6}$
0	1.787
5	1.519
10	1.307
20	1.004
30	0.801
40	0.658
50	0.553
60	0.475
70	0.413
80	0.365
90	0.326
100	0.290

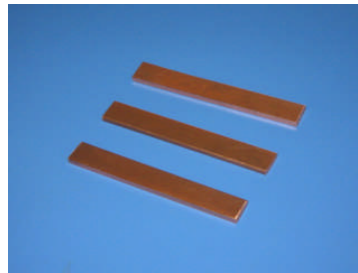
Source: http://www.engineeringtoolbox.com/water-dynamic-kinematic-viscosity_d_596.html
 Visited: 22/02/14



(a) Core insert with copper plate inside



(b) The position of copper plate



(c) Copper plate

Figure 3.12: Copper plates is used for baffle cooling system design at core inserts

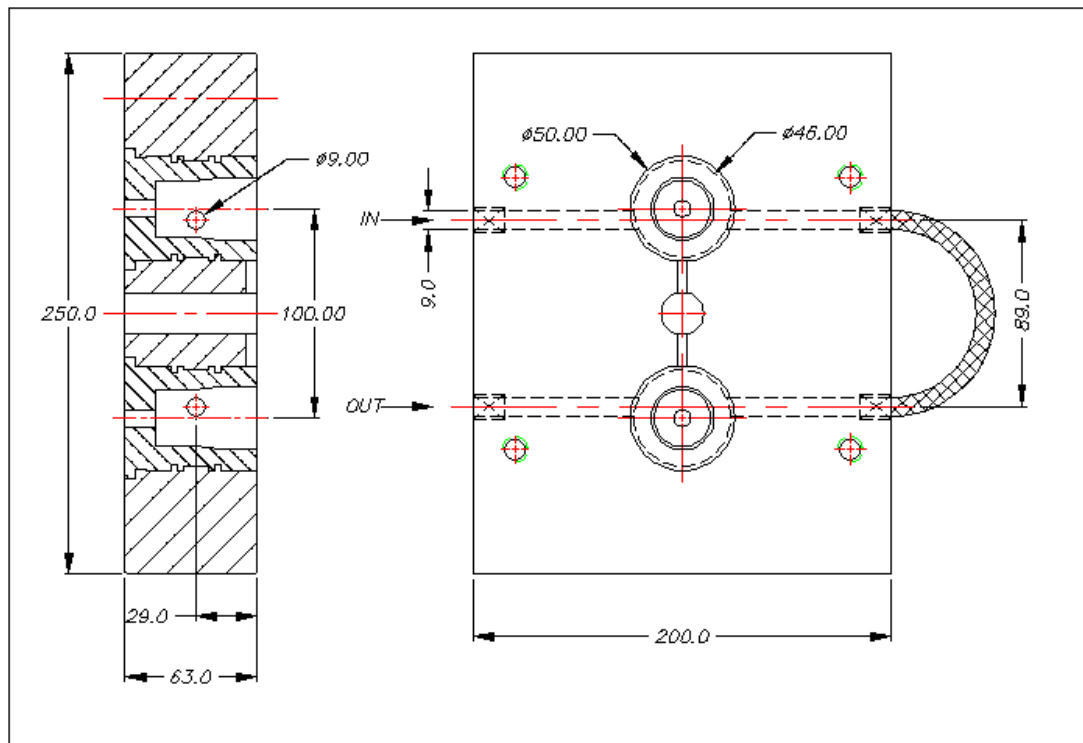


Figure 3.13: A series of cooling system for cavity plate

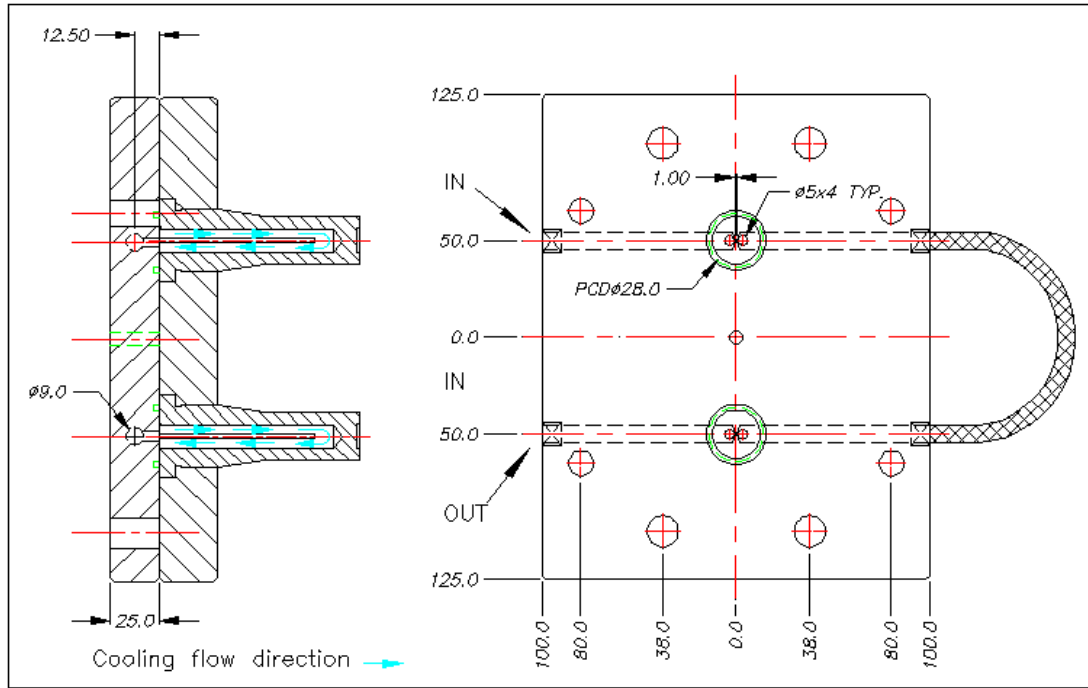


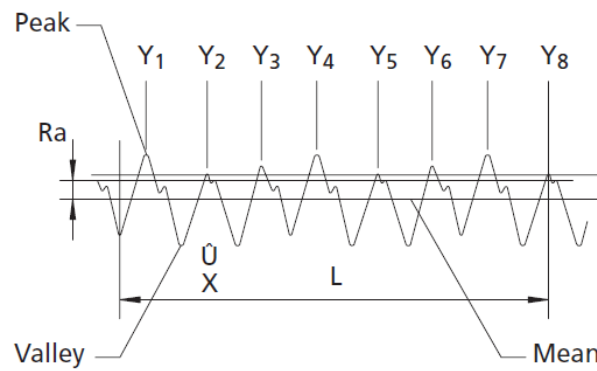
Figure 3.14: A baffle of cooling system for core insert

3.4.8 Surface Roughness

Roughness averages are the most commonly used parameters because they provide a simple value for accept/reject decisions. Arithmetic average roughness, or R_a , can be defined as the arithmetic average height of roughness-component irregularities (peak heights and valleys) from the mean line, measured within the sampling length, L as shown in Figure 3.15. The measurements are taken as the fine point of the stylus on a drive unit which traverses the sampling length on the surface being measured and is defined by the formula,

$$R_a = \frac{1}{n} \sum_{i=1}^n x_i \quad (3.1)$$

Where R_a is the arithmetic mean and x_1, \dots, x_n is a data set containing the values.



Y = Individual measured peak height

Figure 3.15: Sampling length with individual peak height
(Source:<http://www.alphaomegapt.com/pdf%20files/Surface%20Finish%20Definitions.pdf>)

Since the study focuses on the effects of the surface roughness, three sets of surface roughness for core insert and cavity inserts were produced with different ' R_a ' value. Two sets of inserts are employed in EDM process to produce the required surface roughness. Meanwhile another one set of employed polishing method is a produced mirror polished surface roughness by using emery paper and diamond paste (several of grades). The process of producing surface roughness was obtained by means of EDM and polishing process as shown in Appendix B.1 and B.2. Figure 3.16 shows the process of producing the surface roughness for the mould insert. The inserts undergo CNC machining process to obtain the required shape. The cylindrical grinding machine is used for obtaining the allowable dimensioning size before put into EDM and polishing process in order to have a desired surface roughness. For spark erosion surface roughness, R_a value is obtained based on the industries practice. Meanwhile emery paper and diamond paste are used to obtained mirror polish surface. All the R_a value is measured using surface roughness tester.

3.4.9 Measurement of surface roughness

' R_a ' or arithmetical means surface roughness is the recognised standard to evaluate the surface texture. An average value of the core surface was measured perpendicularly to the surface roughness tester, Mitutoyo Surftest SJ-301 at the different four location points around the insert which can be seen in Figure 3.17. The positions of measurement were marked with green colour dot. One dot represents for position 1, two dots represent for position 2, three dots represents for position 3 and four dots represent position 4.

The surface roughness for each position was measured by using surface roughness tester equipment and the average value was taken as the reading for surface roughness. The travelled distance for measuring the surface roughness is 4 mm. Figure 3.18 showed the layout of the equipment set-up for obtaining the surface roughness value for the core inserts. It was comprised with drive/detector (stylus) unit and display unit for recording the surface roughness, dial indicator for parallelism purpose of surface to be measured with the drive/detector (stylus) unit. The equipment and core inserts were placed on the granite table in Metrology Lab at TATIUC to make sure that the perfect position and accurate reading can be obtained. Figure 3.19 showed the correct position of surface core insert and the stylus of the surface roughness equipment. The surface to be measured should be paralleled with the stylus. The data sample for R_a is shown in Appendix I.5 and I.6. Meanwhile the process of obtaining R_a is shown in Appendix I.7.

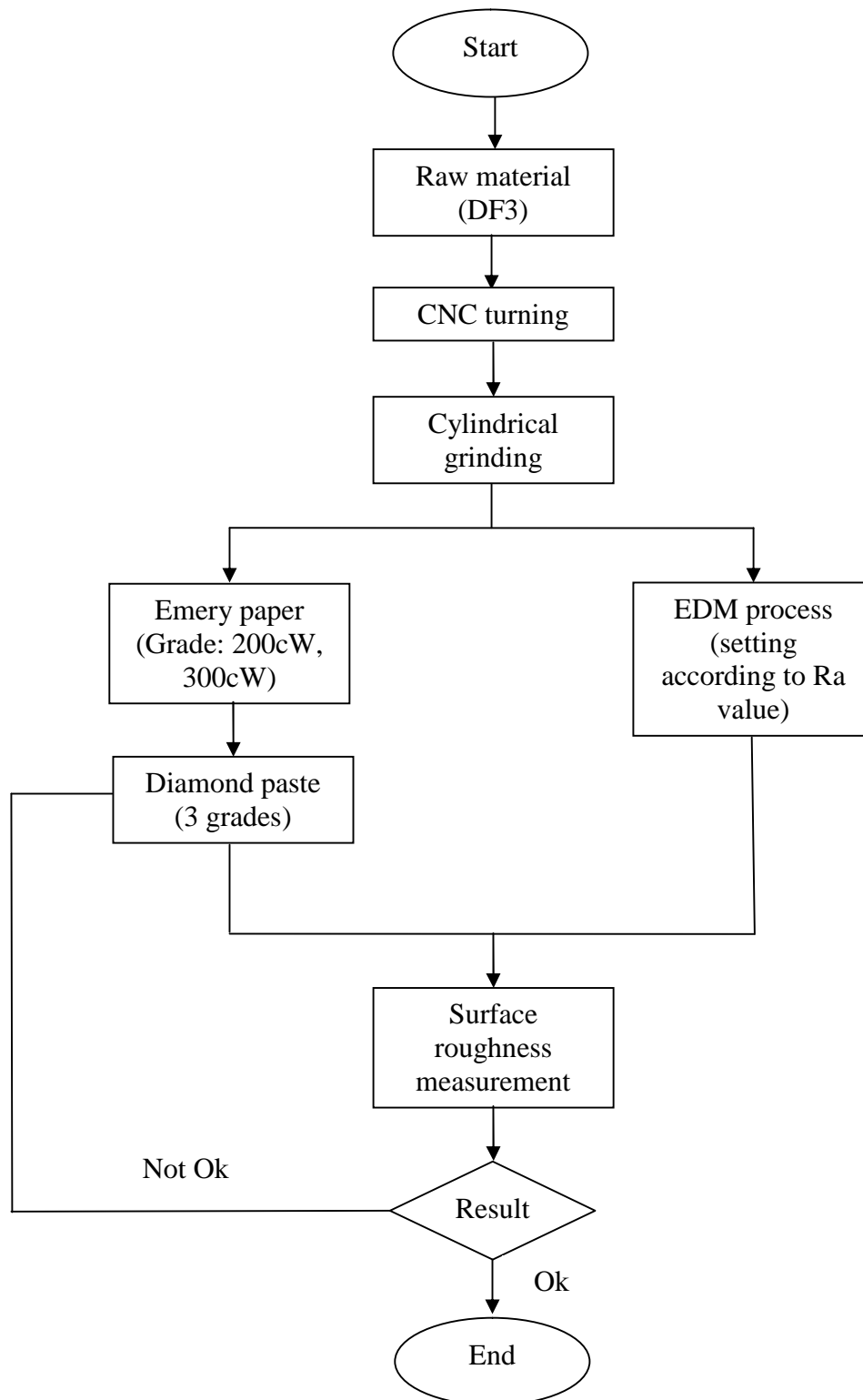


Figure 3.16: Process of producing surface roughness for the mould inserts



Figure 3.17: The position of (green marked) for surface roughness checking

1 dot (green colour) represent position 1, 2 dots represent position 2,
3 dots represent position 3 and 4 dots represent position 4



Figure 3.18: The layout equipment set-up for checking the surface roughness for core inserts

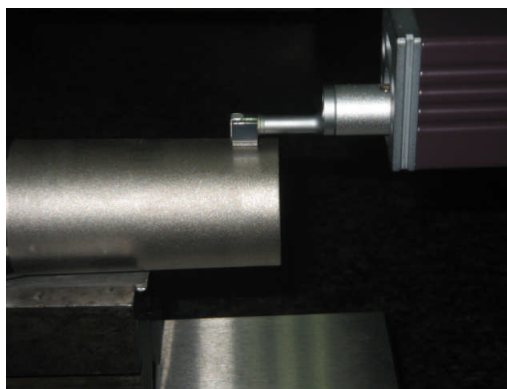


Figure 3.19: The process of measuring the surface roughness
(The drive/detector unit must be parallel with the surface measured)

3.4.10 The matrix combination for core inserts

The matrix combinations for the core inserts and the surface roughness of the insert were produced by the means of EDM and polishing process as shown in Table 3.4. Three sets of surface roughness for core are produced which denoted with S1, S2 and S3. Each set of surface roughness having two inserts which is denoted with “x” and “y” for core insert 1 and core insert 2, respectively. All the core inserts were mark accordingly to avoid mixed-up during changing the core insert during the experiment. By using L₉ Taguchi orthogonal array, the matrix and surface roughness of all core inserts are arranged accordingly as shown in Table 3.5. Each combination of core is having surface roughness value and is denoted with alphabet for further work.

Table 3.4: Matrix combination for core and cavity inserts

Combination		Insert 2		
		S1 _y	S2 _y	S3 _y
Insert –	S1 _x	S1 _x + S1 _y	S1 _x + S2 _y	S1 _x + S3 _y
	S2 _x	S2 _x + S1 _y	S2 _x + S2 _y	S2 _x + S3 _y
	S3 _x	S3 _x + S1 _y	S3 _x + S2 _y	S3 _x + S3 _y

Surface roughness of core; S1 = 0.01 μm , S2 = 1.80 μm and S3 = 3.21 μm
“x” – Core insert 1 and “y” – Core insert 2

Table 3.5: The combination of core surface roughness

Surface of core combination	Surface roughness (μmRa)	Denoted Symbol
S1 _x +S1 _y	0.02	A
S1 _x +S2 _y	1.84	B
S1 _x +S3 _y	3.22	C
S2 _x +S1 _y	1.84	D
S2 _x +S2 _y	3.60	E
S2 _x +S3 _y	5.01	F
S3 _x +S1 _y	3.22	G
S3 _x +S2 _y	5.01	H
S3 _x +S3 _y	6.42	I

S1_x, S2_x and S3_x represent for core insert 1 meanwhile
S1_y, S2_y and S3_y represent for core insert 2

3.4.11 Process of Obtaining Microscopic Core Insert

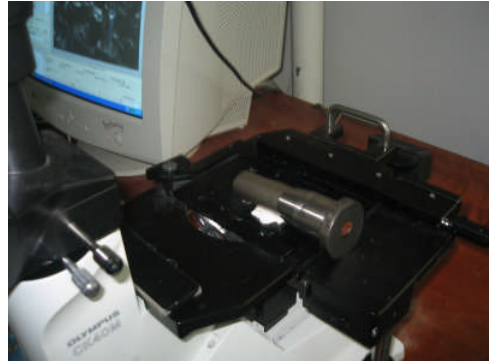
The optical microscope, often referred to as the "light microscope", is a type of microscope which uses visible light and a system of lenses to magnify images of small samples as shown in Figure 3.19(a) and (d). The image from an optical microscope can be captured by normal light-sensitive cameras to generate a micrograph by showing the resulting image directly on a computer screen without the need for eyepieces. The optical microscope used for this research was Olympus CK 40M as shown in Figure 3.19(b) and (c). The stage is a platform below the objective which supports the specimen being viewed. In the centre of the stage is a hole through which light passes to illuminate the specimen. The stage usually has arms to hold slides (rectangular glass plates with typical dimensions of 25×75 mm, on which the specimen is mounted). Refer to Figure 3.19(c).

At magnifications higher than 100× moving a slide by hand is not practical. A mechanical stage, typical of medium and higher priced microscopes, allows tiny movements of the slide via control knobs that reposition the sample/slide as desired. All stages move up and down for focus. With a mechanical stage slides move on two horizontal axes for positioning the specimen to examine specimen details.

Focusing starts at lower magnification in order to centre the specimen by the user on the stage. Moving to a higher magnification requires the stage to be moved higher vertically for re-focus at the higher magnification and may also require slight horizontal specimen position adjustment. Horizontal specimen position adjustments are the reason for having a mechanical stage. The process of obtaining the microscopic of core inserts is shown in Figure 3.19. The results and microscopic images are discussed in Chapter 5.



(a) Layout of optical microscope



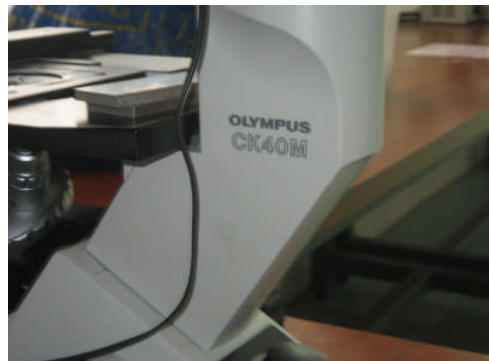
(b) Positioning sparked core insert



(c) Positioning polished core insert



(d) Process checking the microscopic



(e) Olympus CK40M model

Figure 3.20: Process obtaining microscopic core inserts by using optical microscope

3.5 Tooling Construction

The tooling used for the experiment is shown in Figure 3.20 and 3.21. The machining process of fabricating and assembling the tooling is shown in the Appendix C.1. Figure 3.22 showed the tool for conducting the experiment.

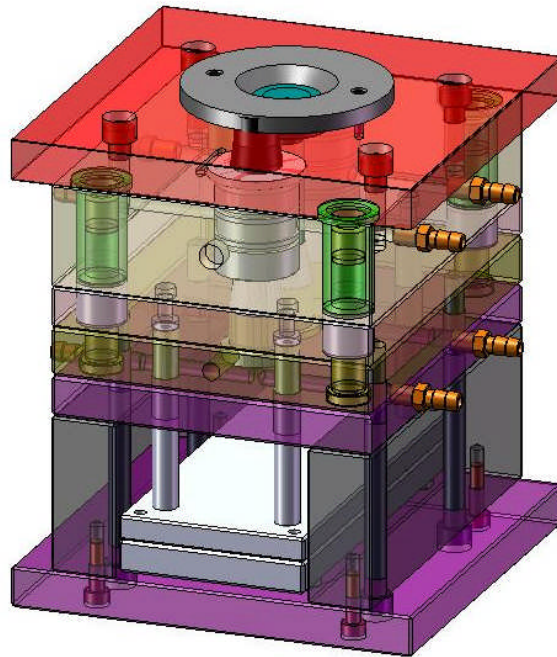


Figure 3.21: The 3D solid modelling test mould for plastic injection moulding



Figure 3.22: Test mould ready for trial out

3.6 Experimental work

The experimental work comprises of the measuring device, injection moulding machine, two-cavity mould and the computer.

3.6.1 Material

Three polymer resins used in the experimental work were high impact polystyrene (HIPS), an acrylonitrile butadiene styrene (ABS) and polyamide (PA6). The typical properties of the resins were Table 3.6.

Table 3.6: Typical properties of polymer resin used

Typical Properties	Units	HIPS	ABS	PA6
Solid density	g/cm ³	1.04	1.03	1.14
The melt mass-flow rate (MFR)	g/10 min	4 (200°C, 5 kg)	1.8 (200°C, 5 kg)	48 (230°C, 2.16 kg)
Melt density	g/cm ³	0.97 (At about 200°C)	0.95 (At about 270°C)	0.95 (At about 270°C)
Thermal conductivity	W/(m °C),	0.16	0.19	0.25
Heat capacity	J/(kg °C)	1340	2013	2600
Manufacturer	-	Idemitsu Petrochemical Co. Ltd.	Chi Mei Corp.	Mitsubishi Group

The resins were then selected based on their availability and necessities for the moulding industries in Malaysia. Appendix D.1, D.2 and D.3 show the specification for the resins from the local supplier in Malaysia.

3.6.2 Equipment and machine set-up

The machine used in injecting the hollow cup was an Engel ES 125 HL-Victory injection moulding machine as shown in Figure 3.23. The machine's capacity is 125 ton and is having $\phi 45\text{mm}$ screw diameter and 90 mm for the injection stroke. The ejection system used for the machine is the hydraulic system which is suitable to carry this study in measuring the ejection force of moulding. The technical specification for the machine is shown in Appendix E.



Figure 3.23: An Engel injection moulding machine (HLV-125)

The packing time and clamping force are kept constantly throughout the experiment for 20 s and 330 kN respectively. Table 3.7 shows the process of parameters of injection moulding that were set up for the experimental work.

Table 3.7: The parameters of moulding conditions for the experiment for the resins

Material	HIPS	ABS	PA6
Melt temperature, A (°C)	195 – 220	200 – 240	250 – 300
Injection pressure, B (MPa)	55 – 69	50 – 77	32 – 57
Packing pressure, C (MPa)	45 – 59	41 – 65	26 – 46
Cooling time, D (s)	16 – 17	17 – 18	17 – 19
Clamping Force (kN)	330	330	330

3.6.3 Instrument Set-up

The measuring device is composed of an injection moulding machine, tool for measuring the ejection force and personal computer. The instrument set up for this study is shown in Figure 3.24 and comprises with force link, trigger switch, connecting cable, signal conditioning platform (SPC). The force during part ejection is measured by a piezoelectric force sensor (Kistler 9331B) mounted at the middle of the ejector rod of the injection moulding machine as shown in Figure 3.25. The piezoelectric force sensor is activated when this ejector rod push the stripper plate for ejecting the part. The acquisition and monitoring of the signal measured by the sensors is based on amplifiers and the signal conditioner, a data acquisition board, type 5063A1, the software DataFlow from Kistler, type 2805A-02 and the signal conditioning platform type 2853A are used and suitable for process visualization, process monitoring and process document for all variation of the injection moulding process and the cyclical processing method. In each cycle the monitoring process is trigger by a switch that is actuated on the top of tool when the tool closed/opened.

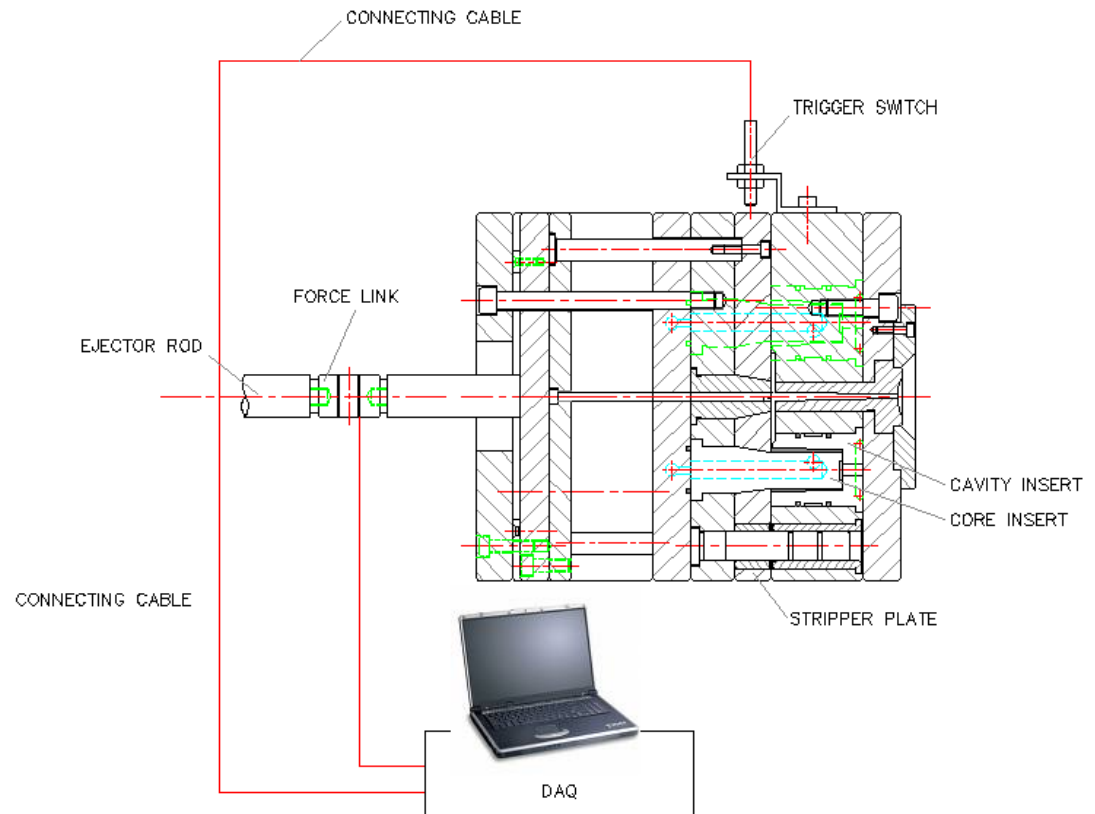


Figure 3.24: Kistler's instrumentation set-up

3.6.4 Force link 9331B

A force sensor link is mounted at the ejector rod cylinder's machine and the force is exerted through the rod to push the ejector plate. The four return pins which are mounted at the ejector plate will push the stripper plate to eject the moulding from the core inserts.

The force transducer will then be fitted at the injection moulding machine's hydraulic cylinder to measure the ejection force. Figure 3.25 showed force link used in this study. The specifications of force link, calibration certificate, test certificate and signal conditioning platform (SPC) are used together with the force link sensor

are shown in Appendix F. Figure 3.26 shows how to fit the force link together with the ejector rod for the injection moulding machine and Figure 3.27 shows the location of the force link at the machine.



Figure 3.25: Force link 9331B



Figure 3.26: Ejector rod and Kistler's link assembly

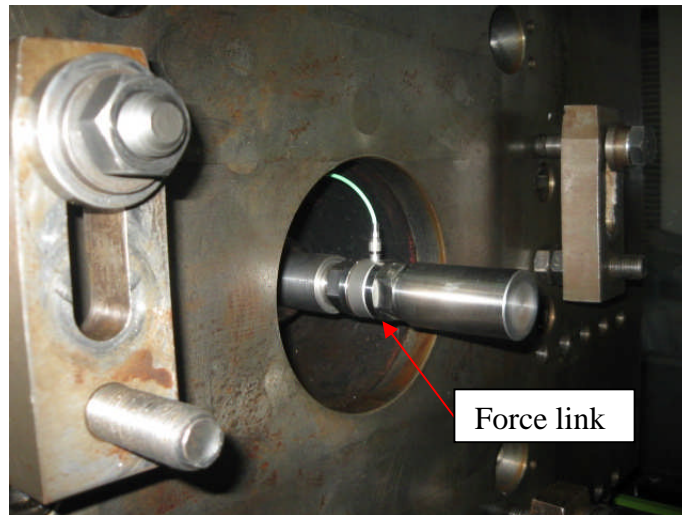


Figure 3.27: Kistler's link position

3.6.5 Experimental Design

3.6.5.1 Taguchi Design of Experiment

Taguchi techniques were developed by Taguchi and Konishi (Taguchi G. and Konishi S., 1987); these techniques have been utilized widely in engineering analysis to optimize the performance characteristics within the combination of design parameters. Taguchi design is also power tool for the design of high quality systems. It introduces an integrated approach that is simple and efficient to find the best range of designs for quality, performance, and computational cost (Taguchi G., 1990).

In Taguchi design, three-stages such as system design, parameter design, and tolerance design are employed (Hasan Oktem et al., 2006). System design consists of the usage of scientific and engineering information required for producing a part. Tolerance design is employed to determine and to analyse tolerances about the optimum combinations suggested by parameter design. Parameter design is used to obtain the optimum levels of process parameters for developing the quality

characteristics and to determine the product parameter values depending optimum process parameter values (Wu Y and Wu A, 2000).

In this study, orthogonal array experiment of L_{81} and L_9 were created to find the optimum levels of process parameters and to determine the ejection force for part exploiting the S/N ratio and ANOVA. Based on orthogonal arrays, the number of experiments which may cause to increase the time and cost can be reduced by using Taguchi technique. It employs a special design of orthogonal arrays to learn the whole parameters space with a small number of experiments only as discussed in Section 3.6.5.2.

Data analysis can be done once the designs of the experiment works are completed. To design the experiment is to develop a scheme or layout of the different conditions to be studied (Ranjit K. Roy, 1995). Set of controlled parameters and the levels of experiment need to be determined before running the experiment. The Taguchi method comprises of two important areas which are a set of orthogonal array for design of experiments purposes, and a standard method for analysis of the result. The Taguchi experiments have put two objectives in order to satisfy the analysis of data that will give a minimal error (error margin < 10%) after the confirmation test has been done. First, the number of trials must be determined. Second, the condition for each trial must be specified. Both the number and conditions of each trial can be transformed by using the orthogonal arrays.

Taguchi offers the use of the S/N ratio to identify the quality characteristics applied for engineering design problems. The S/ N ratio characteristics can be

divided into three steps: the smaller the better, the nominal the best, and the larger the better, signed type (Yong WH and Tang YS, 1998). In this study, the smaller the better quality characteristic is chosen to determine the ejection force for the resins used.

An analysis of variance (ANOVA) can be utilized to present the influence of process parameters on ejection force. In this way, the optimum levels of process parameters can be predicted. The details of the S/N ratio and ANOVA analyses are discussed in the Section 5.3.2.

3.6.5.2 Orthogonal Arrays (OA)

The foundation of designing an experiment using Taguchi methodology is orthogonal arrays (Peace, 1993). The orthogonal arrays provide efficient, meaningful and verifiable conclusion based on the design objectives. In this study, the selection of experimental design is the paramount step before setting up the procedure for the experimental work. While determining the values of the process parameters, the optimal values recommended by MoldFlow material library are considered. Three-levels and six parameters are considered while conducting the experimental work.

The parameters that were involved in this study are the surface roughnesses insert 1, surface roughnesses insert 2, injection pressure, melt temperature, packing pressure and cooling time as shown in table 3 below. With 2 degree of freedom

(DOF) for interactions parameter, L_{81} 's Taguchi orthogonal array (Three-level OA) is the most suitable to be used for this design of experiment. L_{81} means that 81 runs will be conducted with 50 replications (shot) at each run in order to guarantee statistical accuracy. Table 3.8, table 3.9 and table 3.10 show Taguchi's orthogonal array for HIPS, ABS and PA6 respectively, which demonstrate the quality characteristic and allocation level of each parameter.

Table 3.8: The parameter for three levels of selected factors for HIPS

Factors	Level 1	Level 2	Level 3
Core 1, A (μm)	0.01	1.80	3.21
Core 2, B (μm)	0.01	1.80	3.21
Melt temperature, C ($^{\circ}\text{C}$)	195	200	220
Injection pressure, D (MPa)	69	67	55
Packing pressure, E (MPa)	59	56	45
Cooling time, F (s)	16	16	17

Table 3.9: The parameter for three levels of selected factors for ABS

Factors	Level 1	Level 2	Level 3
Core 1, A (μm)	0.01	1.80	3.21
Core 2, B (μm)	0.01	1.80	3.21
Melt temperature, C ($^{\circ}\text{C}$)	200	210	240
Injection pressure, D (MPa)	77	69	50
Packing pressure, E (MPa)	65	56	41
Cooling time, F (s)	17	17	18

Table 3.10: The parameter for three levels of selected factors for PA6

Factors	Level 1	Level 2	Level 3
Core 1, A (μm)	0.01	1.80	3.21
Core 2, B (μm)	0.01	1.80	3.21
Melt temperature, C ($^{\circ}\text{C}$)	250	265	300
Injection pressure, D (MPa)	57	42	32
Packing pressure, E (MPa)	46	35	26
Cooling time, F (s)	17	18	19

3.6.5.3 Order of running the experiments

Whenever possible, the trial condition should be run randomly to avoid the influence of experiment setup. Basically, there are two types of order of running the experiments which include 'repetition' and 'replication'. Based on the Taguchi's method DOE, an $L_{81} (3^{40})$ orthogonal arrays table with 81 rows (corresponding to the number of experiments) were selected for the experiment. For six control factors of three-levels each have been assigned to the columns of standard L_{81} Taguchi array (column no. are 1, 2, 5, 14, 23 and 32) were involved, therefore the remaining columns in the L_{81} orthogonal array were kept unused.

Table 3.11, 3.12 and 3.13 will be used for recording the ejection force data for further analysis as discussed in Chapter 5.

Table 3.11: L₈₁ Taguchi orthogonal array for the experiment of HIPS resin

Expt. No.	Core 1 (μm)	Core 2 (μm)	Melt Temp. ($^{\circ}\text{C}$)	Injection Pressure (MPa)	Packing Pressure (MPa)	Cooling Time (s)	Ejection Force (N)
1	0.01	0.01	195	69	59	16	
2	0.01	0.01	195	67	56	16	
3	0.01	0.01	195	55	45	17	
4	0.01	0.01	200	69	56	17	
5	0.01	0.01	200	67	45	16	
6	0.01	0.01	200	55	59	16	
7	0.01	0.01	220	69	45	16	
8	0.01	0.01	220	67	59	17	
9	0.01	0.01	220	55	56	16	
10	0.01	1.8	195	69	59	16	
11	0.01	1.8	195	67	56	16	
12	0.01	1.8	195	55	45	17	
13	0.01	1.8	200	69	56	17	
14	0.01	1.8	200	67	45	16	
15	0.01	1.8	200	55	59	16	
16	0.01	1.8	220	69	45	16	
17	0.01	1.8	220	67	59	17	
18	0.01	1.8	220	55	56	16	
19	0.01	3.21	195	69	59	16	
20	0.01	3.21	195	67	56	16	
21	0.01	3.21	195	55	45	17	
22	0.01	3.21	200	69	56	17	
23	0.01	3.21	200	67	45	16	
24	0.01	3.21	200	55	59	16	
25	0.01	3.21	220	69	45	16	
26	0.01	3.21	220	67	59	17	
27	0.01	3.21	220	55	56	16	
28	1.8	0.01	195	69	59	16	
29	1.8	0.01	195	67	56	16	
30	1.8	0.01	195	55	45	17	
31	1.8	0.01	200	69	56	17	
32	1.8	0.01	200	67	45	16	
33	1.8	0.01	200	55	59	16	
34	1.8	0.01	220	69	45	16	
35	1.8	0.01	220	67	59	17	
36	1.8	0.01	220	55	56	16	

Table 3.11: Continued

Expt. No.	Core 1 (μm)	Core 2 (μm)	Melt Temp. ($^{\circ}\text{C}$)	Injection Pressure (Mpa)	Packing Pressure (MPa)	Cooling Time (s)	Ejection Force (N)
37	1.8	1.8	195	69	59	16	
38	1.8	1.8	195	67	56	16	
39	1.8	1.8	195	55	45	17	
40	1.8	1.8	200	69	56	17	
41	1.8	1.8	200	67	45	16	
42	1.8	1.8	200	55	59	16	
43	1.8	1.8	220	69	45	16	
44	1.8	1.8	220	67	59	17	
45	1.8	1.8	220	55	56	16	
46	1.8	3.21	195	69	59	16	
47	1.8	3.21	195	67	56	16	
48	1.8	3.21	195	55	45	17	
49	1.8	3.21	200	69	56	17	
50	1.8	3.21	200	67	45	16	
51	1.8	3.21	200	55	59	16	
52	1.8	3.21	220	69	45	16	
53	1.8	3.21	220	67	59	17	
54	1.8	3.21	220	55	56	16	
55	3.21	0.01	195	69	59	16	
56	3.21	0.01	195	67	56	16	
57	3.21	0.01	195	55	45	17	
58	3.21	0.01	200	69	56	17	
59	3.21	0.01	200	67	45	16	
60	3.21	0.01	200	55	59	16	
61	3.21	0.01	220	69	45	16	
62	3.21	0.01	220	67	59	17	
63	3.21	0.01	220	55	56	16	
64	3.21	1.8	195	69	59	16	
65	3.21	1.8	195	67	56	16	
66	3.21	1.8	195	55	45	17	
67	3.21	1.8	200	69	56	17	
68	3.21	1.8	200	67	45	16	
69	3.21	1.8	200	55	59	16	
70	3.21	1.8	220	69	45	16	
71	3.21	1.8	220	67	59	17	
72	3.21	1.8	220	55	56	16	
73	3.21	3.21	195	69	59	16	

Table 3.11: Continued

Expt. No.	Core 1 (μm)	Core 2 (μm)	Melt Temp. (°C)	Injection Pressure (Mpa)	Packing Pressure (MPa)	Cooling Time (s)	Ejection Force (N)
74	3.21	3.21	195	67	56	16	
75	3.21	3.21	195	55	45	17	
76	3.21	3.21	200	69	56	17	
77	3.21	3.21	200	67	45	16	
78	3.21	3.21	200	55	59	16	
79	3.21	3.21	220	69	45	16	
80	3.21	3.21	220	67	59	17	
81	3.21	3.21	220	55	56	16	

Table 3.12: L₈₁ Taguchi orthogonal array for the experiment of ABS resin

Expt. No.	Core 1 (μm)	Core 2 (μm)	Melt Temp. (°C)	Injection Pressure (Mpa)	Packing Pressure (MPa)	Cooling Time (s)	Ejection Force (N)
1	0.01	0.01	200	77	65	17	
2	0.01	0.01	200	69	56	17	
3	0.01	0.01	200	50	41	18	
4	0.01	0.01	210	77	56	18	
5	0.01	0.01	210	69	41	17	
6	0.01	0.01	210	50	65	17	
7	0.01	0.01	240	77	41	17	
8	0.01	0.01	240	69	65	18	
9	0.01	0.01	240	50	56	17	
10	0.01	1.8	200	77	65	17	
11	0.01	1.8	200	69	56	17	
12	0.01	1.8	200	50	41	18	
13	0.01	1.8	210	77	56	18	
14	0.01	1.8	210	69	41	17	
15	0.01	1.8	210	50	65	17	
16	0.01	1.8	240	77	41	17	
17	0.01	1.8	240	69	65	18	
18	0.01	1.8	240	50	56	17	
19	0.01	3.21	200	77	65	17	
20	0.01	3.21	200	69	56	17	
21	0.01	3.21	200	50	41	18	
22	0.01	3.21	210	77	56	18	

Table 3.12: Continued

Expt. No.	Core 1 (μm)	Core 2 (μm)	Melt Temp. ($^{\circ}\text{C}$)	Injection Pressure (Mpa)	Packing Pressure (MPa)	Cooling Time (s)	Ejection Force (N)
23	0.01	3.21	210	69	41	17	
24	0.01	3.21	210	50	65	17	
25	0.01	3.21	240	77	41	17	
26	0.01	3.21	240	69	65	18	
27	0.01	3.21	240	50	56	17	
28	1.8	0.01	200	77	65	17	
29	1.8	0.01	200	69	56	17	
30	1.8	0.01	200	50	41	18	
31	1.8	0.01	210	77	56	18	
32	1.8	0.01	210	69	41	17	
33	1.8	0.01	210	50	65	17	
34	1.8	0.01	240	77	41	17	
35	1.8	0.01	240	69	65	18	
36	1.8	0.01	240	50	56	17	
37	1.8	1.8	200	77	65	17	
38	1.8	1.8	200	69	56	17	
39	1.8	1.8	200	50	41	18	
40	1.8	1.8	210	77	56	18	
41	1.8	1.8	210	69	41	17	
42	1.8	1.8	210	50	65	17	
43	1.8	1.8	240	77	41	17	
44	1.8	1.8	240	69	65	18	
45	1.8	1.8	240	50	56	17	
46	1.8	3.21	200	77	65	17	
47	1.8	3.21	200	69	56	17	
48	1.8	3.21	200	50	41	18	
49	1.8	3.21	210	77	56	18	
50	1.8	3.21	210	69	41	17	
51	1.8	3.21	210	50	65	17	
52	1.8	3.21	240	77	41	17	
53	1.8	3.21	240	69	65	18	
54	1.8	3.21	240	50	56	17	
55	3.21	0.01	200	77	65	17	
56	3.21	0.01	200	69	56	17	
57	3.21	0.01	200	50	41	18	
58	3.21	0.01	210	77	56	18	
59	3.21	0.01	210	69	41	17	

Table 3.12: Continued

Expt. No.	Core 1 (μm)	Core 2 (μm)	Melt Temp. ($^{\circ}\text{C}$)	Injection Pressure (Mpa)	Packing Pressure (MPa)	Cooling Time (s)	Ejection Force (N)
60	3.21	0.01	210	50	65	17	
61	3.21	0.01	240	77	41	17	
62	3.21	0.01	240	69	65	18	
63	3.21	0.01	240	50	56	17	
64	3.21	1.8	200	77	65	17	
65	3.21	1.8	200	69	56	17	
66	3.21	1.8	200	50	41	18	
67	3.21	1.8	210	77	56	18	
68	3.21	1.8	210	69	41	17	
69	3.21	1.8	210	50	65	17	
70	3.21	1.8	240	77	41	17	
71	3.21	1.8	240	69	65	18	
72	3.21	1.8	240	50	56	17	
73	3.21	3.21	200	77	65	17	
74	3.21	3.21	200	69	56	17	
75	3.21	3.21	200	50	41	18	
76	3.21	3.21	210	77	56	18	
77	3.21	3.21	210	69	41	17	
78	3.21	3.21	210	50	65	17	
79	3.21	3.21	240	77	41	17	
80	3.21	3.21	240	69	65	18	
81	3.21	3.21	240	50	56	17	

Table 3.13: L_{81} Taguchi orthogonal array for the experiment of PA6 resin

Expt. No.	Core 1 (μm)	Core 2 (μm)	Melt Temp. ($^{\circ}\text{C}$)	Injection Pressure (Mpa)	Packing Pressure (MPa)	Cooling Time (s)	Ejection Force (N)
1	0.01	0.01	250	57	46	17	
2	0.01	0.01	250	42	35	18	
3	0.01	0.01	250	32	26	19	
4	0.01	0.01	265	57	35	19	
5	0.01	0.01	265	42	26	17	
6	0.01	0.01	265	32	46	18	
7	0.01	0.01	300	57	26	18	

Table 3.13: Continued

Expt. No.	Core 1 (μm)	Core 2 (μm)	Melt Temp. ($^{\circ}\text{C}$)	Injection Pressure (Mpa)	Packing Pressure (MPa)	Cooling Time (s)	Ejection Force (N)
8	0.01	0.01	300	42	46	19	
9	0.01	0.01	300	32	35	17	
10	0.01	1.8	250	57	46	17	
11	0.01	1.8	250	42	35	18	
12	0.01	1.8	250	32	26	19	
13	0.01	1.8	265	57	35	19	
14	0.01	1.8	265	42	26	17	
15	0.01	1.8	265	32	46	18	
16	0.01	1.8	300	57	26	18	
17	0.01	1.8	300	42	46	19	
18	0.01	1.8	300	32	35	17	
19	0.01	3.21	250	57	46	17	
20	0.01	3.21	250	42	35	18	
21	0.01	3.21	250	32	26	19	
22	0.01	3.21	265	57	35	19	
23	0.01	3.21	265	42	26	17	
24	0.01	3.21	265	32	46	18	
25	0.01	3.21	300	57	26	18	
26	0.01	3.21	300	42	46	19	
27	0.01	3.21	300	32	35	17	
28	1.8	0.01	250	57	46	17	
29	1.8	0.01	250	42	35	18	
30	1.8	0.01	250	32	26	19	
31	1.8	0.01	265	57	35	19	
32	1.8	0.01	265	42	26	17	
33	1.8	0.01	265	32	46	18	
34	1.8	0.01	300	57	26	18	
35	1.8	0.01	300	42	46	19	
36	1.8	0.01	300	32	35	17	
37	1.8	1.8	250	57	46	17	
38	1.8	1.8	250	42	35	18	
39	1.8	1.8	250	32	26	19	
40	1.8	1.8	265	57	35	19	
41	1.8	1.8	265	42	26	17	
42	1.8	1.8	265	32	46	18	
43	1.8	1.8	300	57	26	18	
44	1.8	1.8	300	42	46	19	

Table 3.13: Continued

Expt. No.	Core 1 (μm)	Core 2 (μm)	Melt Temp. ($^{\circ}\text{C}$)	Injection Pressure (Mpa)	Packing Pressure (MPa)	Cooling Time (s)	Ejection Force (N)
45	1.8	1.8	300	32	35	17	
46	1.8	3.21	250	57	46	17	
47	1.8	3.21	250	42	35	18	
48	1.8	3.21	250	32	26	19	
49	1.8	3.21	265	57	35	19	
50	1.8	3.21	265	42	26	17	
51	1.8	3.21	265	32	46	18	
52	1.8	3.21	300	57	26	18	
53	1.8	3.21	300	42	46	19	
54	1.8	3.21	300	32	35	17	
55	3.21	0.01	250	57	46	17	
56	3.21	0.01	250	42	35	18	
57	3.21	0.01	250	32	26	19	
58	3.21	0.01	265	57	35	19	
59	3.21	0.01	265	42	26	17	
60	3.21	0.01	265	32	46	18	
61	3.21	0.01	300	57	26	18	
62	3.21	0.01	300	42	46	19	
63	3.21	0.01	300	32	35	17	
64	3.21	1.8	250	57	46	17	
65	3.21	1.8	250	42	35	18	
66	3.21	1.8	250	32	26	19	
67	3.21	1.8	265	57	35	19	
68	3.21	1.8	265	42	26	17	
69	3.21	1.8	265	32	46	18	
70	3.21	1.8	300	57	26	18	
71	3.21	1.8	300	42	46	19	
72	3.21	1.8	300	32	35	17	
73	3.21	3.21	250	57	46	17	
74	3.21	3.21	250	42	35	18	
75	3.21	3.21	250	32	26	19	
76	3.21	3.21	265	57	35	19	
77	3.21	3.21	265	42	26	17	

Table 3.13: Continued

Expt. No.	Core 1 (μm)	Core 2 (μm)	Melt Temp. ($^{\circ}\text{C}$)	Injection Pressure (Mpa)	Packing Pressure (MPa)	Cooling Time (s)	Ejection Force (N)
78	3.21	3.21	265	32	46	18	
79	3.21	3.21	300	57	26	18	
80	3.21	3.21	300	42	46	19	
81	3.21	3.21	300	32	35	17	

3.7 Summary

The methodology used in the study and experimental procedures were discussed. These procedures include instrumentation set-up and materials preparation. It also involves design and tool fabrication as a platform to run the study based on the researcher's knowledge and experience. The facilities available at TATI University College and the supports from Edinburgh Napier University were employed to enhance the study works.

CHAPTER 4

MOLDFLOW ANALYSIS

4.1 Overview

This chapter explains the simulation result by using AMI 2010-R2 software and experimental results on the ejection of moulding for HIPS, ABS and PA6 resins which will be explained in Chapter 5. The objective of using MoldFlow software is to create an analytical method in examining associated problems which may arise during filling, packing and curing during the cycle time of the moulding. It is analytical because the result from analysis will guide a solution path that will change processing parameters of the injection moulding machine depending on the problem and choice to fix the problem. The simulation results obtained from Moldflow software will be used in setting up machine parameters prior to trial on the injection moulding machine. For this research, melting temperature at a different level for HIPS, ABS and PA6 were put into software specially designed for the analysis. Whilst the software suggested on the injection pressure, packing pressure and cooling time are the main parameters used when conducting the experiment for this research. Apart from that, several counteracts can be considered to solve any negative problem arousals while conducting the analysis such as air trap or weld

mark problem. Appendix G.1, G.2, and G.3 showed the analysis log result for different type of resin.

The usage of computer simulation software package in dealing with the current study enables the prediction of initial result for filling and pressure distribution prior to the experimental works. By utilising filling analysis the processing characteristics of an injection mould can be investigated and optimized at design stage. The benefits are improvements in part quality of weld lines, eliminating gas traps, balancing pressure drops and reducing stress levels.

4.2 Moldflow Analysis Result

Manufacturers have been doing injection moulding plastic parts since long before simulation technology arrived on scene. It was apparent from early days that process variations affected part quality, because of the complex interplay among the process physics, material properties and geometric complexity of the part and mould, successful injection moulding was considered almost an art form. Experience gained through trial and error was the only means of dealing with problems encountered in the process (Swan, 2004). In the simulation environment, the optimal filling time and pressure distribution were combined with other processing criteria from Moldflow in order to determine an optimal, feasible fill time and pressure generated.

4.2.1 Gate Location Analysis Result

The analysis has been done using AMI 2010-R2 software in identifying the best gate location. Placing a gate correctly is the most challenging and critical factor whilst filling the resin in cavity so to obtain good and high quality product of moulding. The analysis result, the gate location on the moulding may be preset or appeared with two or three choices, and then the optimum gate locations may need to be examined by running the filling analysis at different best gate locations. The ability of the software in predicting gate location will help designers at the earliest before placing it into the machining works.

As shown in Figure 4.1, the gate analysis indicates that the best injection location is in the centre of the model (blue area) and the least good injection location (red area) is slightly located below the centre, where the thickness of model is less compared to the top of the model. The injection location was placed on the top of the model to facilitate the ejection of stripper plate in ejecting the moulding from the core while measuring the ejection force.

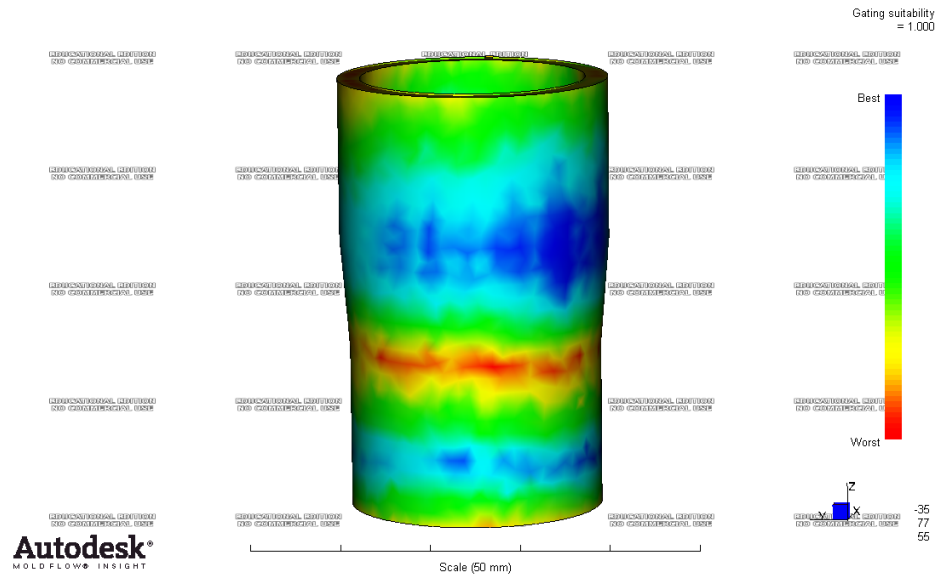


Figure 4.1: Suggested gating suitability for the moulding

4.2.2 Mould Filling Analysis Result

4.2.2.1 Flow Analysis

A comparison study between different types of polymer resin was made according to the process conditions in AMI 2010-R2 which was shown in Table 4.1. All of these parameters were set in AMI 2010-R2 before the analysis was carried out. Different melting temperatures were set for the materials and the packing time was set to be 20 s. The software was capable to predict the fill pattern, fill time, air trap, weld line, temperature and pressure distribution for the moulding. The resin flow started from the thicker section of the part which is 2 mm through rectangular gate (1 mm x 1 mm x 1 mm) and the full round runner system with Ø5 mm.

Table 4.1: Process condition for HIPS, PA6 and ABS

Resins	Melt temperature (°C)	Packing/holding time (s)
HIPS	195	20
	200	
	220	
ABS	200	20
	210	
	240	
PA6	250	20
	265	
	300	

4.2.2.2 Fill Time Result

The fill time results show the progression of the resin entrance inside the cavity. One of the reason in selecting gate location is to ensure the uniformed flow paths in the cavity fill (Imihezri S. S. S. et al., 2004) and filling completed rapidly as soon as possible without any problem. Figure 4.2 shows the fill time results for HIPS, ABS and PA6. The fill time for PA6 is 0.9690 s which indicates quicker fill time compared to HIPS and ABS, 1.889 s and 1.6360 s respectively. This is useful to estimate the short-shot, weld line, air entrapment, hesitation and over packing. The filling flow phase was illustrated through colour coded contour that ranged from blue to red as shown in Figure 4.2. The injection location influenced the melt resin flow which contributed to weld line and air entrapment of the moulding. The overall flow analysis results were tabulated in Table 4.2 based on selected melting temperature.

4.2.2.3 Pressure Result

The maximum pressure that should be used is under the limit of the moulding machine tonnage capacity. The pressure distribution should be balanced much like the fill time with little over packing and uniformed pressure distribution during packing. The pressure and fill time plots should look very similar for there is little or no underflow in the part which short-shot or flashing problem can be avoided. The 3D mesh of the part model enables the analysis of pressure distribution through the flow path inside the mould. Pressure at the end of filling represents pressure distribution. The pressure results indicated that PA6 requires low injection pressure of 43.24 MPa compared to ABS and HIPS that require 94.96 MPa and 70.15 MPa respectively as shown in Figure 4.3. The magnitude of the pressure depends on the resistance of the polymer in the mould and a higher injection pressure was an indicative of an occurrence of higher shear rate and shear stress levels (Moldflow Plastic Insight Manual 6.0, 2006).

Table 4.2: Flow analysis results

Result	HIPS	ABS	PA6
Melting temperature (°C)	200	210	265
Fill time (s)	1.889	1.636	0.969
Projected area (cm ²)	8.08	8.08	8.07
Volume (cm ³)	18.77	18.77	18.77
Part weight (g)	16.64	16.46	16.54
Weld line	Exist	Exist	Exist
Air bubble	Exist	Exist	Exist
Freeze time (s)	19.08	24.85	13.96
Max. Clamping force (tonne)	3.25	3.93	2.02
Volumetric shrinkage (%)	6.817	4.825	16.06
Pressure (MPa)	70.15	94.96	43.24

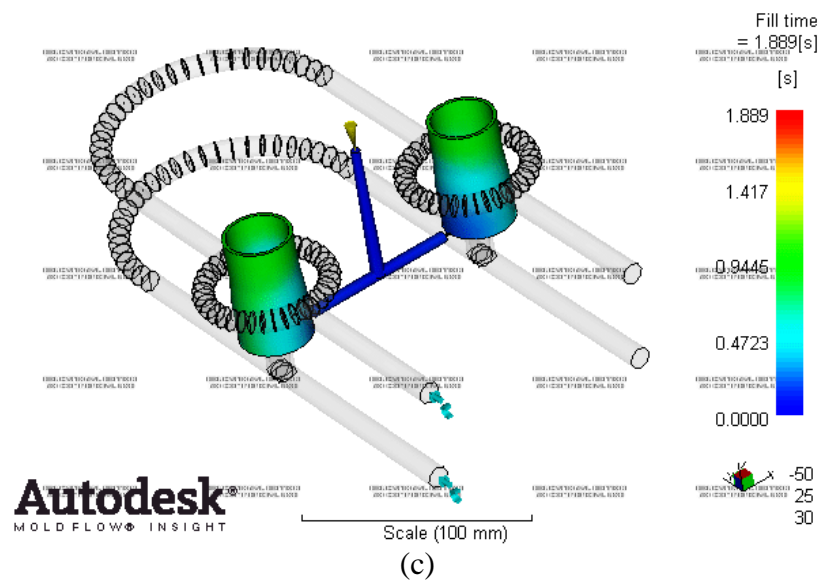
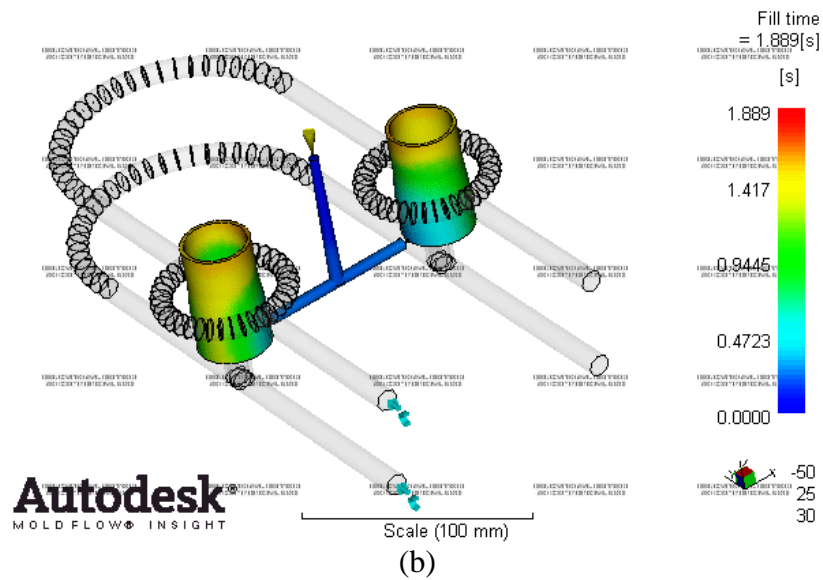
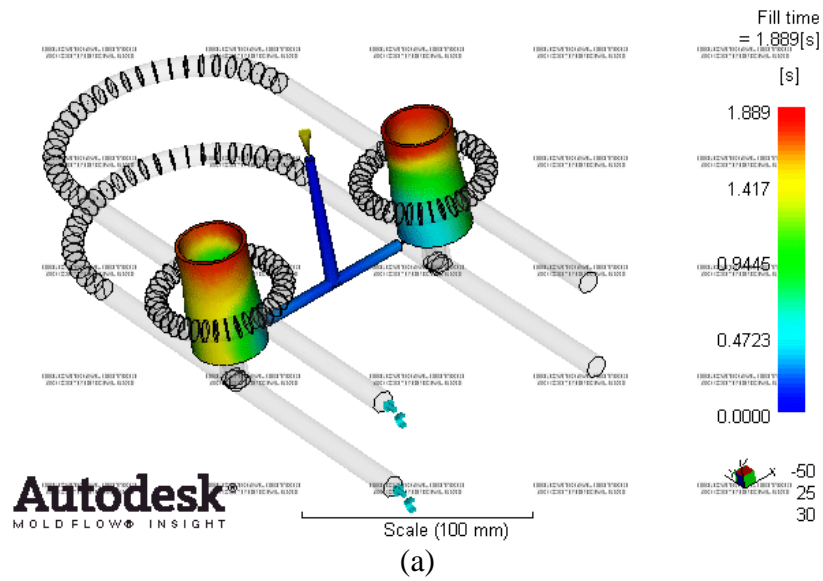


Figure 4.2: Fill time. (a) HIPS. (b) ABS. (c) PA6

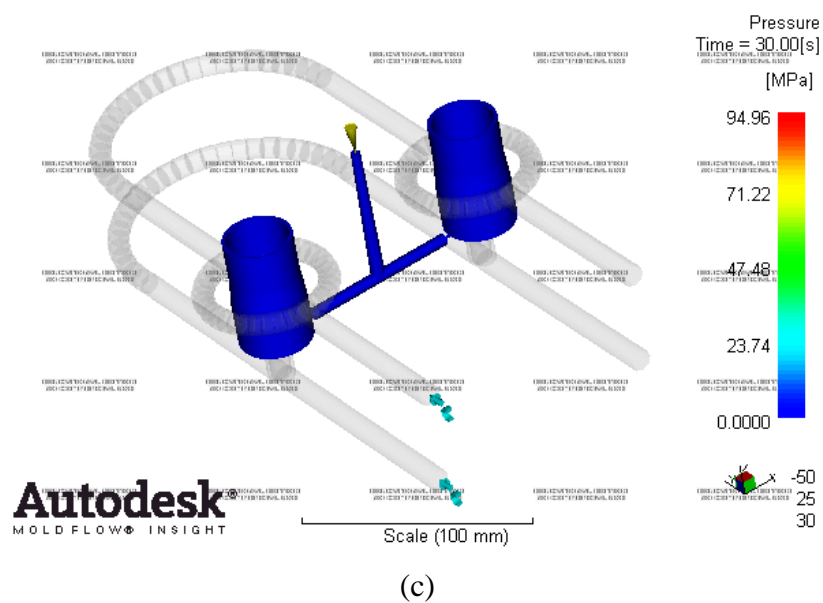
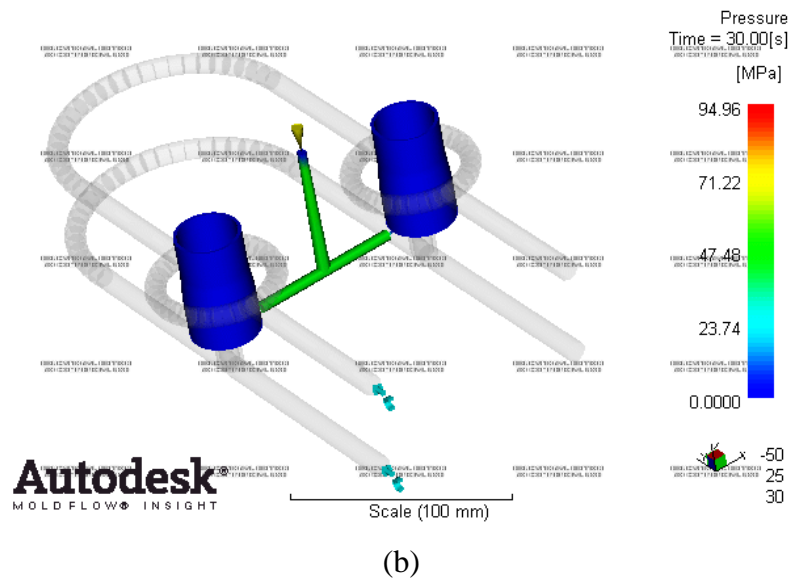
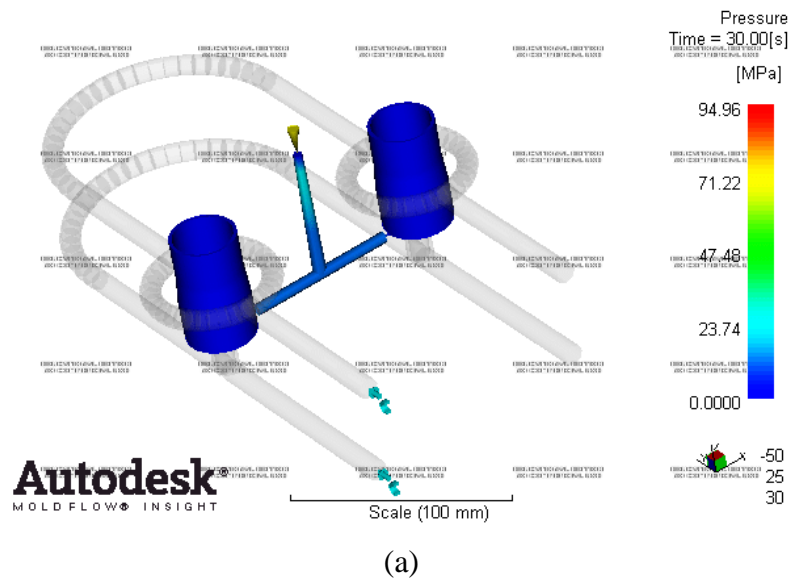


Figure 4.3: Pressure at the end of fill. (a) HIPS. (b) ABS. (c) PA6

4.2.2.4 Shear Stress at Wall Result

Shear stress at wall occurs at the frozen of molten layer interface. This is the location of the cross section where the shear stress will be the highest. The shear stress within the part should be below the material limit specified in the material database. Shear stress should be kept to minimum because shear stress can cause warp problem, blemish and low strength of the part. High injection pressure indicates an occurrence of high shear rate and shear stress level. As shown in Appendix H.1, the maximum shear stress at wall for HIPS is 2.824×10^6 l/s and ABS and PA6 are 9.859×10^6 l/s and 1.0×10^7 l/s respectively.

4.2.2.5 Air Traps Result

The result will show air traps that might be possible to develop in the part during the filling. The results revealed that all thermoplastics material showed an air entrapment at the same location (Figure 4.4(a), 4.4(b) and 4.4(c)). Air traps should be eliminated by using several approaches such as changing the wall thickness, gate locations or injection speed. Air traps indicate the presence of surface defects such as burn marks, blemishes and short-shots (Jay Shoemaker, 2006). This is due to the different polymer resins which have different viscosity. Hence, a flow channel should be provided to aid air evacuation from the cavity. The ventilation design system was discussed in Chapter 3 (Section 3.4.6).

4.2.2.6 Weld lines result

Weld line occurs when two materials flow and converged at one location, or flow front splits and comes back together as it happens around hole. Occasionally weld lines are formed at the interface between the thick and thin section. It happens when there is significant race tracking where the material in the thick section is racing around and the thin is lagging. Weld line basically will cause poor appearance and reduces the strength of the part. Figure 4.5 shows the visualisation of the weld lines that might occur.

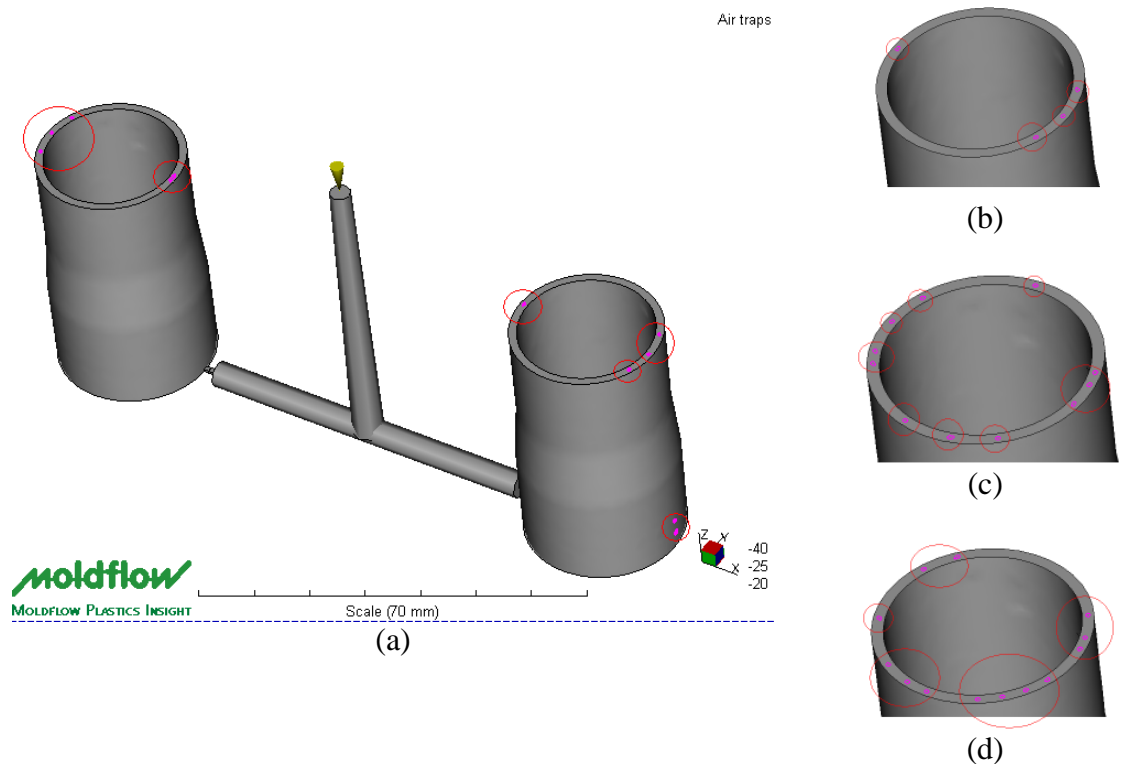


Figure 4.4: (a) Air entrapment marked with circle. (b) HIPS. (c) PA6. (d) ABS

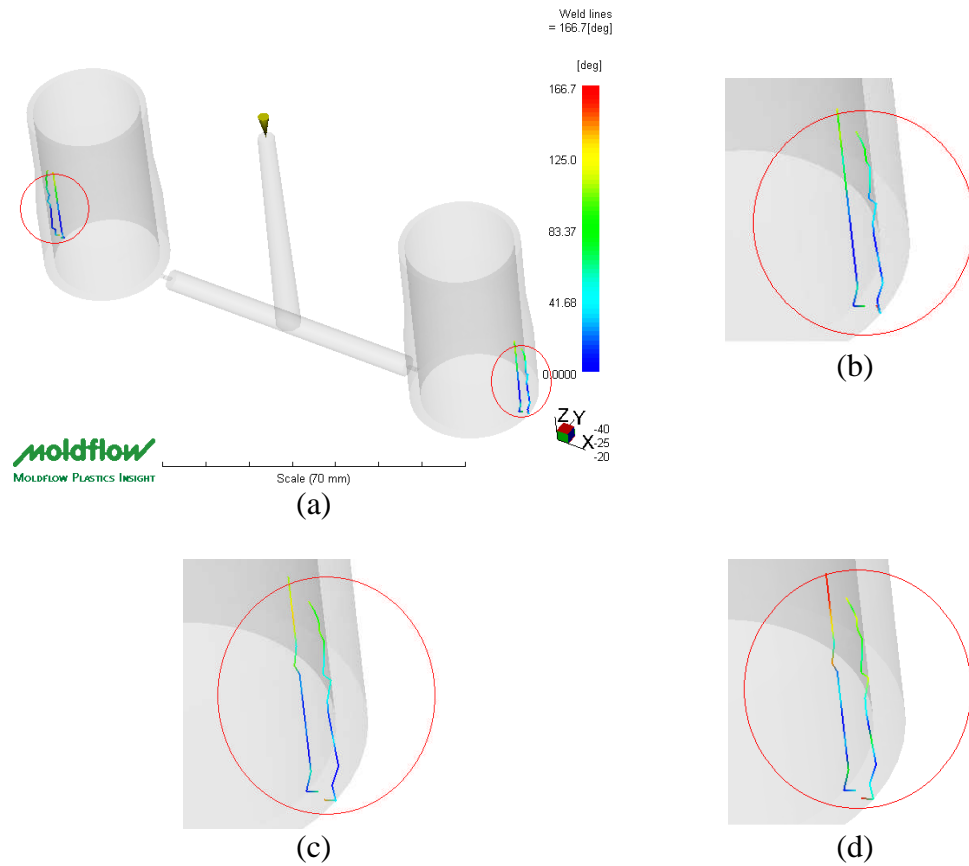


Figure 4.5: (a) Weld lines position with circle marked. (b) HIPS. (c) ABS. (d) PA6

4.2.2.7 Clamp force result

The clamp tonnage is calculated based on the cavity area at the parting line. The clamp force is calculated in each element using the projected area on the XY plane and the pressure in that element. Clamp force may become very sensitive when there is balanced of fill and pack pressure for such resin. Appendix H.2 shows the graph of clamp force and the value of maximum clamping force values are shown in Appendix H.2. The maximum clamping force for HIPS is 3.2534 tonnes and ABS and PA6 are 3.9275 tonnes and 2.0226 tonnes respectively.

4.2.2.8 Volumetric Shrinkage Result

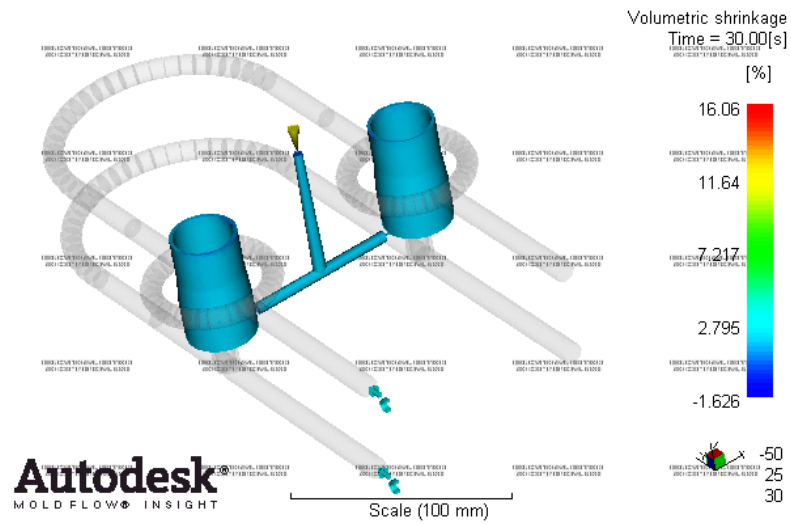
The volumetric shrinkage for such plastic resins indicates the volume reduction of the element which is shown in percentage due to packing of the part. The higher the packing pressure the lower the shrinkage. Figure 4.6 shows the volumetric shrinkage result. The maximum percentage of volumetric shrinkage was PA6 16%. Meanwhile for HIPS and ABS were 7 % and 5 % respectively.

4.2.2.9 Polymer Fill region

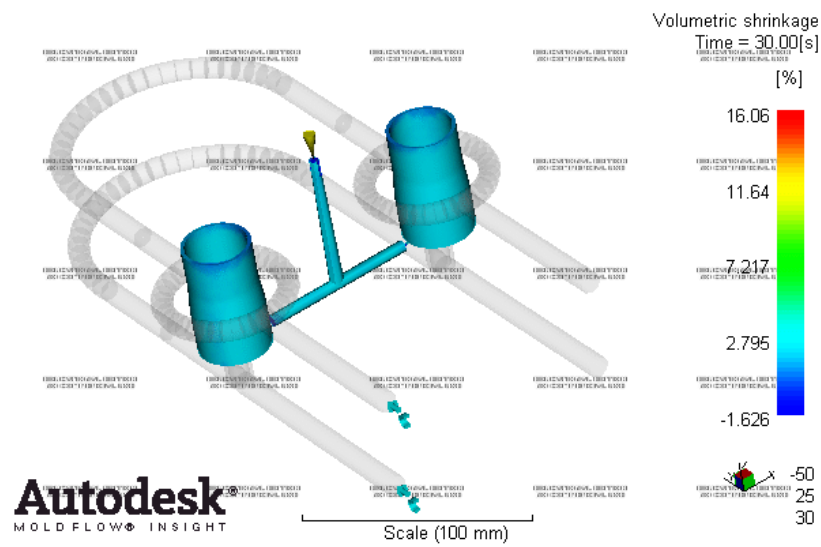
This result will predict the probability of the molten plastic resin which enters inside the cavity. From Figure 4.7, all resins indicate green colour which means high probability of the molten plastic resin to enter inside the cavity. The quality result is based on the injection pressure and melting temperature setting. The time taken for HIPS to fill the cavity is 1.889 s. Meanwhile for ABS and PA6 were 1.636 s and 0.9690 s respectively.

4.2.2.10 Time to Freeze Result

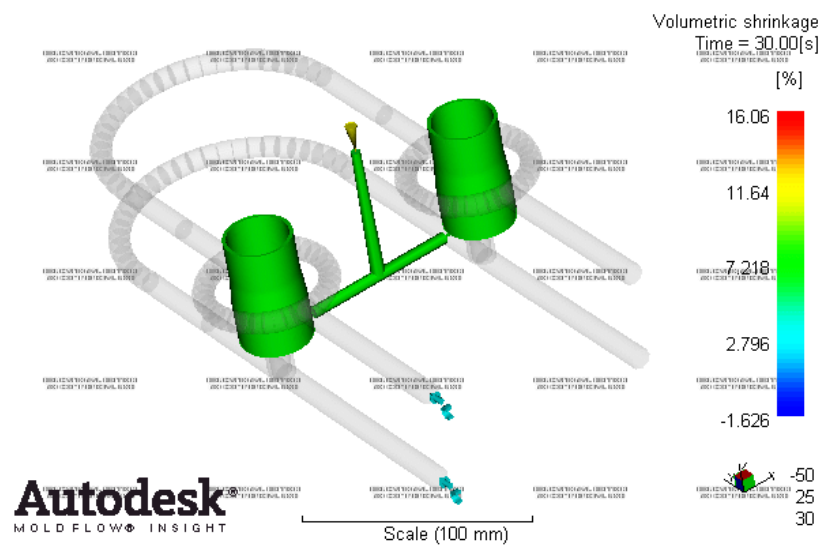
Time to freeze results indicate the time required for resin polymer to reach the solid state. This will affect the cycle time for the part. Parallel freezing time and fast cooling are needed as these affect the product properties and cycle time. As shown in Figures H.3.1, H.3.2 and H.3.3 (Appendix H.3), the time to freeze for HIPS is 19.08 s while for ABS and PA6 recorded 24.85 s and 13.96 s respectively.



(a)



(b)



(c)

Figure 4.6: Volumetric shrinkage (a) HIPS. (b) ABS. (c) PA6

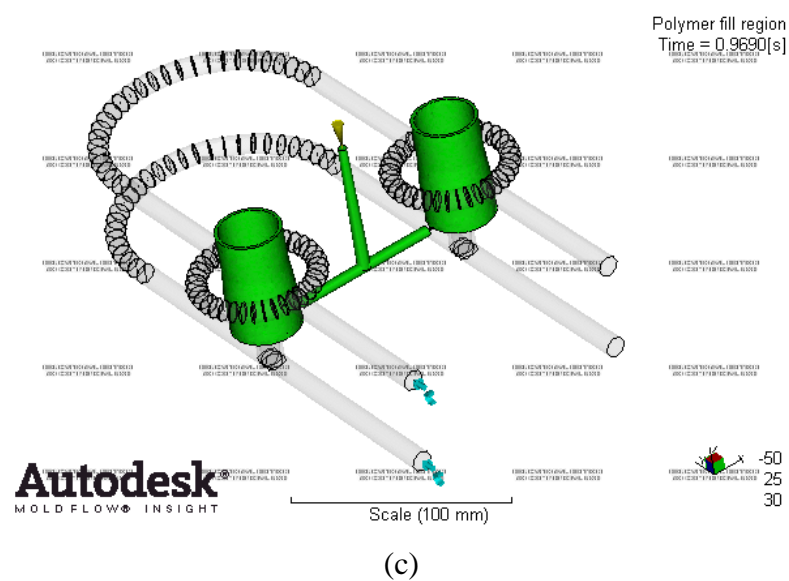
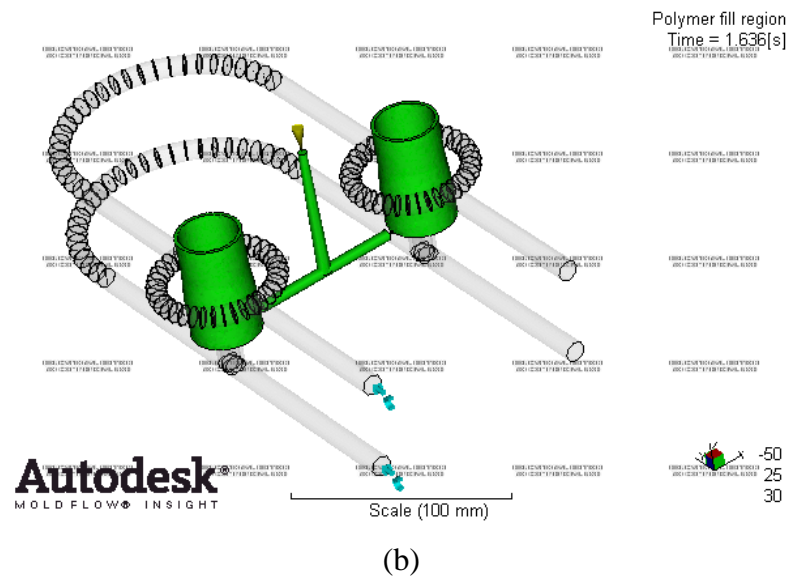
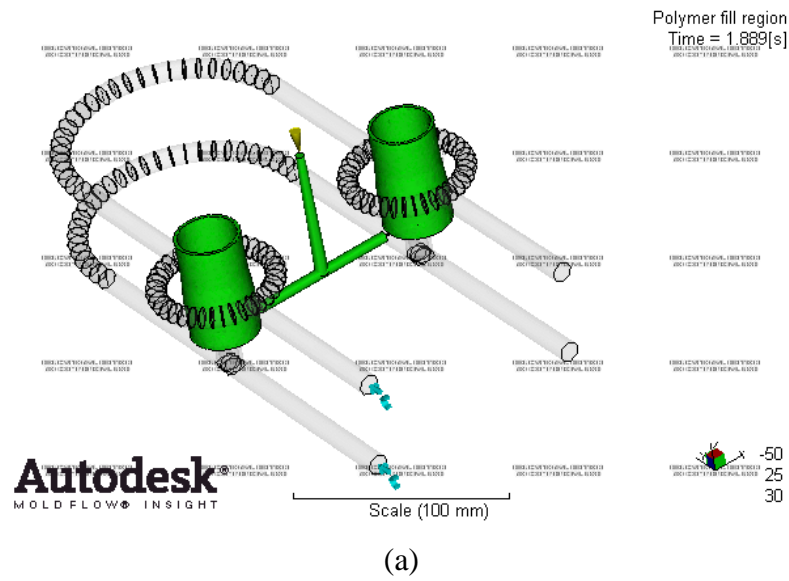


Figure 4.7: Polymer Fill region (a) HIPS. (b) ABS. (c) PA6

4.3 Conclusion

This analysis is to establish process condition for injection moulding machine to be used in experimental work. The simulation work was performed on the MoldFlow according to the actual tool condition such as cooling channel layout and the feeding system used. The actual materials used are obtained from MoldFlow's library system which are the same materials used for this experiment. By doing the analysis, MoldFlow has given the processing parameter (injection pressure, packing pressure, cooling time, etc.) for the setting purposes on the injection moulding. For this research, three levels of melting temperature for each material were put as parameters for analysis purpose. Then other parameters' values such as injection pressure, packing pressure and cooling time were obtained respectively from analysis log. These values were used while running the experimental work. Apart from that, problems' possibilities were highlighted as remedies for designer. In this case, weld line and air entrapment are the major issues which need to be measured thoroughly. So, the air vent and a proper cooling channel should be provided on the tool as described in Chapter 3 for this research. So, the MoldFlow software helps the designer to have access to flow analysis and their interpretations, including the simulation of cooling, to aid the successful design and manufacture of parts and tools.

4.4 Summary

This chapter explained the process of simulation work using the MoldFlow software and possibilities in problems which might occur during the process. The software enables to tell the designer on the ability of filling process for suitable area of gating first before doing any further analysis. Some of the processing parameters can be obtained automatically and can be accessed in analysis log for the software. The software can help designer in advance before the actual tool is put on the actual production by comparing ‘trial and error’ method which consumes time and cost in traditional approach.

CHAPTER 5

RESULT AND DISCUSSION

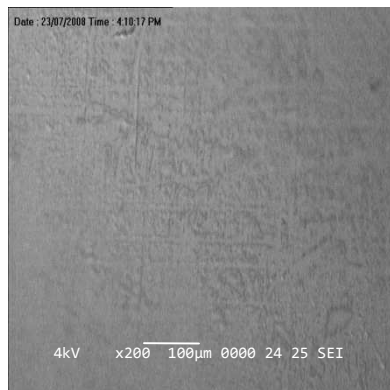
5.1 Overview

This chapter explains the experimental results on the ejection of moulding for HIPS, ABS and PA6 resins. The objective is to achieve the optimum ejection force based on the setting parameters and conditions and model building for predicting response function. The essential parameters include surface roughness of cavity inserts, injection pressure, melting temperature, packing pressure and cooling time which was discussed in Chapter 3. The control effect factor and noise factor were elaborated including ANOVA for analysis purposes. Hence, the mathematical model was developed to show the relationship between the three types of resins parallel to the surface roughness of the insert and parameters used.

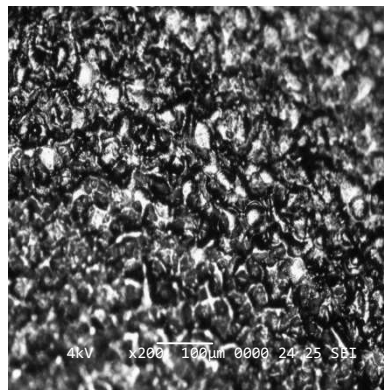
5.2 Ejection Force Experiment Results

5.2.1 Surface roughness of the core inserts

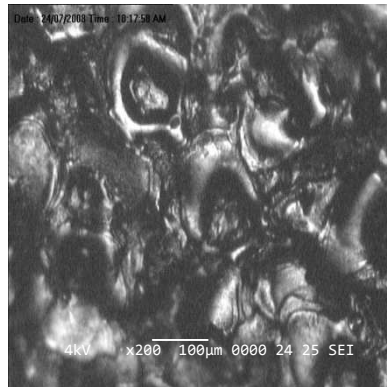
The microscopically examination of the core insert surface was observed by using the Olympus CK40M optical microscope as shown in Figure 5.1 (see 3.4.9 surface roughness measurement). Meanwhile Figure 5.2 shows the part for this experiment.



(a) 0.01 μmRa



(b) 1.80 μmRa



(c) 3.2 μmRa

Figure 5.1: Microscopic for core insert surface roughness x100 (a) Polished insert, and (b, c) Sparked insert

The value of Ra for the inserts was obtained by using surface roughness tester (SurfTest Mitutoyo SJ – 301). Appendix I.1, I.2, I.3, I.4, I.5 and I.6 show the value of Ra for the inserts used for the experiment.



Figure 5.2: Part sample of HIPS

5.2.2 Surface roughness of part

The surface of moulding was observed by using SEM as shown in Figure 5.3, objectively to investigate the possible causes of ejection force. The part samples were coated with platinum by using Auto Fine Coater, JFC-1600 model. The ejection force decreases as the combination surface roughness decreased from 0.14 μmRa and was minimum when the combinations core surface roughness was 1.65 μmRa . The ejection force then started to increase from the combination surface roughness of 1.35 μmRa , decreasing rapidly from 1.65 μmRa . The surface roughness as shown in Figure 5.5 illustrates the relation between surface of core combinations and ejection of ABS. The ejection force increases as the surface of core combination decreases from 0.05 μmRa , was minimum at 2.30 μmRa .

For moulding with surface roughness of 1.17 μmRa to 4.14 μmRa , various depth of crater mark appeared which indicates a strong relation to types of resins used with the generated ejection force. On the other hand, for moulding with surface roughness of 0.05 μmRa to 0.14 μmRa , the surface texture is quite smooth for ABS and PA6 except for HIPS. Figure 5.6(a) shows the relation between surface of core combinations and ejection force of PA6. The ejection force decreases as the moulding surface roughness decreased from 0.07 μmRa , and started to increase from 1.41 μmRa .

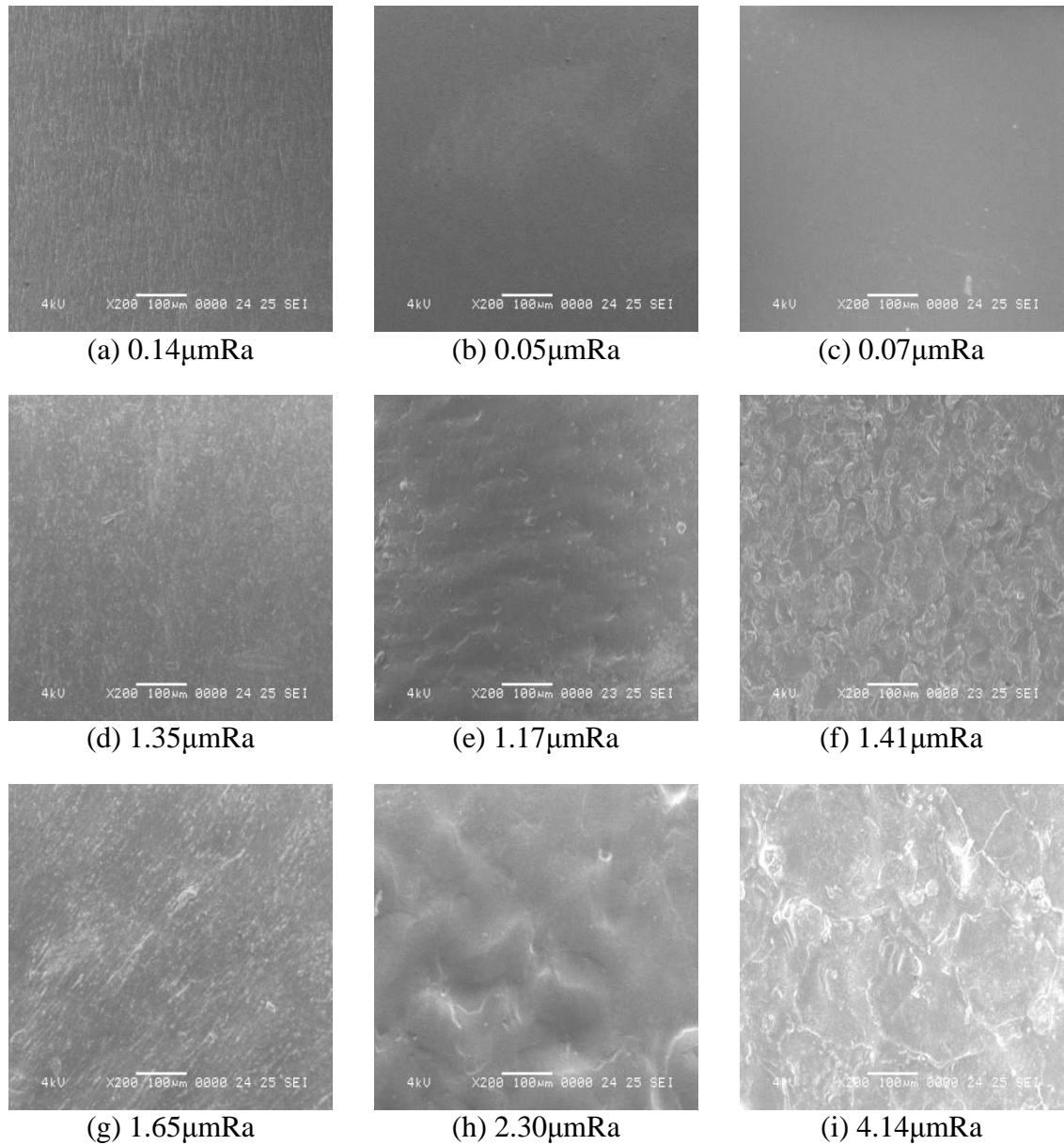


Figure 5.3: SEM image for mouldings at different levels of surface roughness for different types of thermoplastic (a) (d) (g) HIPS. (b) (e) (h) ABS. (c) (f) (i) PA6 resin

5.2.3 Mechanical bonding and van der Waal effect of the ejection force

The mechanical bonding state and van der Waal principle also have influence in studying the ejection force for surface roughness. For instance, two important aspects; shrinkage and friction influence the ejection force model. Unfortunately, due to unavailable instrument, these factors are not considered during experiment.

Shrinkage is the end product caused by thermal contraction and directional distortion. While atoms move closer in atomic vibration at a low energy level, and directional distortion results from orientation of polymer molecules during the flow and once the flow ends, their following relaxation goes back to a coiled state; this phenomenon is called thermal contraction. One condition of shrinkage can be massively predisposed by ejection temperature and hence varies for amorphous (HIPS and ABS) and semi-crystalline polymers (PA6). Semi-crystalline polymers (PA6) possess an enhanced state of shrinkage due to phase transformation of crystalline portion. Meanwhile, prior towards the subject mentioned (PA6), HIPS and PA6 contract in even more gradually. The basic idea of having friction between thermoplastic part and injection mould core does not mainly concerns on the mechanical relationship between the two surfaces; instead, it also depends on adhesive component inherent towards the properties of these materials at processing conditions. Following towards this occurrence, the mechanical component of friction usually be inclined to a simpler concept definition; that is, the high complexion of adhesion component. In addition to such matter, heat helps in increasing on the abilities of the adhesive to primarily absorb, dissolve and disperse. For polymers, the surface forces consist of van der Waals, coulombic and possibly hydrogen bonding forces. Subjectively referring to when the surface free energy of polymer increases, the adhesive force becomes greater. States such as extremely clean metal surfaces promote chemical bonding. In relation to this experimental work, ejection forces for HIPS, ABS and PA6 were all determined experimentally.

5.2.4 The effect of ejection forces on the surface roughness

Table 5.1 summarizes the ejection force on the surface combination for HIPS. Nine surface combinations denoted A to Z representing different core inserts for each combination. Each surface combination produce a different core surface measured in micrometer (μm). For each surface combination, nine experiments were performed with different processing parameters applied at each experiment. The parameters were summarized in Table 5.2.

Table 5.1: Average ejection force for HIPS

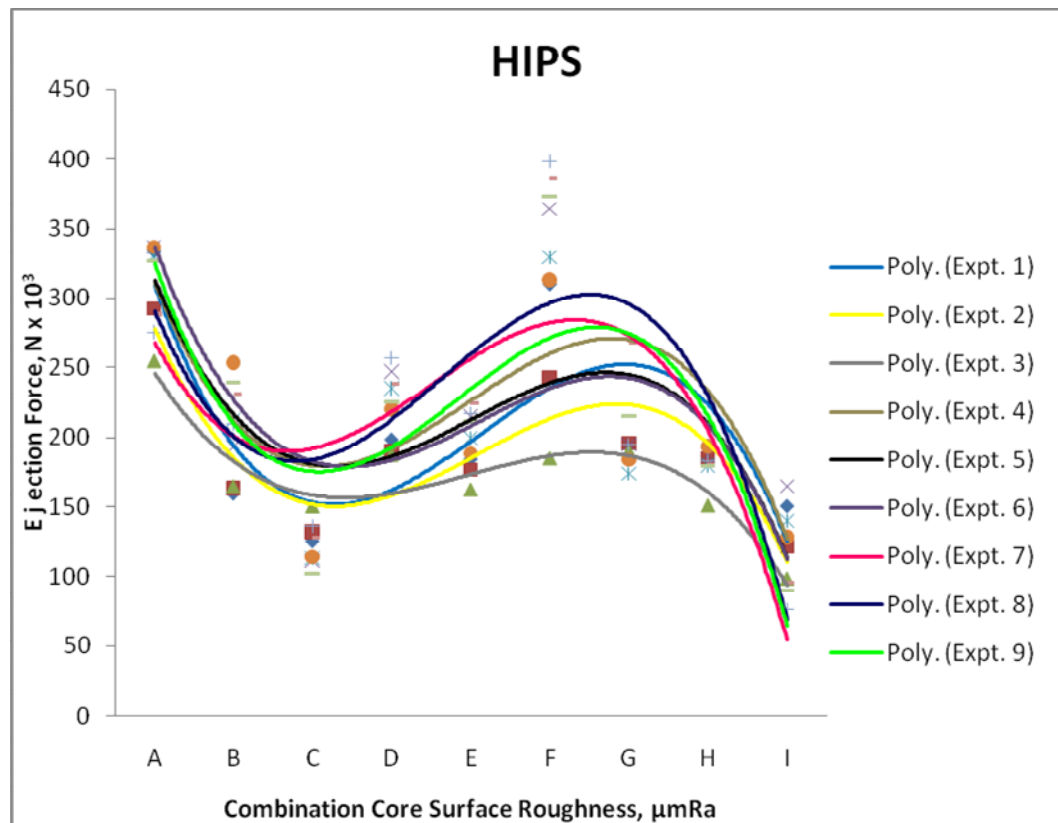
Combination Surface	Denoted Symbol	Core Surface (μm)	Ejection Force (N) $\times 10^3$								
			Expt. 1	Expt. 2	Expt. 3	Expt. 4	Expt. 5	Expt. 6	Expt. 7	Expt. 8	Expt. 9
$S1_x+S1_y$	A	0.02	334	292.1	254.8	336.4	329.8	336.8	275.5	288.2	326.6
$S1_x+S2_y$	B	1.84	158.9	163	164.7	193.1	212.4	253.4	209.9	230.6	239.2
$S1_x+S3_y$	C	3.22	124.8	131.6	150.4	111.2	113.6	113.9	136.4	128	102
$S2_x+S1_y$	D	1.84	198.3	189.5	187.7	246.6	235.1	220.1	256.8	237.9	225.4
$S2_x+S2_y$	E	3.6	184	176.5	162.4	214.4	199.6	188.3	217.3	224	211.5
$S2_x+S3_y$	F	5.01	310.3	242.6	185.1	363.8	329.3	313.3	398.1	386	373
$S3_x+S1_y$	G	3.22	195.4	195.6	190.5	194.9	174.1	184	195.2	268	214.8
$S3_x+S2_y$	H	5.01	194	184.1	150.9	186.9	180	193.4	183.2	180.3	179.4
$S3_x+S3_y$	I	6.42	150	121.3	98.6	164.3	140.1	128.1	76.9	95.8	90.4

$S1_x$, $S2_x$ and $S3_x$ represent for core insert 1 meanwhile $S1_y$, $S2_y$ and $S3_y$ represent for core insert 2

Table 5.2: The parameter setting for HIPS for the experiment

Expt. No.	Melt Temp. (°C)	Injection Pressure (MPa)	Packing Pressure (MPa)	Cooling Time (s)
1	195	69	59	16
2	195	67	56	16
3	195	55	45	17
4	200	69	56	17
5	200	67	45	16
6	200	55	59	16
7	220	69	45	16
8	220	67	59	17
9	220	55	56	16

The melting temperatures for the experiments were divided into three groups of 195°C, 200°C and 220°C. The melting temperature was selected according to the range of the recommended material's temperature. The results are summarized in Figure 5.4.

**Figure 5.4:** The combination of surface roughness and ejection force for HIPS

As seen in Figure 5.4, the graph's characteristic to all experiments possesses similarity in the graph's pattern. However, the ejection force for the three groups at different temperature shows a slightly different value. The higher the temperature the higher the ejection force and it shows that the ejection force was affected with the increment of melting temperature. However, despite any melting temperatures, each experiment abides the relationship of the ejection force and the surface roughness which the ejection force is inversely proportional with the surface roughness.

By referring to Table 5.2, it can be observed that the melting temperatures are the same for experiment 1 to 3. i.e. 195 °C. The graph also depicted a similarity in trend for point E ($S_{2x} + S_{2y}$), F ($S_{2x} + S_{3y}$), G ($S_{3x} + S_{1y}$), H ($S_{3x} + S_{2y}$) and ($S_{3x} + S_{3y}$). Following such a case, the observed phenomena for these surface roughness combinations is when the surface roughness increases, the ejection force will decrease as shown in Figure 5.4 (a). As the melting temperature increases, the ejection force also increase which can be seen clearly at the melting temperature of 200°C and 220°C. It can be concluded that, the melting temperature is influenced with the ejection force for HIPS. At the point E ($S_{2x} + S_{2y}$) onwards, the ejection forces are decreased when the surface roughness are increased.

Figure 5.5 summarizes the error of the ejection force for different combination surface with 5% error calculated. The selected error is complying with the Taguchi method.

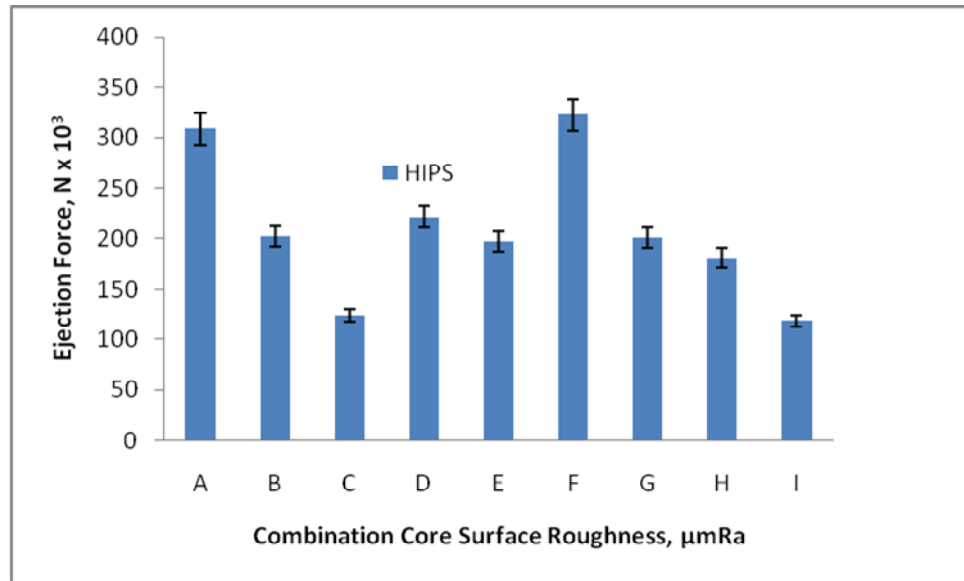


Figure 5.5: The error of the ejection force for different combination surface for HIPS

The same methods were applied to ABS with Table 5.3 and 5.4 which summarized the ejection force on the surface combination and the processing parameters.

Table 5.3: The parameter setting for ABS for the experiment

Expt. No.	Melt Temp. (°C)	Injection Pressure (MPa)	Packing Pressure (MPa)	Cooling Time (s)
1	200	77	65	17
2	200	69	56	17
3	200	50	41	18
4	210	77	56	18
5	210	69	41	17
6	210	50	65	17
7	240	77	41	17
8	240	69	65	18
9	240	50	56	17

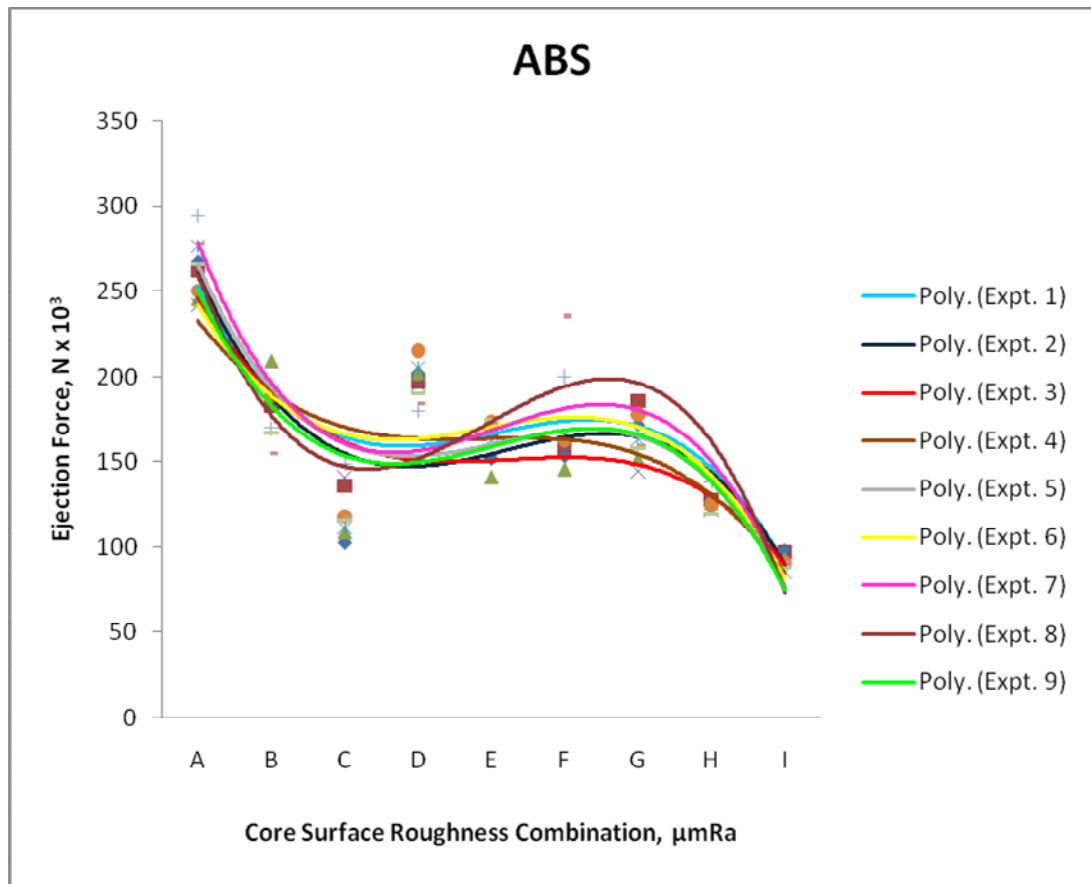
Figure 5.6 represents the relation of the ejection force and the surface combination. The characteristic for ABS is almost similar to HIPS. As seen for Experiment 3, the ejection force shows a constant value throughout the process.

Experiment 8 shows an inversely proportional of ejection force to the surface combination due to the core surface roughness value are increased at a proportionate value. For experiment 7, the trend of graph behaviour looked almost similar to experiment 8 but the value of ejection force is small. Experiment 1, 6 and 9 showed the same behaviour among them but for experiment 6, it started to increase at core surface roughness C which is lower than what can be observed from Experiment 1. These experiments (Experiment 1, 6 and 9) share the same injection pressure but different melting temperatures.

Table 5.4: Average ejection force for ABS

Combination Surface	Denoted Symbol	Core Surface (μm)	Average Ejection Force (N) x 10^3								
			Expt. 1	Expt. 2	Expt. 3	Expt. 4	Expt. 5	Expt. 6	Expt. 7	Expt. 8	Expt. 9
S1 _x +S1 _y	A	0.02	262.3	267.4	246	242	276.3	249.9	294.6	277.9	265.7
S1 _x +S2 _y	B	1.84	183.4	193.4	209.6	183.7	191.2	188.7	169.9	154.8	166.7
S1 _x +S3 _y	C	3.22	136.5	103	108.7	141.3	111.5	117.8	149.1	118.2	115.87
S2 _x +S1 _y	D	1.84	197.5	202.4	202.3	195.8	205.4	215.2	179.87	184	190.5
S2 _x +S2 _y	E	3.60	167.9	152.4	141.4	166.5	163.6	173.2	170.4	173	174.3
S2 _x +S3 _y	F	5.01	157	153.7	146	165.6	161.9	162	200.5	235.5	165
S3 _x +S1 _y	G	3.22	185.9	172	151.87	145	163.2	177.6	158.6	158.9	157.9
S3 _x +S2 _y	H	5.01	128.1	127.6	126	122.3	122.8	124.9	138.4	142	120.1
S3 _x +S3 _y	I	6.42	97.7	98.4	92.8	91.4	85.4	91	87.7	91	88.5

S1_x, S2_x and S3_x represent for core insert 1 meanwhile S1_y, S2_y and S3_y represent for core insert



5.6: The combination of surface roughness and ejection force for ABS

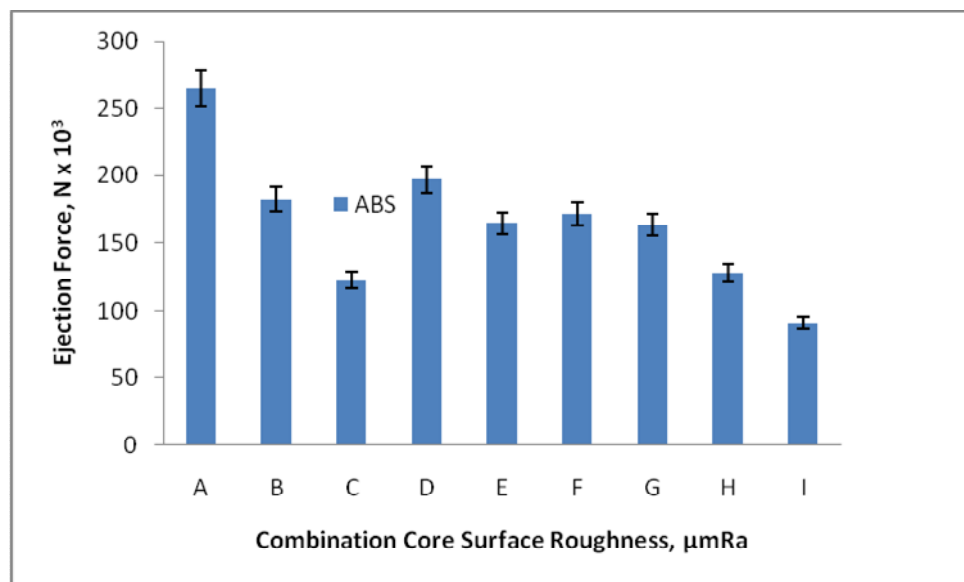


Figure 5.7: The error of the ejection force for different combination surface for ABS

Table 5.5: Average ejection force and standard error for PA6

Combination Surface	Denoted Symbol	Surface (μm)	Average Ejection Force (N)								
			Expt. 1	Expt. 2	Expt. 3	Expt. 4	Expt. 5	Expt. 6	Expt. 7	Expt. 8	Expt. 9
$S1_x+S1_y$	A	0.02	127.6	114	98.5	106	103.5	99	94.7	101.2	76.7
$S1_x+S2_y$	B	1.84	95.7	76.4	57.5	114.1	101	89.2	154.9	144.9	114.5
$S1_x+S3_y$	C	3.22	62.1	38.3	32.5	95.5	46.6	47.1	111.6	97.8	73.6
$S2_x+S1_y$	D	1.84	97.9	83.9	76.9	130	91.2	80.5	154.6	137.1	113
$S2_x+S2_y$	E	3.60	132.9	116.4	63	165.9	175.7	158	151.8	135.9	78
$S2_x+S3_y$	F	5.01	154.1	155.2	89.2	147.5	155.6	179.8	194.2	202.5	130.3
$S3_x+S1_y$	G	3.22	107.4	103.5	87.2	98	86.1	92.3	95.1	86.6	62
$S3_x+S2_y$	H	5.01	149.9	64.8	53.3	164	147.1	120.1	214.7	155.7	116.7
$S3_x+S3_y$	I	6.42	110	110.8	100.1	96.8	100.8	111.4	103.1	121.4	134.5

$S1_x$, $S2_x$ and $S3_x$ represent for core insert 1 meanwhile $S1_y$, $S2_y$ and $S3_y$ represent for core insert 2

Table 5.6: The parameter setting for PA6 for the experiment

Expt. No.	Melt Temp. (°C)	Injection Pressure (MPa)	Packing Pressure (MPa)	Cooling Time (s)
1	250	57	46	17
2	250	42	35	18
3	250	32	26	19
4	265	57	35	19
5	265	42	26	17
6	265	32	46	18
7	300	57	26	18
8	300	42	46	19
9	300	32	35	17

For PA6, a shared melting temperature of 265°C for experiment 5 and 6 showed the same behaviour where the ejection force is higher at the core surface roughness value 0.02 μmRa . Experiment 4, 7 and 8 constituted the same behaviour and starting point. Similarly with experiment 1, 2 and 3, the same behaviour can be observed as shown in Figure 5.8 due to their similar melting temperature of 250 °C. Meanwhile experiment 5 and 6 depicted the same behaviour due to their similar melting temperature of 265°C. On the other hand, experiment 4 and 7 composed of same graphs' trend and possess same injection pressure. It can be concluded that when ejection force for all stated experiments falls at different melting temperatures, the injection pressure cannot be lowered; which can be seen in experiment 9. It can be stated that, when the core surface roughness is high for all the ejection force for PA6, it results to a high ejection force.

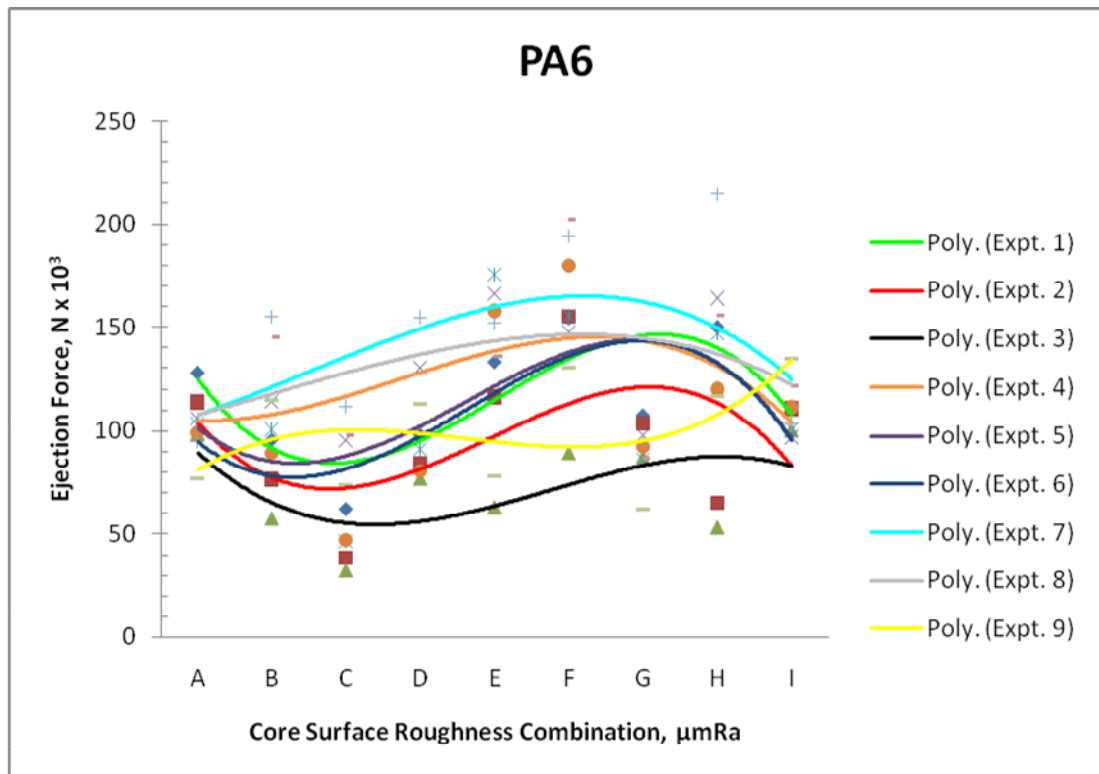


Figure 5.8: The combination of surface roughness and ejection force for PA6

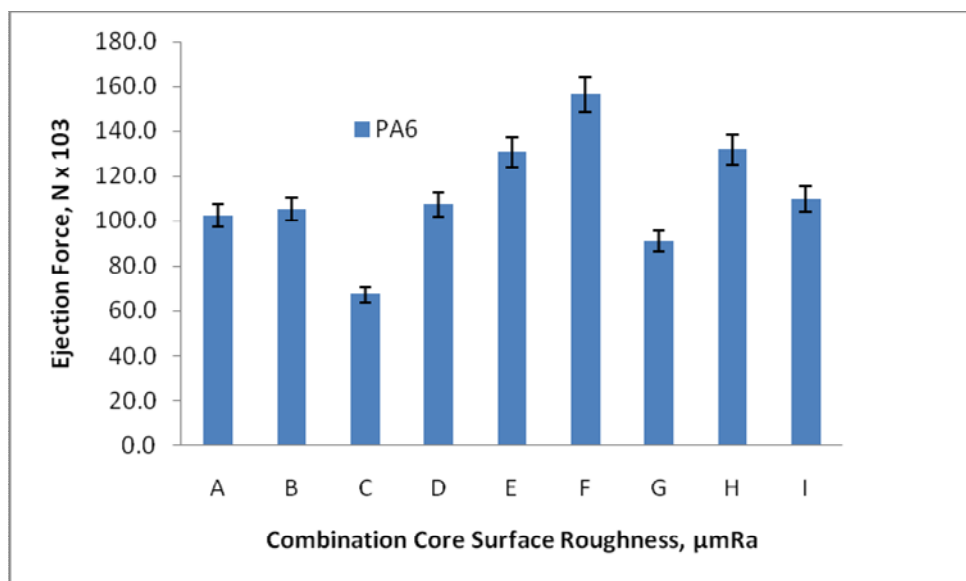


Figure 5.9: The error of the ejection force for different combination surface for PA6

In short, when these three materials were compared, HIPS showed a consistent of ejection force according to the increased of melting temperature which is slightly different with ABS material. The physical properties such as density and melt flow index are not the same even though they are amorphous.

Figure 5.7 shows the ejection force of HIPS on the varieties of surface roughness combination. The ejection force increases as the core surface roughness decreased which can be seen in $S1_x+S1_y$ ($S1_x$ – core insert 1 and $S1_y$ – core insert 2). The same phenomenon can be observed for ABS in Figure 5.8. HIPS and ABS exhibit the same character whereas when the surface roughness increases, the ejection forces decreased. Meanwhile for PA6 in Figure 5.9, the ejection force is high for surface roughness combination of $S2_x+S3_y$ and low for $S1_x+S3_y$ combination.

5.2.5 Ejection Force Experiment Data

The process of how to obtain the ejection force data was discussed in Chapter 3. The ejection force for HIPS, ABS and PA6 were taken after subtracting the force with moulding and without moulding. The value then will be recorded in the table for STATISCA analysis. The results from the experiments are shown in Table 5.7, 5.8 and 5.9 below. Appendix J shows the graph for obtaining the ejection force without moulding and after ejecting the moulding part by using data acquisition (DAQ).

Table 5.7: Table of result from ejection force experiment for HIPS

Expt No.	Core 1 (μm)	Core 2 (μm)	Melt temp. (°C)	Inj. Pressure (MPa)	Pack. Pressure (MPa)	Cooling time (s)	Ejection force (N)
1	0.01	0.01	195	69	59	16	333955.7
2	0.01	0.01	195	67	56	16	292138.7
3	0.01	0.01	195	55	45	17	254834.4
4	0.01	0.01	200	69	56	17	336354.6
5	0.01	0.01	200	67	45	16	329753
6	0.01	0.01	200	55	59	16	336825.6
7	0.01	0.01	220	69	45	16	275475.6
8	0.01	0.01	220	67	59	17	288241.5
9	0.01	0.01	220	55	56	16	326621.2
10	0.01	1.80	195	69	59	16	158897.7
11	0.01	1.80	195	67	56	16	163011.9
12	0.01	1.80	195	55	45	17	164672.6
13	0.01	1.80	200	69	56	17	193096.4
14	0.01	1.80	200	67	45	16	212358.6
15	0.01	1.80	200	55	59	16	253447.3
16	0.01	1.80	220	69	45	16	209939.4
17	0.01	1.80	220	67	59	17	230581.6
18	0.01	1.80	220	55	56	16	239157.3
19	0.01	3.21	195	69	59	16	124774.2
20	0.01	3.21	195	67	56	16	131631.9
21	0.01	3.21	195	55	45	17	150416.4
22	0.01	3.21	200	69	56	17	111199
23	0.01	3.21	200	67	45	16	113553.8
24	0.01	3.21	200	55	59	16	113879
25	0.01	3.21	220	69	45	16	136403.4
26	0.01	3.21	220	67	59	17	127985.4
27	0.01	3.21	220	55	56	16	102033.5
28	1.80	0.01	195	69	59	16	198270.4
29	1.80	0.01	195	67	56	16	189540.7
30	1.80	0.01	195	55	45	17	187706.9
31	1.80	0.01	200	69	56	17	246591.3
32	1.80	0.01	200	67	45	16	235053.5
33	1.80	0.01	200	55	59	16	220097.68
34	1.80	0.01	220	69	45	16	256835.4
35	1.80	0.01	220	67	59	17	237939.2
36	1.80	0.01	220	55	56	16	225446.8

Table 5.7: Continued.

Expt No.	Core 1 (μm)	Core 2 (μm)	Melt temp. (°C)	Inj. Pressure (MPa)	Pack. Pressure (MPa)	Cooling time (s)	Ejection force (N)
37	1.80	1.80	195	69	59	16	183941.53
38	1.80	1.80	195	67	56	16	176515.38
39	1.80	1.80	195	55	45	17	162407.08
40	1.80	1.80	200	69	56	17	214390.2
41	1.80	1.80	200	67	45	16	199557.63
42	1.80	1.80	200	55	59	16	188267.78
43	1.80	1.80	220	69	45	16	217278.48
44	1.80	1.80	220	67	59	17	224044.54
45	1.80	1.80	220	55	56	16	211503.86
46	1.80	3.21	195	69	59	16	310274
47	1.80	3.21	195	67	56	16	242632.2
48	1.80	3.21	195	55	45	17	185119.4
49	1.80	3.21	200	69	56	17	363806.6
50	1.80	3.21	200	67	45	16	329319
51	1.18	3.21	200	55	59	16	313306.4
52	1.18	3.21	220	69	45	16	398123.5
53	1.18	3.21	220	67	59	17	386030.9
54	1.18	3.21	220	55	56	16	372975.1
55	3.21	0.01	195	69	59	16	195371.43
56	3.21	0.01	195	67	56	16	195607.63
57	3.21	0.01	195	55	45	17	190485.33
58	3.21	0.01	200	69	56	17	194937.83
59	3.21	0.01	200	67	45	16	174082.13
60	3.21	0.01	200	55	59	16	184004.43
61	3.21	0.01	220	69	45	16	195200.33
62	3.21	0.01	220	67	59	17	267971.13
63	3.21	0.01	220	55	56	16	214826.93
64	3.21	1.80	195	69	59	16	193903
65	3.21	1.80	195	67	56	16	184141.48
66	3.21	1.80	195	55	45	17	150868.1
67	3.21	1.80	200	69	56	17	186908.4
68	3.21	1.80	200	67	45	16	180035.4
69	3.21	1.80	200	55	59	16	193362.1
70	3.21	1.80	220	69	45	16	183157.3
71	3.21	1.80	220	67	59	17	180327.1
72	3.21	1.80	220	55	56	16	179392.5
73	3.21	3.21	195	69	59	16	149998.7
74	3.21	3.21	195	67	56	16	121307.5

Table 5.7: Continued.

Expt No.	Core 1 (μm)	Core 2 (μm)	Melt temp. (°C)	Inj. Pressure (MPa)	Pack. Pressure (MPa)	Cooling time (s)	Ejection force (N)
75	3.21	3.21	195	55	45	17	98627.7
76	3.21	3.21	200	69	56	17	164294.1
77	3.21	3.21	200	67	45	16	140092.3
78	3.21	3.21	200	55	59	16	128104.9
79	3.21	3.21	220	69	45	16	76855.9
80	3.21	3.21	220	67	59	17	95841.5
81	3.21	3.21	220	55	56	16	90363.6

Table 5.8: Table of result from ejection force experiment for ABS

Expt No.	Core 1 (μm)	Core 2 (μm)	Melt temp. (°C)	Inj. Pressure (MPa)	Pack. Pressure (MPa)	Cooling time (s)	Ejection force (N)
1	0.01	0.01	200	77	65	17	262353
2	0.01	0.01	200	69	56	17	267434
3	0.01	0.01	200	50	41	18	246012
4	0.01	0.01	210	77	56	18	241876
5	0.01	0.01	210	69	41	17	276288
6	0.01	0.01	210	50	65	17	249873
7	0.01	0.01	240	77	41	17	294599
8	0.01	0.01	240	69	65	18	277914
9	0.01	0.01	240	50	56	17	265682
10	0.01	1.80	200	77	65	17	183377
11	0.01	1.80	200	69	56	17	193428
12	0.01	1.80	200	50	41	18	209613
13	0.01	1.80	210	77	56	18	183748
14	0.01	1.80	210	69	41	17	191222
15	0.01	1.80	210	50	65	17	188676
16	0.01	1.80	240	77	41	17	169871
17	0.01	1.80	240	69	65	18	154806
18	0.01	1.80	240	50	56	17	166714
19	0.01	3.21	200	77	65	17	136466
20	0.01	3.21	200	69	56	17	103036
21	0.01	3.21	200	50	41	18	108716

Table 5.8: Continued.

Expt No.	Core 1 (μm)	Core 2 (μm)	Melt temp. (°C)	Inj. Pressure (MPa)	Pack. Pressure (MPa)	Cooling time (s)	Ejection force (N)
22	0.01	3.21	210	77	56	18	141284
23	0.01	3.21	210	69	41	17	111495
24	0.01	3.21	210	50	65	17	117829
25	0.01	3.21	240	77	41	17	149134
26	0.01	3.21	240	69	65	18	118246
27	0.01	3.21	240	50	56	17	115755
28	1.80	0.01	200	77	65	17	197466
29	1.80	0.01	200	69	56	17	202361
30	1.80	0.01	200	50	41	18	202324
31	1.80	0.01	210	77	56	18	195808
32	1.80	0.01	210	69	41	17	205380
33	1.80	0.01	210	50	65	17	215221
34	1.80	0.01	240	77	41	17	179755
35	1.80	0.01	240	69	65	18	183988
36	1.80	0.01	240	50	56	17	190458
37	1.80	1.80	200	77	65	17	167913
38	1.80	1.80	200	69	56	17	152365
39	1.80	1.80	200	50	41	18	141431
40	1.80	1.80	210	77	56	18	166526
41	1.80	1.80	210	69	41	17	163597
42	1.80	1.80	210	50	65	17	173247
43	1.80	1.80	240	77	41	17	170354
44	1.80	1.80	240	69	65	18	172987
45	1.80	1.80	240	50	56	17	174323
46	1.80	3.21	200	77	65	17	157043
47	1.80	3.21	200	69	56	17	153703
48	1.80	3.21	200	50	41	18	145981
49	1.80	3.21	210	77	56	18	165632
50	1.80	3.21	210	69	41	17	161854
51	1.80	3.21	210	50	65	17	162020
52	1.80	3.21	240	77	41	17	200471
53	1.80	3.21	240	69	65	18	235502
54	1.80	3.21	240	50	56	17	164969
55	3.21	0.01	200	77	65	17	185935
56	3.21	0.01	200	69	56	17	171995
57	3.21	0.01	200	50	41	18	151784
58	3.21	0.01	210	77	56	18	145053
59	3.21	0.01	210	69	41	17	163223
60	3.21	0.01	210	50	65	17	177563

Table 5.8: Continued.

Expt No.	Core 1 (μm)	Core 2 (μm)	Melt temp. (°C)	Inj. Pressure (MPa)	Pack. Pressure (MPa)	Cooling time (s)	Ejection force (N)
61	3.21	0.01	240	77	41	17	158639
62	3.21	0.01	240	69	65	18	158859
63	3.21	0.01	240	50	56	17	157872
64	3.21	1.80	200	77	65	17	128136
65	3.21	1.80	200	69	56	17	127589
66	3.21	1.80	200	50	41	18	125980
67	3.21	1.80	210	77	56	18	122273
68	3.21	1.80	210	69	41	17	122778
69	3.21	1.80	210	50	65	17	124852
70	3.21	1.80	240	77	41	17	138369
71	3.21	1.80	240	69	65	18	142026
72	3.21	1.80	240	50	56	17	120144
73	3.21	3.21	200	77	65	17	97680.2
74	3.21	3.21	200	69	56	17	98448.7
75	3.21	3.21	200	50	41	18	92808.9
76	3.21	3.21	210	77	56	18	91436.4
77	3.21	3.21	210	69	41	17	85397.9
78	3.21	3.21	210	50	65	17	90987.3
79	3.21	3.21	240	77	41	17	87651
80	3.21	3.21	240	69	65	18	90547.9
81	3.21	3.21	240	50	56	17	88484.8

Table 5.9: Table of result from ejection force experiment for PA6

Expt No.	Core 1 (μm)	Core 2 (μm)	Melt temp. (°C)	Inj. Pressure (MPa)	Pack. Pressure (MPa)	Cooling time (s)	Ejection force (N)
1	0.01	0.01	250	57	46	17	127617
2	0.01	0.01	250	42	35	18	114034
3	0.01	0.01	250	32	26	19	98471
4	0.01	0.01	265	57	35	19	105959
5	0.01	0.01	265	42	26	17	103546
6	0.01	0.01	265	32	46	18	99047
7	0.01	0.01	300	57	26	18	94740.2
8	0.01	0.01	300	42	46	19	101270
9	0.01	0.01	300	32	35	17	76713

Table 5.9: Continued.

Expt No.	Core 1 (μm)	Core 2 (μm)	Melt temp. (°C)	Inj. Pressure (MPa)	Pack. Pressure (Mpa)	Cooling time (s)	Ejection force (N)
10	0.01	1.80	250	57	46	17	95690.7
11	0.01	1.80	250	42	35	18	76432.4
12	0.01	1.80	250	32	26	19	57459.7
13	0.01	1.80	265	57	35	19	114081
14	0.01	1.80	265	42	26	17	101047
15	0.01	1.80	265	32	46	18	89151.2
16	0.01	1.80	300	57	26	18	154892
17	0.01	1.80	300	42	46	19	144945
18	0.01	1.80	300	32	35	17	114549
19	0.01	3.21	250	57	46	17	62142.3
20	0.01	3.21	250	42	35	18	38312.7
21	0.01	3.21	250	32	26	19	32480.2
22	0.01	3.21	265	57	35	19	95468.1
23	0.01	3.21	265	42	26	17	46570.7
24	0.01	3.21	265	32	46	18	47065.8
25	0.01	3.21	300	57	26	18	111555
26	0.01	3.21	300	42	46	19	97772.2
27	0.01	3.21	300	32	35	17	73566
28	1.80	0.01	250	57	46	17	97922.4
29	1.80	0.01	250	42	35	18	83894.7
30	1.80	0.01	250	32	26	19	76943
31	1.80	0.01	265	57	35	19	129963
32	1.80	0.01	265	42	26	17	91240.9
33	1.80	0.01	265	32	46	18	80471.9
34	1.80	0.01	300	57	26	18	154641
35	1.80	0.01	300	42	46	19	137063
36	1.80	0.01	300	32	35	17	112955
37	1.80	1.80	250	57	46	17	132875
38	1.80	1.80	250	42	35	18	116396
39	1.80	1.80	250	32	26	19	62907
40	1.80	1.80	265	57	35	19	165884
41	1.80	1.80	265	42	26	17	175658
42	1.80	1.80	265	32	46	18	157919
43	1.80	1.80	300	57	26	18	151820
44	1.80	1.80	300	42	46	19	135909
45	1.80	1.80	300	32	35	17	78014.6
46	1.80	3.21	250	57	46	17	154115
47	1.80	3.21	250	42	35	18	155236
48	1.80	3.21	250	32	26	19	89242.3

Table 5.9: Continued.

Expt No.	Core 1 (μm)	Core 2 (μm)	Melt temp. (°C)	Inj. Pressure (MPa)	Pack. Pressure (Mpa)	Cooling time (s)	Ejection force (N)
49	1.80	3.21	265	57	35	19	147493
50	1.80	3.21	265	42	26	17	155616
51	1.80	3.21	265	32	46	18	179839
52	1.80	3.21	300	57	26	18	194219
53	1.80	3.21	300	42	46	19	202530
54	1.80	3.21	300	32	35	17	130306
55	3.21	0.01	250	57	46	17	107350
56	3.21	0.01	250	42	35	18	103529
57	3.21	0.01	250	32	26	19	87238.7
58	3.21	0.01	265	57	35	19	98021.6
59	3.21	0.01	265	42	26	17	86059.5
60	3.21	0.01	265	32	46	18	92301.3
61	3.21	0.01	300	57	26	18	95099.6
62	3.21	0.01	300	42	46	19	86550.7
63	3.21	0.01	300	32	35	17	61980.9
64	3.21	1.80	250	57	46	17	149899
65	3.21	1.80	250	42	35	18	64760.1
66	3.21	1.80	250	32	26	19	53342.5
67	3.21	1.80	265	57	35	19	164048
68	3.21	1.80	265	42	26	17	147149
69	3.21	1.80	265	32	46	18	120066
70	3.21	1.80	300	57	26	18	214658
71	3.21	1.80	300	42	46	19	155658
72	3.21	1.80	300	32	35	17	116721
73	3.21	3.21	250	57	46	17	110039
74	3.21	3.21	250	42	35	18	110760
75	3.21	3.21	250	32	26	19	100124
76	3.21	3.21	265	57	35	19	96781.7
77	3.21	3.21	265	42	26	17	100820
78	3.21	3.21	265	32	46	18	111441
79	3.21	3.21	300	57	26	18	103055
80	3.21	3.21	300	42	46	19	121370
81	3.21	3.21	300	32	35	17	134466

5.2.6 Validation of Melting Temperature, Injection Pressure, Packing Pressure and Cooling Times against Ejection Force

Before continuing with other analysis, the data need to be checked for validity. The observed values against predicted values for HIPS, ABS and PA6 need to be generated to check the validity of the data gathered. STATISCA software was used to generate observed values against predicted values plot at confidence interval of 95% (Kuo-Ming Tsai et al., 2009 and Douglas C. Montgomery et al., 2006). The results of the various predictions were presented on Figures 5.10, 5.11 and 5.12 respectively. Figure 5.10, 5.11 and 5.12 indicate the experimental actual ejection force for HIPS, ABS and PA6 materials respectively. The solid straight line on the Figure 5.10 to 5.12 represents the perfect correlation between the actual and predicted values i.e. one to one correspondence if the predicted life was exactly equivalent to the actual life. The two straight line dotted lines represent a three times factor indicating a goodness band. Data points that fall above the solid line represent non-conservative estimates, while points below solid line represent conservative predictions in comparison to the experimental results.

It can be seen that the correlation between the observed and predicted results are well correlated within the expected scatter band for both method and materials. It can be also seen that the ejection force tended to be slightly conservative due to the most points concentrated on the lower band i.e. with the solid line and the lower dotted line. These show that the data can be used for further analysis.

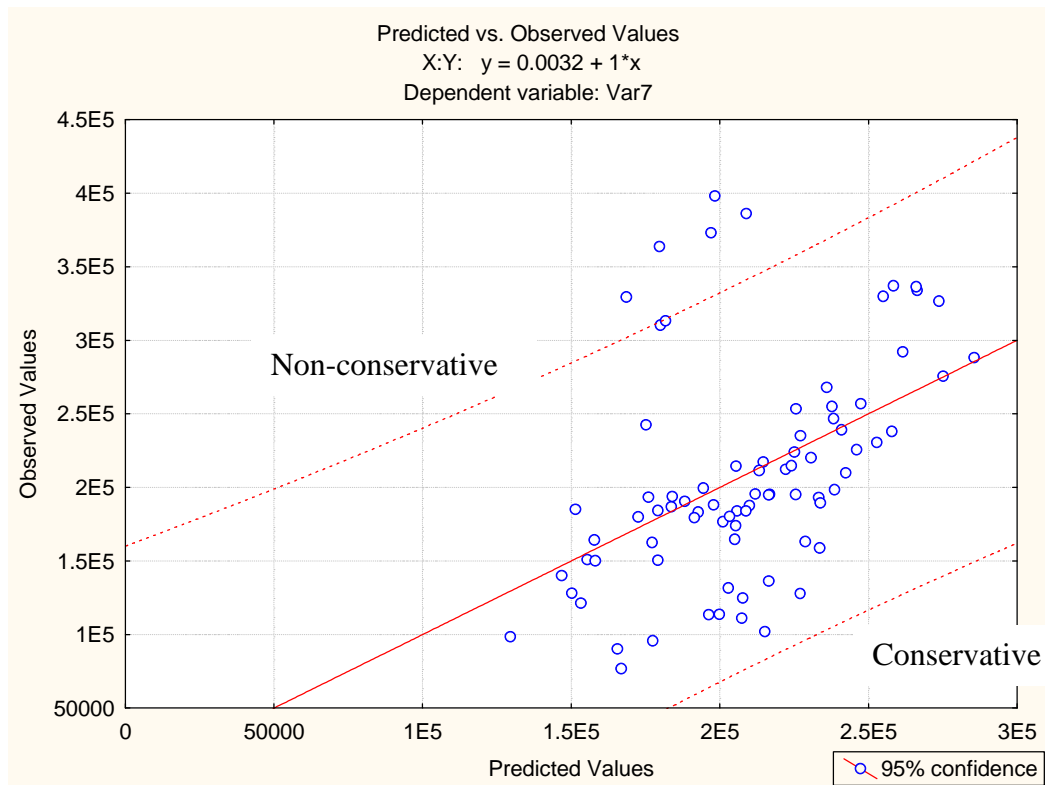


Figure 5.10: Comparison between the observed to predicted values in ejection force for the HIPS material

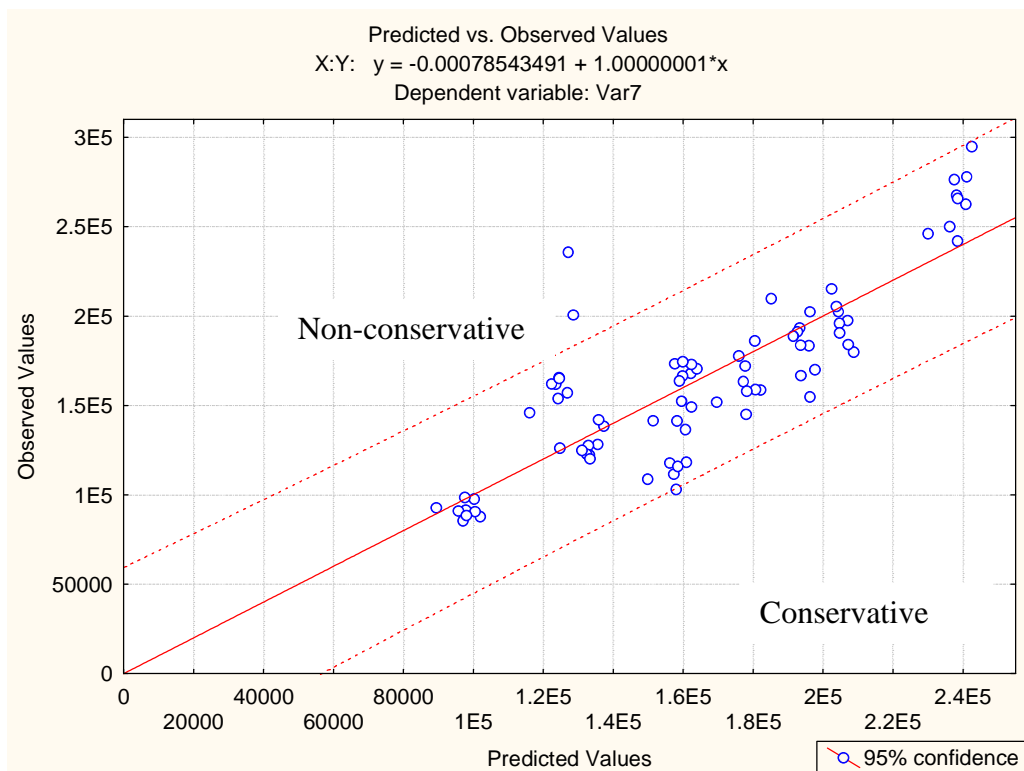


Figure 5.11: Comparison between the observed to predicted values in ejection force for the ABS material

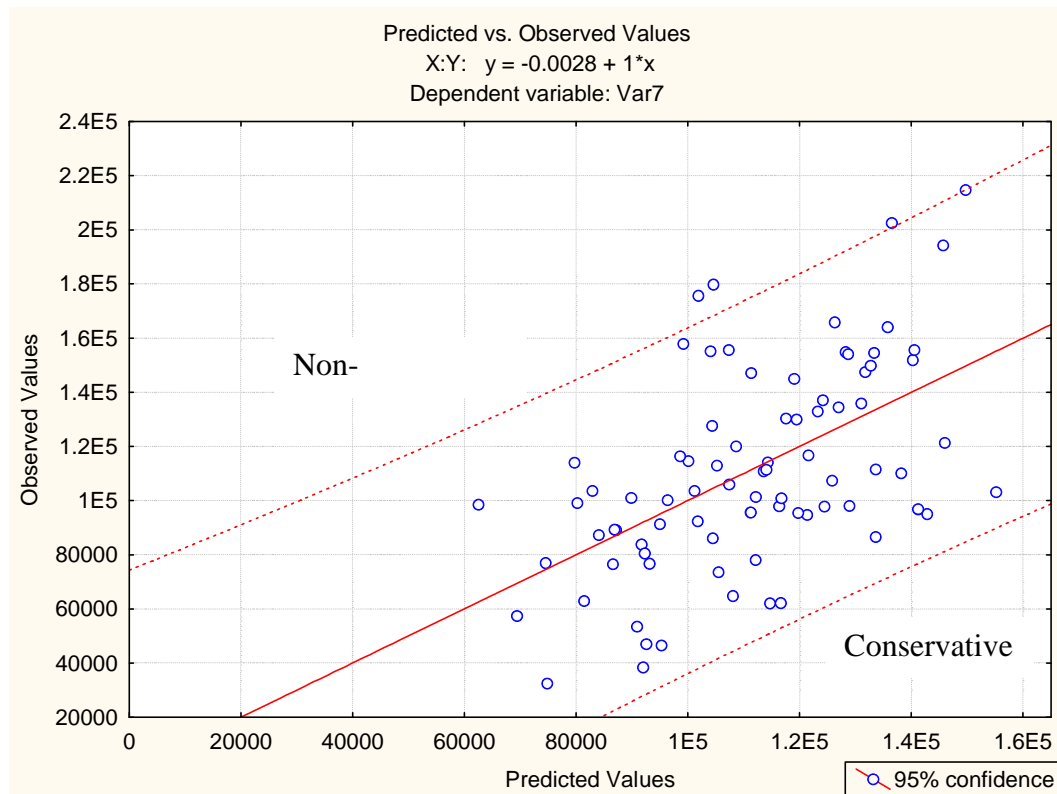


Figure 5.12: Comparison between the observed to predicted values in ejection
For the PA6 material

Table 5.10, 5.11 and 5.12 showed the result of effect estimates for ejection force against all independent variables that had been generated using STATISTICA software. From the table 5.4 for HIPS material, it can be seen that the highlighted columns which are the core insert 1 (A), core insert 2 (B) and melting temperature (C), gave the significant effect to the ejection force when $P < 0.05$. The other variable which is the injection pressure (D), packing pressure (E) and cooling time (F) did not give significant effect to the ejection force. From STATISTICA, the surface plot for dependent variable for HIPS material are discussed and generated in Section 5.2.5 (Figure 5.13, 5.16, 5.19 and 5.22).

Meanwhile for ABS as shown in Table 5.11, the core insert 1 (A), core insert 2(B) and melting temperature (c), gave the significant effect to the ejection force. This is similar to HIPS material. The surface plots for dependent variable for ABS material are shown in Figure 5.14, 5.17, 5.20 and 5.23.

For PA6 material (Figure 5.12), the core insert 1 (A), core insert 2 (B), melt temperature (C) and injection pressure (D), gave the significant effect to the ejection force. The other variable which is the packing pressure (E) and cooling time (F) did not give significant effect to the ejection force. The surface plots for dependent variable for PA6 material are shown in Figure 5.15, 5.18, 5.21 and 5.24.

Table 5.10: Effect estimate table of ejection force for HIPS

Effect Estimates; Var.:Var7; R-sqr=.91747; Adj.:.81661 (Spreadsheet_HIPS) 1 2-level factors, 5 3-level factors, 81 Runs DV: Var7; MS Residual=999806 x 10³

Factor	Effect	Std.Err.	t(36)	p
Mean/Interc.	133122	12547.82	10.60919	0.000000
(1) A (L)	-357498	37088.44	-9.63907	0.000000
A (Q)	287872	32194.93	8.94154	0.000000
(2) B (L)	-336999	37088.44	-9.08636	0.000000
B (Q)	114427	32194.93	3.55421	0.001082
(3) C (L)	-20433	20634.19	-0.99024	0.328665
C (Q)	3374	18603.45	0.18135	0.857107
(4) D (L)	3957	20535.80	0.19270	0.848279
D (Q)	781	19014.73	0.04109	0.967455
(5) E (L)	20007	20558.83	0.97316	0.336968
E (Q)	-8197	19981.57	-0.41025	0.684057
(6) F (L)	6721	18247.80	0.36833	0.714786
AL by BL	-483671	54287.31	-8.90947	0.000000
AL by BQ	275494	47124.55	5.84608	0.000001
AQ by BL	502165	47124.55	10.65612	0.000000
AQ by BQ	-243136	40906.86	-5.94366	0.000001
AL by CL	-87016	23920.34	-3.63774	0.000855
AL by CQ	-34098	21923.36	-1.55535	0.128612
AQ by CL	78211	20764.26	3.76664	0.000592
AQ by CQ	26936	19030.75	1.41538	0.165550
AL by DL	-26741	23920.34	-1.11791	0.271008
AL by DQ	17319	22408.03	0.77288	0.444638
AQ by DL	36318	20764.26	1.74905	0.088805
AQ by DQ	-16527	19451.48	-0.84967	0.401124
AL by EL	13706	23920.34	0.57300	0.570207
AL by EQ	-1896	21813.89	-0.08693	0.931211
AQ by EL	-9356	20764.26	-0.45060	0.654980
AQ by EQ	3731	18935.73	0.19701	0.844928
AL by FL	8421	20715.63	0.40652	0.686770
AQ by FL	-2315	17982.37	-0.12876	0.898263
BL by CL	-8220	23920.34	-0.34363	0.733124
BL by CQ	-915	21923.36	-0.04172	0.966956
BQ by CL	9397	20764.26	0.45254	0.653597
BQ by CQ	3067	19030.75	0.16117	0.872861
BL by DL	35615	23920.34	1.48889	0.145225
BL by DQ	-14631	22408.03	-0.65294	0.517942
BQ by DL	-25128	20764.26	-1.21016	0.234103
BQ by DQ	9203	19451.48	0.47313	0.638974
BL by EL	-607	23920.34	-0.02538	0.979894
BL by EQ	967	21813.89	0.04434	0.964876

Table 5.10: Continued.

Effect Estimates; Var.:Var7; R-sqr=.91747; Adj:.81661 (Spreadsheet_HIPS) 1 2-level factors, 5 3-level factors, 81 Runs DV: Var7; MS Residual=999806 x 10³

Factor	Effect	Std.Err.	t(36)	p
BQ by EL	-1702	20764.26	-0.08198	0.935117
BQ by EQ	-1981	18935.73	-0.10462	0.917258
BL by FL	5314	20715.63	0.25651	0.799016
BQ by FL	-6981	17982.37	-0.38819	0.700162
CL by DL	-9952	15579.45	-0.63876	0.527020

A – Core insert1, B – Core Insert 2, C – Melting temperature, D – Injection pressure, E – Packing pressure and F – Cooling time

Table 5.11: Effect estimate table of ejection force for ABS

Effect Estimates; Var.:Var7; R-sqr=.95183; Adj:.89295 (Spreadsheet_ABS) 1 2-level factors, 5 3-level factors, 81 Runs DV: Var7; MS Residual=261934 x 10³

Factor	Effect	Std.Err.	t(36)	p
Mean/Interc.	144031	6227.34	23.12888	0.000000
(1) A (L)	-155059	18665.75	-8.30713	0.000000
A (Q)	85578	16202.96	5.28160	0.000006
(2) B (L)	-152581	18665.75	-8.17441	0.000000
B (Q)	19420	16202.96	1.19857	0.238526
(3) C (L)	-2467	10446.33	-0.23615	0.814657
C (Q)	-8155	9364.91	-0.87077	0.389651
(4) D (L)	14056	10475.02	1.34182	0.188056
D (Q)	-2443	9243.06	-0.26428	0.793072
(5) E (L)	1793	10691.65	0.16772	0.867743
E (Q)	-3998	9695.87	-0.41233	0.682540
(6) F (L)	-9309	9207.45	-1.01108	0.318725
AL by BL	-112495	27786.65	-4.04853	0.000262
AL by BQ	59301	24120.43	2.45855	0.018892
AQ by BL	139072	24120.43	5.76574	0.000001
AQ by BQ	-50735	20937.94	-2.42309	0.020546
AL by CL	-23954	12243.49	-1.95646	0.058203
AL by CQ	-12356	11036.13	-1.11957	0.270313
AQ by CL	21729	10628.07	2.04448	0.048272
AQ by CQ	10209	9580.01	1.06566	0.293671
AL by DL	-794	12243.49	-0.06486	0.948645
AL by DQ	-3397	10892.55	-0.31185	0.756950
AQ by DL	-3047	10628.07	-0.28671	0.775980
AQ by DQ	6399	9455.37	0.67680	0.502862
AL by EL	-3062	12243.49	-0.25010	0.803935
AL by EQ	2124	10713.05	0.19823	0.843977
AQ by EL	10694	10628.07	1.00617	0.321051
AQ by EQ	-2746	9299.56	-0.29525	0.769501
AL by FL	-7065	10603.17	-0.66629	0.509475

Table 5.11: Continued.

Effect Estimates; Var.:Var7; R-sqr=.95183; Adj.:.89295 (Spreadsheet_ABS) 1 2-level factors, 5 3-level factors, 81 Runs DV: Var7; MS Residual=261934 x 10³

Factor	Effect	Std.Err.	t(36)	p
AQ by FL	6914	9204.17	0.75122	0.457401
BL by CL	22331	12243.49	1.82394	0.076472
BL by CQ	-2183	11036.13	-0.19778	0.844327
BQ by CL	-12511	10628.07	-1.17712	0.246871
BQ by CQ	2585	9580.01	0.26982	0.788841
BL by DL	16852	12243.49	1.37642	0.177194
BL by DQ	-2420	10892.55	-0.22221	0.825405
BQ by DL	-9377	10628.07	-0.88229	0.383472
BQ by DQ	-1727	9455.37	-0.18267	0.856083
BL by EL	7566	12243.49	0.61795	0.540501
BL by EQ	-4055	10713.05	-0.37847	0.707305
BQ by EL	-5808	10628.07	-0.54645	0.588125
BQ by EQ	3995	9299.56	0.42958	0.670059
BL by FL	7317	10603.17	0.69005	0.494586
BQ by FL	1371	9204.17	0.14892	0.882451
CL by DL	5222	8017.77	0.65136	0.518952

A – Core insert1, B – Core Insert 2, C – Melting temperature, D – Injection pressure, E – Packing pressure and F – Cooling time

Table 5.12: Effect estimate table of ejection force for PA6

Effect Estimates; Var.:Var7; R-sqr=.83225; Adj.:.58062 (Spreadsheet_PA6) 6 3-level factors, 1 Blocks, 81 Runs; MS Residual=598305 x 10³ DV: Var7

Factor	Effect	Std.Err.	t(32)	p
Mean/Interc.	63864	8999.05	7.09679	0.000000
(1) A (L)	-104064	27515.19	-3.78205	0.000643
A (Q)	116244	23884.79	4.86688	0.000029
(2) B (L)	-119860	27515.19	-4.35614	0.000128
B (Q)	93468	23884.79	3.91327	0.000447
(3) C (L)	57	15702.09	0.00361	0.997146
C (Q)	-24231	13956.33	-1.73621	0.092148
(4) D (L)	2499	15702.09	0.15914	0.874558
D (Q)	-6327	13688.77	-0.46219	0.647073
(5) E (L)	7694	15702.09	0.48999	0.627480
E (Q)	6179	13621.06	0.45360	0.653176
(6) F (L)	5844	15702.09	0.37216	0.712225
F (Q)	-4454	13598.41	-0.32756	0.745379
AL by BL	-122659	41995.42	-2.92078	0.006352
AL by BQ	88267	36454.47	2.42129	0.021313
AQ by BL	141051	36454.47	3.86924	0.000505
AQ by BQ	-79592	31644.61	-2.51520	0.017114
AL by CL	-15812	18504.23	-0.85450	0.399179

Table 5.12: Continued.

Effect Estimates; Var.:Var7; R-sqr=.83225; Adj.:.58062 (Spreadsheet_PA6) 6 3-level factors, 1 Blocks, 81 Runs; MS Residual=598305 x 10³ DV: Var7

Factor	Effect	Std.Err.	t(32)	p
AL by CQ	-18570	16446.92	-1.12910	0.267247
AQ by CL	12209	16062.75	0.76011	0.452754
AQ by CQ	21337	14276.89	1.49452	0.144837
AL by DL	-12490	18504.23	-0.67500	0.504521
AL by DQ	-18452	16131.61	-1.14381	0.261186
AQ by DL	11803	16062.75	0.73481	0.467807
AQ by DQ	16701	14003.18	1.19268	0.241763
AL by EL	-7468	18504.23	-0.40356	0.689220
AL by EQ	2814	16051.82	0.17530	0.861946
AQ by EL	7645	16062.75	0.47593	0.637357
AQ by EQ	-5384	13933.92	-0.38642	0.701745
AL by FL	-8899	18504.23	-0.48091	0.633852
AL by FQ	-13776	16025.13	-0.85963	0.396390
AQ by FL	3465	16062.75	0.21570	0.830588
AQ by FQ	15237	13910.75	1.09534	0.281544
BL by CL	-17780	18504.23	-0.96084	0.343836
BL by CQ	-32062	16446.92	-1.94943	0.060054
BQ by CL	34023	16062.75	2.11811	0.042026
BQ by CQ	34913	14276.89	2.44544	0.020151
BL by DL	-40016	18504.23	-2.16256	0.038156
BL by DQ	-1313	16131.61	-0.08140	0.935629
BQ by DL	37302	16062.75	2.32229	0.026737
BQ by DQ	2921	14003.18	0.20857	0.836109
BL by EL	11278	18504.23	0.60950	0.546497
BL by EQ	14689	16051.82	0.91509	0.366989
BQ by EL	-5111	16062.75	-0.31817	0.752425
BQ by EQ	-14707	13933.92	-1.05546	0.299121
BL by FL	9203	18504.23	0.49734	0.622353
BL by FQ	1621	16025.13	0.10117	0.920046
BQ by FL	-11451	16062.75	-0.71291	0.481068
BQ by FQ	1251	13910.75	0.08996	0.928882

A – Core insert1, B – Core Insert 2, C – Melting temperature, D – Injection pressure, E – Packing pressure and F – Cooling time

From Table 5.4 and 5.5, it can be observed that the highlighted columns which are the surface roughness, melting temperature and injection pressure, showed a significant effect to the ejection force for HIPS and ABS resins. Meanwhile for PA6, the highlighted columns which include the surface roughness, melting temperature

injection pressure and packing pressure, also showed a significant effect to the ejection force as shown in Table 5.6.

5.2.7 Model graph and surface contour plot

By referring to 3-D surface plot model as shown below, the relationship between independent variables and dependent variable in this experiment can be observed. In Figure 5.13, 5.14 and 5.15, the melting temperature plays an important role in determining the ejection force particularly for PA6 where whilst increasing the surface roughness, it gradually increases the ejection force. For injection pressure, PA6 showed the ejection force which will increase when the injection pressure is increased (Figure 5.18). Different for HIPS and ABS, the ejection force pressure was increased at the surface roughness level decrease and high injection pressure as shown in Figure 5.16 and 5.17.

The packing pressure for HIPS and ABS does not give much effect to ejection force (Figure 5.19 and 5.20) compared to PA6 when at the surface roughness of 1.84 μm , the ejection force is high as shown in Figure 5.21. The cooling time does not give significant effect for all resins used in this experiment as shown in Figure 5.22, 5.23 and 5.24.

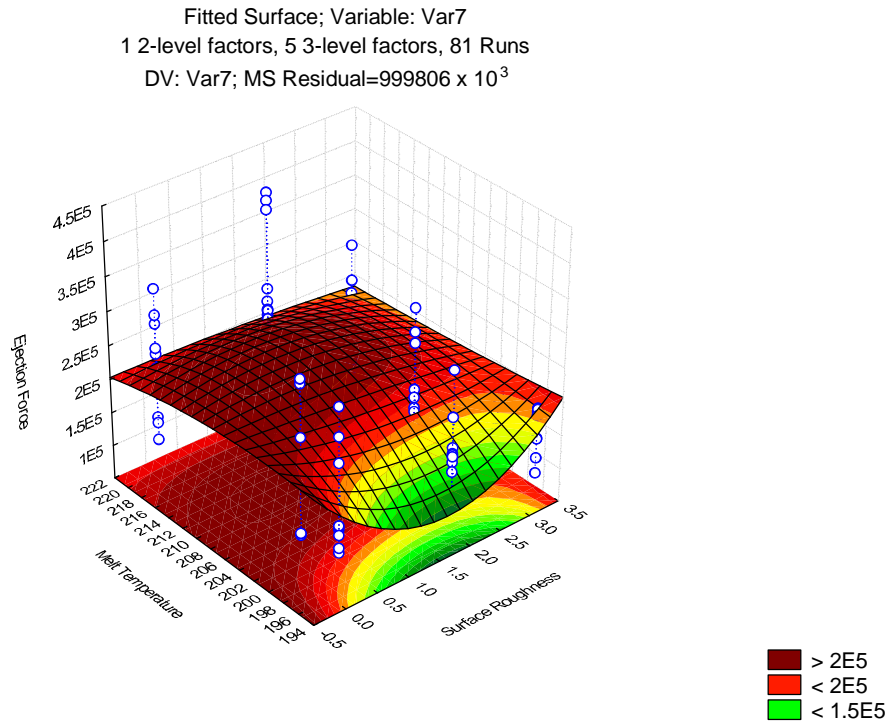


Figure 5.13: Surface plot of surface roughness and melting temperature against ejection force for HIPS

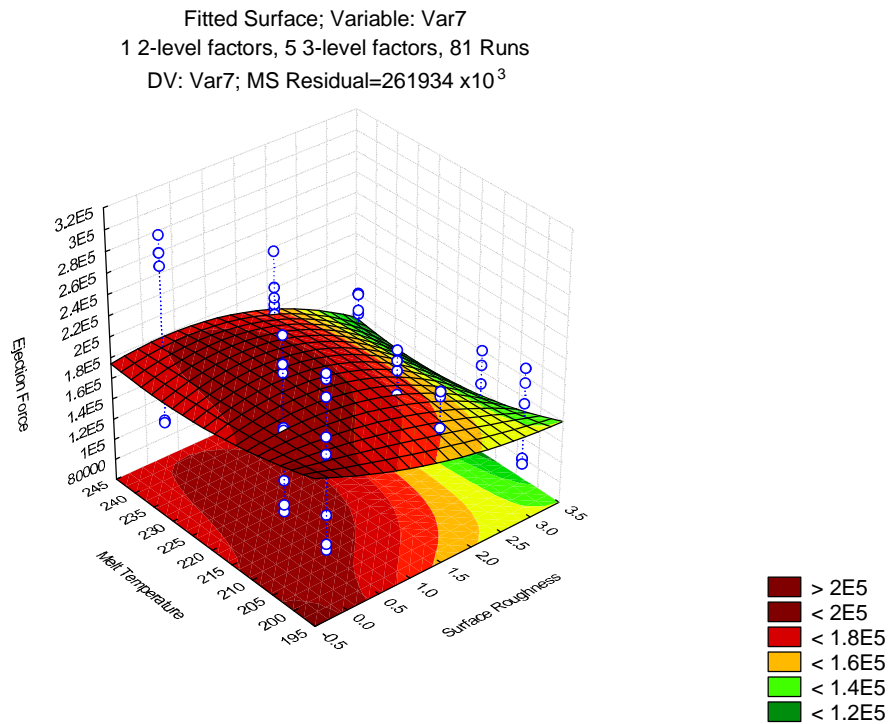


Figure 5.14: Surface plot of surface roughness and melting temperature against ejection force for ABS

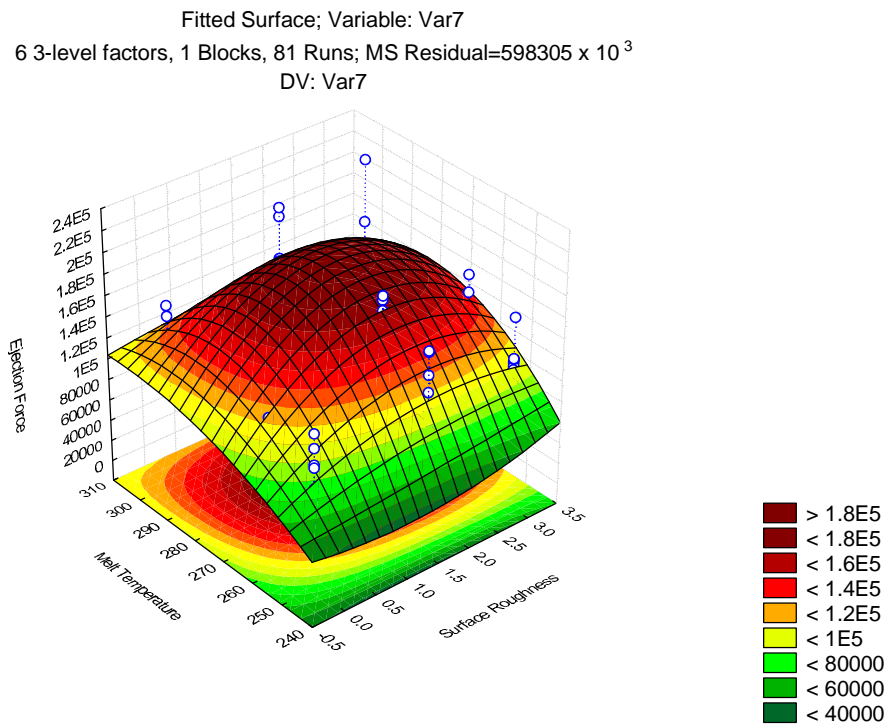


Figure 5.15: Surface plot of surface roughness and melting temperature against ejection force for PA6

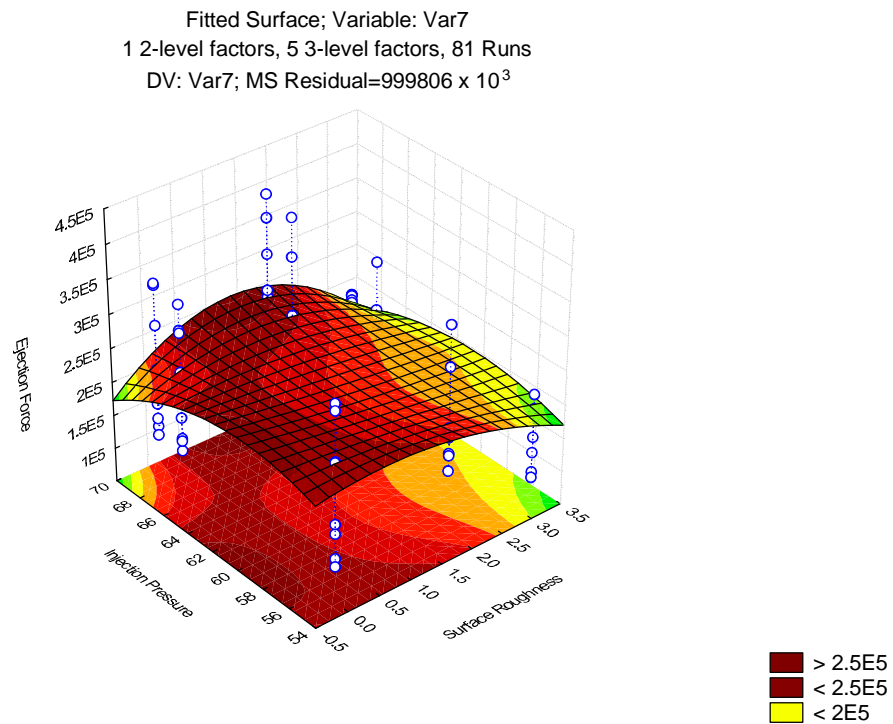


Figure 5.16: Surface plot of surface roughness and injection pressure against ejection force for HIPS

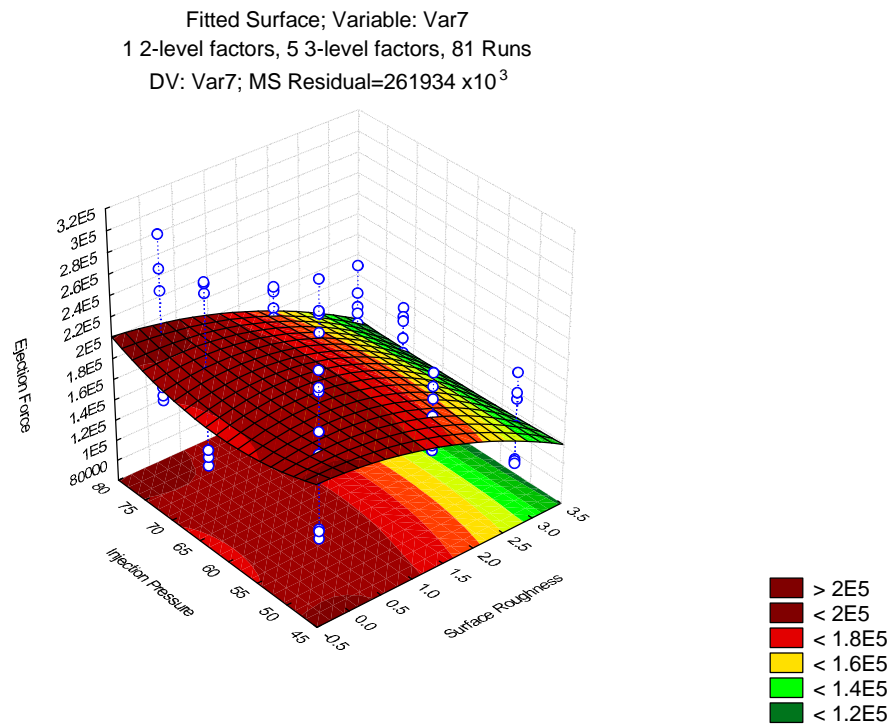


Figure 5.17: Surface plot of surface roughness and injection pressure against ejection force for ABS

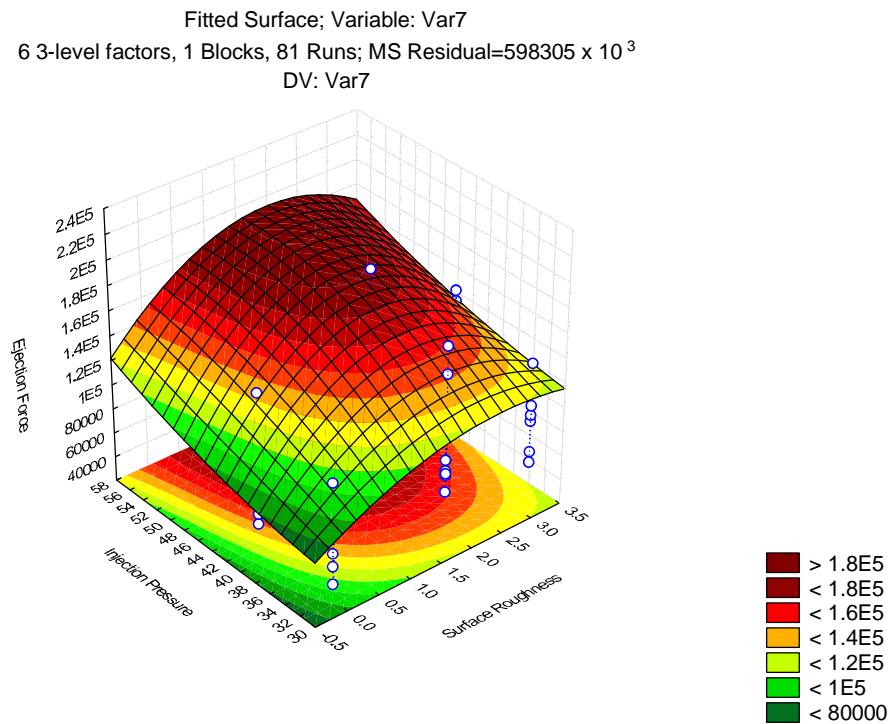


Figure 5.18: Surface plot of surface roughness and injection pressure against ejection force for PA6

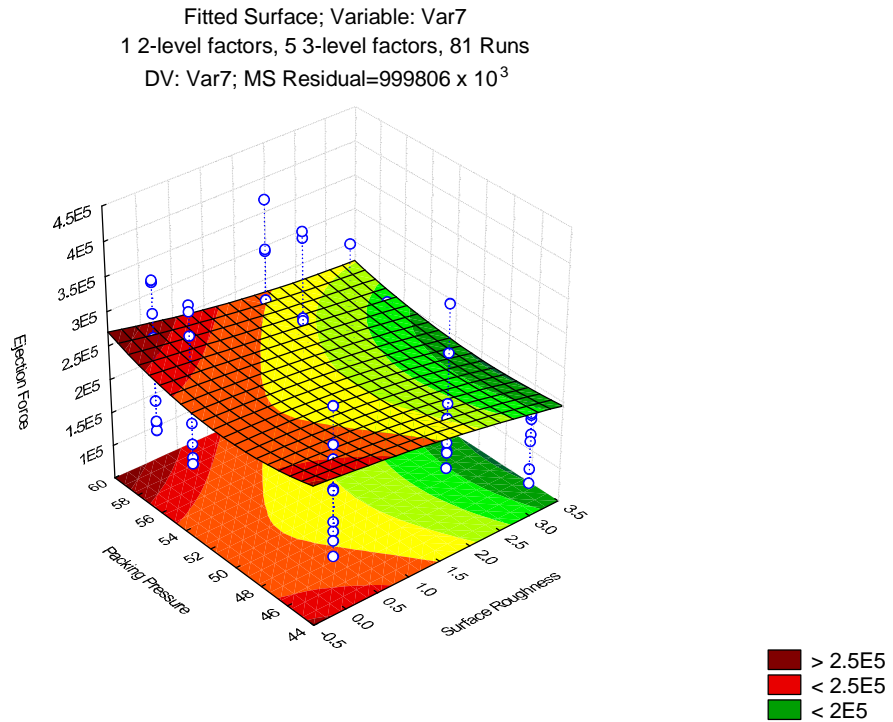


Figure 5.19: Surface plot of surface roughness and packing pressure against ejection force for HIPS

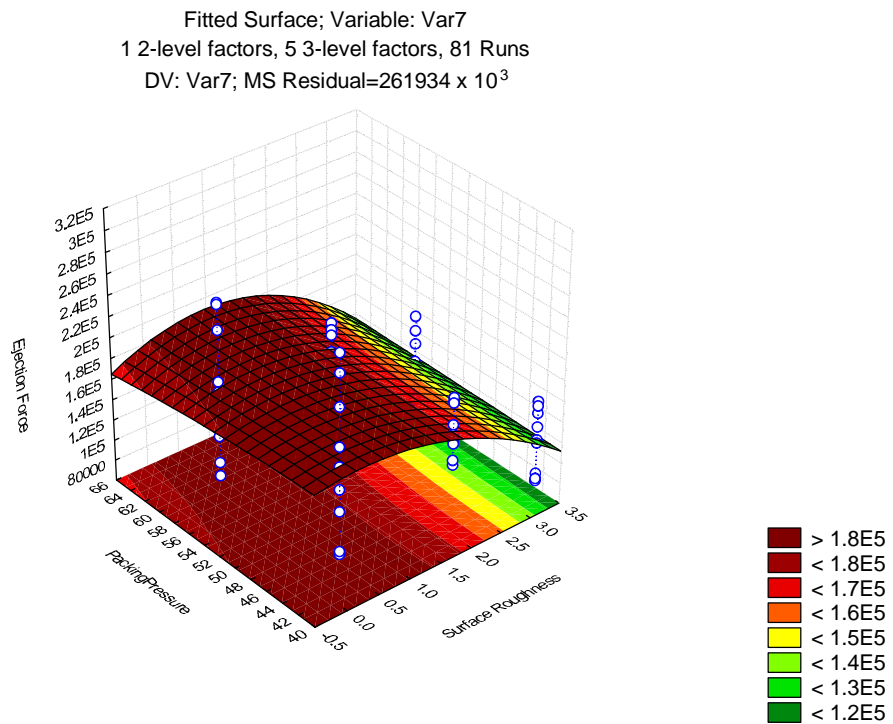


Figure 5.20: Surface plot of surface roughness and packing pressure against ejection force for ABS

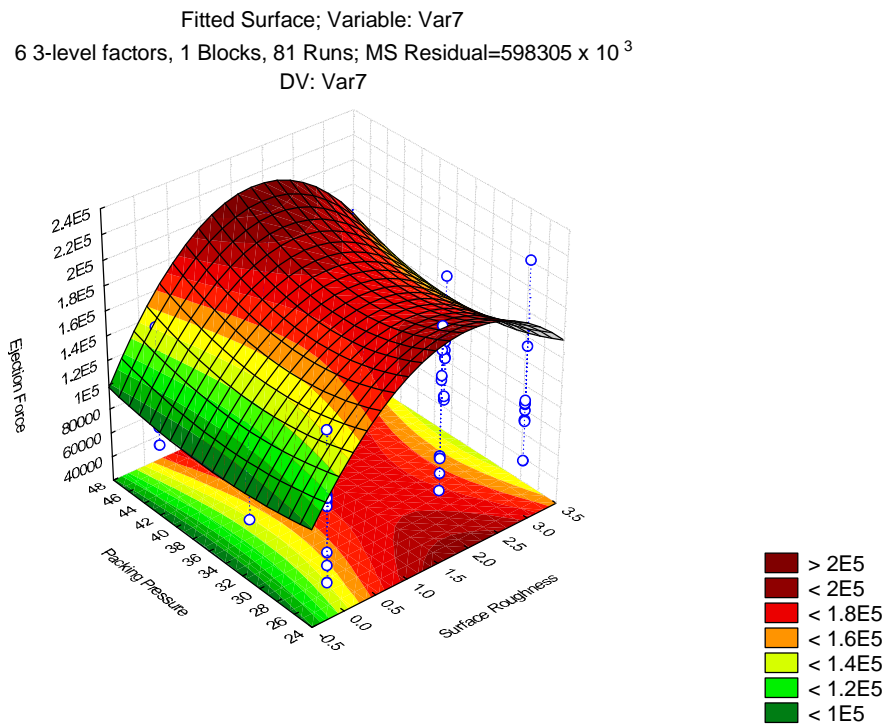


Figure 5.21: Surface plot of surface roughness and packing pressure against ejection force for PA6

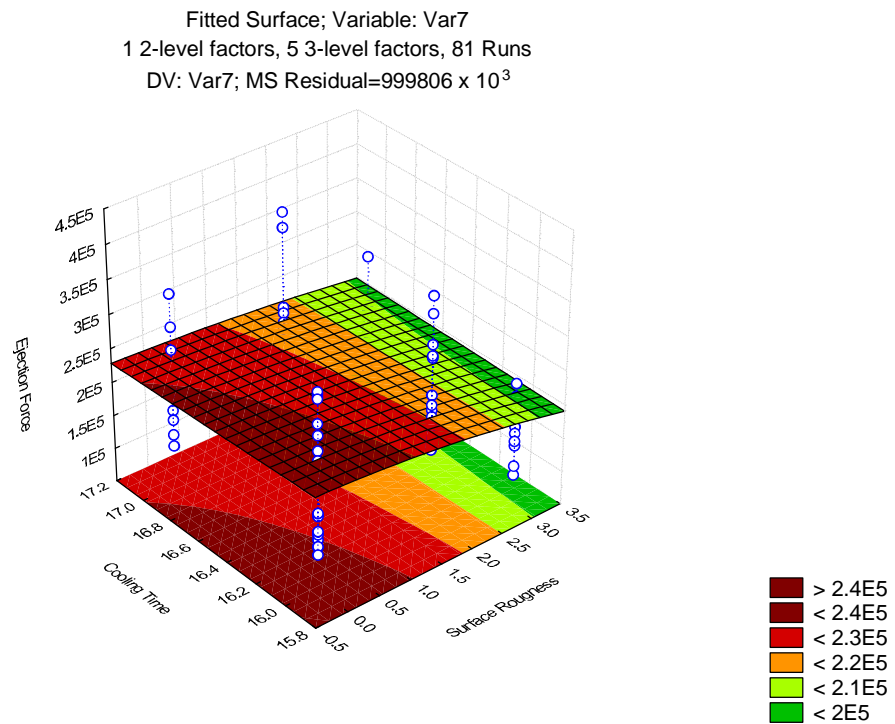


Figure 5.22: Surface plot of surface roughness and cooling time against ejection force for HIPS

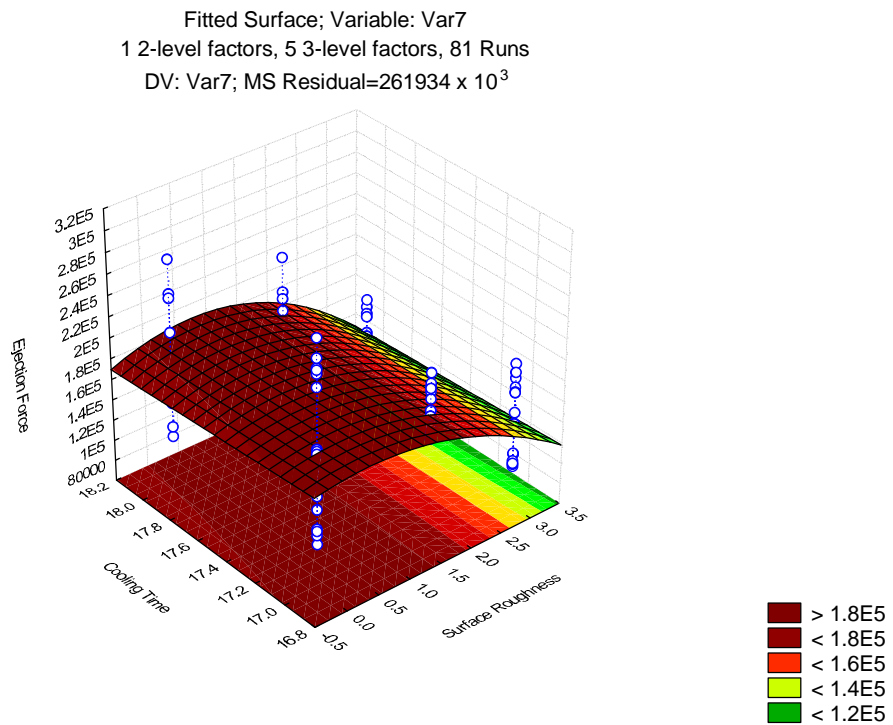


Figure 5.23: Surface plot of surface roughness and cooling time against ejection force for ABS

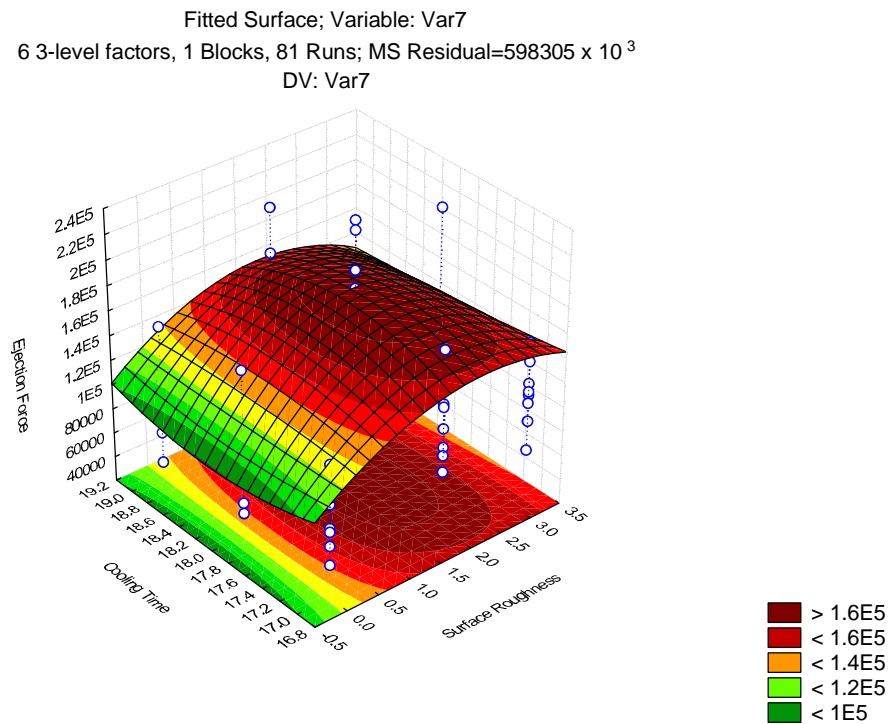


Figure 5.24: Surface plot of surface roughness and cooling time against ejection force for PA6

5.3 Effect of Control Factors

The effect and control of control factors were investigated through the analysis of variance (ANOVA). The control factors considered for ANOVA are surface roughness1 (A), surface roughness 2 (B), melting temperature (C), injection pressure (D), packing pressure (E) and cooling time (F) which are indicated in Table 5.7 to 5.12. The influence of various design factors and the degree of sensitivity of the result with different factors affecting the quality of characteristics can be observed.

5.3.1 Analysis of Variance (ANOVA)

An ANOVA is an analysis of variation present in an experiment. It is a test of hypothesis that the variation in an experiment gives no greater than that due to normal variation of individuals' characteristics and error in their measurement. The reason for doing an ANOVA is to see any difference between groups on some variables.

In an ANOVA, variation will come from a number of sources depending upon the layout of the experiment. The concept behind experimental design and the formulation of an ANOVA model is to identify the sources of variation and construct proper tests to compare them.

The basis for every statistical test is to phrase the question in terms of a null hypothesis, essentially that everything is equal, and then to test whether that can be accepted within a certain probability. If the null hypothesis is rejected, that allows the

researcher to say that "significant differences were found in ... with a probability <0.05 ."

The tests in an ANOVA are based on the F-ratio: the variation due to an experimental treatment or effect divided by the variation due to experimental error. The null hypothesis is this ratio equals 1.0, or the treatment effect is the same as the experimental error. This hypothesis is rejected if the F-ratio shows a significantly large enough number that the possibility of it equalling to 1.0 which can be smaller than some pre-assigned criteria such as 0.05 (one in twenty). In Taguchi method, the signal to noise (S/N) ratio is expressed as a log transformation of the mean-squared deviation (MSD) as the measure for analysis of experimental results (Roy, 2001). Pooling is a process of disregarding an individual factor's contribution and then subsequently adjusting the contributions of other factors.

5.3.2 ANOVA and regression analysis

First analysis to be considered was based on the ANOVA output. It has produced statistic concepts such as the Sum of Square (SS), Mean Square (MS), Estimate Coefficient, Standard Error, F-test value and Prob $> F$ to fit models in crossed design. From the analysis, full factorial of mixing 2-level and 3-level was chosen for HIPS and ABS and 3-level for PA6 to fit the six factors in this study. Every individual and its interaction effects have a single degree of freedom and their SS values were computed and tabulated in Table 5.13 (for ejection force of HIPS), Table 5.14 (for ejection force of ABS) and Table 5.15 (for ejection force of PA6). The analyses were carried out for a 95% confidence level. It was found that the

highlighted column represents the significant value for the analysis of variance in this experiment. For HIPS and ABS, the surface roughness core 1, surface roughness core 2 and melting temperature give influence to the ejection force. The probability value for these two materials was less than 0.05. The rest of the factors showed lack of fit because the probability value is greater than 0.05 ($P > 0.05$), which means there are insignificant values present as shown in Table 5.13 and 5.14. Meanwhile for PA6, the surface roughness core 1, surface roughness core 2, melting temperature and injection pressure give influence to the ejection force as shown in Figure 5.15. The rest of the factors are insignificant because probability value is greater than 0.05.

Table 5.13: ANOVA table of ejection force for HIPS

ANOVA; Var.:Var7; R-sqr=.91747; Adj.:.81661 (Spreadsheet_PS) 1 2-level factors,
5 3-level factors, 81 Runs DV: Var7; MS Residual=999806 x 10³

Factor	SS	df	MS	F	p
(1) A (L)	9.289370 x 10 ¹⁰	1	9.289370 x 10 ¹⁰	92.9117	0.000000
A (Q)	7.993554 x 10 ¹⁰	1	7.993554 x 10 ¹⁰	79.9511	0.000000
(2) B (L)	8.254584 x 10 ¹⁰	1	8.254584 x 10 ¹⁰	82.5619	0.000000
B (Q)	1.262992 x 10 ¹⁰	1	1.262992 x 10 ¹⁰	12.6324	0.001082
(3) C (L)	9.803892 x 10 ⁸	1	9.803892 x 10 ⁸	0.9806	0.328665
C (Q)	3.288300 x 10 ⁷	1	3.288300 x 10 ⁷	0.0329	0.857107
(4) D (L)	3.712507 x 10 ⁷	1	3.712507 x 10 ⁷	0.0371	0.848279
D (Q)	1.687681 x 10 ⁶	1	1.687681 x 10 ⁶	0.0017	0.967455
(5) E (L)	9.468569 x 10 ⁸	1	9.468569 x 10 ⁸	0.9470	0.336968
E (Q)	1.682692 x 10 ⁸	1	1.682692 x 10 ⁸	0.1683	0.684057
(6) F (L)	1.356394 x 10 ⁸	1	1.356394 x 10 ⁸	0.1357	0.714786
AL by BL	7.936332 x 10 ¹⁰	1	7.936332 x 10 ¹⁰	79.3787	0.000000
AL by BQ	3.417006 x 10 ¹⁰	1	3.417006 x 10 ¹⁰	34.1767	0.000001
AQ by BL	1.135309 x 10 ¹¹	1	1.135309 x 10 ¹¹	113.5529	0.000000
AQ by BQ	3.532020 x 10 ¹⁰	1	3.532020 x 10 ¹⁰	35.3271	0.000001
AL by CL	1.323056 x 10 ¹⁰	1	1.323056 x 10 ¹⁰	13.2331	0.000855
AL by CQ	2.418632 x 10 ⁹	1	2.418632 x 10 ⁹	2.4191	0.128612
AQ by 3L	1.418482 x 10 ¹⁰	1	1.418482 x 10 ¹⁰	14.1876	0.000592
AQ by CQ	2.002917 x 10 ⁹	1	2.002917 x 10 ⁹	2.0033	0.165550
AL by DL	1.249491 x 10 ⁹	1	1.249491 x 10 ⁹	1.2497	0.271008
AL by DQ	5.972287 x 10 ⁸	1	5.972287 x 10 ⁸	0.5973	0.444638
AQ by DL	3.058584 x 10 ⁹	1	3.058584 x 10 ⁹	3.0592	0.088805
AQ by DQ	7.217999 x 10 ⁸	1	7.217999 x 10 ⁸	0.7219	0.401124
AL by EL	3.282642 x 10 ⁸	1	3.282642 x 10 ⁸	0.3283	0.570207
AL by EQ	7.554957 x 10 ⁶	1	7.554957 x 10 ⁶	0.0076	0.931211
AQ by EL	2.030013 x 10 ⁸	1	2.030013 x 10 ⁸	0.2030	0.654980
AQ by EQ	3.880552 x 10 ⁷	1	3.880552 x 10 ⁷	0.0388	0.844928
AL by FL	1.652234 x 10 ⁸	1	1.652234 x 10 ⁸	0.1653	0.686770
AQ by FL	1.657641 x 10 ⁷	1	1.657641 x 10 ⁷	0.0166	0.898263
BL by CL	1.180578 x 10 ⁸	1	1.180578 x 10 ⁸	0.1181	0.733124
BL by CQ	1.739857 x 10 ⁶	1	1.739857 x 10 ⁶	0.0017	0.966956
BQ by CL	2.047502 x 10 ⁸	1	2.047502 x 10 ⁸	0.2048	0.653597
BQ by CQ	2.597071 x 10 ⁷	1	2.597071 x 10 ⁷	0.0260	0.872861
BL by DL	2.216363 x 10 ⁹	1	2.216363 x 10 ⁹	2.2168	0.145225
BL by DQ	4.262508 x 10 ⁸	1	4.262508 x 10 ⁸	0.4263	0.517942
BQ by DL	1.464206 x 10 ⁹	1	1.464206 x 10 ⁹	1.4645	0.234103
BQ by DQ	2.238118 x 10 ⁸	1	2.238118 x 10 ⁸	0.2239	0.638974
BL by EL	6.438779 x 10 ⁵	1	6.438779 x 10 ⁵	0.0006	0.979894
BL by EQ	1.965935 x 10 ⁶	1	1.965935 x 10 ⁶	0.0020	0.964876
BQ by EL	6.719408 x 10 ⁶	1	6.719408 x 10 ⁶	0.0067	0.935117

Table 5.7: Continued.

ANOVA; Var.:Var7; R-sqr=.91747; Adj.:.81661 (Spreadsheet_PS) 1 2-level factors,
5 3-level factors, 81 Runs DV: Var7; MS Residual=999806 x 10³

Factor	SS	df	MS	F	p
BQ by EQ	1.094311 x 10 ⁷	1	1.094311 x 10 ⁷	0.0109	0.917258
BL by FL	6.578539 x 10 ⁷	1	6.578539 x 10 ⁷	0.0658	0.799016
BQ by FL	1.506615 x 10 ⁸	1	1.506615 x 10 ⁸	0.1507	0.700162
CL by DL	4.079399 x 10 ⁸	1	4.079399 x 10 ⁸	0.4080	0.527020
Error	3.599301 x 10 ⁸	36	9.998057 x 10 ⁸		
Total SS	4.361413 x 10 ¹¹	80			

A – Core insert1, B – Core Insert 2, C – Melting temperature, D – Injection pressure, E – Packing pressure and F – Cooling time, L – Linear and Q – Quadratic, L – Linear and Q - Quadratic

The reliability level of generated quadratic model for HIPS was verified through the high values of R² (0.91747) and Adj-R² (0.81661) which were obtained from statistical analysis, as shown in Table 5.7. The R² value of 0.91747 indicated that the quadratic model was able to fit more than 92% of the variability of the responses obtained from experimental data. In case of ABS and PA6, the values of R² are 0.95183 and 0.83225 respectively. Meanwhile for the Adj-R² for ABS and PA6 are 0.81661 and 0.58062 respectively as shown in Table 5.8 and 5.9. It means that all R² values obtained for the resins used in the experiment were able to fit in the model.

Table 5.14: ANOVA table of ejection force for ABS

ANOVA; Var.:Var7; R-sqr=.95183; Adj.:.89295 (Spreadsheet_ABS) 1 2-level factors, 5 3-level factors, 81 Runs DV: Var7; MS Residual=261934 x 10³

Factor	SS	df	MS	F	p
(1) A (L)	1.807561 x 10 ¹⁰	1	1.807561 x 10 ¹⁰	69.00834	0.000000
A (Q)	7.306730 x 10 ⁹	1	7.306730 x 10 ⁹	27.89534	0.000006
(2) B (L)	1.750266 x 10 ¹⁰	1	1.750266 x 10 ¹⁰	66.82095	0.000000
B (Q)	3.762858 x 10 ⁸	1	3.762858 x 10 ⁸	1.43657	0.238526
(3) C (L)	1.460682 x 10 ⁷	1	1.460682 x 10 ⁷	0.05577	0.814657
C (Q)	1.986076 x 10 ⁸	1	1.986076 x 10 ⁸	0.75824	0.389651
(4) D (L)	4.716085 x 10 ⁸	1	4.716085 x 10 ⁸	1.80049	0.188056
D (Q)	1.829443 x 10 ⁷	1	1.829443 x 10 ⁷	0.06984	0.793072
(5) E (L)	7.368150 x 10 ⁶	1	7.368150 x 10 ⁶	0.02813	0.867743
E (Q)	4.453378 x 10 ⁷	1	4.453378 x 10 ⁷	0.17002	0.682540

Table 5.14: Continued.

ANOVA; Var.:Var7; R-sqr=.95183; Adj.:.89295 (Spreadsheet_ABS) 1 2-level factors, 5 3-level factors, 81 Runs DV: Var7; MS Residual=261934 x 10³

Factor	SS	df	MS	F	p
(6) F (L)	2.677717 x 10 ⁸	1	2.677717 x 10 ⁸	1.02229	0.318725
AL by BL	4.293250 x 10 ⁹	1	4.293250 x 10 ⁹	16.39060	0.000262
AL by BQ	1.583253 x 10 ⁹	1	1.583253 x 10 ⁹	6.04448	0.018892
AQ by BL	8.707672 x 10 ⁹	1	8.707672 x 10 ⁹	33.24381	0.000001
AQ by BQ	1.537907 x 10 ⁹	1	1.537907 x 10 ⁹	5.87136	0.020546
AL by CL	1.002612E+09	1	1.002612 x 10 ⁹	3.82773	0.058203
AL by CQ	3.283145 x 10 ⁸	1	3.283145 x 10 ⁸	1.25343	0.270313
AQ by CL	1.094861 x 10 ⁹	1	1.094861 x 10 ⁹	4.17992	0.048272
AQ by CQ	2.974626 x 10 ⁸	1	2.974626 x 10 ⁸	1.13564	0.293671
AL by DL	1.101892 x 10 ⁶	1	1.101892 x 10 ⁶	0.00421	0.948645
AL by DQ	2.547384 x 10 ⁷	1	2.547384 x 10 ⁷	0.09725	0.756950
AQ by DL	2.153129 x 10 ⁷	1	2.153129 x 10 ⁷	0.08220	0.775980
AQ by DQ	1.199792 x 10 ⁸	1	1.199792 x 10 ⁸	0.45805	0.502862
AL by EL	1.638347 x 10 ⁷	1	1.638347E+07	0.06255	0.803935
AL by EQ	1.029316 x 10 ⁷	1	1.029316 x 10 ⁷	0.03930	0.843977
AQ by EL	2.651743 x 10 ⁸	1	2.651743 x 10 ⁸	1.01237	0.321051
AQ by EQ	2.283306 x 10 ⁷	1	2.283306 x 10 ⁷	0.08717	0.769501
AL by FL	1.162827 x 10 ⁸	1	1.162827 x 10 ⁸	0.44394	0.509475
AQ by FL	1.478188 x 10 ⁸	1	1.478188 x 10 ⁸	0.56434	0.457401
BL by CL	8.713871 x 10 ⁸	1	8.713871 x 10 ⁸	3.32675	0.076472
BL by CQ	1.024645 x 10 ⁷	1	1.024645 x 10 ⁷	0.03912	0.844327
BQ by CL	3.629395 x 10 ⁸	1	3.629395 x 10 ⁸	1.38562	0.246871
BQ by CQ	1.906929 x 10 ⁷	1	1.906929 x 10 ⁷	0.07280	0.788841
BL by DL	4.962402 x 10 ⁸	1	4.962402 x 10 ⁸	1.89453	0.177194
BL by DQ	1.293380 x 10 ⁷	1	1.293380 x 10 ⁷	0.04938	0.825405
BQ by DL	2.039000 x 10 ⁸	1	2.039000 x 10 ⁸	0.77844	0.383472
BQ by DQ	8.740161 x 10 ⁶	1	8.740161 x 10 ⁶	0.03337	0.856083
BL by EL	1.000210 x 10 ⁸	1	1.000210 x 10 ⁸	0.38186	0.540501
BL by EQ	3.751910 x 10 ⁷	1	3.751910 x 10 ⁷	0.14324	0.707305
BQ by EL	7.821658 x 10 ⁷	1	7.821658 x 10 ⁷	0.29861	0.588125
BQ by EQ	4.833774 x 10 ⁷	1	4.833774 x 10 ⁷	0.18454	0.670059
BL by FL	1.247258 x 10 ⁸	1	1.247258 x 10 ⁸	0.47617	0.494586
BQ by FL	5.808624 x 10 ⁶	1	5.808624 x 10 ⁶	0.02218	0.882451
CL by DL	1.111300 x 10 ⁸	1	1.111300 x 10 ⁸	0.42427	0.518952
Error	9.429612 x 10 ⁹	36	2.619337 x 10 ⁸		
Total SS	1.957399 x 10 ¹¹	80			

A – Core insert1, B – Core Insert 2, C – Melting temperature, D – Injection pressure, E – Packing pressure and F – Cooling time, L – Linear and Q - Quadratic

Table 5.15: ANOVA table of ejection force for PA6

ANOVA; Var.: Var7; R-sqr=.83225; Adj.:.58062 (Spreadsheet_PA6) 6 3-level factors, 1 Blocks, 81 Runs; MS Residual=598305 x 10³ DV: Var7

Factor	SS	df	MS	F	p
(1)Var1 (L)	8.558118 x 10 ⁹	1	8.558118 x 10 ⁹	14.30393	0.000643
Var1 (Q)	1.417176 x 10 ¹⁰	1	1.417176 x 10 ¹⁰	23.68650	0.000029
(2)Var2 (L)	1.135344 x 10 ¹⁰	1	1.135344 x 10 ¹⁰	18.97599	0.000128
Var2 (Q)	9.162265 x 10 ⁹	1	9.162265 x 10 ⁹	15.31369	0.000447
(3)Var3 (L)	7.777133 x 10 ³	1	7.777133 x 10 ³	0.00001	0.997146
Var3 (Q)	1.803539 x 10 ⁹	1	1.803539 x 10 ⁹	3.01441	0.092148
(4)Var4 (L)	1.515259 x 10 ⁷	1	1.515259 x 10 ⁷	0.02533	0.874558
Var4 (Q)	1.278090 x 10 ⁸	1	1.278090 x 10 ⁸	0.21362	0.647073
(5)Var5 (L)	1.436500 x 10 ⁸	1	1.436500 x 10 ⁸	0.24009	0.627480
Var5 (Q)	1.231049 x 10 ⁸	1	1.231049 x 10 ⁸	0.20576	0.653176
(6)Var6 (L)	8.286855 x 10 ⁷	1	8.286855 x 10 ⁷	0.13851	0.712225
Var6 (Q)	6.419492 x 10 ⁷	1	6.419492 x 10 ⁷	0.10729	0.745379
1L by 2L	5.104117 x 10 ⁹	1	5.104117 x 10 ⁹	8.53096	0.006352
1L by 2Q	3.507643 x 10 ⁹	1	3.507643 x 10 ⁹	5.86263	0.021313
1Q by 2L	8.957241 x 10 ⁹	1	8.957241 x 10 ⁹	14.97102	0.000505
1Q by 2Q	3.785007 x 10 ⁹	1	3.785007 x 10 ⁹	6.32621	0.017114
1L by 3L	4.368671 x 10 ⁸	1	4.368671 x 10 ⁸	0.73017	0.399179
1L by 3Q	7.627658 x 10 ⁸	1	7.627658 x 10 ⁸	1.27488	0.267247
1Q by 3L	3.456789 x 10 ⁸	1	3.456789 x 10 ⁸	0.57776	0.452754
1Q by 3Q	1.336366 x 10 ⁹	1	1.336366 x 10 ⁹	2.23358	0.144837
1L by 4L	2.726065 x 10 ⁸	1	2.726065 x 10 ⁸	0.45563	0.504521
1L by 4Q	7.827658 x 10 ⁸	1	7.827658 x 10 ⁸	1.30831	0.261186
1Q by 4L	3.230522 x 10 ⁸	1	3.230522 x 10 ⁸	0.53995	0.467807
1Q by 4Q	8.510845 x 10 ⁸	1	8.510845 x 10 ⁸	1.42249	0.241763
1L by 5L	9.744059 x 10 ⁷	1	9.744059 x 10 ⁷	0.16286	0.689220
1L by 5Q	1.838651 x 10 ⁷	1	1.838651 x 10 ⁷	0.03073	0.861946
1Q by 5L	1.355226 x 10 ⁸	1	1.355226 x 10 ⁸	0.22651	0.637357
1Q by 5Q	8.933776 x 10 ⁷	1	8.933776 x 10 ⁷	0.14932	0.701745
1L by 6L	1.383729 x 10 ⁸	1	1.383729 x 10 ⁸	0.23127	0.633852
1L by 6Q	4.421210 x 10 ⁸	1	4.421210 x 10 ⁸	0.73896	0.396390
1Q by 6L	2.783803 x 10 ⁷	1	2.783803 x 10 ⁷	0.04653	0.830588
1Q by 6Q	7.178281 x 10 ⁸	1	7.178281 x 10 ⁸	1.19977	0.281544
2L by 3L	5.523667 x 10 ⁸	1	5.523667 x 10 ⁸	0.92322	0.343836
2L by 3Q	2.273730 x 10 ⁹	1	2.273730 x 10 ⁹	3.80028	0.060054
2Q by 3L	2.684228 x 10 ⁹	1	2.684228 x 10 ⁹	4.48638	0.042026
2Q by 3Q	3.577982 x 10 ⁹	1	3.577982 x 10 ⁹	5.98019	0.020151
2L by 4L	2.798066 x 10 ⁹	1	2.798066 x 10 ⁹	4.67665	0.038156
2L by 4Q	3.964628 x 10 ⁶	1	3.964628 x 10 ⁶	0.00663	0.935629
2Q by 4L	3.226666 x 10 ⁹	1	3.226666 x 10 ⁹	5.39301	0.026737
2Q by 4Q	2.602606 x 10 ⁷	1	2.602606 x 10 ⁷	0.04350	0.836109
2L by 5L	2.222639 x 10 ⁸	1	2.222639 x 10 ⁸	0.37149	0.546497
2L by 5Q	5.010137 x 10 ⁸	1	5.010137 x 10 ⁸	0.83739	0.366989
2Q by 5L	6.056660 x 10 ⁷	1	6.056660 x 10 ⁷	0.10123	0.752425

A – Core insert1, B – Core Insert 2, C – Melting temperature, D – Injection pressure, E – Packing pressure and F – Cooling time

Table 5.15: Continued

ANOVA; Var.:Var7; R-sqr=.83225; Adj.:.58062 (Spreadsheet_PA6) 6 3-level factors, 1 Blocks, 81 Runs; MS Residual=598305 x 10³ DV: Var7

Factor	SS	df	MS	F	p
2Q by 5Q	6.665040 x 10 ⁸	1	6.665040 x 10 ⁸	1.11399	0.299121
2L by 6L	1.479864 x 10 ⁸	1	1.479864 x 10 ⁸	0.24734	0.622353
2L by 6Q	6.123932 x 10 ⁶	1	6.123932 x 10 ⁶	0.01024	0.920046
2Q by 6L	3.040830 x 10 ⁸	1	3.040830 x 10 ⁸	0.50824	0.481068
2Q by 6Q	4.841700 x 10 ⁶	1	4.841700 x 10 ⁶	0.00809	0.928882
Error	1.914577 x 10 ¹⁰	32	5.983053 x 10 ⁸		
Total SS	1.141322 x 10 ¹¹	80			

A – Core insert1, B – Core Insert 2, C – Melting temperature, D – Injection pressure, E – Packing pressure and F – Cooling time

Table 5.16, 5.17 and 5.18 below show the regression coefficient of ejection force for HIPS, ABS and PA6. These tables are used to produce the mathematical model of the resin used in this study.

Table 5.16: Regression coefficient table of ejection force for HIPS

Regr. Coefficients; Var.:Var7; R-sqr=.91747; Adj.:.81661 (Spreadsheet_PS) 1 2-level factors, 5 3-level factors, 81 Runs DV: Var7; MS Residual=999806 x 10³

Factor	Regressn - Coeff.	Std.Err.	t(36)	p
Mean/Interc.	-8102506	8365260	-0.96859	0.339213
(1) A (L)	-9591112	10217946	-0.93865	0.354164
A (Q)	3494937	3110126	1.12373	0.268566
(2) B (L)	-2825070	10217946	-0.27648	0.783760
B (Q)	858432	3110126	0.27601	0.784117
(3) C (L)	79176	74440	1.06361	0.294586
C (Q)	-181	178	-1.01441	0.317159
(4) D (L)	26850	95364	0.28155	0.779898
D (Q)	-129	759	-0.16948	0.866364
(5) E (L)	-25632	60418	-0.42425	0.673911
E (Q)	256	584	0.43912	0.663196
(6) F (L)	-740	17539	-0.04220	0.966575
AL by BL	-41360	26915	-1.53670	0.133110
AL by BQ	44193	8192	5.39440	0.000004
AQ by BL	19460	8192	2.37538	0.022977
AQ by BQ	-14821	2494	-5.94366	0.000001
AL by CL	110398	90914	1.21431	0.232536
AL by CQ	-258	218	-1.18215	0.244894
AQ by CL	-40123	27672	-1.44993	0.155735
AQ by CQ	94	66	1.41538	0.165550
AL by DL	-90106	114648	-0.78594	0.437048

Table 5.16: Continued.

Regr. Coefficients; Var.:Var7; R-sqr=.91747; Adj.:.81661 (Spreadsheet_PS) 1 2-level factors, 5 3-level factors, 81 Runs DV: Var7; MS Residual=999806 x 10³

Factor	Regressn - Coeff.	Std.Err.	t(36)	p
AL by DQ	754	930	0.81060	0.422925
AQ by DL	28910	34896	0.82844	0.412879
AQ by DQ	-240	283	-0.84967	0.401124
AL by EL	16274	67943	0.23953	0.812056
AL by EQ	-162	658	-0.24587	0.807181
AQ by EL	-3872	20680	-0.18722	0.852542
AQ by EQ	39	200	0.19701	0.844928
AL by FL	1213	20628	0.05880	0.953439
AQ by FL	808	6279	0.12876	0.898263
BL by CL	20346	90914	0.22380	0.824179
BL by CQ	-48	218	-0.21959	0.827430
BQ by CL	-4576	27672	-0.16535	0.869592
BQ by CQ	11	66	0.16117	0.872861
BL by DL	34382	114648	0.29989	0.765982
BL by DQ	-290	930	-0.31168	0.757082
BQ by DL	-15976	34896	-0.45781	0.649842
BQ by DQ	134	283	0.47313	0.638974
BL by EL	-9256	67943	-0.13623	0.892397
BL by EQ	87	658	0.13171	0.895950
BQ by EL	2222	20680	0.10746	0.915018
BQ by EQ	-21	200	-0.10462	0.917258
BL by FL	-8890	20628	-0.43096	0.669064
BQ by FL	2437	6279	0.38819	0.700162
CL by DL	-57	89	-0.63876	0.527020

A – Core insert1, B – Core Insert 2, C – Melting temperature, D – Injection pressure, E – Packing pressure and F – Cooling time, L – Linear and Q - Quadratic

Table 5.17: Regression coefficient table of ejection force for ABS

Regr. Coefficients; Var.:Var7; R-sqr=.95183; Adj.:.89295 (Spreadsheet_ABS) 1 2-level factors, 5 3-level factors, 81 Runs DV: Var7; MS Residual=261934 x 10³

Factor	Regressn - Coeff.	Std.Err.	t(36)	p
Mean/Interc.	1119801	1498810	0.74713	0.459839
(1) A (L)	-2115677	1823893	-1.15998	0.253693
A (Q)	702775	555154	1.26591	0.213677
(2) B (L)	-578778	1823893	-0.31733	0.752826
B (Q)	130371	555154	0.23484	0.815666
(3) C (L)	-4134	13266	-0.31161	0.757136
C (Q)	8	30	0.25390	0.801018
(4) D (L)	-1711	7999	-0.21396	0.831783
D (Q)	-1	58	-0.02424	0.980799
(5) E (L)	-2538	7328	-0.34633	0.731110
E (Q)	22	69	0.31155	0.757179
(6) F (L)	-15231	8839	-1.72317	0.093439
AL by BL	8845	13776	0.64207	0.524893

Table 5.17: Continued.

Regr. Coefficients; Var.:Var7; R-sqr=.95183; Adj.:.89295 (Spreadsheet_ABS) 1 2-level factors, 5 3-level factors, 81 Runs DV: Var7; MS Residual=261934 x 10³

Factor	Regressn - Coeff.	Std.Err.	t(36)	p
AL by BQ	9024	4193	2.15195	0.038183
AQ by BL	319	4193	0.07618	0.939695
AQ by BQ	-3093	1276	-2.42309	0.020546
AL by CL	15443	16205	0.95296	0.346967
AL by CQ	-34	37	-0.92238	0.362473
AQ by CL	-5418	4932	-1.09839	0.279328
AQ by CQ	12	11	1.06566	0.293671
AL by DL	7364	8970	0.82091	0.417100
AL by DQ	-60	71	-0.83633	0.408484
AQ by DL	-1828	2730	-0.66935	0.507542
AQ by DQ	15	22	0.67680	0.502862
AL by EL	-2029	8319	-0.24395	0.808655
AL by EQ	26	79	0.32581	0.746453
AQ by EL	597	2532	0.23584	0.814892
AQ by EQ	-7	24	-0.29525	0.769501
AL by FL	7680	10558	0.72737	0.471702
AQ by FL	-2414	3214	-0.75122	0.457401
BL by CL	4433	16205	0.27354	0.786001
BL by CQ	-11	37	-0.28732	0.775517
BQ by CL	-1215	4932	-0.24623	0.806905
BQ by CQ	3	11	0.26982	0.788841
BL by DL	-4006	8970	-0.44659	0.657849
BL by DQ	30	71	0.41803	0.678408
BQ by DL	625	2730	0.22897	0.820189
BQ by DQ	-4	22	-0.18267	0.856083
BL by EL	3271	8319	0.39322	0.696477
BL by EQ	-33	79	-0.41754	0.678762
BQ by EL	-1011	2532	-0.39918	0.692122
BQ by EQ	10	24	0.42958	0.670059
BL by FL	6971	10558	0.66020	0.513328
BQ by FL	-479	3214	-0.14892	0.882451
CL by DL	10	15	0.65136	0.518952

A – Core insert1, B – Core Insert 2, C – Melting temperature, D – Injection pressure, E – Packing pressure and F – Cooling time, L – Linear and Q - Quadratic

Table 5.18: Regression coefficient table of ejection force for PA6

Regr. Coefficients; Var.:Var7; R-sqr=.83225; Adj.:.58062 (Spreadsheet_PA6) 6 3-level factors, 1 Blocks, 81 Runs; MS Residual=598305 x 10³ DV: Var7

Factor	Regressn - Coeff.	Std.Err.	t(32)	p
Mean/Interc.	2736331	4643412	0.58929	0.559802
(1) A (L)	-9736619	5687531	-1.71192	0.096588
A (Q)	2877944	1731164	1.66243	0.106192
(2) B (L)	-6942703	5687531	-1.22069	0.231123
B (Q)	1874824	1731164	1.08298	0.286908

Table 5.18: Continued.

Regr. Coefficients; Var.:Var7; R-sqr=.83225; Adj.:.58062 (Spreadsheet_PA6) 6 3-level factors, 1 Blocks, 81 Runs; MS Residual=598305 x 10³ DV: Var7

Factor	Regressn - Coeff.	Std.Err.	t(32)	p
(3) C (L)	-12280	14078	-0.87227	0.389561
C (Q)	22	25	0.87986	0.385497
(4) D (L)	951	7873	0.12082	0.904590
D (Q)	-1	87	-0.01049	0.991696
(5) E (L)	1787	9564	0.18686	0.852947
E (Q)	-23	132	-0.17710	0.860546
(6) F (L)	-120646	469068	-0.25720	0.798668
F (Q)	3504	13028	0.26897	0.789683
AL by BL	-20377	20821	-0.97871	0.335065
AL by BQ	14676	6337	2.31579	0.027133
AQ by BL	8917	6337	1.40698	0.169071
AQ by BQ	-4852	1929	-2.51520	0.017114
AL by CL	27173	17244	1.57578	0.124912
AL by CQ	-49	31	-1.57036	0.126167
AQ by CL	-7890	5249	-1.50325	0.142580
AQ by CQ	14	9	1.49452	0.144837
AL by DL	11006	9643	1.14128	0.262220
AL by DQ	-118	107	-1.10085	0.279173
AQ by DL	-3625	2935	-1.23495	0.225842
AQ by DQ	39	33	1.19268	0.241763
AL by EL	-5136	11714	-0.43842	0.664027
AL by EQ	77	161	0.47923	0.635032
AQ by EL	1234	3565	0.34604	0.731577
AQ by EQ	-19	49	-0.38642	0.701745
AL by FL	649846	574542	1.13107	0.266432
AL by FQ	-18044	15957	-1.13078	0.266552
AQ by FL	-192131	174878	-1.09866	0.280115
AQ by FQ	5320	4857	1.09534	0.281544
BL by CL	43957	17244	2.54913	0.015794
BL by CQ	-78	31	-2.50559	0.017506
BQ by CL	-13008	5249	-2.47842	0.018659
BQ by CQ	23	9	2.44544	0.020151
BL by DL	4154	9643	0.43077	0.669524
BL by DQ	-29	107	-0.26696	0.791215
BQ by DL	-1126	2935	-0.38363	0.703792
BQ by DQ	7	33	0.20857	0.836109
BL by EL	-12128	11714	-1.03533	0.308276
BL by EQ	167	161	1.03515	0.308360
BQ by EL	3824	3565	1.07244	0.291546
BQ by EQ	-52	49	-1.05546	0.299121
BL by FL	108144	574542	0.18823	0.851888
BL by FQ	-3202	15957	-0.20068	0.842219
BQ by FL	-13730	174878	-0.07851	0.937908
BQ by FQ	437	4857	0.08996	0.928882

A – Core insert1, B – Core Insert 2, C – Melting temperature, D – Injection pressure, E – Packing pressure and F – Cooling time, L – Linear and Q - Quadratic

5.4 Analysis Method

In analysing the result, Taguchi had introduced the use of signal-to-noise (S/N) ratio to determine the quality of characteristics in products. The S/N ratio characteristics can be divided into three categories; the-nominal-the-best, the-smaller-the-better and the-larger-the-better while the quality characteristics is continuous. The S/N ratio is a measure of performance aimed at developing products and processes insensitive to noise factors (Oktem et al., 2007). The aim of study is to minimise the ejection force within the process parameters, the-smaller-the-better method has been selected. The MSD for the-smaller-the-better written as;

$$\eta = -10 \log(M.S.D), \quad (5.1)$$

Where $M.S.D = \frac{1}{n} \sum_{i=1}^n y_i^2$

$$M.S.D. = \frac{1}{N} \left(\sum_{i=1}^n Y_i^2 \right), \quad (5.2)$$

Where M.S.D is the mean square deviation, Y_i the observation or data and n is the number of tests in a trial.

5.5 Effect of machining parameter on ejection force, F_e

In this study, decreasing in surface roughness may result in increasing the ejection force. At optimum condition, the levels of machining parameter found are intended to produce less ejection force as shown in Figure 5.25, 5.26 and 5.27. Table

5.19, 5.20, 5.21, 5.22, 5.23 and 5.24 show the value ejection force recorded based on the machine parameters used during the experiment.

In the case of injection pressure as shown in Figure 5.25, 5.26 and 5.27, as the injection of pressure becomes high, the injection force also shows an increase except for PA6, in which, the melting temperature is at 300 °C (Figure 5.27c). At this temperature, the viscosity of subjected resin is high. For HIPS, an increase in injection pressure resulted to an increase of ejection force except at high temperature (220 °C) as shown in Figure 5.27a. The same phenomenon can be observed for ABS, where the increased in injection pressure showed an increasing in ejection force except for the surface roughness of 6.32 μm (Figure 5.27b). For PA6; behaved the same result as HIPS and ABS except at temperature 300 °C, the ejection force was decreasing (Figure 5.27c). This indicates that higher melting temperature will influence the ejection force of the moulding due to high viscosity which causes higher pressure losses (Menges et al., 2001). The higher injection pressure loss, the more energy is dissipated during the injection as can be seen in Figure 5.27c for PA6.

In the case of packing pressure, generally high packing pressures resulted in the ejection force which can be seen in Figure 5.25, 5.26 and 5.27. It is desirable to keep from 80 % - 100 % of the pressure applied to fill the moulding. However, the packing pressure can be much higher or lower (Jay shoemaker, 2006).

Table 5.19: Ejection force for injection pressure and melting temperature for $S1_x + S1_y$ surface roughness combinations

Resin	Melting Temperature	Injection Pressure x 10^3 (MPa)			
		55	67	69	Error
PS	195°C	255	292	334	22.8
	200°C	337	330	336	2.2
	220°C	327	288	275	15.6
		50	69	77	Error
ABS	200°C	246	257	262	4.7
	210°C	250	276	242	10.3
	220°C	266	278	295	8.4
		32	42	57	Error
PA6	250°C	98	114	128	8.7
	265°C	99	104	106	2.1
	300°C	77	101	95	7.2

Table 5.20: Ejection force for melting temperature and packing pressure for $S1_x + S1_y$ surface roughness combinations

Resin	Melting Temperature	Packing Pressure x 10^3 (MPa)			
		45	56	59	Error
PS	195°C	255	292	334	22.8
	200°C	330	336	337	2.2
	220°C	275	327	288	15.6
		41	56	65	Error
ABS	200°C	246	267	262	6.3
	210°C	276	242	250	10.3
	220°C	295	266	278	8.4
		26	35	46	Error
PA6	250°C	98	114	128	8.7
	265°C	104	106	99	2.1
	300°C	95	77	101	7.2

Table 5.21: Ejection force for injection pressure and melting temperature for $S2_x + S2_y$ surface roughness combinations

Resin	Melting Temperature	Injection Pressure x 10^3 (MPa)			
		55	67	69	Error
PS	195°C	162	177	184	6.5
	200°C	188	200	214	7.5
	220°C	212	224	217	3.5
		50	69	77	Error
ABS	200°C	141	152	168	7.8
	210°C	174	164	167	3.0
	240°C	174	173	170	1.2
		32	42	57	Error
PA6	250°C	63	116	133	21.1
	265°C	158	176	166	5.2
	300°C	78	136	152	22.5

Table 5.22: Ejection force for packing pressure and melting temperature for $S2_x + S2_y$ surface roughness combinations

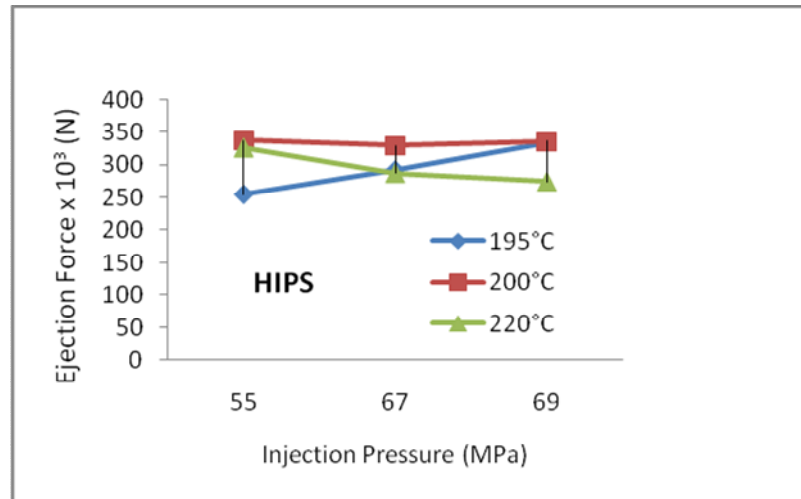
Resin	Melting Temperature	Packing Pressure x 10^3 (MPa)			
		45	56	59	Error
PS	195°C	162	177	184	6.5
	200°C	200	214	188	7.5
	220°C	217	212	224	3.5
		41	56	65	Error
ABS	200°C	141	152	168	7.8
	210°C	164	167	173	2.6
	240°C	170	174	173	1.2
		26	35	46	Error
PA6	250°C	63	116	134	21.3
	265°C	176	166	158	5.2
	300°C	152	78	136	22.5

Table 5.23: Ejection force for Injection pressure and melting temperature for S3_x + S3_y surface roughness combinations

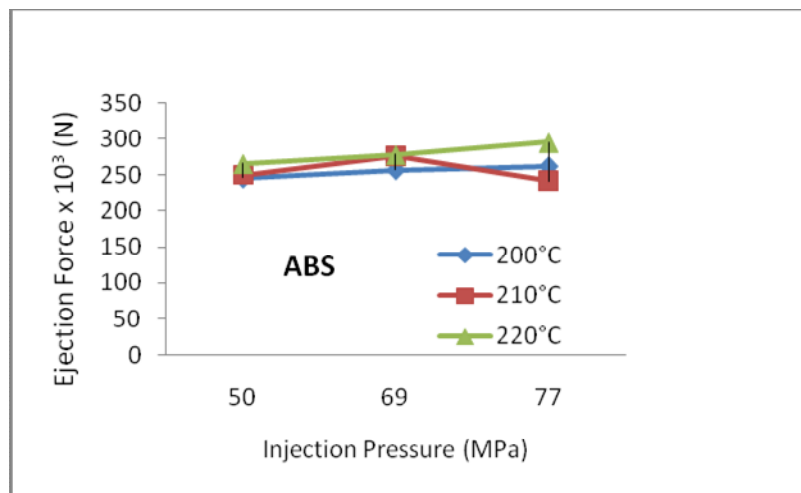
Resin	Melting Temperature	Injection Pressure x 10 ³ (MPa)			
		55	67	69	Error
HIPS	195°C	99	121	150	14.8
	200°C	128	140	164	10.6
	220°C	90	96	77	5.6
		50	69	77	Error
ABS	200°C	100	111	110	3.5
	210°C	111	101	97	4.2
	240°C	134	121	103	9.0
		32	42	57	Error
PA6	250°C	93	98	98	1.7
	265°C	91	85	91	2.0
	300°C	88	91	88	1.0

Table 5.24: Ejection force for packing pressure and melting temperature for S3_x + S3_y surface roughness combinations

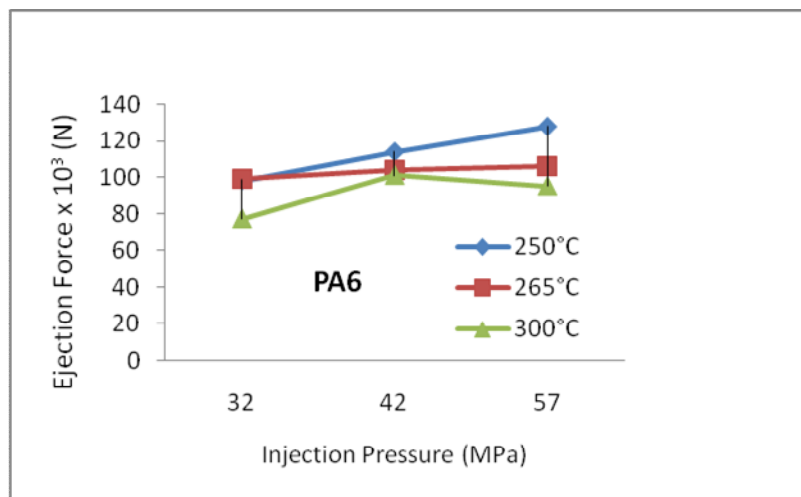
Resin	Melting Temperature	Packing Pressure x 10 ³ (MPa)			
		45	56	59	Error
PS	195°C	99	121	150	14.8
	200°C	140	164	128	10.6
	220°C	77	90	96	5.6
		41	56	65	Error
ABS	200°C	100	111	110	3.5
	210°C	101	97	111	4.2
	240°C	103	134	121	9.0
		26	35	46	Error
PA6	250°C	93	98	98	1.7
	265°C	85	91	91	2.0
	300°C	87	88	91	1.2



(a) HIPS

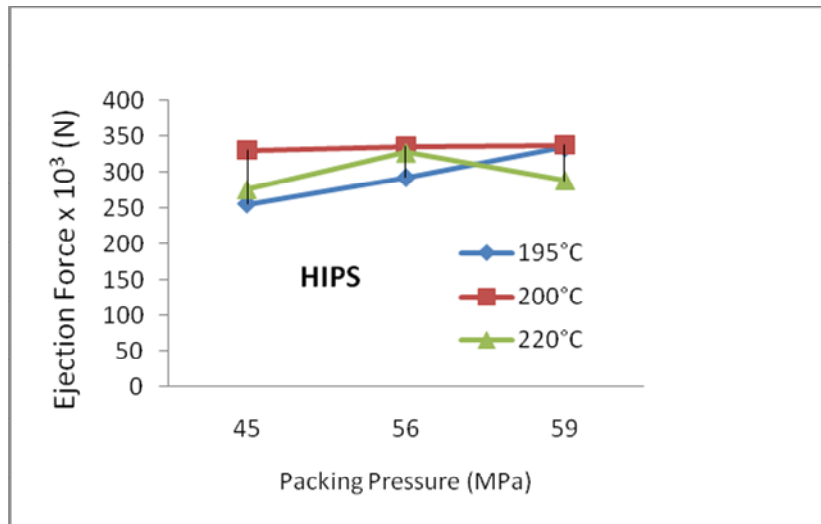


(b) ABS

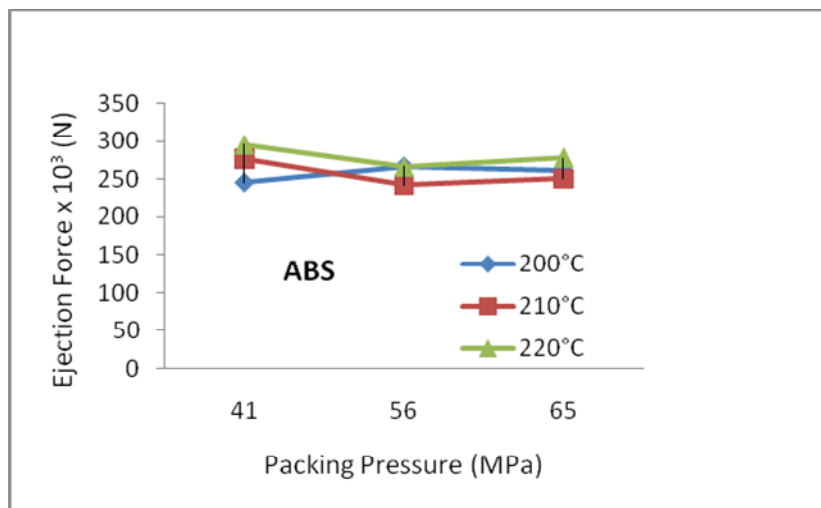


(c)

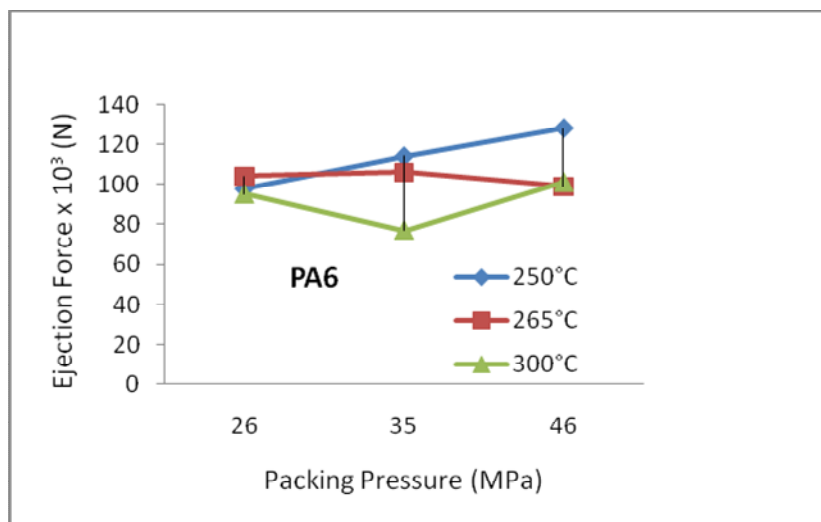
Figure 5.25: (a) HIPS, (b) ABS and (c) PA6. Ejection force versus injection pressure for surface roughness S1x + S1y



(a)

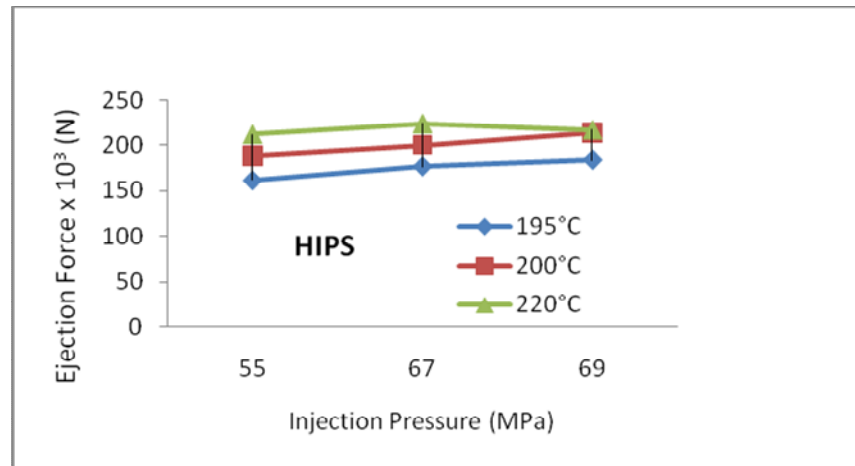


(b)

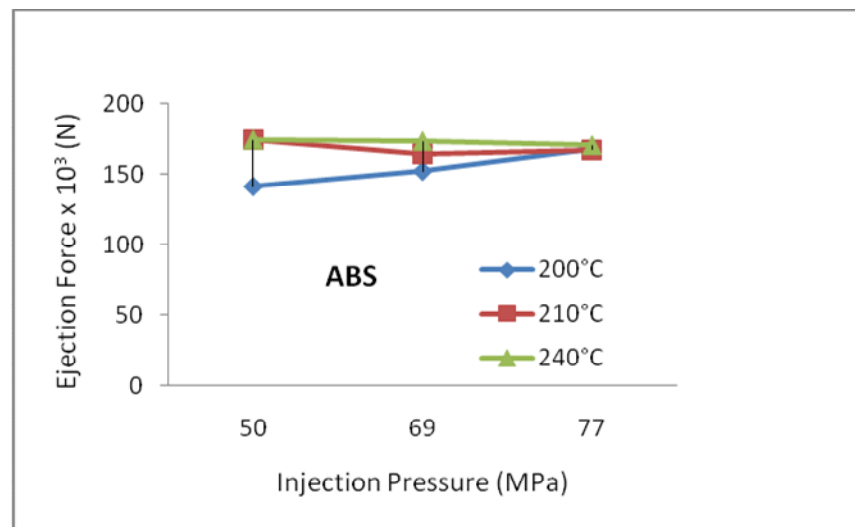


(c)

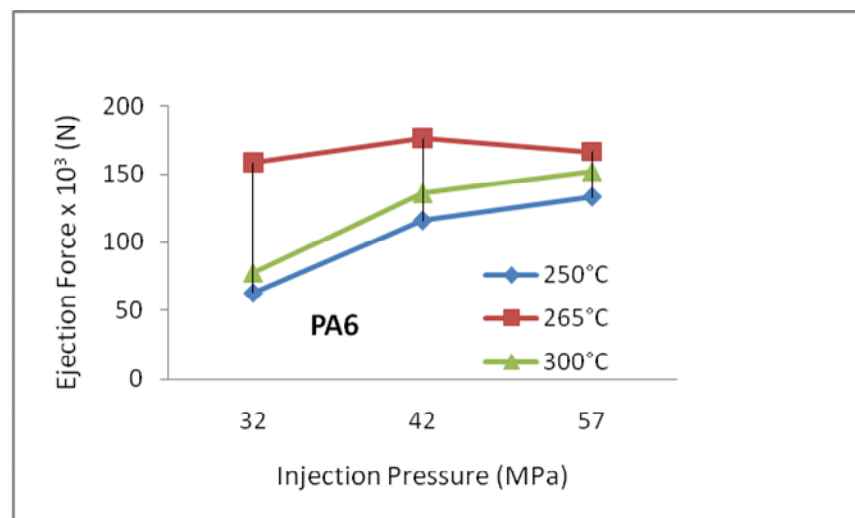
Figure 5.26: (a) HIPS, (b) ABS and (c) PA6. Ejection force versus packing pressure for surface roughness S1x + S1y



(a)

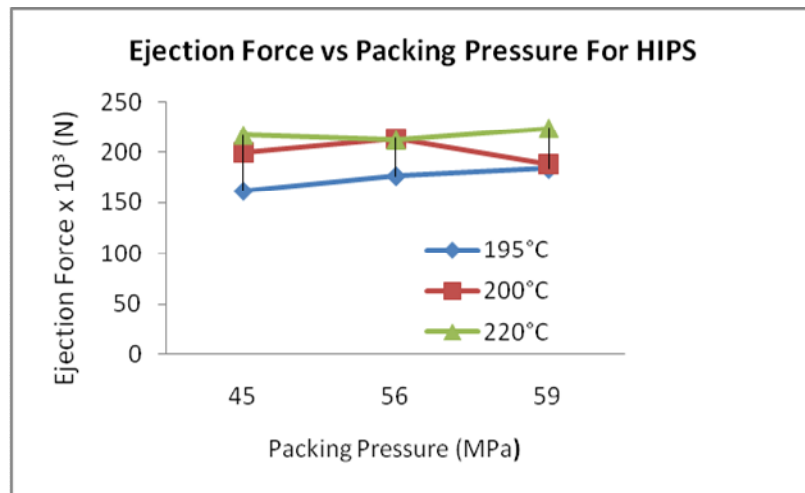


(b)

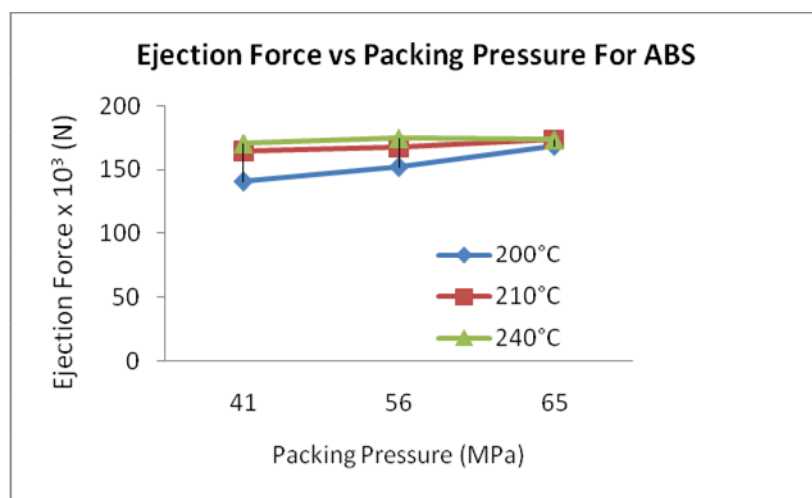


(c)

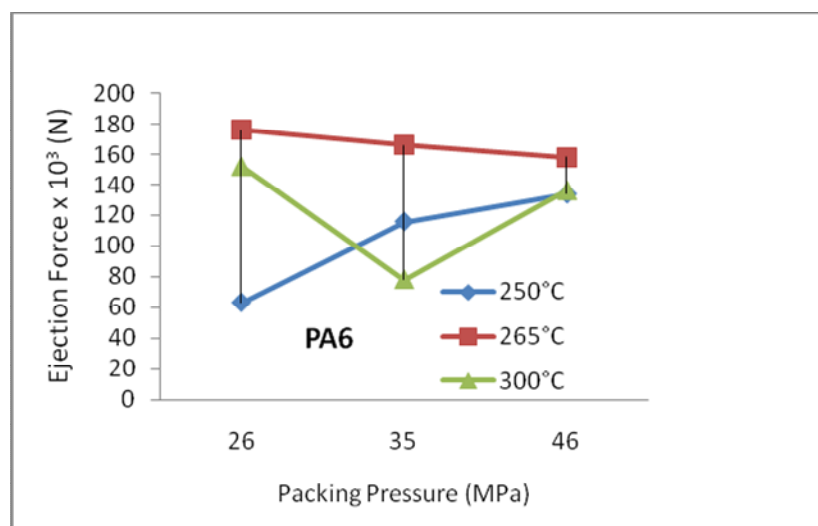
Figure 5.27: (a) HIPS, (b) ABS and (c) PA6. Ejection force versus injection pressure for surface roughness S2x + S2y



(a)

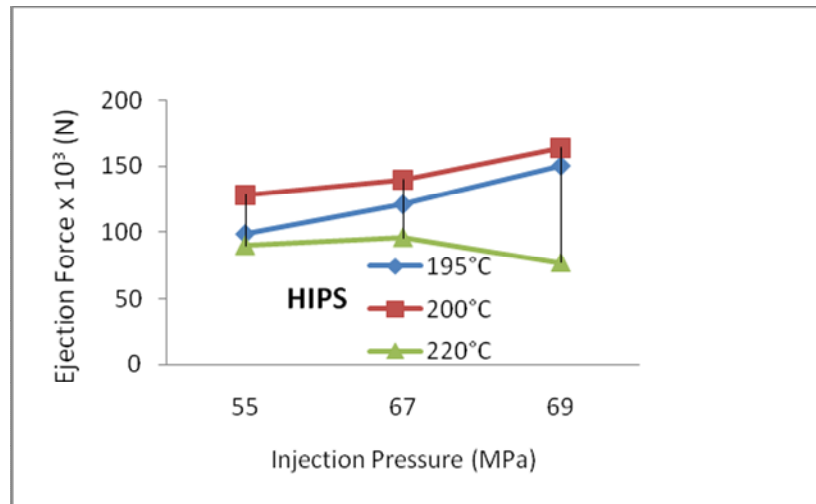


(b)

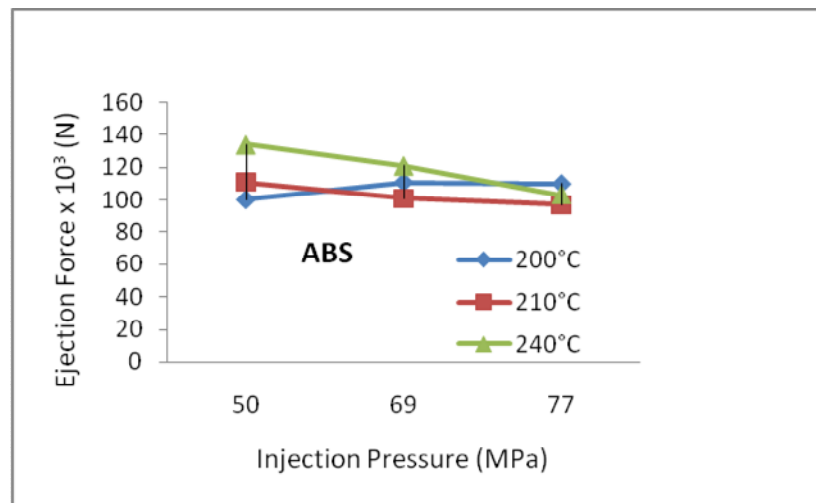


(c)

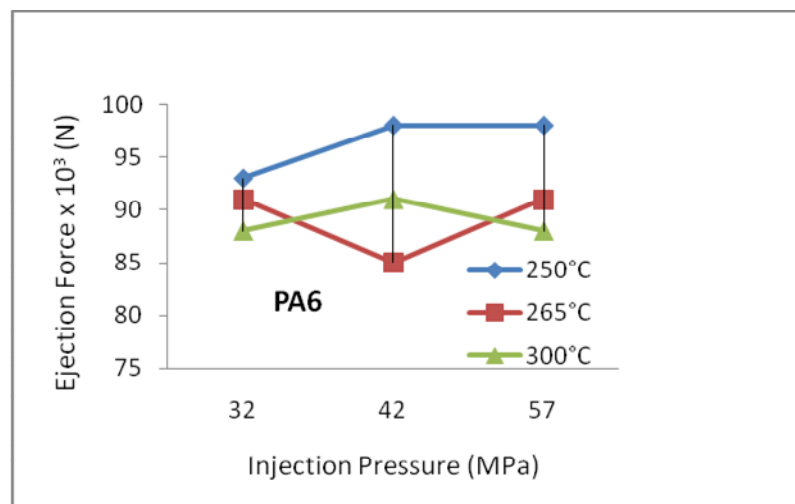
Figure 5.28: (a) HIPS, (b) ABS and (c) PA6. Ejection force versus packing pressure for surface roughness S2x + S2y



(a)

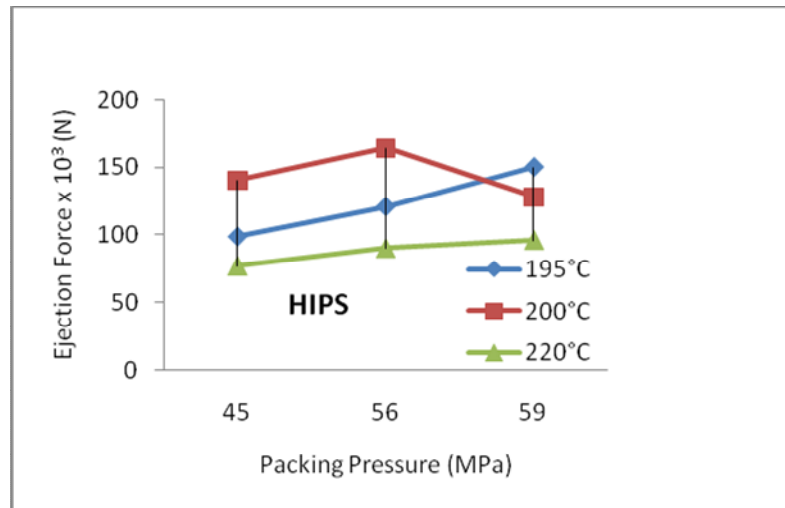


(b)

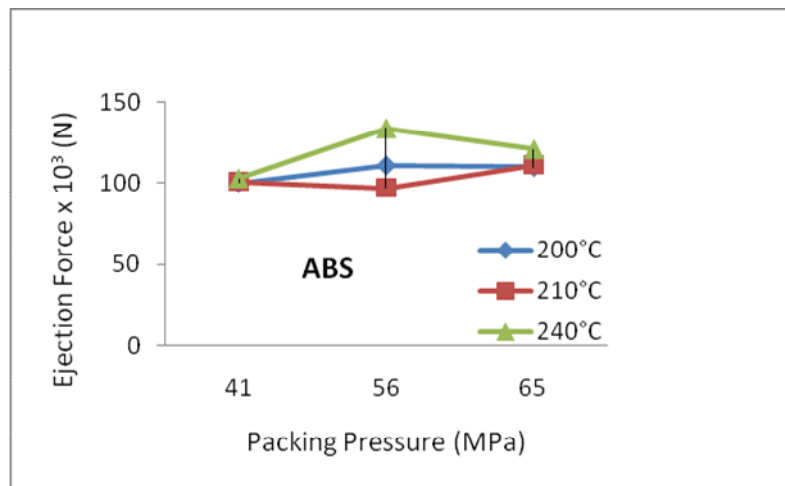


(c)

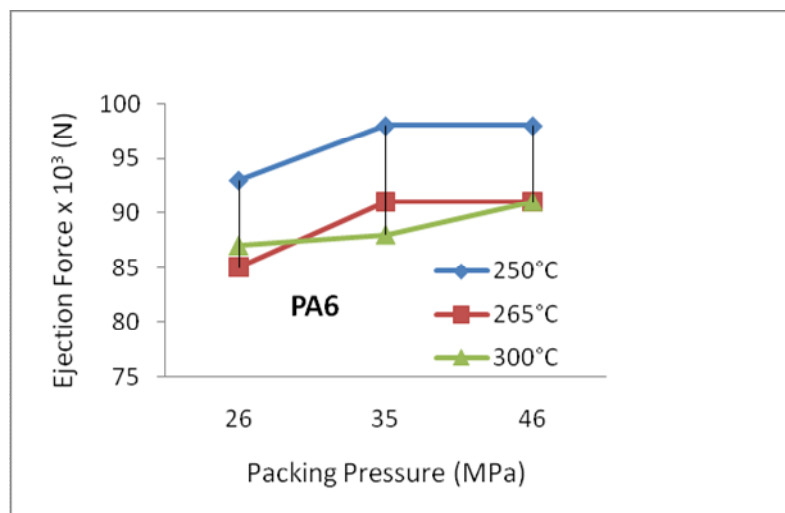
Figure 5.29: (a) HIPS, (b) ABS and (c) PA6. Ejection force versus injection pressure for surface roughness S3x + S3y



(a)



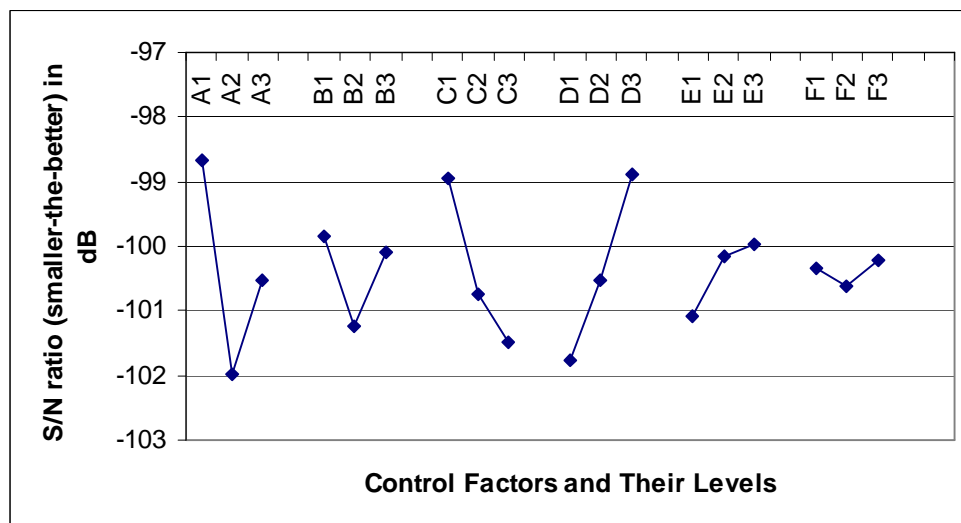
(b)



(c)

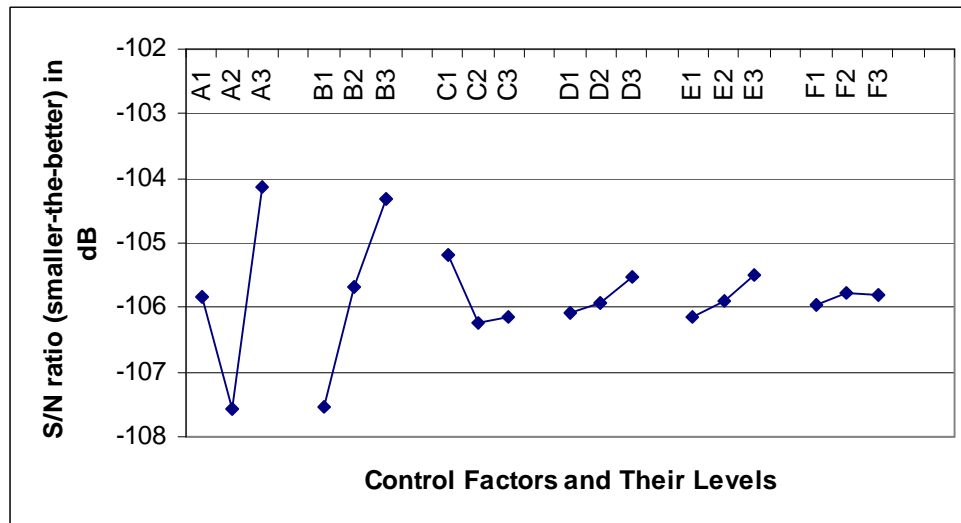
Figure 5.30: (a) HIPS, (b) ABS and (c) PA6. Ejection force versus packing pressure for surface roughness S3x + S3y

All of the independent factors were optimised simultaneously through Taguchi method. The optimum condition represents the combination of control factor levels that is expected to produce the best performance. The average S/N ratio for each factor level indicates the relative effects of the various factors on ejection force generated. Taguchi analysis observes that the bigger value of mean S/N ratio will demonstrate a better quality characteristic of a product. Therefore, based on the average S/N ratio for each factor level as illustrated in Figure 5.31, 5.32 and 5.33, the optimum machining performance for ejection force was obtained at all levels. The optimum parametric combination for HIPS is A1B1C1D3E3F3. Meanwhile for ABS and PA6 were A3B3C1D3E3F2 and A3B3C1D3E2F3 respectively. Appendix K.1, K.2 and K.3 show the tabulated data for orthogonal array, L_{81} of HIPS, ABS and PA6 to obtain the optimum machining performance. The reason why this analysis is performed is to optimize value according to the average signal-noise ratio value and its control factor for three levels of the material used. This analysis can reduce the number of experiment. The analysis is carried out by using L_{81} orthogonal array.



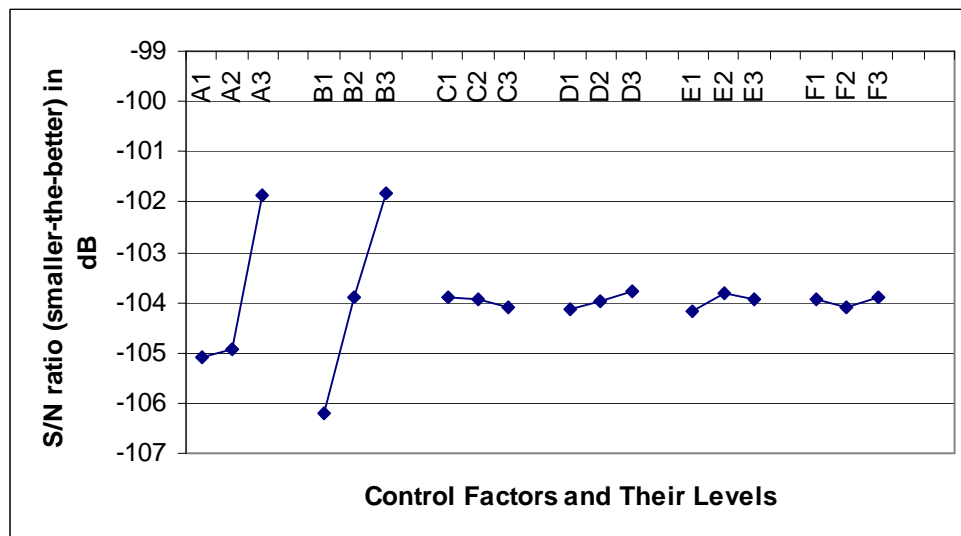
A – Core insert 1, B – Core insert 2, C – Melting temperature,
D – Injection pressure, E – Packing pressure and F – Cooling time

Figure 5.31: Average S/N ratio by control factor and their levels for HIPS



A – Core insert 1, B – Core insert 2, C – Melting temperature,
D – Injection pressure, E – Packing pressure and F – Cooling time

Figure 5.32: Average S/N ratio by control factor and their levels for ABS



A – Core insert 1, B – Core insert 2, C – Melting temperature,
D – Injection pressure, E – Packing pressure and F – Cooling time

Figure 5.33: Average S/N ratio by control factor and their levels for PA6

5.6 Mathematical Models

To predict ejection force, the responses's regression model was generated as shown in Table 5.10, 5.11 and 5.12. The generated model was fitted to the experiment data to predict the optimum condition. The interaction model was also considered.

$$Y(x) = \beta_0 + \sum \beta_i x_i + \sum \beta_{ii} x_i^2 + \sum \sum \beta_{ij} x_i x_j \quad (5.3)$$

where the dependent variable $Y(x)$ represents the value of F_e predicted; β_0 is constant, β_i are the first order or linear effect coefficients, β_{ii} are the second order or quadratic effect coefficients and β_{ij} are the interaction effect coefficients.

The model for HIPS was;

$$F_{eHIPS} = -8102506 + AB + AC + AB^2 + AC^2 + A^2C + A^2B^2 + A^2C^2 \quad (5.4)$$

Substitutes the above equation, the model of ejection force for HIPS as follow;

Mathematical model of ejection force for HIPS;

$$F_{eHIPS} = -8102506 - 41360x_1x_2 + 110398x_1x_3 + 44193x_1x_2^2 - 258x_1x_3^2 + 19460x_1^2x_2 - 14821x_1^2x_2^2 + 94x_1^2x_3^2 \quad (5.5)$$

The model for ABS was;

$$F_{eABS} = 1119801 + A + B + F + AB^2 + AC^2 + A^2B^2 + A^2C^2 \quad (5.6)$$

Substitutes the above equation, the model of ejection force for HIPS as follow;

Mathematical model ejection force for ABS;

$$F_{eABS} = 2736331 - 2115677x_1 - 578778x_2 - 152316x_6 + 702775x_1^2 - 5418x_1^2 x_3 + 12 x_1^2 x_3^2 \quad (5.7)$$

The model for PA6 was;

$$F_{ePA6} = 2736331 + A + E^2 + AB^2 + BC + BC^2 + B^2C + A^2B^2 \quad (5.8)$$

Where A is the core insert1, B is the Core Insert 2, C is the melting temperature, D is the injection pressure and E is the packing pressure and F is the cooling time.

Mathematical model ejection force for PA6;

$$F_{ePA6} = 2736331 - 9736619x_1 - 23x_5^2 + 14676x_1x_2^2 + 43957x_2x_3 - 78x_2x_3^2 - 13008x_2^2x_3 - 485x_1^2x_2^2 \quad (5.9)$$

Where x_1 is the core insert 1 (μm), x_2 is the core insert 2, x_3 (μm) is the melting temperature ($^{\circ}\text{C}$), x_4 is the injection pressure (MPa), x_5 is the packing pressure (MPa) and x_6 is the cooling time (s).

To justify the normal distribution assumption, Normal Probability plot can be used and the graph can be generated from the STATISTICA. Normal distribution is accepted as the normal values are scattered nearby to the solid line. Figure 5.34, 5.35 and 5.36 showed the Normal Probability plot for the dependent variables in the experiment.

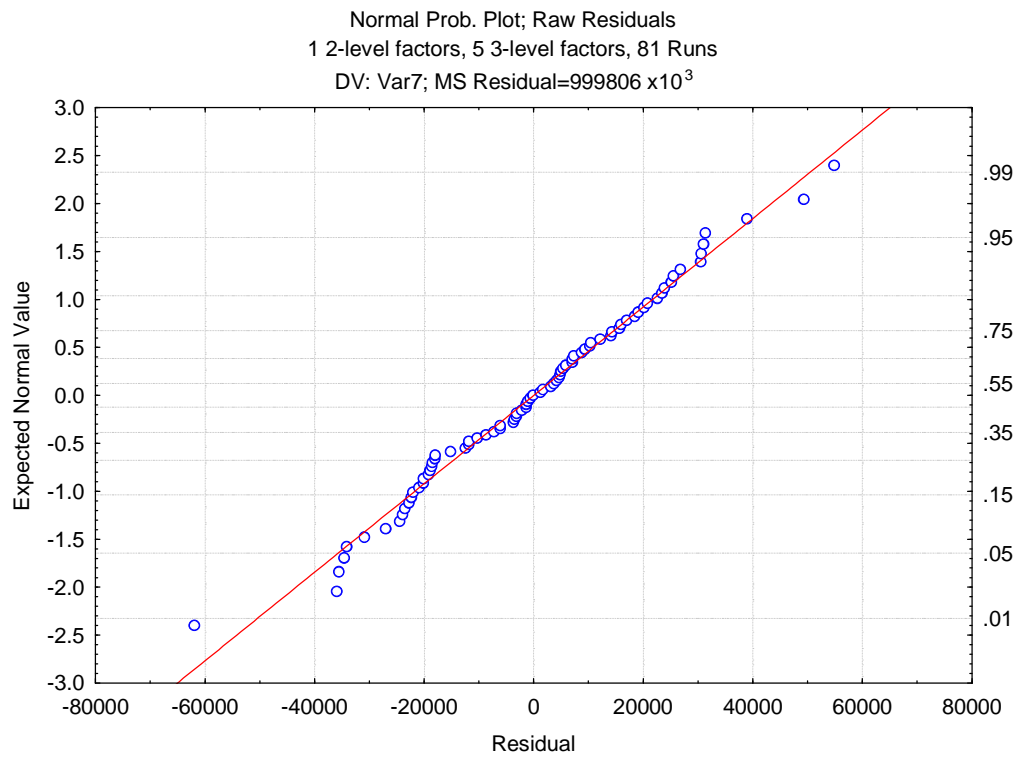


Figure 5.34: Normal probability plot of ejection force for HIPS

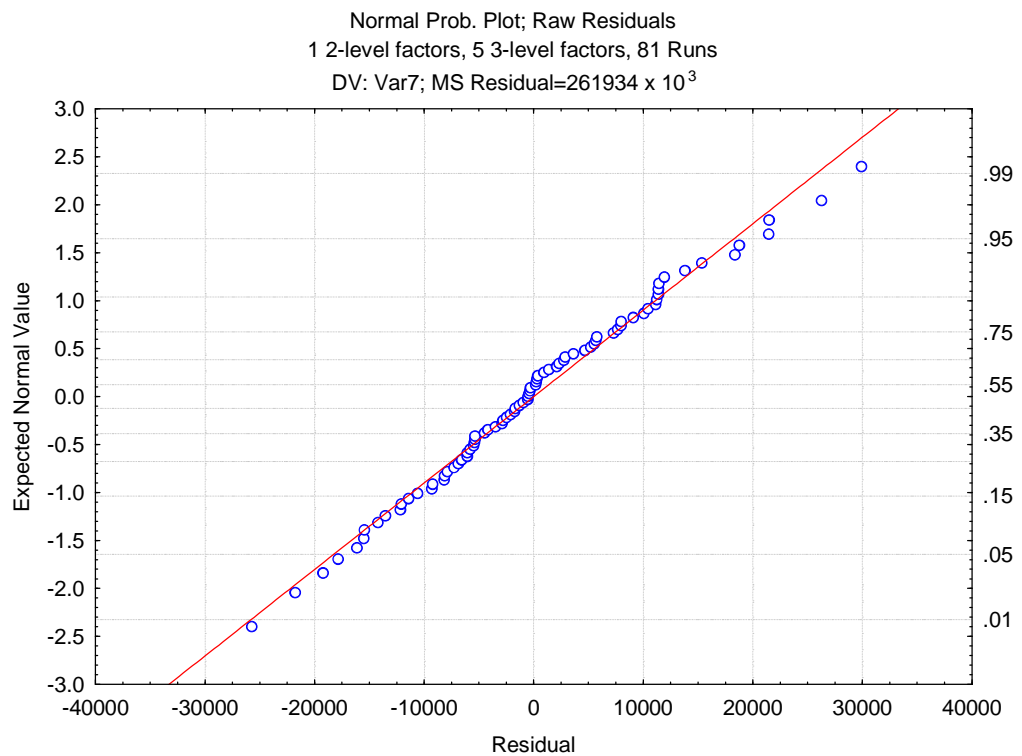


Figure 5.35: Normal probability plot of ejection force for ABS

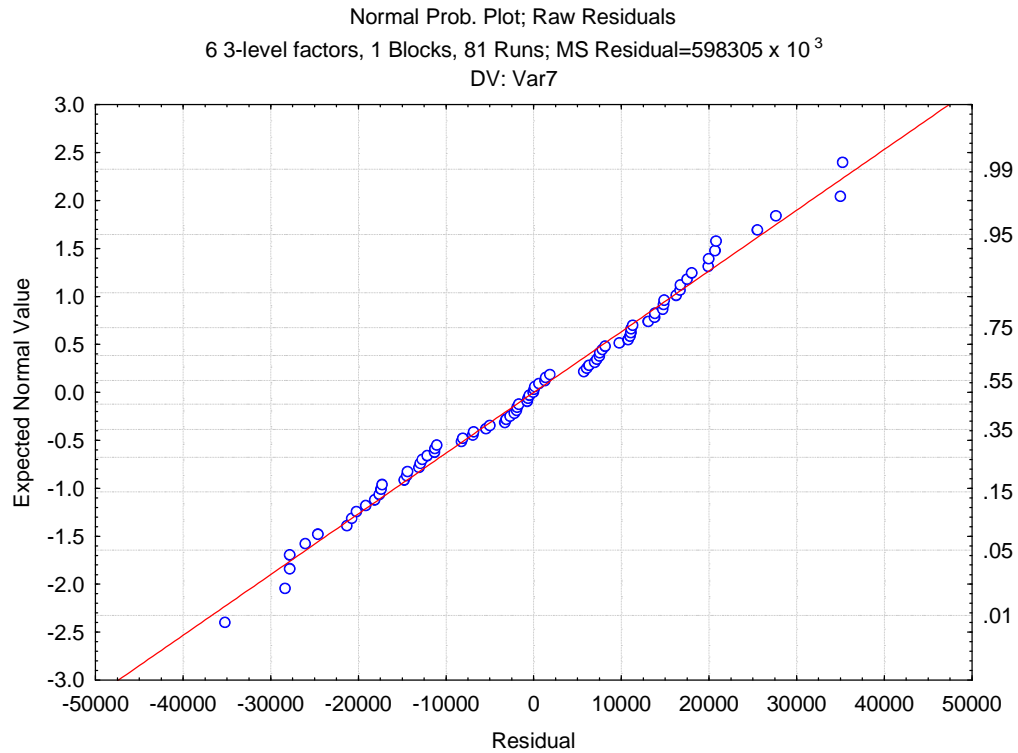


Figure 5.36: Normal probability plot of ejection force for PA6

5.7 Summary

This section explained the experimental work of this research and how the analysis is performed by using Statistica Release 7 software. The relationship between the ejection force and the level of different surface roughness are discussed and elaborated thoroughly in this chapter. In such a case, a mathematical model for HIPS, ABS and PA6 are developed further future analysis. The optimizations of parameters are later given using ANOVA and regression analysis.

CHAPTER 6

CONCLUSIONS AND RECOMMENDATIONS

6.1 Conclusion

The following conclusions are drawn based on the results throughout the study on mould filling and ejection of moulding for HIPS, ABS and PA6. The relationship of surface roughness and ejection force generated was analysed. It can be observed that the surface roughness of core substantially influences the ejection force. The following results obtained lead to several conclusions that;

1. The usage of simulation software package enables the prediction of initial result for filling and pressure distribution prior to the experimental works. By utilising filling analysis, the processing characteristics of an injection mould can be investigated and optimized at the design stage. This will be improved in quality part of weld lines, eliminating gas traps, balancing pressure drops and reducing stress levels.
2. In the simulation environment, the optimal fill time and pressure distribution combined with other processing criteria from Moldflow were used to determine an optimal, feasible fill time and pressure generated.

3. HIPS and ABS showed minimum ejection force when the combination core surface roughness was about 6.42 μmRa whereas, PA6 showed the minimum ejection forces near 3.22 μmRa . It indicates that the optimum core surface roughness exists for the ejection force.
4. The results in 3 above suggest that the amorphous materials exhibit same behaviour compared to crystalline material. PA6 generates more ejection force compared to HIPS and ABS due to the material in which it has a high viscosity characteristic. It is suggested that a minimum ejection force produces a good moulding with the least deformation caused by the ejection force.
5. The ejection force generated with regards to different levels of surface roughness which can be summarised in the following sequence; PA6 > HIPS > ABS.

6.2 Contribution to knowledge

Measuring ejection forces in actual operating conditions has been less reported in the literature due to the mechanical complexity associated to a suitable tool. The principal contributions of this research are as follow.

The test tool developed in this work enables the on-line monitoring of the ejection force. The force sensor mounted in this tool does not require modification on the tool itself. By doing this, the actual mould can be used to measure the ejection force without any modification. The same idea can be adopted by research on how to mount the sensor and where to locate it.

One of the major contribution knowledge of this research is developing the mathematical model for HIPS, ABS and PA6 which are not available data in industrial and research community. One does not require doing a trial and error on checking force. In this model, the pre-setting of surface roughness can be set earlier and the variable of processing parameter such as melting temperature, injection pressure, packing pressure as well as cooling time can be used as per recommended or manufacturer's data sheet. It is a necessity to develop model ejection force for amorphous and crystalline resin which can later help people in moulding industries in planning the undertaken job and also improving easy manufacture of the plastic parts.

The optimum levels of processing parameters towards production of plastic components for plastic parts (HIPS, ABS and PA6) can be determined by exploiting the S/N ratio and ANOVA.

6.3 Recommendation for Further Work

There are still few areas for further study in order to improve the accuracy in predicting the model for ejection force of moulding. This section describes some of the possibilities for extending the work investigated based on the obtained result and observations. Profoundly, effective recommendations for further work benefits shall be suggested as below.

1. The details of tool information may also be added to the Moldflow software in order to allow the calculation of the resin performance over the range of typical mould. The possibility of reducing cycle time and heating conditions should be explored further together with trial and the software before being placed on production.
2. There is a possibility to explore on plastic resin field in this study which is found widely available in Malaysia but not in the list of Moldflow library. Resins such as polyethylene (PE) and propylene (PP) up to certain grades are not in the list. Hence, such resins cannot be simulated prior to production.

3. The mould heating system can be used to suit the temperature range. For instance an “intelligent” manifold system can be developed further for such resin usage. It may work like the valve system and integrates with the sensor to on/off in response to the required temperature range.
4. The sensor for pressure cavity should be employed to measure the pressure generated inside the cavity. The pressure gives a significant effect to eject the force generated. Unfortunately the sensor is unavailable to be used in this study.

REFERENCES

- A. J. Pontes, A. S. Pouzada, R. Pantani and G. Titomanlio, "Ejection force of tubular injection molding. Part II: A Prediction Model," *Polymer Engineering and Science*, vol. 45, pp. 325-332, March 2005.
- A. J. Pontes and A. S. Pouzada, "Ejection force in tubular injection moldings. Part I: Effect of Processing Conditions," *Polymer Engineering and Science*, vol. 44, pp. 891-897, May 2004.
- A. J. Pontes, A. M. Brito and A. S. Pouzada, "Assessment of the ejection force in tubular injection moldings," *Journal of Injection Molding Technology* vol. 6 pp. 343-352, December 2002.
- A. Kumar, P. S. Ghoshdastidar and M. K. Muju, "Computer simulation of transport process during injection mold-filling and optimization of the molding conditions," *Journal of Materials Processing Technology* 120, pp. 438-449, November 2001.
- A. Özdemir, O. Uluer and A. GÜltaş, "Flow front advancement of molten thermoplastic materials during filling stage of a mold cavity," *Journal of Polymer Testing* 23, pp. 957-966, April 2004.
- A.S. Pouzada, E.C. Fereira and A.J. Pontes, "Friction properties of moulding thermoplastics," *Polymer Testing* 25, pp. 1017-1023, June 2006.
- Buchmann, R. Theriault and T. A. Osswald, "Polymer flow length simulation during injection mold filling ," *Polymer Engineering and Science*, vol. 37, pp. 667-671, March 1997.
- B. H. Min, "A study on quality monitoring of injection-molded part," *Journal of Material Processing Technology* 136, pp. 1-6, June 2002.

- B. S. Chen and W. H. Liu, "Numerical simulation of the post-filling stage in injection molding with a two-phase model," *Polymer Engineering and Science*, vol. 34, pp. 835-846, May 1994.
- B. Pramujati, R. Dubay and J. G. Han, "Injection velocity control in plastic injection molding," *ANTEC 2005*, pp. 734-738
- C. G. Gogos and C. F. Huang, "The process of cavity filling including the fountain flow in injection molding," *Polymer Engineering and Science*, vol. 26, pp.1457-1466, November 1986.
- C. H. Che Haron, B. Md. Deros, A. Ginting and M. Fauziah, "Investigation on the influence of machining parameters when machining tool steel using EDM," *Journal of Material Processing Technology 116*, pp. 84-87, 2001.
- C. Collins, "Monitoring cavity pressure perfects injection molding," *Automation Assembly*, Vol. 19, pp. 197-202, 1999.
- D. O. Kazmer, P. Knepper and S. Johnston, "A review of in-mold pressure and temperature instrumentation," *ANTEC 2005*, pp. 3300-3304.
- D. H. Chun, "Cavity filling analyses of injection molding simulation: bubble and weld line formation," *Journal of Materials Processing Technology 89-90*, pp. 177-181, 1999.
- D. M. Gao, S. Reymond and A. Garcia-Rejon, "Modeling of the effect of mold venting on the injection moulding process," *Journal of Injection Molding Technology*, vol. 2, pp.136-140, September 1998.
- F. L. Amorim and W. L. Weingaertner, "The influence of generator actuation mode and process parameters on the performance of finish EDM of a stool steel," *Journal of Materials Processing Technology, 166*, pp. 411-416, 2005.

- Hasan Oktem , Tuncay Erzurumlu and Ibrahim Uzman , “ Application of Taguchi optimization technique in determining plastic injection molding process parameters for a thin-shell part,” *Journal of Materials and Design* 28, pp. 1271–1278, 2006.
- H. L. Zhang, N. S. Ong and Y. C. Lam, “Mold surface roughness effects on cavity filling of polymer melt in micro injection molding,” *International Journal Advanced Manufacturing Technology*, April 2007.
- Ho-Sang Lee, “Finite element analysis for the flow characteristics along the thickness direction in injection molding,” *Polymer Engineering and Science*, vol. 37, pp. 559-567, March 1997.
- H. Yokoi, N. Masuda and H. Mitsuhashi, “Visualization analysis of flow front behavior during filling process of injection mold cavity by two-axis tracking system,” *Journal of Materials Processing Technology* 130-131, pp. 328-333, 2002.
- J. F. Héty, D. M. Gao, A. Garcia-Rejon and G. Sallaoum, “3D Finite element method for the simulation of the filling stage in injection molding,” *Polymer Engineering and Science*, vol. 38, pp. 223-236, 1998.
- J. Koszkuł and J. Nabialek, “Viscosity models in simulation of the filling stage of the injection molding process,” *Journal of Materials Processing Technology* 157-158, pp. 183-187, 2004.
- J. P. Beaumont, J. H. Young and M. J. Jaworski, “ Solving mold filling imbalances in multi-cavity injection molds,” *Journal of Injection Molding Technology*, vol. 2, pp. 47-58, June 1998.
- Kuo-Ming Tsai, Chung-Yu Hsieh, Wei-Chun Lo, “A study of the effects of process parameters for injection molding on surface quality of optical lenses,” *Journal of Materials processing technology*, vol. 209, pp.3469-3477, 2009

- L. G. Reifschneider, "Reliability of mold filling simulation for part design," *Journal of Injection Molding Technology*, vol. 5, pp. 38-47, March 2001.
- Lee Hornberger and Ken Lown, "Thinning injection molded computer walls," *Specialized Molding Techniques*, pp. 133-141, 2001.
- M. R. Kamal and V. Tan, "Orientation in injection molded polystyrene," *Polymer Engineering and Science*, vol. 19, pp. 558-572, 1979.
- M. W. Darlington, A. J. Scott and A. C. Smith, "Pressure losses in the packing stage of injection molding," *Polymer Engineering and Science*, vol. 26, pp. 1282-1289, 1986.
- N. Dontula, P. C. Sukanek, H. Devanathan and G.A. Campbell, "An experimental and theoretical investigation of transient melt temperature during injection molding," *Polymer Engineering and Science*, vol. 31, pp. 1674-1683, December 1991.
- N. Vitelli and C. Kirschner, "Design of an instrumented mold to verify air gap formation during cooling in box-shaped parts," *ANTEC 2005*, pp. 930-934.
- Qin Sheng, Fred F. Farshad and Shangyu Duan, "A simulation of crystallinity gradients developed in slowly crystallizing injection molded polymer via parallel splitting," *Engineering Computations*, vol. 16, pp. 892-912, 1999.
- R. Dubay, "Predictive control of cavity pressure during injection filling," *Journal of Injection Molding Technology*, vol. 5, pp. 72-79, June 2001.
- S. K. Soh and C. J. Chang, "Boundary conditions in the modelling of injection mold-filling of thin cavities," *Polymer Engineering and Science*, vol. 26, pp. 893-899, July 1986.

- S. G. Kim and N. P. Suh, "Performance prediction of weld line structure in amorphous polymers," *Polymer Engineering and Science*, vol. 26, pp. 1200-1207, September 1986.
- S. Singh, S. Maheshwari and P. C. Pandey, "Some investigations into the electric discharge machining of hardened tool steel using different electrode materials," *Journal of Materials Processing Technology* 149, pp. 272-277, November 2003.
- Swan M., "History of Injection Molding simulation – The state of the technology after its first quarter century." Mold Flow Corporation 2004.
- T. Sazaki, N. Koga, K. Shirai, Y. Kobayashi and A. Toyoshima, "An experimental study on ejection forces of injection molding," *Journal of Precision Engineering*, pp. 270-273, 2000.
- X. Chen, F. Gao and G. Chen, "A soft sensor development for melt-flow-length measurement during injection mold filling," *Material Science Engineering, A* 384, pp. 245-254, June 2004.
- X. Chen and F. Gao, "Profiling of injection velocity for uniformity mold filling," *Advances in Polymer Technology*, vol. 25, pp. 13-21, 2006.
- Yash P. Gupta, "A simplified predictive control approach for handling constraints through linear programming," *Computers in Industry*, Vol. 21, Issue 3, April 1993, pp. 255–265.
- Y. H. Guu, "AFM surface imaging of AISI D2 tool steel machined by the EDM process," *Applied Surface Science* 242, pp. 245-250, 2004.
- Yong WH and Tang YS., "Design optimization of cutting parameters for turning operations based on Taguchi method," *Journal of Material Process Technology* 84, pp.122–129, 1998.

BIBLIOGRAPHY

- A. W. Birley and M. J. Scott, "Plastic Materials – Properties and Applications," Blackie and Son Limited, 1982.
- Belofsky.H, "Plastics: Product Design and Process Engineering," Hanser Publisher, 1995.
- C-Mold Design Guide. Center of Robotic and Manufacturing System University of Kentucky, 1999. Information on C-Mold, <http://www.rms.engr.uk.edu//pages/cmold/>. Accessed on 19 March 2003.
- Callister W D., "Fundamentals of Materials Science and Engineering, 2nd Edition," John Wiley & Sons Inc., 2005.
- Crawford R J., "Plastics Engineering, 2nd Editions," Pergamon Press, 1990.
- Douglas C. Montgomery, Elizabeth A. Peck and G. Geoffrey vining, "Introduction to linear regression analysis," Fourth Edition, Wiley Interscience, 2006
- Glen Stuart Peace, "Taguchi Methods – A hands – On Approach," Addison Wesley Publishing Company, Inc., 1993.
- G. Gruenwald, "Plastics – How Structure Determines Properties," Hanser Publisher, 1992.
- Hary, C. Moser, "When do you need EDM," President Charmilles Technologies Corporation Linconshire, Illinois, Modern Machine Shop Publication, 2000.
- <http://www.ensinger-online.com/en/materials/basics-of-plastics/plastics-classification/>. Visited: 03/02/14

Jay Shoemaker, "Moldflow Design Guide – A Resource for Plastics Engineers,"
Hanser Publisher, 2006.

John P. Beaumont, "Runner and Gating Design Handbook," Hanser, 2004.

J. P. Holman, "Experimental Methods for Engineers," McGraw-Hill, 2001.

J. P. Beaumont, R. Nagel and R. Sherman, "Successful Injection Molding," pp.162-
163, Hanser, 2002.

Michael L. Berins, "Plastics Engineering Handbook of the Society of the Plastics
Industry, Inc.," 5th. Edition, Kluwer Academic Publishers, 2000.

Moldflow Plastic Insight Manual 6.0, 2006

Osswald, Turng and Gramann, "Injection Molding Handbook," Hanser, 2002.

Phillip J. Ross, "Taguchi Techniques for Quality Engineering," Second Edition,
McGraw – Hill, 1996.

Rosato Dominick V., Rosato Donald V. and Rosato Marlene G., "Injection Molding
Handbook, Third Edition, "Kluwer Academic Publisher, 2000)

Taguchi G, Konishi S. Taguchi methods, orthogonal arrays and linear graphs, tools
for quality American supplier institute. American Supplier Institute; pp. 8–35,
1987.

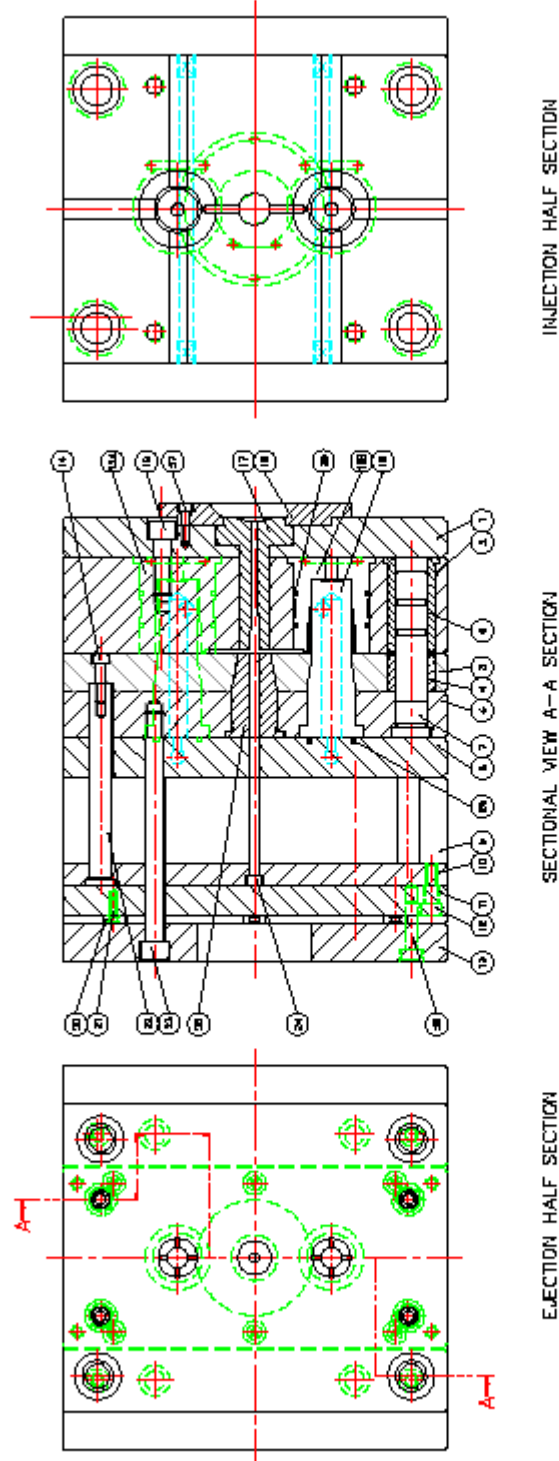
Taguchi G., " Introduction to quality engineering," New York: McGraw-Hill, 1990.

Wu Y and Wu A, "Taguchi methods for robust design,' The Park Avenue, New
York: The American Society of Mechanical Engineers; 2000.

APPENDICES




APPENDIX A
Tool Drawings

APPENDIX A.1



Notes:-

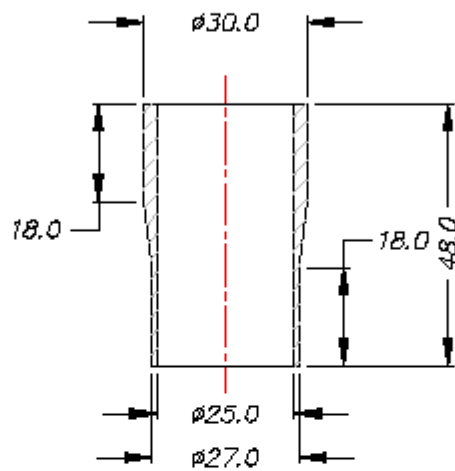
1. For component detail drawings: refer to Drawing No.: C05012936-01-01
2. For BOM: refer to Drawing No.: B05012936-01-02
3. Injection Moulding Machine: E5950/ENGEL 125HL-V Pro-Series (125T)

 Edinburgh Napier <small>UNIVERSITY</small>	 <small>BRITISH SOCIETY OF PLASTICS ENGINEERS</small>	TITLE: The Effect Surface Finish on The Mould Filling and The Ejection of Moulding		DATE: 25.05.08
		NAME: 1,2,5	DGR1: ADP	ADP
			DGR1: ADP	ADP
		HANDING: - 1 -	DGR1: ADP	ADP
		DRAWING NO: A3	DGR1: ADP	ADP
EDINBURGH, SCOTLAND		TEREHONGTAN MALAYSIA		

APPENDIX A.2

30					
29	O-RING	2	STANDARD	Ø3	OD = 30 mm
28	O-RING	4	STANDARD	Ø3	OD = 50 mm
27	SHCS	2	--	M5 x 0.8	L = 20 mm
26	SHCS	4	--	M8 x 1.25	L = 30 mm
25	SPRUE PULLER BUSH	1	MOLD STEEL	438 x 55	50-52HRC
24	SPRUE PULLER PIN	1	MOLD STEEL	Ø10 x 152	55-58HRC
23	BOLT	4	--	M12 x 1.75	L = 150 mm
22	RETURN PIN	4	EN31	Ø20 x 131.5	54-56HRC
21	CSK SCREW	4	--	M5 x 0.8	L = 12 mm
20	REST BUTTON	6	EN31	Ø15 x 5	54-56HRC
19	SHCS	4	--	M12 x 1.75	L = 35 mm
18	REGISTER RING	1	MILD STEEL	Ø125 x 15	--
17	SPRUE BUSH	1	EN31	Ø50 x 89.5	54-56HRC
16	CORE INSERT	2	MOLD STEEL	Ø42 x 103.24	50-52HRC
15B	CAVITY INSERT	1	MOLD STEEL	Ø58 x 63	50-52HRC
15A	CAVITY INSERT	1	MOLD STEEL	Ø58 x 63	50-52HRC
14	SHCS	4	--	M6 x 1.0	L = 25 mm
13	BOTTOM PLATE	1	MILD STEEL	250 x 250 x 25	--
12	SHCS	4	--	M8 x 1.25	L = 25 mm
11	EJECTOR BACK PLATE	1	MILD STEEL	116 x 250 x 20	--
10	EJECTOR RETAINER PLATE	1	MILD STEEL	116 x 250 x 15	--
9	SPACER BLOCK	2	MILD STEEL	40 x 96 x 250	--
8	CORE BACK PLATE	1	MILD STEEL	200 x 250 x 25	--
7	GUIDE PILLAR	4	EN31	Ø25 x 108	60HRC
6	GUIDE BUSH (CV)	4	EN31	Ø30 x 61	60HRC
5	CORE PLATE	1	MILD STEEL	200 x 250 x 30	--
4	GUIDE BUSH (ST)	4	EN31	Ø30 x 24	60HRC
3	STRIPPER PLATE	1	MILD STEEL	200 x 250 x 25	--
2	CAVITY PLATE	1	MILD STEEL	200 x 250 x 63	--
1	TOP PLATE	1	MILD STEEL	250 x 250 x 25	--
ITEM	DESCRIPTION	NO.	MATERIAL	FINISHED SIZE	REMARKS
TITLE: The Effect Surface Finish on The Mould Filling and The Ejection of Moulding				SCALE 1:1	DGN Alias 25.05.08
					DRN Alias 25.05.08
					CHD Colin 06.06.08
					APPD Colin 06.06.08
				Hand.Hrs - ± -	Op. N7/
				Drawing No.:	DRG. SIZE A4
				B05012936-01-02	SHEET NO. 1 OF 1
EDINBURGH, SCOTLAND		TERENGGANU MALAYSIA			

APPENDIX A.3

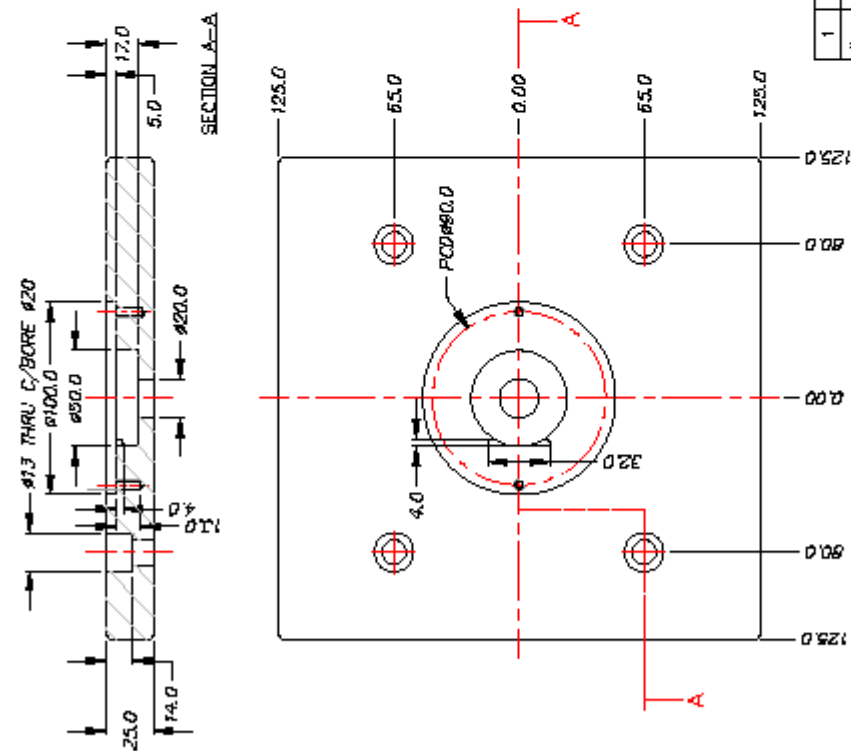


Notes:

1. The component is modeled on AutoDesk Inventor Prof. 10
2. Materials : HIPS, ABS and PA6
3. Weight: ± 8.0 grams
4. Density: Refer to material's specifications
5. All dimensions in mm




TITLE: The Effect Surface Finish on The Mould Filling and The Ejection of Moulding		SCALE 1:1	DGN	Alias	25.05.08
			DRN	Alias	25.05.08
 EDINBURGH, SCOTLAND		 TERENGGANU MALAYSIA	CHD	Calin	25.05.08
			APPD	Calin	25.05.08
		Hard.Hrc - ± -	Op. N7/ 	DWG. SIZE A4	
		Drawing No.: C05012936-01-01			SHEET NO. 1 OF 1

APPENDIX A.4

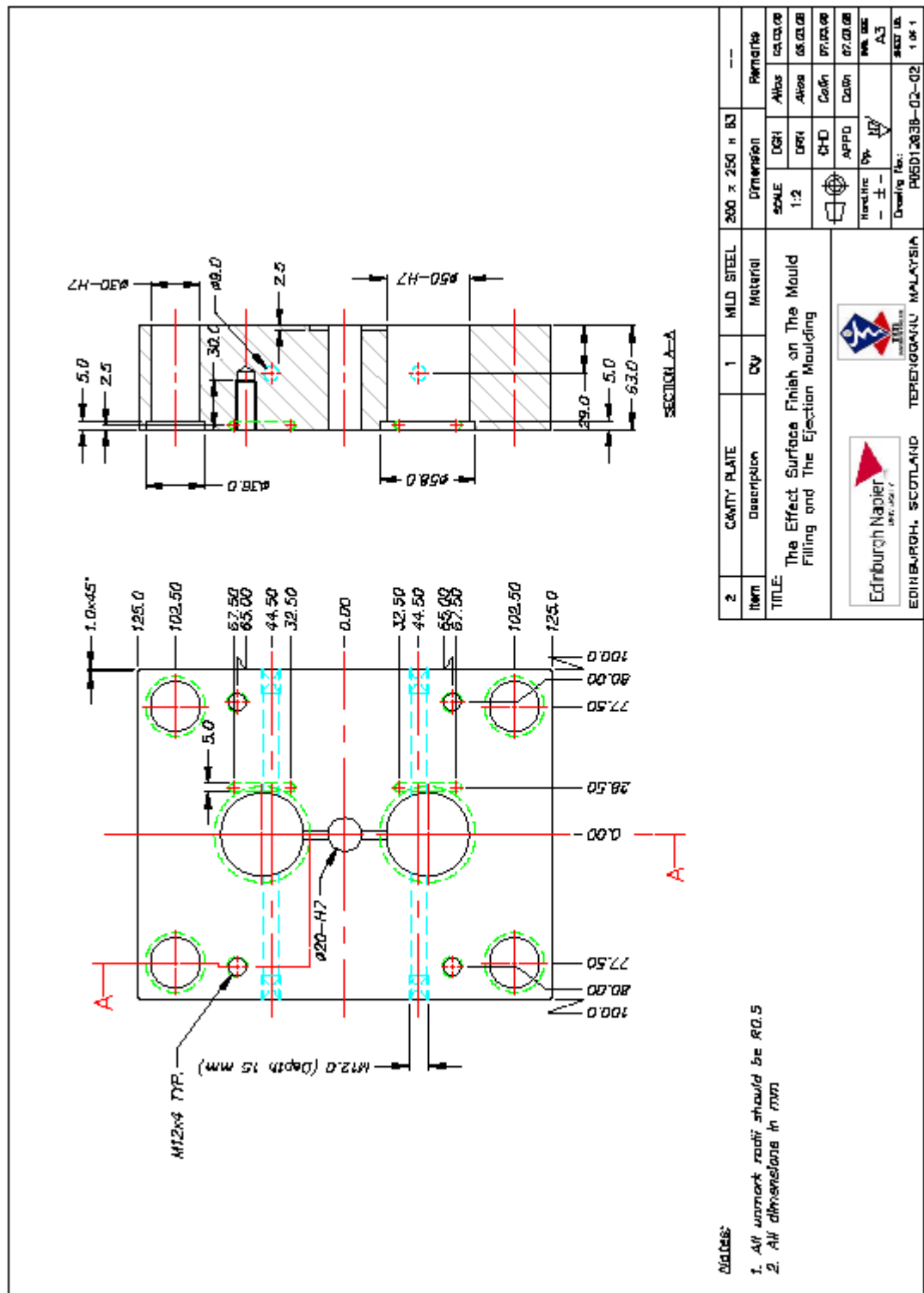


Notes

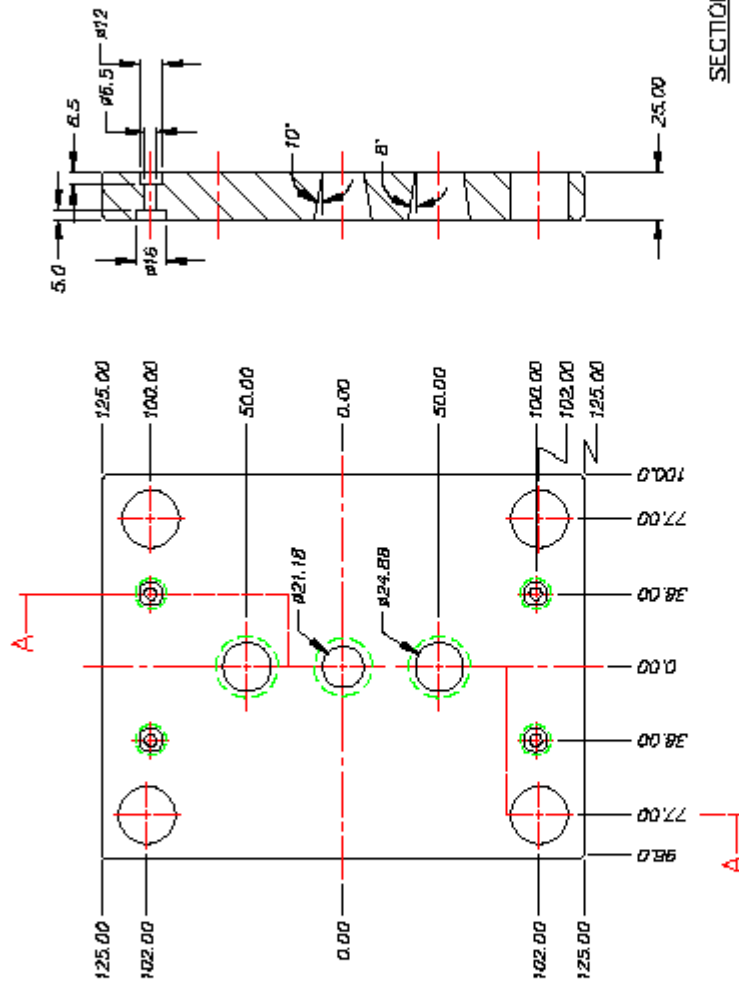
1. All unmark radii should be R0.5
2. All dimensions in mm

1	TOP PLATE	1	MILD STEEL	250 X 250 X 25	Remains
<p>TITLE: The Effect Surface Finish on The Mould Filling and The Ejection Moulding</p>					
					
Edinburgh Napier UNIVERSITY		TERENGGANU MALAYSIA		Moulding Machine	
EDINBURGH, SCOTLAND		TERENGGANU MALAYSIA		Moulding Machine	

APPENDIX A.5



APPENDIX A.6



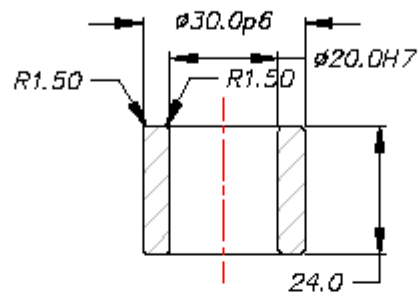
SECTION A-A

3	STRIPPER PLATE	1	MILD STEEL	200 X 250 X .25	Remains
TITLE: The Effect Surface Finish on The Mould Filling and The Ejection Moulding					
Description		Qty	Material	Dimension	Remarks
SOALE		1-2	DRH	ALUM	ALUM
		CHD	Cañ	Cañ	ALUM
		APPD	Cañ	Cañ	ALUM
Hardness Op. $\frac{H}{V}$		-	AJ	100.55	100.55
Drawing No.:		PDS012035-03-02			
Drawing Scale:		1:1			

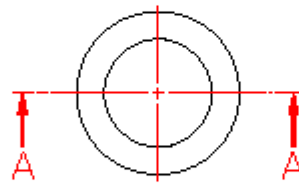
Notes:

1. All unmark radii should be R0.5
2. All dimensions in mm
3. All sharp corner should be chamfered 1.5 X 45°

APPENDIX A.7





SECTION A-A

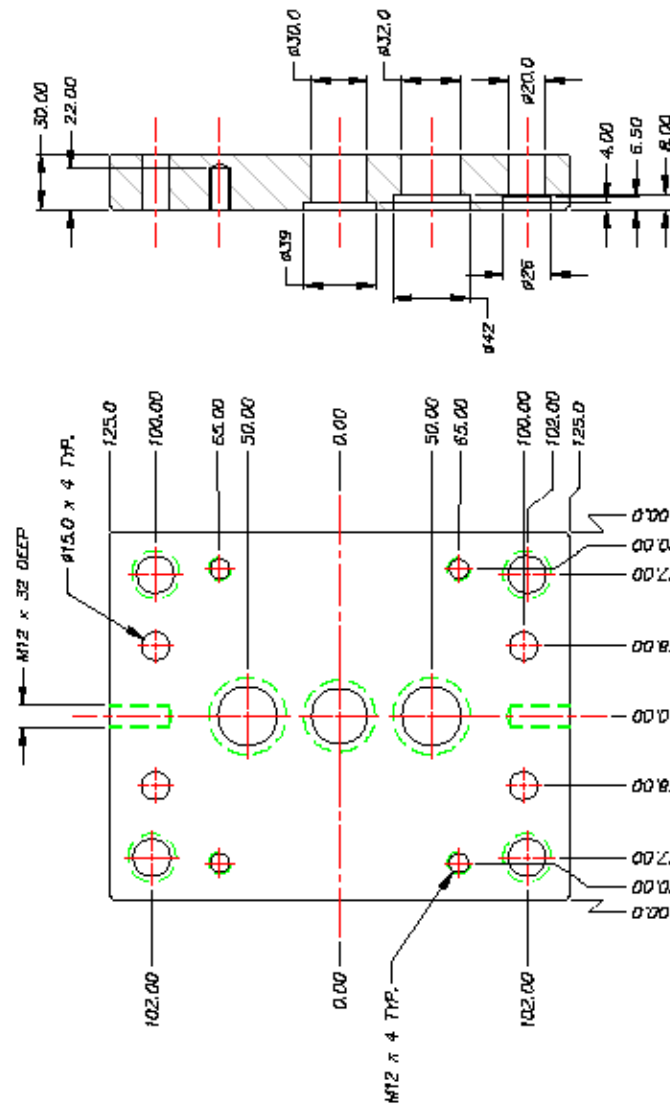


Notes:

1. All unmark radii should be R0.5
2. All dimensions in mm

4	GUIDE BUSH (ST)	4	EN31	30 x 24	60HRC
Item	Description	Qty	Material	Dimension	Remarks
TITLE: The Effect Surface Finish on The Mould Filling and The Ejection of Moulding				SCALE 1:1	DGN Alias 23.04.08
					DRN Alias 23.04.08
					CHD Colin 25.04.08
					APPD Colin 25.04.08
				Hard.Hrc ± ± ±	Op. NZ/ DWG. SIZE A4
 EDINBURGH, SCOTLAND				 TERENGGANU MALAYSIA	
				Drawing No.: P05012936-04-02	SHEET NO. 1 OF 1

APPENDIX A.8

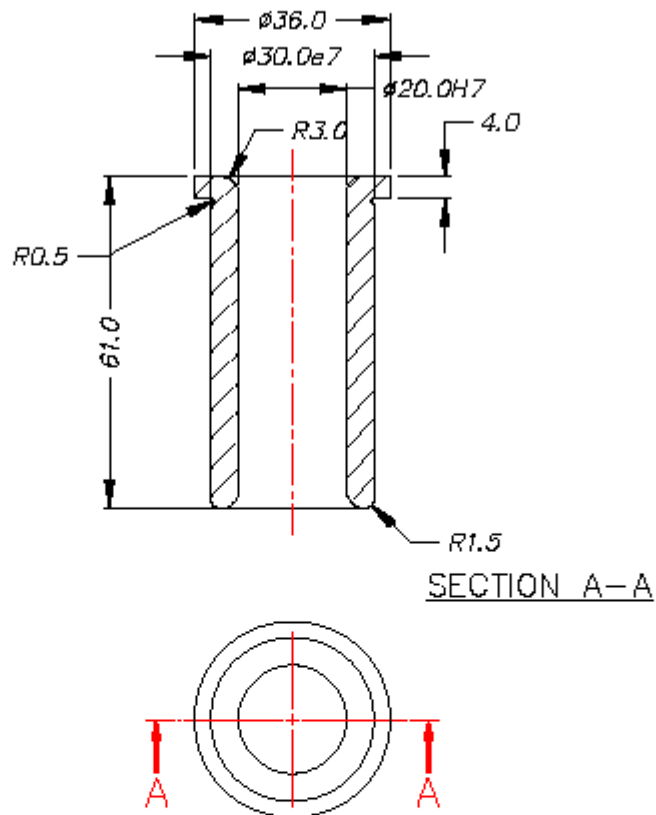


Note:

1. All parameters remain constant in time
2. All simulations are in mean

[illegible]

APPENDIX A.9

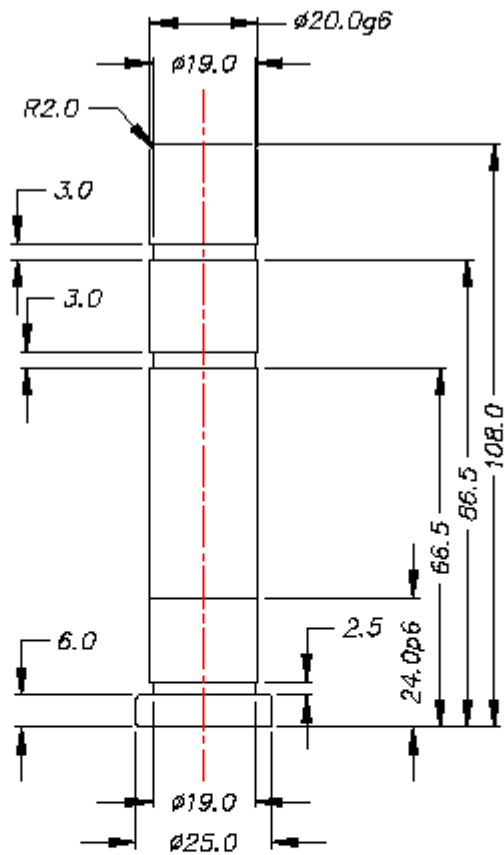


Notes:

1. All unmark radii should be R0.5
2. All dimensions in mm



6	GUIDE BUSH (CV)	4	EN31	30 x 61	60HRC
Item	Description	Qty	Material	Dimension	Remarks
TITLE: The Effect Surface Finish on The Mould Filling and The Ejection of Moulding				SCALE 1:1	DGN Alias 10.03.08
					DRN Alias 10.03.08
					CHD Colin 12.03.08
					APPD Colin 12.03.08
				Hard.Hrc - ± -	Qp. DMS. 03.08 A4
 EDINBURGH, SCOTLAND				 TERENGGANU, MALAYSIA	
				Drawing No.: P05012936-06-02	SHEET NO. 1 OF 1

APPENDIX A.10

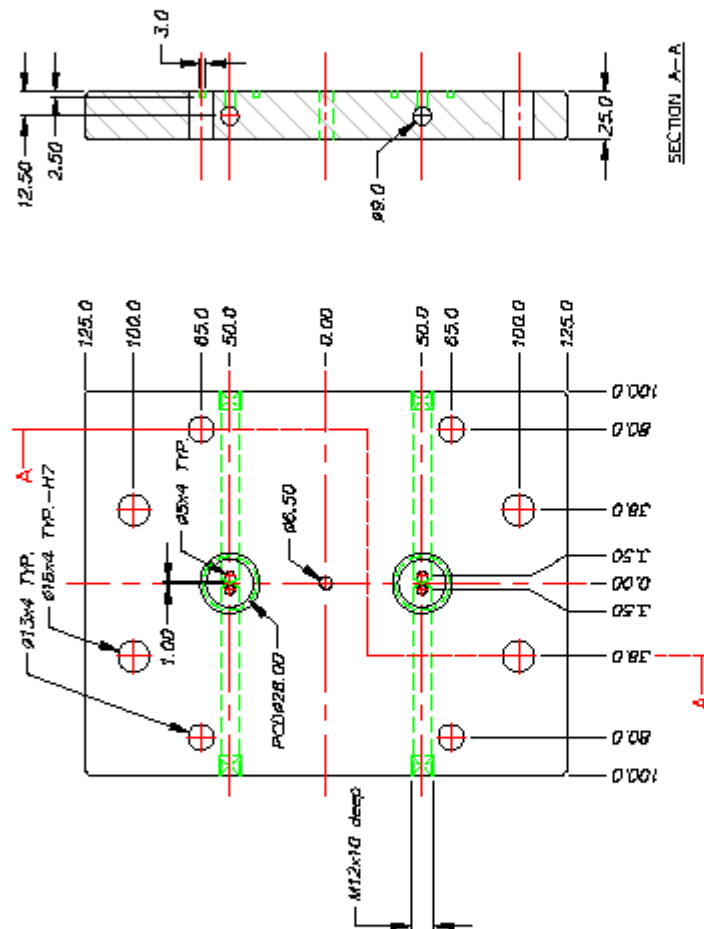


Notes:

1. All unmark radii should be R0.5
2. All dimensions in mm

7	GUIDE PILLAR	4	EN31	Ø25 x 108	60HRC
Item	Description	Qty	Material	Dimension	Remarks
TITLE: The Effect Surface Finish on The Mould Filling and The Ejection of Moulding				SCALE 1:1	DGN Alias 21.04.08
					DRN Alias 21.04.08
					CHD Colin 24.04.08
					APPD Colin 24.04.08
				Hard.Hrc - ± -	Op. N7/ DMC SIZE A4
 				Drawing No.: P05012936-07-02	SHEET NO. 1 OF 1
EDINBURGH, SCOTLAND TERENGGANU MALAYSIA					

APPENDIX A.11



Notes:

1. All unmarked radii should be R0.5
2. All dimensions in mm

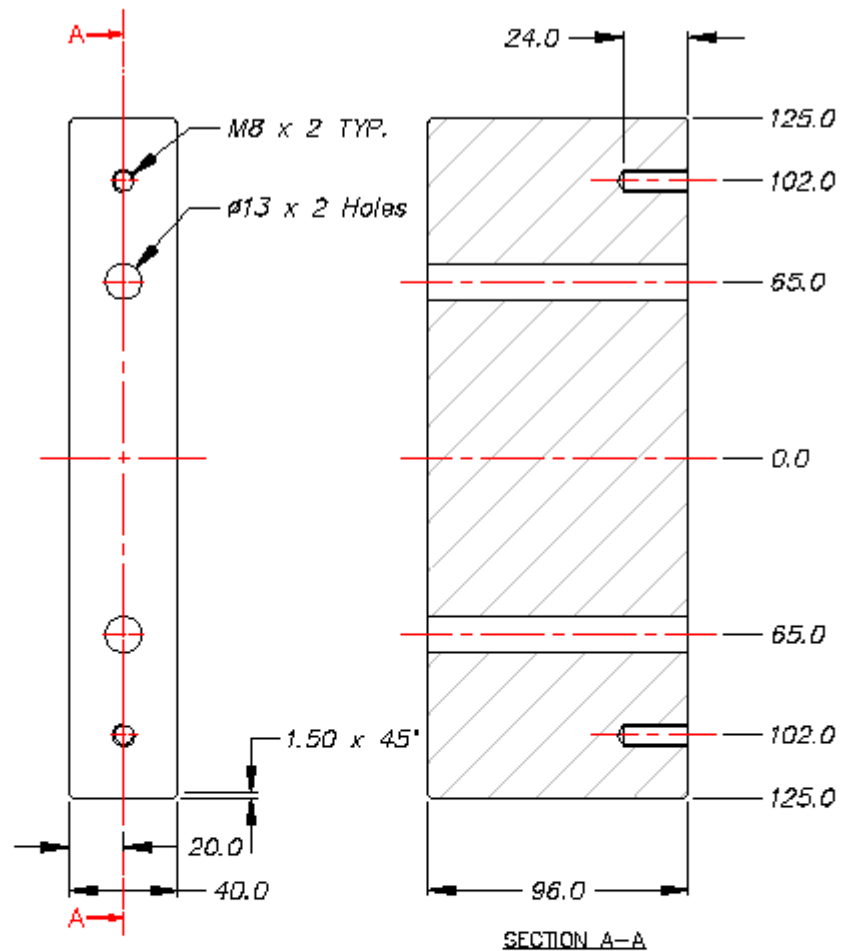
Item	Core Back Plate	1	MILD STEEL	200 X 250 X 25	Dimension	Remarks
Description		Qty	Material	SCALE	DSH	Alcoa
TITLE:		The Effect Surface Finish on The Mould Filling and The Ejection Moulding		1:2	DRH	Alcoa
				CHD	Coon	Alcoa
				APPD	Coon	Alcoa
				Handwritten	Coon	Alcoa
				Drawing No.	PD501283B-01B-02	1 of 1



Edinburgh Napier
University



EDINBURGH, SCOTLAND TERENURE, IRELAND

APPENDIX A.12

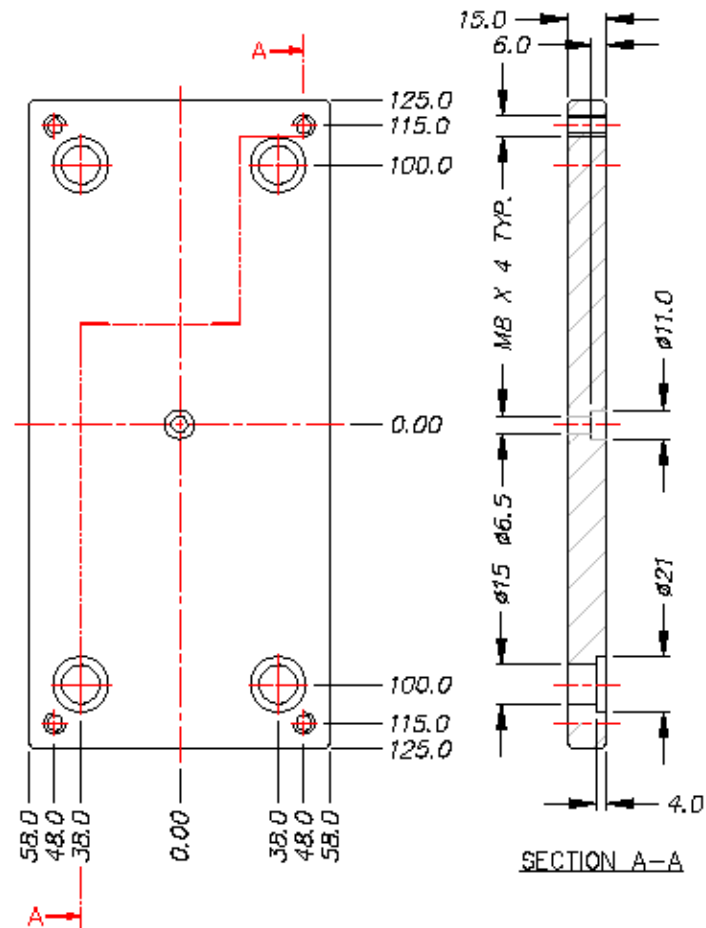


Notes:

1. All unmark radii should be R0.5
2. All dimensions in mm



9	SPACER BLOCK	2	MILD STEEL	40 x 96 x 250	--
Item	Description	Qty	Material	Dimension	Remarks
TITLE: The Effect Surface Finish on The Mould Filling and The Ejection of Moulding				SCALE 1:2	DGN Alias 10.03.08
					DRN Alias 10.03.08
					CHD Colin 12.03.08
					APPD Colin 12.03.08
				Hard.Hrc - ± -	Op. NZ DWA. SIZE A4
 				Drawing No.: P05012936-09-02	SHEET NO. 1 OF 1
EDINBURGH, SCOTLAND				TERENGGANU MALAYSIA	

APPENDIX A.13

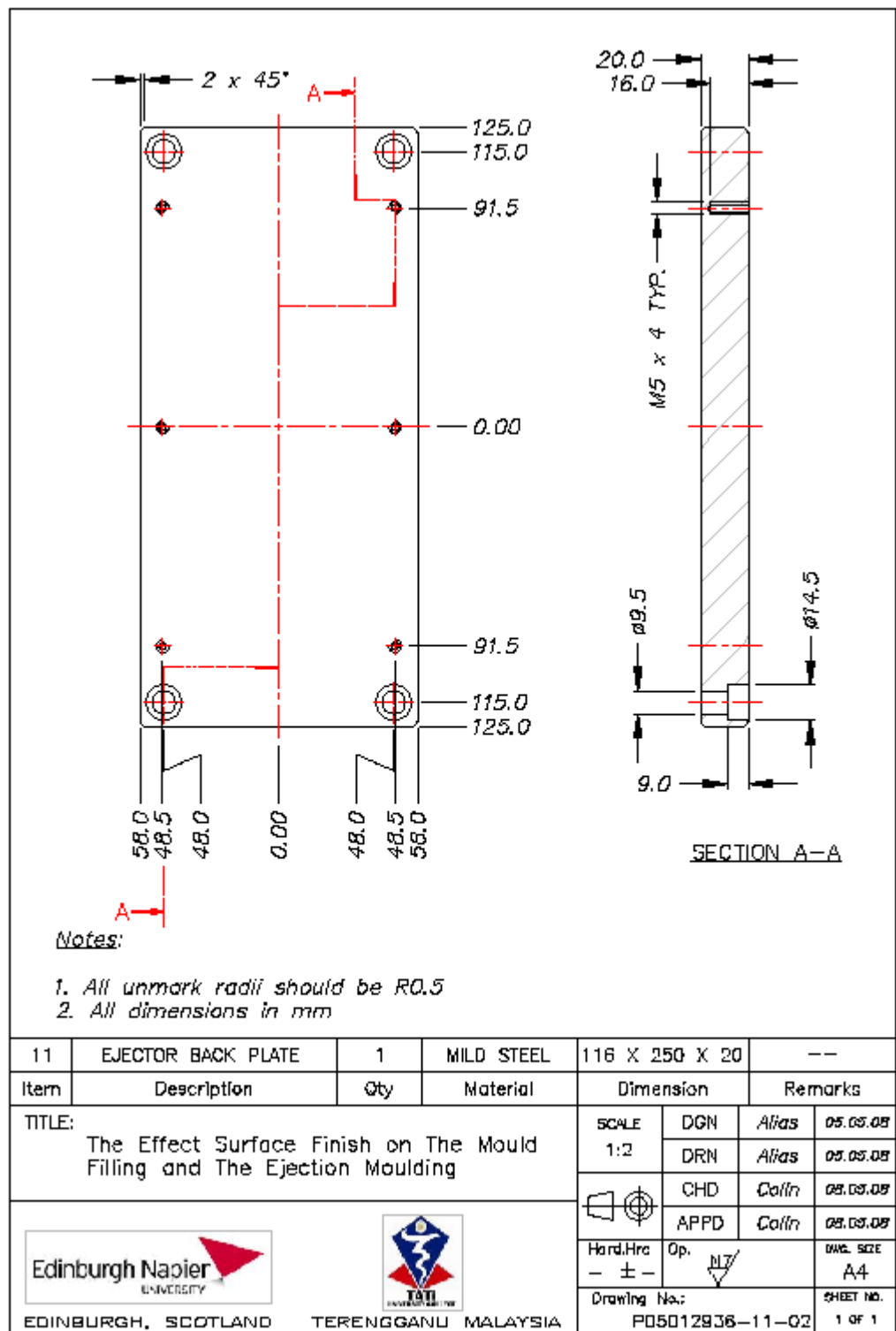


Notes:

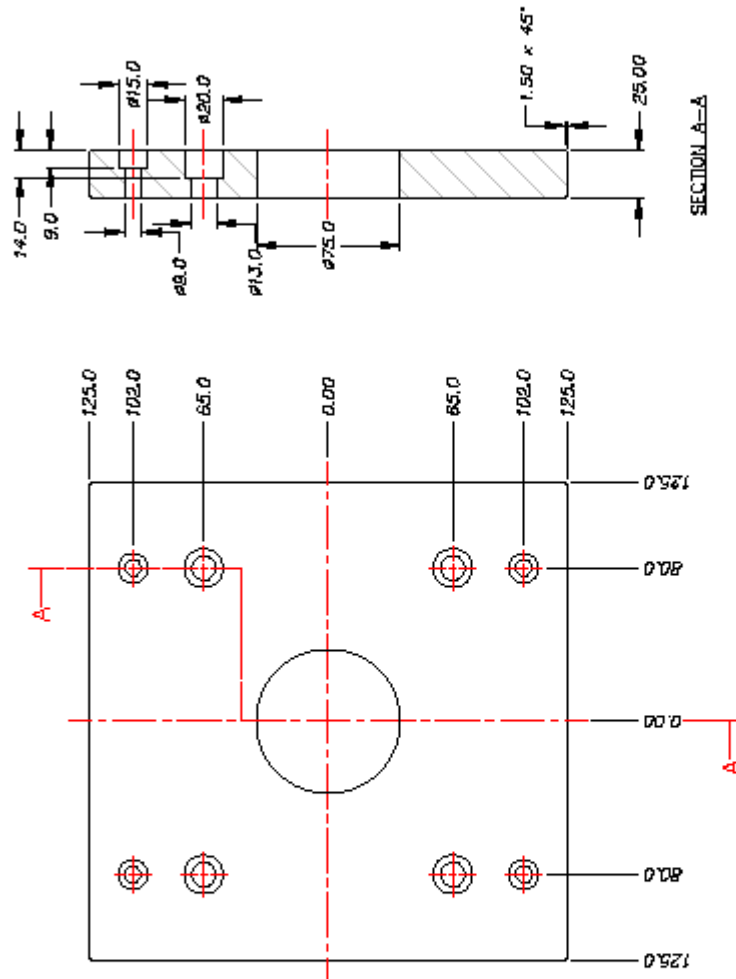
1. All unmark radii should be R0.5
2. All dimensions in mm

10	EJECTOR RETAINER PLATE	1	MILD STEEL	116 X 250 X 15	—
Item	Description	Qty	Material	Dimension	Remarks
TITLE:				SCALE	DGN
The Effect Surface Finish on The Mould Filling and The Ejection Moulding				1:2	Alias
				DRN	Alias
				CHD	Colin
				APPD	Colin
 				Hand.Hrs	Dwg. Size
				— ± —	A4
EDINBURGH, SCOTLAND				Drawing No.:	SHEET NO.
TERENGGANU, MALAYSIA				P05012936-10-02	1 OF 1



APPENDIX A.14



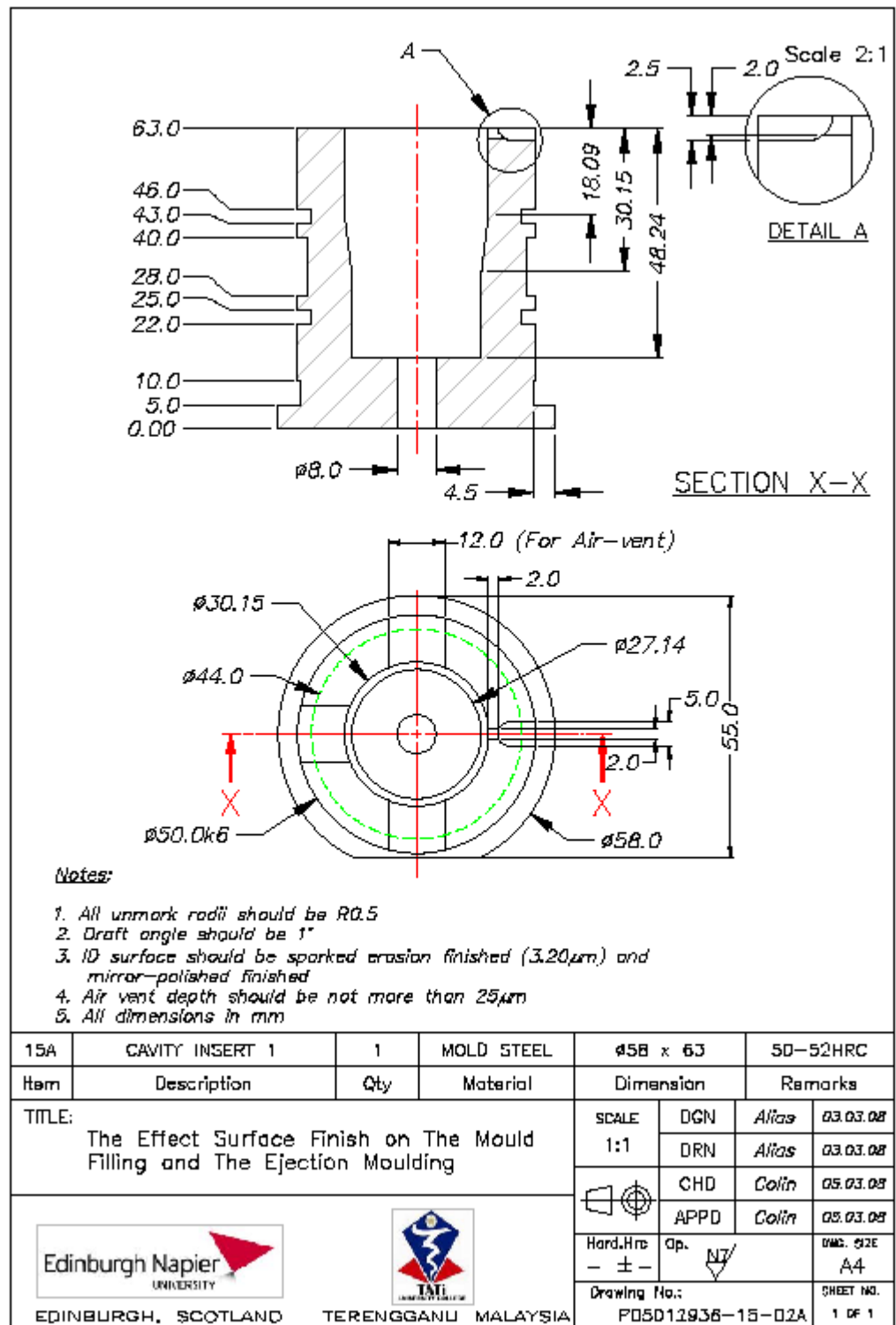
APPENDIX A.15

Notes:

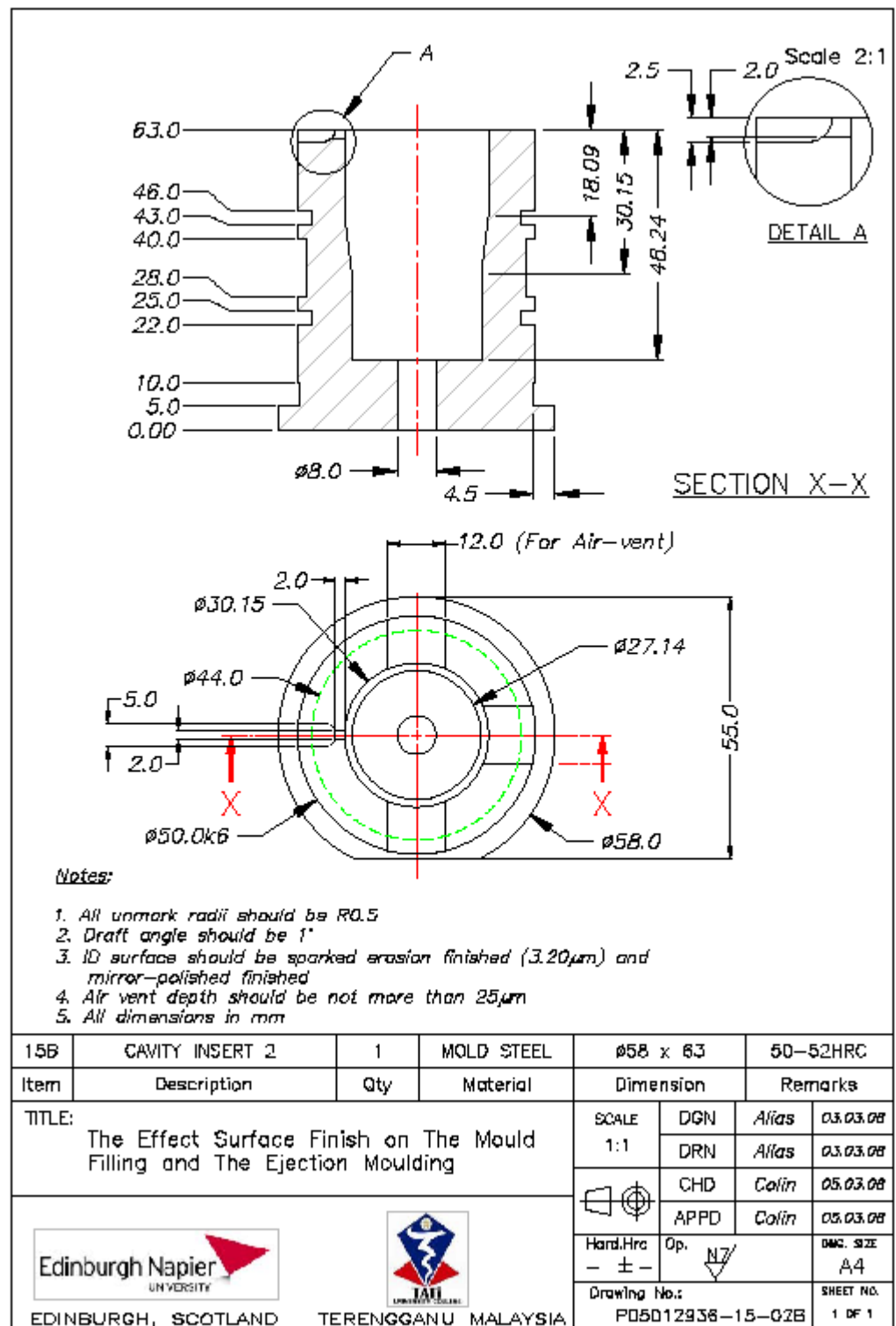
1. All unmark radii should be RQ.5
2. All dimensions in mm

13	BOTTOM PLATE	1	MILD STEEL	550 x 250 x 25	Remarks
TITLE: The Effect Surface Finish on The Mould Filling and The Ejection Moulding					
 					
Edinburgh Napier UNIVERSITY		TERENGGANU MALAYSIA			
		EDINBURGH, SCOTLAND		PUJ01 2835-13-02	
		1 of 1		08/07/09	

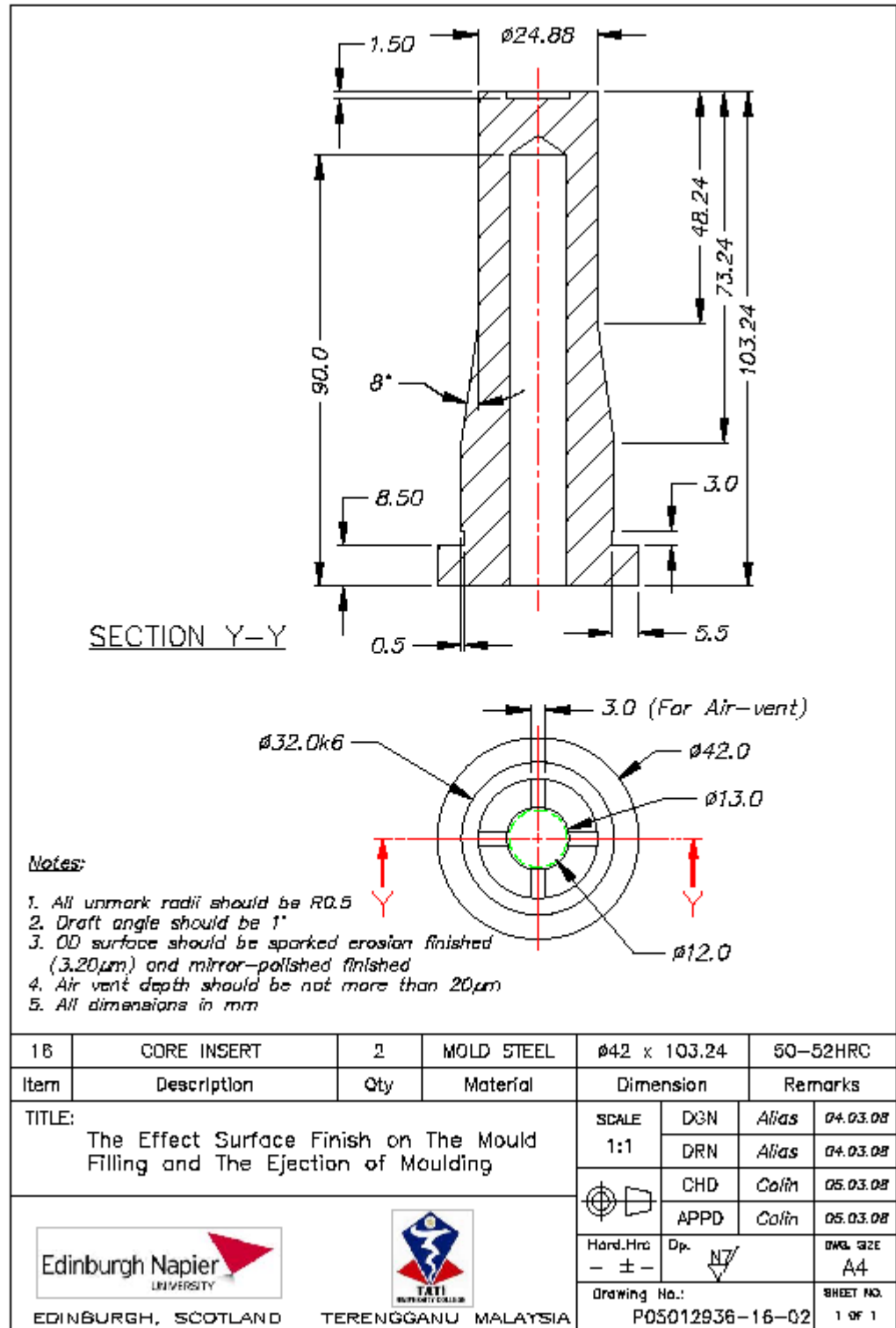
APPENDIX A.16



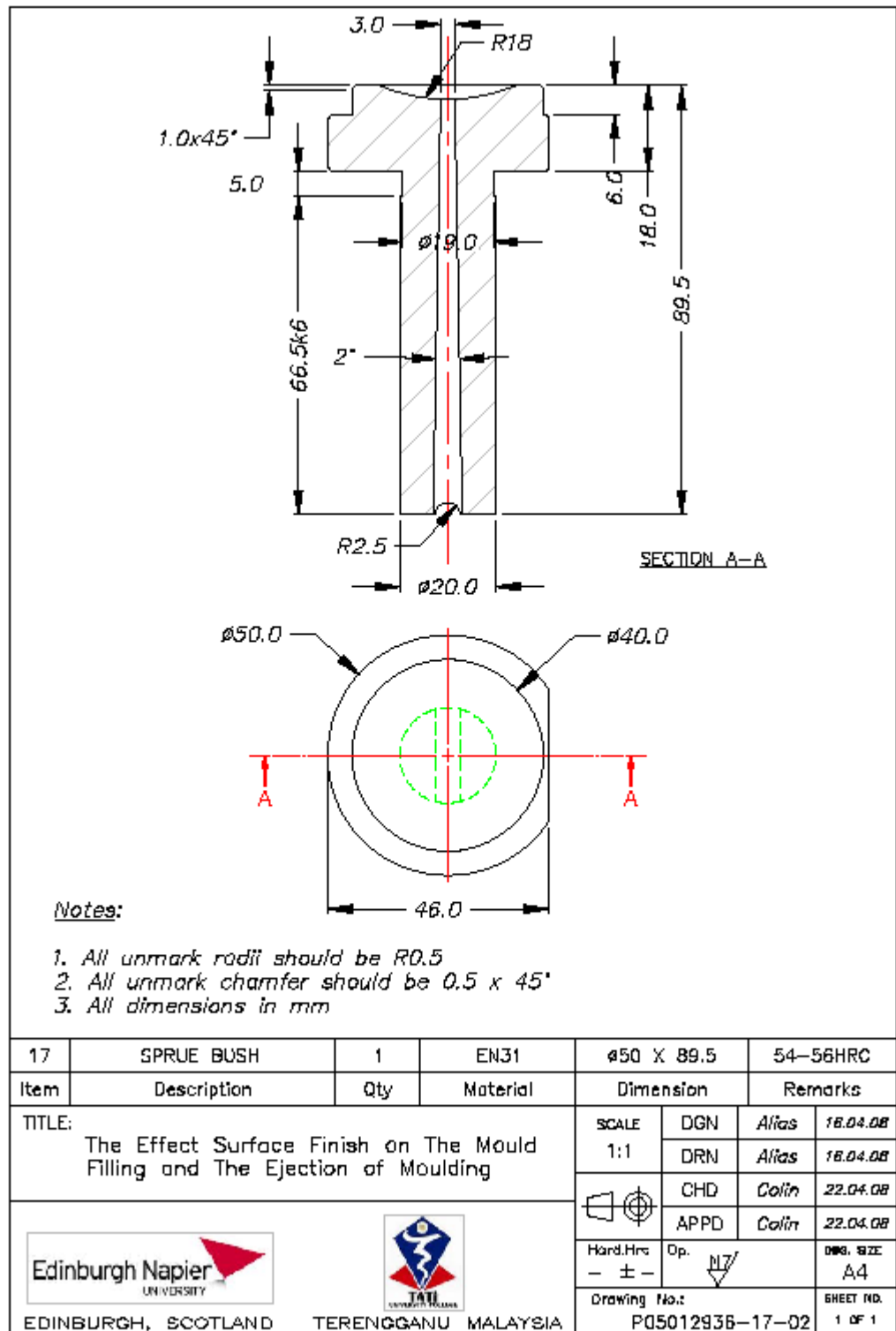
APPENDIX A.17



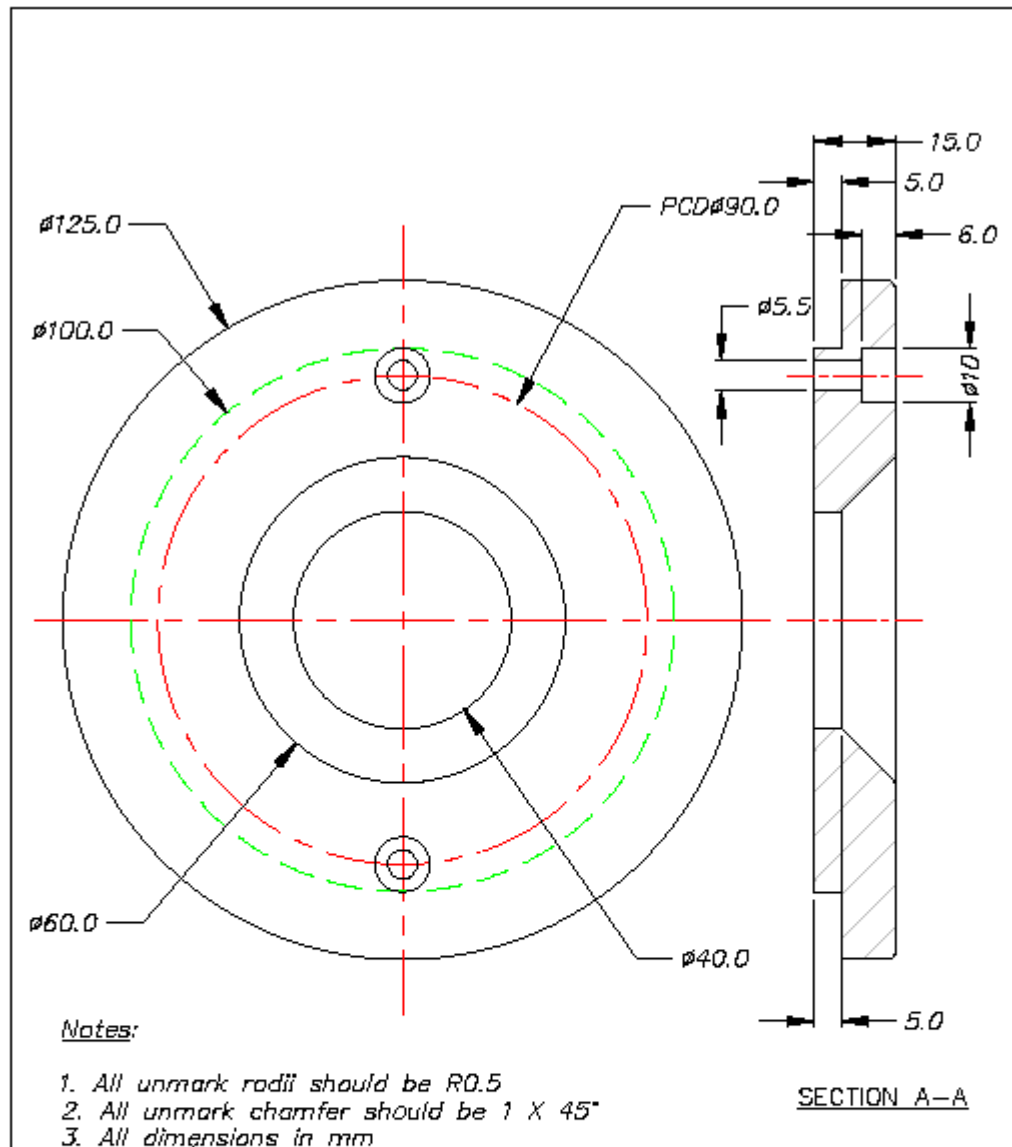
APPENDIX A.18



APPENDIX A.19

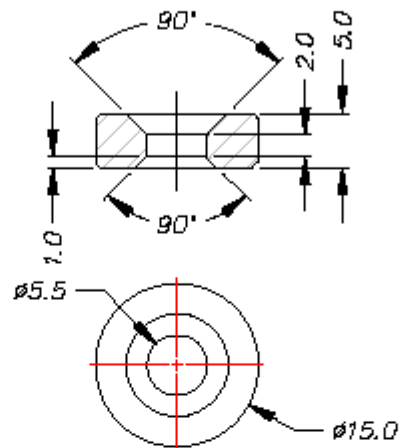


APPENDIX A.20



18	REGISTER RING	1	MILD STEEL	125 X 15	--
Item	Description	Qty	Material	Dimension	Remarks
TITLE: The Effect Surface Finish on The Mould Filling and The Ejection Moulding				SCALE 1:1	DGN Alias 18.03.08
					DRN Alias 18.03.08
					CHD Colin 20.03.08
					APPD Colin 20.03.08
				Hard.Hrc - ± -	Op. N7
				Drawing No.: P05012938-18-02	
 EDINBURGH, SCOTLAND				 TERENGGANU MALAYSIA	
				DWG. SIZE A4 SHEET NO. 1 OF 1	

APPENDIX A.21

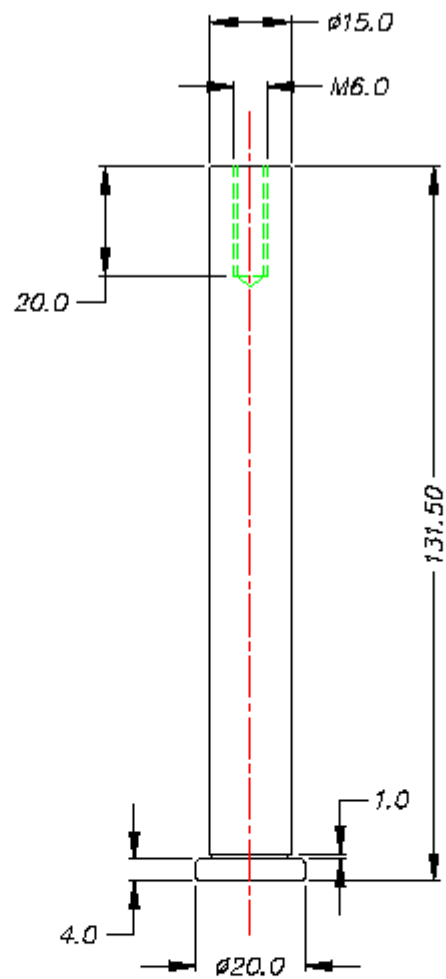


Notes:

1. All unmark chamfer should be $0.5 \times 45^\circ$
2. All dimensions in mm



20	REST BUTTON	6	EN31	15 X 5	54-56HRC
Item	Description	Qty	Material	Dimension	Remarks
TITLE: The Effect Surface Finish on The Mould Filling and The Ejection of Moulding				SCALE 2:1	DGN Alias 23.04.08
					DRN Alias 23.04.08
					CHD Colin 25.04.08
					APPD Colin 25.04.08
				Hard.Hrc - ± -	Op. N7/
				Drawing No.: P05012936-20-02	
 EDINBURGH, SCOTLAND				 TERENGGANU MALAYSIA	
					DWG. SIZE A4
					SHEET NO. 1 OF 1

APPENDIX A.22

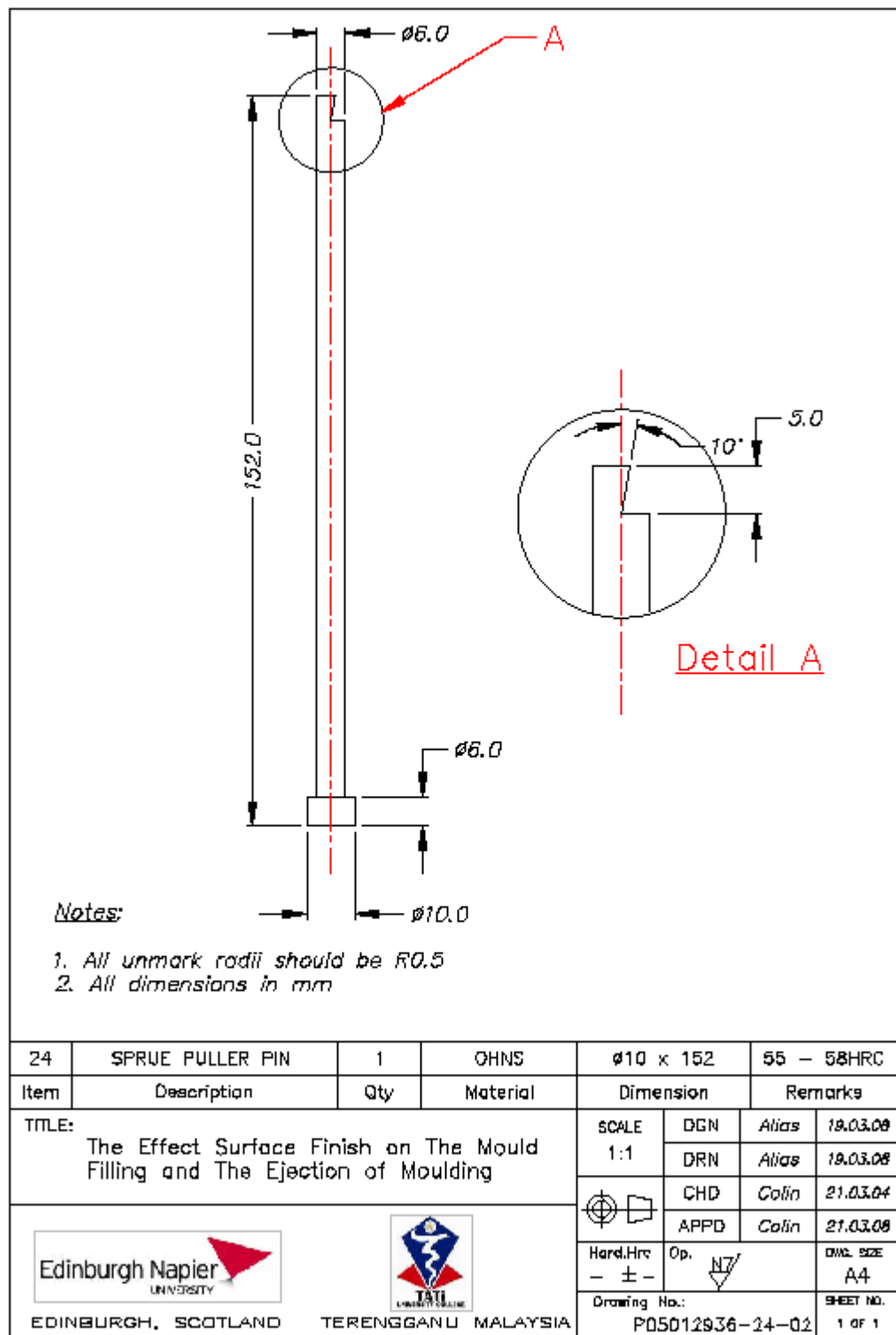


Notes:

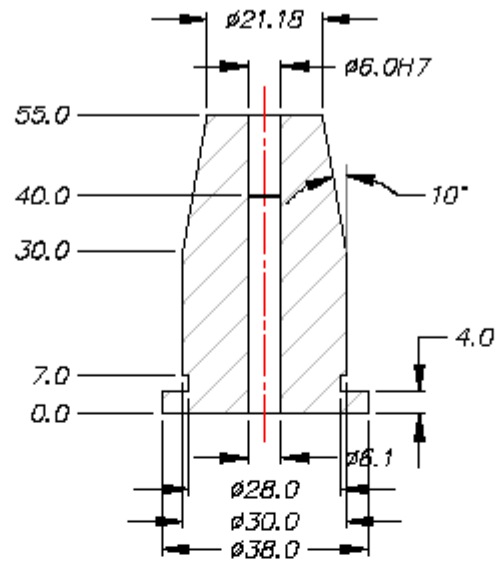
1. All unmark radii should be R0.5
2. All dimensions in mm

22	RETURN PIN	4	MOLD STEEL	Ø20 x 131.5	50-52HRC
Item	Description	Qty	Material	Dimension	Remarks
TITLE: The Effect Surface Finish on The Mould Filling and The Ejection of Moulding				SCALE 1:1	DGN Alias 18.03.08
				DRN Alias 18.03.08	
				CHD Colin 21.03.08	
				APPD Colin 21.03.08	
				Hand.Hrc - ± -	Op. N7 DWC. SIZE A4
				Drawing No.: P05012938-22-02	SHEET NO. 1 OF 1
 EDINBURGH, SCOTLAND		 TERENGGANU MALAYSIA			

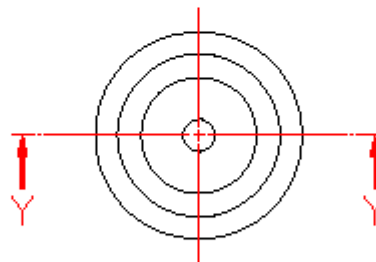
APPENDIX A.23



APPENDIX A.24





SECTION Y-Y



Notes:

1. All unmark radii should be R0.5
2. All dimensions in mm

25	SPRUE PULLER BUSH	1	MOLD STEEL	38 x 55	50-52HRC
Item	Description	Qty	Material	Dimension	Remarks
TITLE: The Effect Surface Finish on The Mould Filling and The Ejection of Moulding				SCALE 1:1	DGN Alias 18.04.08
					DRN Alias 18.04.08
					CHD Colin 23.04.08
					APPD Colin 23.04.08
				Hard.Hrc - ± -	Op. N7
 				DWG. SIZE A4	SHEET NO. 1 OF 1
EDINBURGH, SCOTLAND TERENGGANU MALAYSIA				Drawing No.: P05012936-25-01	

APPENDIX B
Surface Roughness

APPENDIX B.1

Mirror polishing techniques



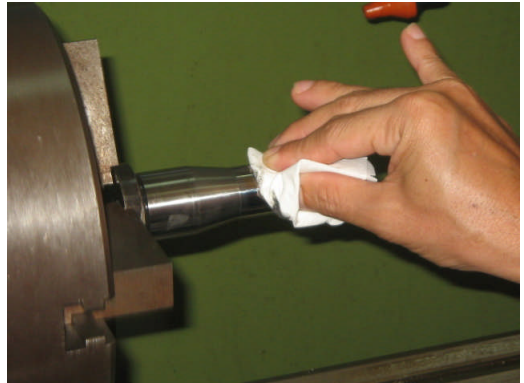
(a) Setting up the insert on the machine



(b) Applied different grade of sand paper



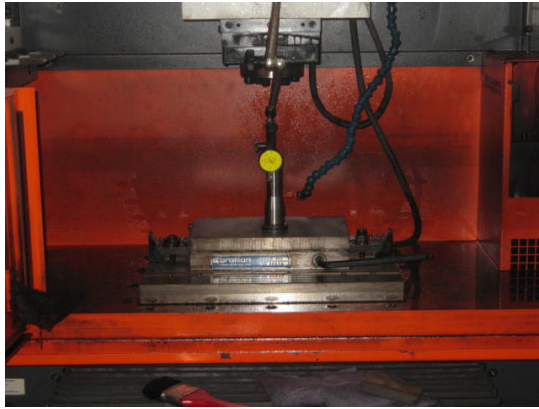
(c) Apply light pressure



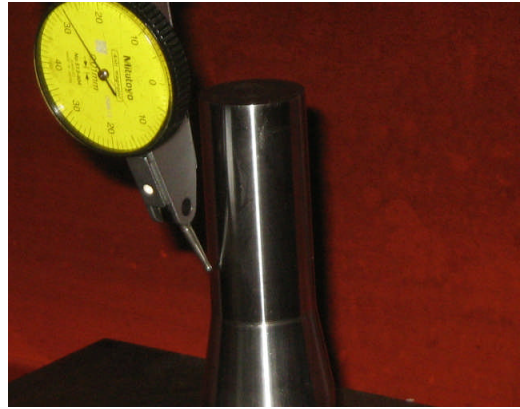
(d) Finish with Kemet KD compound paste on the surface insert

APPENDIX B.2

Process of producing the spark erosion for the core inserts



(a) Setting up the core insert



(b) Close-up setting by using dial indicator
(Before EDM process)



(c) Surface roughness after EDM process

APPENDIX C
Tooling Fabricating

APPENDIX C.1

Machining works to fabricate the tool.



(a) Cavity insert after heat treatment



(b) Cavity insert after heat treatment



(a) Cavity insert after heat treatment



(b) Cylindrical grinding (CG) process for cavity insert



(c) After OD (out side diameter) machining

Continued.



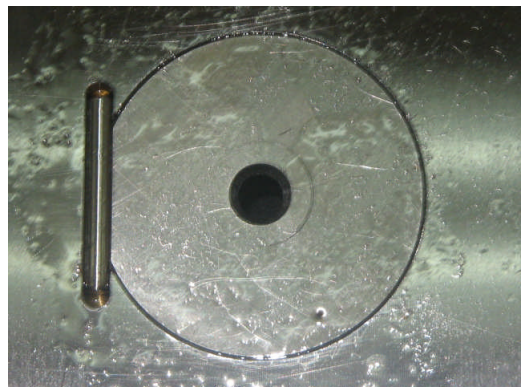
(d) Some of mold base parts waiting for machining



(e) Setting cavity plate prior machining process



(f) After machining process for cavity plate



(g) Fitting cavity insert and dowel pin



(h) Fitting 2 cavity inserts and dowel pins

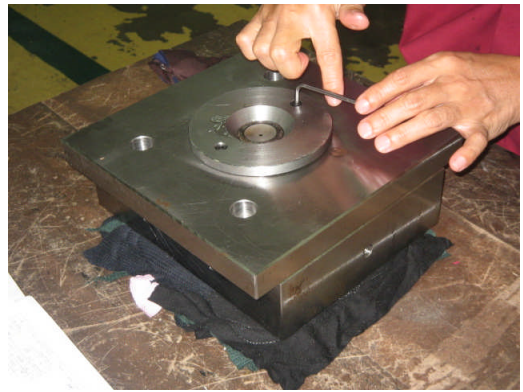


(i) Fitting top plate

Continued.



(j) Fitting sprue bush



(k) Tighten the register ring



(l) Fitting top plate



(m) Fitting core inserts



(n) Fitting Test mould



(o) Test mould in open position

APPENDIX D
Resin Specification

APPENDIX D.1

IDEMITSU PS ® - PETROCHEMICAL (MALAYSIA) SDN. BHD.

Properties of IDEMITSU PS

PROPERTY		TESTING MODE	RESIN	General Purpose PS					High Impact PS					
			GRADE	HF – 10	HH – 30G	HH – 30	HH – 35	US – 320	HT40	HT50	HT54	HT560	ET63	MS500
			UNIT/ TYPE	High Flow	Good Flow	High Heat	High Heat Mold Release	High Strength Mold Flow	Good Flow	High Impact	High Gloss	High Flow	Thick Sheet	High Flow
Specific Gravity		ASTM – D792	–	1.04	1.04	1.04	1.04	1.04	1.05	1.05	1.05	1.05	1.05	1.05
Melt index (200 °C)		ASTM – D1238	g/10 min	29	8.6	5.3	6.3	3.0	6.5	3.7	2.2	16	2.4	4.8
Tensile Properties	Strength	ASTM – D638	kg/cm ²	370	400	460	400	470	230	280	290	200	280	290
	Elongation		%	2.2	2.4	2.6	2.6	3.0	50	45	64	37	50	40
Flexural Properties	Strength	ASTM – D790	kg/cm ²	560	720	890	890	900	460	560	560	410	500	600
	Modulus			31,000	31,000	31,000	31,000	20,000						
Izod Impact Strength		ASTM – D256	kg. cm/cm	1.1	1.2	1.2	1.2	1.3	8.5	8.4	12	8.9	9.4	7.3
Heat Distortion Temp.		ASTM – D648	° C	75	80	86	86	86	81	85	86	79	85	85
Rockwell Hardness		ASTM – D785	–	M 60	M 60	M 60	M 60	M 65	L 55	L 60	L 60	L 48	L 56	L 68
Glossiness		ASTM – D523	%	–	–	–	–	–	49	47	80	60	53	53
Flammability		UL - 94		1/16’’ HB	1/16’’ HB	1/16’’ HB	1/16’’ HB	1/16’’ HB	1/16’’ HB	1/16’’ HB	1/16’’ HB	1/16’’ HB	1/16’’ HB	1/16’’ HB
APPLICATION		–		House hold Goods	Audio Cassette	House hold Goods	House hold Goods	Audio Cassette	Audio & TV Housing					

APPENDIX D.2

ABS Characteristics POLYLAC ®

Typical Properties	ASTM Test	Units	General Purpose					
			PA – 707	PA – 757	PA – 717C	PA – 727	PA – 747	PA - 709
Tensile Strength	D - 638	Kg/cm ² (lb/in ²)	500 (7,090)	480 (6,800)	450 (6,380)	485 (6,870)	385 (5,470)	400 (5,670)
Tensile Elongation	D - 638	%	15	20	25	20	30	40
Flexural Modulus	D – 790	10 ⁴ kg/cm ² (10 ⁵ lb/in ²)	2.9 (4.1)	2.7 (3.8)	2.5 (3.5)	2.7 (3.8)	2.2 (3.1)	2.3 (3.2)
Flexural Strength	D – 790	Kg/cm ² (lb/in ²)	860 (12,200)	790 (11,200)	720 (10,200)	780 (11,000)	620 (8,800)	640 (9,070)
Rockwell Hardness	D - 785		R – 116	R – 116	R – 115	R – 110	R – 108	R – 102
IZOD Impact Strength (Notched)	D – 256	1/8" kg-cm/cm (ft-lb/in)	14 (2.6)	20 (3.7)	28 (5.2)	26 (4.8)	41 (7.5)	45 (8.4)
		1/4" kg-cm/cm (ft-lb/in)	14 (2.6)	18 (3.3)	25 (4.6)	23 (4.2)	36 (6.6)	40 (7.4)
Vicat Softening Temp	D – 1525	°C (°F)	105 (221)	105 (221)	104 (219)	105 (221)	103 (217)	105 (221)
H. D. T	D – 648 (annealed) (unannealed)	°C (°F)	99 (210) 88 (190)	99 (210) 88 (190)	98 (208) 87 (189)	99 (210) 88 (190)	97 (206) 86 (187)	98 (208) 88 (190)
Specific Gravity	D – 792	23/23 °C	1.06	1.05	1.04	1.04	1.03	1.03
Melt Flow Index	D – 1238	200 °C x 5 kg g/10 min (Cond. G)	1.9	1.8	1.2	1.8	1.2	0.5
	ISO – 1133*	220 °C x 10 kg g/10 min	20	22	12	19	13	5

Typical Properties	ASTM Test	Units	General Purpose					
			PA – 707	PA – 757	PA – 717C	PA – 727	PA – 747	PA - 709
Flammability		File No. E56070 UL & C – UL	1/16” HB	1/16” HB	1/16” HB	1/16” HB	1/16” HB	1/16” HB
Product Description			High gloss High Rigid	High gloss Medium Impact	Medium Impact	Electro- Plating	High Impact	Super Impact

All tests were run under laboratory condition. ASTM where applicable testing procedure. * ISO testing condition.

The data listed here fall within the normal range of product properties, but they should not be used to establish specification limits or used alone as a basis for design. This information is not intended as a warranty of any kind. Buyers must make their own representative tests and assume all risks of use whether used alone or in combination with other products. Chi Mei Corporation assumes no obligation or liability of any advice furnished by it or its employees or representatives. Test results obtained with respect to these products are for reference only. All warranties expressed or implied including warranties of merchantability for a particular purpose or use are excluded and disclaimed.

APPENDIX D.3

TYPICAL PROPERTIES AND PROCESSING CONDITIONS OF NOVAMID ®

- A. Injection molding
- Typical Properties (Dry-as-Molded)

PROPERTY	ASTM (Test Method)	UNIT	NOVAMID ®					
			1010C 2	1010C R	1020C	1010N 2	1015G	1018F 2
PHYSICAL								
Specific gravity	D1505	–	1.13	1.13	1.13	1.16	1.35	1.42
GF Content	–	Wt. %	–	–	–	–	30	–
MECHANICAL								
Tensile strength at yield	D638	kg/cm ²	800	810	780	800	1800	850
Elongation	D638	%	100	60	200	11	4	8
Flexural strength	D790	kg/cm ²	1,050	1,050	1,000	1,150	2,100	1,300
Flexural modulus	D790	kg/cm ²	26,500	28,000	26,000	32,000	80,000	70,000
Izod impact strength (Notched)	D256	kg.cm/cm	4.2	4.4	4.7	3.7	9	7.5
Hardness (Rockwell)	D785	–	120	120	120	110	120	120
Taber abrasion (CS-17, 1000 gr.)	D1044	mg/1000 rpm	7	7	–	7	15	12
THERMAL								
Melting point	DSC (2°C/min)	°C	224	224	224	224	224	224
Deflexion, temperature (4.6 kg/cm ²)	D648	°C	160	160	–	170	220	195
(18.6 kg/cm ²)	D648	°C	65	67	57	75	208	165
ELECTRICAL								
Volume sensitivity	D257	Ω . cm	10 ¹⁵	10 ¹⁵	10 ¹⁵	10 ¹⁵	10 ¹⁵	10 ¹⁵
Dielectric strength (3.2 mm thickness)	D149	kV/min	20	20	20	20	15	20
Dielectric constant (10 ⁶ Hz)	D150	–	4 – 5	4 – 5	4 – 5	4 – 5	4 – 6	3 – 4
Dissipation factor (16 ⁶ Hz)	D150	–	0.03	0.03	0.03	0.03	0.02	0.02
Arc resistance (Tungsten)	D495	sec.	124	124	–	123	132	–
OTHERS								
Flammability (Minimum thickness, colour)	UL94	–	94V-2 (1/32”, all)	94V-2 (1/32”, all)	–	94V-0 (1/32”, all)	94HB (1/32”, all)	–
Mold shrinkage (3 mm thickness)	–	%	1.0 – 1.5	1.0 – 1.5	1.0 – 1.5	1.0 – 1.5	0.2 – 0.8	0.4 – 0.9

Typical Processing conditions

Type of NOVAMID ®	: NOVAMID ® 1010C2
Molding machine	: Screw-in-line type (Nissei Plastic TS-100)
Machine capacity	: 3.5 oz
Product	: Plate (80 mm x 80 mm X 3 mm) (Side gate: 4.0 mm x 1.0 mm)
Cylinder temperature	
rear	: 240 °C
center	: 250 °C
front	: 250 °C
Nozzle temperature	: 260 °C
Mold temperature	: 80 °C
Injection pressure	: 320 kg/cm ²
Back pressure	: 50 kg/cm ²
Screw speed	: 40 rpm
Cycle time	
injection time	: 10 sec.
Cooling time	: 10 sec.
Total time	: 20 sec.

APPENDIX E
Injection Moulding Machine Specification

APPENDIX E.1

ENGEL	TECHNICAL DATA ES 650/125 HL-Victory		1999-05-06	
International size designation		650/125		
INJECTION UNIT				
Screw diameter	mm	40	45	50
Metering stroke	mm	200		
Screw speed	min ⁻¹	5 – 290		
Plasticizing rate	g/sec	26	35	46
Injection rate	cm ³ /sec	127	161	199
	cm ³ /sec	95	120	149
Maximum stroke volume	cm ³	251	318	392
	g	226	286	353
Specific injection pressure	bar	1930	1520	1230
Specific injection pressure increased	bar	2400	2040	1650
Nozzle stroke	mm	350		
Nozzle contact pressure	kN	67		
Heating capacity		12,3	13,3	15,3
Number of heating zone		5		
CLAMPING UNIT				
Clamping force	kN	1250		
Opening stroke	mm	600		
Ejector force	kN	61		
Ejector stroke	mm	130		
Platen distance maximum	mm	850		
Mould height minimum	mm	250		
Total size	mm	740 x 480		
Enlarged mould fixing platen	mm	740 x 700		
	mm	470		
DRIVE				
Pump drive power	kW	22		
Oil filling	l	310		
WEIGHT				
Net	kg	9000		

APPENDIX F
Force Link and Signal Processing
Conditioning Specification

APPENDIX F.1

Force – FSP

KISTLER

1 ... 4

Quarz-Kraftmesselemente Elements de mesure de force à quartz Quartz Force Links

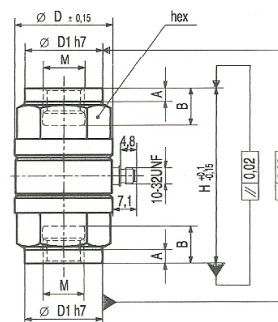
9301B/9371B

Kraftsensoren für das Messen dynamischer und quasistatischer Zug- und Druckkräfte.

Capteurs destiné à mesurer des forces dynamiques et quasi-statiques de traction et de compression.

Force sensors for measuring dynamic and quasistatic tensile and compression forces.

- Kalibriertes Kraftmesselement
Elément de mesure étalonné
Calibrated force link
- Einfache Montage
Simplicité de montage
Simple installation
- Zentriersitze für exakten Einbau
Portée de centrage pour montage exact
Centering seats for accurate fitting
- Masseisoliert
Isolément par rapport à la masse
Ground-Isolated
- Zubehör für optimale Krafteinleitung
Accessoires pour une transmission optimale des forces
Accessories for optimum force introduction



	Bereich / Gamme / Range Fz										Kalibrierter Teilbereich / Gamme partielle étalonnée / Calibrated partial range										Überlast / Surcharge / Overload										Steifigkeit / Rigidité / Rigidity (N / μm)										Eigenfrequenz / fréquence propre / Natural frequency										Kapazität / Capacité / Capacitance										Drehmoment / couple / torque (max., F _{x,y} , F _z = 0)										Biegemoment / couple de flexion bending moment (max., F _z = 0)										Schubkraft / force de cisaillement / shear force (max., F _z = 0)										Gewicht / Poids / Weight										Dimensionen / Dimensions / Dimensions / mm									
Type	kN		N		kN		N/μm		kHz		pF		Nm		Nm		kN		g		D	D1	H	A	B	hex	M																																																																																			
9301B	±	2,5	25	±	2,75	±	300	≈	90	±	8	2	5	0,35	14	11	8,5	25	2	5	9	M5																																																																																								
9311B	±	5	50	±	5,5	±	600	≈	70	±	23	3	15	0,75	28	15	12,5	30	3	5	13	M6																																																																																								
9321B	±	10	100	±	11	±	900	≈	55	±	37	14	60	1,5	90	23	18	45	5	10	19	M10																																																																																								
9331B	±	20	200	±	22	±	1000	≈	45	±	55	30	120	3	170	29	23	52	5	11	24	M12																																																																																								
9341B	±	30	300	±	33	±	1800	≈	40	±	65	50	240	4,5	330	35	31	62	6	14	32	M16																																																																																								
9351B	±	40	400	±	44	±	2000	≈	33	±	65	90	370	6	480	41	35	72	7	18	36	M20																																																																																								
9361B	±	60	600	±	66	±	2800	≈	28	±	150	190	830	9	1020	53	45	88	9	22	46	M24																																																																																								
9371B	±	120	1200	±	132	±	4000	≈	22	±	200	430	2500	18	2500	76	64	108	10	28	65	M30																																																																																								

Technical drawing of a force transducer. The drawing shows a cross-section of the device with various dimensions labeled. Key dimensions include: D1 h7 (inner diameter), M (thread), A (height), B (width), H (total height), and H 2/15 (height of a specific part). Internal components like a 10-32 NF thread and a 10-32 NF nut are also shown. The drawing includes a scale bar indicating 10.02 and 10.03 mm.

Technische Daten

Données techniques

Technical Data*

Empfindlichkeit	Sensibilité	Sensitivity	pC/N	≈ -4
Ansprechschwelle	Seuil de réponse	Threshold	N	≤ 0,02
Linearität	Linéarité	Linearity	% FSO	± 0,5
Hysteresis	Hystérésis	Hysteresis	% FSO	± 0,5
Isolationswiderstand	Résistance d'isolement	Isolation resistance	TΩ	≥ 50
Masseisolation	Isolément par rapport à la masse	Ground-isolation	MΩ	≥ 100
Temperatur-Koeffizient	Coefficient de température	Temperature coefficient	%/°C	-0,02
Betriebstemperatur-Bereich	Gamme de température de service	Operating temperature range	°C	-40 ... 120

* In all Kistler documents, the decimal sign is a comma on the line (ISO 31-0:1992)

Kistler Instrumente AG Winterthur, CH-8408 Winterthur, Switzerland, Tel. (052) 224 11 11 Kistler Instrument Corp., Amherst, NY 14228-2171, USA, Phone (716) 691-5100

Beschreibung

Der Kraftsensor ist unter Vorspannung zwischen zwei Muttern eingebaut und kann daher sowohl Druck- wie auch Zugkräfte messen. Das Quarzelement gibt eine der wirkenden Kraft proportionale elektrische Ladung ab. Diese wird durch eine Elektrode abgenommen und über den Steckeranschluss nach aussen geführt. Das Ladungssignal wird weiter über ein abgeschirmtes Kabel zu einem Ladungsverstärker geführt, welcher dieses in eine proportionale Ausgangsspannung umwandelt. Durch eine entsprechende Auswertelektronik kann der Messwert erfasst und weiterverarbeitet werden.

Der Sensor ist masseisoliert eingebaut. Damit werden Erdschleifenprobleme weitgehend ausgeschaltet.

Anwendung

Das Kraftmesselement eignet sich, dank seiner grossen Steifigkeit, speziell für das Messen von rasch ändernden Zug- und Druckkräften. Das elastische Verhalten des Messobjektes wird dabei praktisch nicht verändert. Quasistatische Messungen sind ebenfalls möglich. **Das Kraftmesselement wird kalibriert geliefert.** Nach einem korrekten Einbau ist es ohne Nachkalibrierung sofort einsatzbereit.

Einsatzbeispiele

Automobilindustrie

- Sicherheitstechnik, Überwachung von Aufprallkräften
- Kraftstösse in Fahrwerken
- Kräfte an Auswuchtmaschinen

Materialprüfung

- Schlagprüfung, Wechselfestigkeit

Werkzeugmaschinen

- Überwachung an Pressen, Stanz-, Präge- und Schweissmaschinen
- Kraftmessungen an Längsführungen

Allgemein Maschinenindustrie

- Überwachung von Abstützkräften (Kraftschwingungen) an Maschinen, welche auf Dämpfungselementen gelagert sind
- Einspannvorgänge, z.B. Kraftsensor kombiniert mit Hydraulikzylinder
- Fügetechnik (Einschieben, Einpressen von Montageteilen)

Qualitätskontrolle

- Kraftmessungen an Schaltern
- Überwachung von Montageautomaten

Montage

Die Kontaktflächen, welche die Kraft auf das Messelement übertragen, müssen plan, steif und sauber sein. Die Befestigungsschrauben dürfen nicht in den Sackgewinden des Kraftmesselementes aufstehen. Es ist ein Spiel S (siehe Fig. A, Seite 3) von mindestens 0,5 mm einzuhalten. Die Schrauben sind genügend stark anzuziehen, sodass auch bei der grössten Zugkraft kein Spalt zwischen Kontaktflächen auftritt.

Das Kraftmesselement hat beidseitig Zentriersitze, die den genauen Einbau erleichtern.

Description

Le capteur de force est monté sous précontrainte entre deux écrous et peut donc mesurer des forces de compressions et de traction. L'élément à quartz engendre une charge électrique proportionnelle à la force. Cette charge électrique est captée par une électrode puis acheminée vers l'extérieur par le biais d'un connecteur. Par l'intermédiaire d'un câble blindé, le signal de charge est ensuite acheminé à un amplificateur de charge qui le transforme en une tension de sortie qui lui est proportionnelle. Un système électronique permet alors de saisir et de traiter la valeur mesurée.

Le capteur est moulé avec isolement par rapport à la masse, ce qui permet d'éviter en grande partie les problèmes de circuits de retour par la terre.

Utilisation

Grâce à sa grande rigidité, l'élément de mesure convient parfaitement à mesures de forces de traction et de compression dynamiques. Le comportement élastique de l'objet à mesurer ne se trouve pas modifié de manière notable. Des mesures quasi-statiques sont possibles aussi. **L'élément de mesure est livré étalonné.** Monté correctement, il peut être mis en oeuvre immédiatement sans réétalonnage.

Exemples d'utilisation

Industrie automobile

- Technique de sécurité, surveillance des forces de collision
- Etude des impulsions sur les châssis
- Mesure des forces s'exerçant sur les machines à équilibrer les roues

Essais de matériaux

- Essais aux chocs, résistance aux efforts alternés

Machines-outils

- Surveillance des presses, machines à découper, presse à estamper et machines à souder
- Mesures des forces sur les glissières longitudinales

Construction mécanique générale

- Surveillance des forces d'appui (vibrations) s'exerçant sur des machines montées sur des éléments stabilisateurs
- Processus de fixation, p. ex. capteur de force associé à un cylindre hydraulique
- Technique d'assemblage (insertion, encastrement d'éléments de montage)

Contrôles de qualité

- Mesure de forces sur les commutateurs
- Surveillance des robots de montage

Montage

Les surfaces de contact qui transmettent la force aux éléments de mesure doivent être planes, rigides et propres. Les vis de fixation ne doivent pas toucher le fond des alésages filetés de l'élément de mesure. Un jeu S (voir fig. A, page 3) de 0,5 mm au minimum est à respecter. Les vis doivent être serrées suffisamment pour éviter qu'une fente s'ouvre entre les surfaces de contact sous la force de tension la plus grande.

L'élément de mesure a des rebords de centrage des deux côtés qui facilitent le montage exact.

Description

The force sensor is mounted under preload between two nuts and, therefore can measure compression and tensile forces. The quartz element yields an electric charge which is proportional to the force. This is picked off by an electrode and transferred via a connector. The charge signal is fed via a screened cable to a charge amplifier, which converts it into a proportional output voltage. An appropriate evaluation circuit can record and further process the measurand.

The sensor is moulded ground-isolated. This largely eliminates ground loop problems.

Application

As a result of its great rigidity, the force link is particularly suitable for measuring rapidly changing tensile and compression forces. The elastic behaviour of the test object is practically not influenced. Quasistatic measurements, are possible, too. **The force link is supplied calibrated.** After correct installation, it is immediately ready for use without recalibration.

Exemples of use

Automobile industry

- Safety technology, monitoring of collision forces
- Mechanical shocks in chassis
- Forces on balancing machines

Material testing

- Impact testing, alternate strength testing

Machine tools

- Monitoring on presses, punching, embossing and welding machines

- Force measurements on longitudinal guideways

General machine building

- Monitoring of supporting forces (force oscillations) on machinery mounted on damping elements
- Clamping processes, e.g. force sensor combined with hydraulic cylinder
- Joining technique (insertion, press fit of components)

Quality control

- Force measurements on switches
- Monitoring of automatic assembly machines

Mounting

The contact faces which transmit the force to the force link must be flat, rigid and clean. The fixing bolts must not touch the bottom of the threaded holes of the force link. A play S (see fig. A, page 3) of at least 0,5 mm must be assured. The bolt must be tightened sufficiently as to avoid that a gap could open between the contact faces under the highest tensile force.

The force link has centering shoulders on both ends which precise mounting easier.

Krafteinleitung

Nach Möglichkeit soll diese konzentrisch zur Achse erfolgen. Exzentrische Krafteinleitung, Biegemomente, Drehmomente sowie Schubkräfte sind nur bis zu einem gewissen Mass zulässig.

Kraftmesselement mit SCS Kalibrierschein

Kistler ist die akkreditierte Kalibrierstelle Nr. 049 des SCS (Swiss Calibration Service) für Kraft. Deshalb können Kraftmesselemente gegen Aufpreis auch mit einem SCS-Kalibrierschein geliefert werden. Sie können dann z. B. als Bezugsnorm im betriebsinternen Kalibrierdienst verwendet werden. Kalibriert wird dann nur der Druckkraftbereich (100 %FS, 10 %FS und 1 %FS). Wir empfehlen, die Druckkappe und den Flansch (siehe Seite 4) zu verwenden, um reproduzierbare Messungen zu gewährleisten.

Transmission des forces

Dans la mesure du possible, la transmission des forces doit s'effectuer le long de l'axe. L'application excentrique de forces, l'application de moments de flexion, de couples de rotation et d'efforts de cisaillement ne sont admissibles que dans certaines limites.

Élément de mesure de force avec certificat d'étalonnage SCS

Kistler est le laboratoire d'étalonnage no. 049 accrédité par SCS (Swiss Calibration Service) pour la force. Les éléments de mesure peuvent alors être livrés (contre un supplément) avec un certificat d'étalonnage SCS. Ils serviront p. ex. comme étalons de référence dans le service d'étalonnage interne. Alors seulement la gamme de force en compression (100 %FS, 10 %FS et 1 %FS) sera étalonnée. Nous recommandons d'utiliser la calotte et la bride (voir page 4) pour assurer une bonne reproductibilité des mesures.

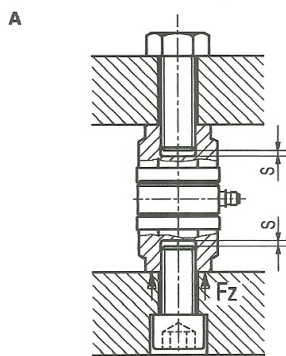
Force introduction

As far as possible, this should be concentric to the axis. Eccentric force introduction, bending moments, torques and shear forces are permitted only to a certain extent.

Force link with SCS Calibration Certificate

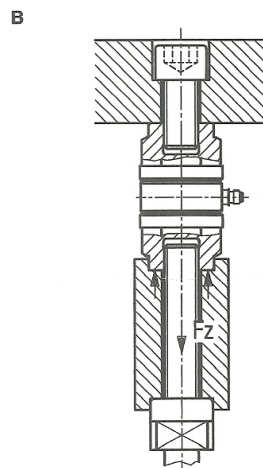
Kistler is the calibration laboratory no. 049 accredited by the SCS (Swiss Calibration Service) for force. Therefore, the force links can be supplied (at an extra charge) with an SCS Calibration Certificate. They can then be used e. g. as reference standards in an internal calibration service. Only the range for compression force will be calibrated (100 %FS, 10 %FS and 1 %FS). We recommend to use the force distribution cap and the flange (see page 4) to assure a good reproducibility of the measurements.

Einbaubeispiele, verschiedene Arten der Krafteinleitung



Krafteinleitung von Druckkräften
Transmission des forces de pression
Force introduction of compression forces

Exemples de montage - Différents types de transmission des forces

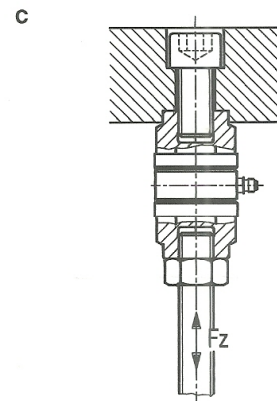


Belastung durch Zug- und Druckkräfte über ein Verlängerungsstück. Die Vorspannkraft auf die Hülse darf beim Wirken von Zugkräften einen Minimalwert nicht unterschreiten.

Application de forces de traction et de compression par l'intermédiaire d'une rallonge. La force de précontrainte s'exerçant sur le manchon ne doit pas être inférieure à la valeur minimale en cas d'application de forces de traction.

Loading from tensile and compression forces via an extension piece. The preloading force on the sleeve must not be less than a minimum value under the effect of tensile forces.

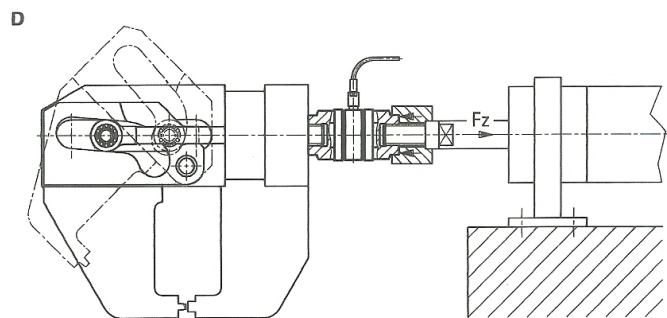
Mounting examples, different types of force introduction



Krafteinleitung von Zug- und Druckkräften, direkt auf den Gewindeanschluss. In diesem Fall sollte stets eine Gegenmutter verwendet werden.

Transmission des forces de traction et de compression directement sur le raccord fileté. Dans ce cas, un contre-écrou sera systématiquement utilisé.

Force introduction of tensile and compression forces directly onto the threaded connection. In this case, a lock nut should always be used.



Einbaubeispiel eines Kraftmesselementes in einer hydraulischen Spannvorrichtung. Überwachung von Zug- und Druckkräften.

Exemple de montage d'un élément de mesure dans un dispositif de fixation hydraulique. Surveillance des forces de traction et de compression.

Mounting example of a force link in a hydraulic clamping device. Monitoring of tensile and compression forces.

Zubehör**Anschlusskabel**

Die verschiedenen Kabelarten passend zum Steckeranschluss 10-32 UNF neg. sind aus dem Kistler Datenblatt Nr. 15.011 ersichtlich.

Druckkappe und Flansch

Für eine optimale Krafteinleitung kann in Kombination zum Kraftmesselement eine Druckkappe und ein Flansch eingesetzt werden. Die Teile sind ebenfalls als Präzisionsteile gefertigt und weisen eine Oberflächenhärte von 400 ... 490 HV (Vickers) auf.

Accessoires**Câbles de connexion**

Les différentes variantes de câbles s'adaptant au connecteur 10-32 UNF nég. sont décrites dans la notice technique No 15.011 Kistler.

Calotte distributrice de force et bride

Pour une transmission optimale des forces, il est possible d'utiliser un calotte distributrice de force et une bride en association avec un élément de mesure des forces. Il s'agit de pièces de précision qui présentent une dureté de surface de 400 ... 490 (dureté Vickers).

Accessories**Connecting cable**

The different cable types suitable for connector Type 10-32 UNF neg. are listed in Kistler data sheet No. 15.011.

Force distributing cap and flange

A force distributing cap and a flange can be used in combination with the force link to provide optimum force introduction. These components are also manufactured as precision parts and have a surface hardness of 400 ... 490 HV (Vickers).

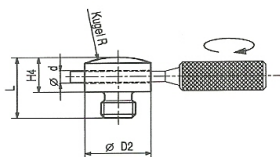
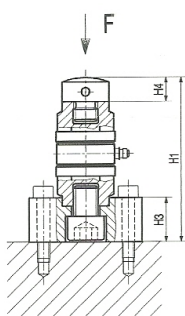


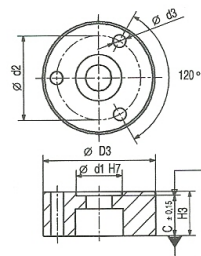
Fig. 1

**Druckkappe / Calotte distributrice de force / Force distributing cap (Typ 9500A...)**

Mit einem zylindrischen Werkzeug kann die Druckkappe eingeschraubt werden.

Le calotte distributrice de force peut être vissée à l'aide d'un outil cylindrique.

The force distributing cap can be screwed in with a cylindrical tool.

**Flansch / Bride / Flange (Typ 9501A...)**

Eine Zylinderschraube mit Innensechskant gehört zum Lieferumfang des Flansches.

Une vis à tête cylindrique à six pans creux est livrée avec la bride.

A socket head cap screw is supplied with the flange.

Fig. 1

Kraftmesselement mit Flansch und Druckkappe. Einsatz für Druckkraftbelastungen.

Élément de mesure de forces avec bride et calotte distributrice de force. Utilisation pour les forces de pression.

Force link with flange and pressure distributing cap. Insert for compression force loading.

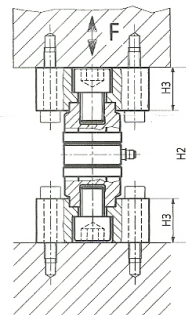
Fig. 2

Kraftmesselement mit beidseitig montierten Flanschen. Einsatz für Zug- und Druckkraftbelastungen.

Élément de mesure de forces à brides des deux côtés. Utilisation pour les forces de traction et de pression.

Force link with flanges fitted on both sides. Insert for compression force loading.

Fig. 2



000-107m-12.96 (DB06.013m-12.96)

Kraftmesselemente Eléments de mesure de force Quartz force links	Druckkappe Calotte distributrice de force Force distributing cap						Flansch / Bride / Flange							Fig. 1	Fig. 2	
	Type	Type	D2	L	H4	R	d	Type	D3	H3	d1	d2	d3	C	H1	H2
9301B	9500A0	8,5	8	4	R10	2,2		9501A0	25	9	8,5	18	3,2	8	37	41
9311B	9500A1	12,5	10	6	R15	3,2		9501A1	34	11	12,5	24	4,3	9	45	48
9321B	9500A2	18	17	9	R25	4,3		9501A2	44	18	18	33	5,3	16	70	77
9331B	9500A3	23	21	12	R35	4,3		9501A3	56	22	23	42	6,4	20	84	92
9341B	9500A4	31	28	15	R45	6,4		9501A4	70	29	31	52	8,4	27	104	116
9351B	9500A5	35	33	18	R50	6,4		9501A5	84	37	35	62	10,5	35	125	142
9361B	9500A6	45	41	22	R65	8,4		9501A6	102	44	45	77	13	42	152	172
9371B	9500A7	64	57	32	R90	8,4		9501A7	136	53	64	106	17	51	191	210

Signal Conditioning Platform (SCP)

Type 2853A...

Universal Measuring Platform

With the SCP, Kistler Instrumente AG offers a practical signal conditioning unit in a standardized and modular design for use in the following sectors: "Acceleration", "Plastics processing" and "Combustion engines". The SCP consists of a standardized base unit and application-orientated modules.

The SCP features the following characteristics:

- Rack-mounted or desktop unit in a standardized 19" construction
- Normal and remote control using standardized communication protocols
- Menu-driven configuration via a GUI (Graphical User Interface)
- Application-specific modules for charge amplification, piezoresistive amplification, universal low-voltage amplification as well as signal conditioning individually tailored for each sensor
- Complete integration into Kistler software ("Plastics" field)
- Consisting of a base unit (Master) expandable by one additional (Slave) unit ("Combustion engines" sector)
- Optional automatic sensor detection (for "Combustion engines" and "Acceleration" sectors)

The application-specific modules are described in the relevant data sheets:

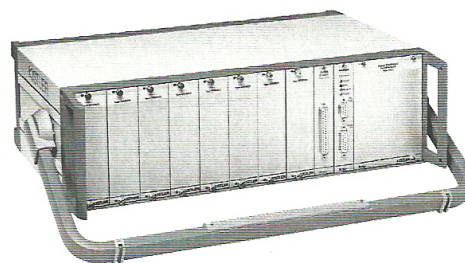
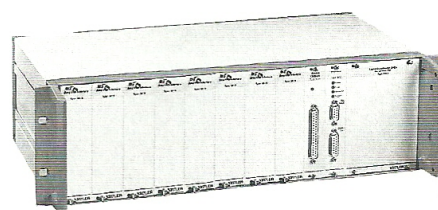
"Plastics processing"	Data sheet 000-408e
"Combustion engines"	Data sheet 000-409e
"Acceleration"	Data sheet 000-410e

Description of SCP

The SCP consists of a base unit and the application-specific modules.

A base unit consists of the chassis (Type 2853A) in 19" construction together with the module cards for the power supply, data communication (Type 5615) and for the signal output (Type 5225A).

The power supply is an integral part of the base unit and contains a universal voltage conditioning system with high interference immunity. External data communication between SCP and a higher level computer is carried out by the module for data communication (Type 5615) via an RS 232C interface. All analog measuring signals from the application-specific modules are made available for further processing by the signal output module (Type 5225A).



The base unit (Master) can be supplemented by one 19" additional unit (Slave), in which data communication continues to take place via the base unit. ("Combustion engines" sector).

A maximum of 8 slots is available per unit for modules with up to four measuring channels. Therefore, the base unit can provide a maximum of 32 measuring channels or, with the additional unit, a maximum of 64 measuring channels. In addition, up to 4 potential-free outputs are available to drive external equipment. The internal and external processes can be synchronized with trigger signals.

Parameters can be set for all SCP functions via the SCP configuration software (5.590.239) for Windows 98SE, NT, 2000 as well as XP. Standardized protocols for data communication ensure comprehensive compatibility with higher level computer and data acquisition systems.

Orders can be placed using the information from the data sheets for the field of application concerned.

2853A_000-374e-10.06

This information corresponds to the current state of knowledge. Kistler reserves the right to make technical changes. Liability for consequential damage resulting from the use of Kistler products is excluded.

Page 1/4
©2006, Kistler Instrumente AG, PO Box, Eulachstr. 22, CH-8408 Winterthur
Tel +41 52 224 11 11, Fax +41 52 224 14 14, info@kistler.com, www.kistler.com

Technical Data

Chassis

Module cards	max.	8
Channels	max.	32 per rack
	max.	2 rack combination
Power supply	VAC	100 ... 240 V $\pm 10\%$
Max. power input	W	53
Degree of protection	IP	40
Operating temperature	°C	0 ... 60
	°F	32 ... 140
Dimensions		19" / 3 HE 84 TE
Weight (without modules)	kg	25,6
Software		COM components for Microsoft Windows 98, XP, 2000, NT

Analog interface card (Type 5225A1)

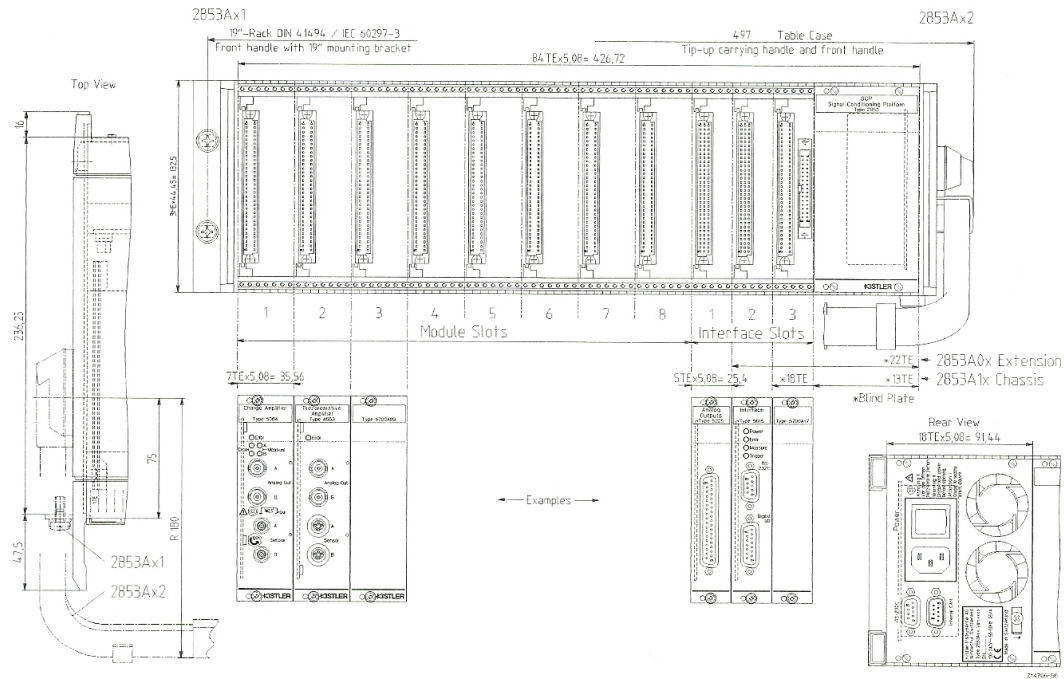
Analog outputs		32
Voltage	V	± 10
Current	mA	0 ... ± 2 (pro Kanal)
Error	%	$< \pm 0,1$
Trigger output	V	High $> 2,4$
	V	Low $< 0,8$
		(electrically isolated)
Connection	Type	Sub. D 37pol. female

CPU interface card Type 5615 (Type 2853A11 and Type 2853A12)

Interface	RS232	
Trigger input voltage	V	High 3 ... 30
(connected to 5225 trigger output)	V	Low < 2
Current input High	mA	2 ... 29
Digital outputs	floating switches with photo/MOS relay	
Current load (continuous)	mA	< 100
Voltage (continuous)	V	$< \pm 42$
Connection RS232	Type	Sub D 9 pol. female
Connection Operate		
Outputs	Type	Sub D 15 pol. female

2853A_000-374e-10.06

Dimensions



Accessories Included

2853A11 and 2853A12:

- Software on CD
- CPU interface card
- Analog interface card

Art. No./Type

7.643.014
5615
5225A1

- A/D card 16 channel PC card
16 bit resolution
- A/D card 16 channel PCI card
16 bit resolution
- A/D card 64 channel PCI card
16 bit resolution
- A/D card 16 channel ISA card
12 bit resolution
- A/D card 64 channel ISA card
12 bit resolution

Art. No./Type

2855A5
2855A4
2855A6
2855A3
2855A2

2853A01 and 2853A02:

- Analog interface card
- CAN connecting cable 0,5 m

5225A1
5.590.239

Accessories

2853A11 and 2853A12:

- CPU interface card
- Analog interface card

5615
5225A1

2853A01 and 2853A02:

- Analog interface card

5225A1

Optional Accessories

- Communication cable serial 5 m
- Dummy front panel modules
- A/D card 16 channel PC card
12 bit resolution

1200A27
5700A09
2855B1

Connecting cable A/D card SCP chassis

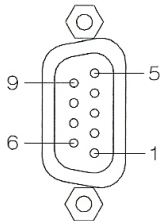
- A/D card 2855B1
- A/D card 2855A5
- A/D card 2855A4
- A/D card 2855A6
- A/D card 2855A3
- A/D card 2855A2
- Grounding cable

1200B21
1200B21
1200A13
1200A41
1200A13
1200A41
5.590.175

This information corresponds to the current state of knowledge. Kistler reserves the right to make technical changes. Liability for consequential damage resulting from the use of Kistler products is excluded.

©2006, Kistler Instrumente AG, PO Box, Eulachstr. 22, CH-8408 Winterthur
Tel +41 52 224 11 11, Fax +41 52 224 14 14, info@kistler.com, www.kistler.com

Pin Allocation Sub 9

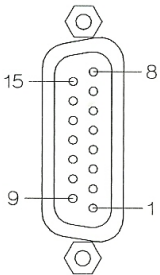


Pin Layout:

1	1, 6, 4
6	1, 6, 4
2	RxD
7	7,8
3	TxD
8	7, 8
4	1, 6, 4
9	NC
5	GND RS

Pin allocation Type 5615A RS232 interface

Pin Allocation Sub 15

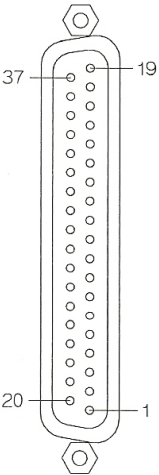


Pin Layout:

1	TRIGGER+
9	TRIGGER-
2	Remote OP+
10	Remote OP-
3	DOUT A1
11	DOUT A3
4	DOUT B1
12	DOUT B3
5	DOUT A2
13	+24 V
6	DOUT B2
14	DOUT A4
7	NC
15	DOUT B4
8	EGND

Pin allocation Type 5615 operate and digital outputs

Pin Allocation Sub 37



Pin Layout:

1	AGND	29	Analog 5C
20	Analog 1A	11	Analog 5D
2	Analog 1B	30	Analog 6A
21	Analog 1C	12	Analog 6B
3	Analog 1D	31	Analog 6C
22	Analog 2A	13	Analog 6D
4	Analog 2B	32	Analog 7A
23	Analog 2C	14	Analog 7B
5	Analog 2D	33	Analog 7C
24	Analog 3A	15	Analog 7D
6	Analog 3B	34	Analog 8A
25	Analog 3C	16	Analog 8B
7	Analog 3D	35	Analog 8C
26	Analog 4A	17	Analog 8D
8	Analog 4B	36	AGND
27	Analog 4C	18	TRIG OUT+
9	Analog 4D	37	TRIG OUT-
28	Analog 5A	19	GND RS
10	Analog 5B		

Pin allocation Type 5225A1 analog outputs and trigger

2853A_000-374e-10.06

APPENDIX F.3

Measure & Analyze – MCS

KISTLER
measure. analyze. innovate.

SCP for Plastics Processing Modules for Signal Conditioning System

Type 2853A..., 2207A...,
5063A..., 5227A...,
5613A...

The SCP is a modular system for conditioning measuring signals from piezoelectric, piezoresistive and thermocouple sensors. Voltages from external sources can also be measured in addition. The SCP consist of a base unit and application specific module.

- Maximum flexibility for applications in plastic processing
- Fully supported by DataFlow Software

Description

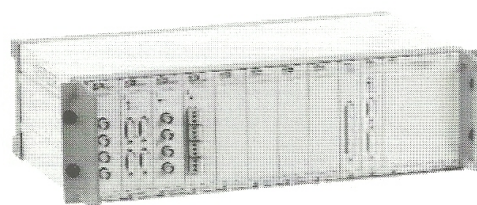
The SCP modules are modules for the SCP base unit Type 2853A... and signal conditioner Type 2859A... . These are described in detail in the data sheets of the corresponding Types. The SCP base unit is a stationary system which can be equipped with up to 8 modules. Up to 32 input channels are available. The signal conditioner Type 2859A... is the mobile version of this system. 4 piezoelectric pressure inputs and 4 temperature inputs are integrated in this system as standard. A vacant module slot allows the system to be expanded as required by up to 12 input channels.

The following modules are available for plastics processing:

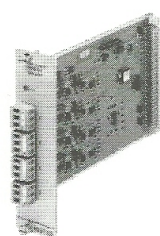
- 4-channel thermocouple amplifier Type 2207A
- 4-channel charge amplifier Type 5063A1 for the connection of 4 piezoelectric sensors
- 4-channel voltage amplifier Type 5227A1 for the connection of 4 external «voltage sources» ± 10 V
- 4-channel amplifier interface Type 5613A1/A2 for the supply, remote control and signal transmission from 4 external amplifiers or transmitters. The module provides an excitation voltage of 24 V and ± 15 V respectively for the external amplifiers

Application

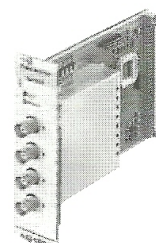
When used with the DataFlow software Type 2805A-02-x, the SCP Type 2853A... and the signal conditioner Type 2859A... is suitable for process visualization, process monitoring and process documentation for all variations of the injection molding process and other cyclical processing methods. For further information on DataFlow, see corresponding data sheet.



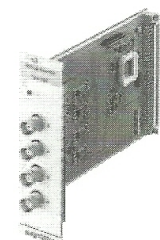
SCP «Plastics Processing» in typical configurations



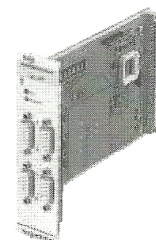
Type 2207A



Type 5063A1



Type 5227A1



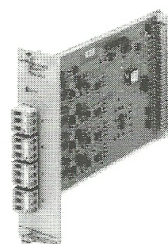
Type 5613A1/A2

000-408e-02.03 (DB19.001e)

This information corresponds to the current state of knowledge. Kistler reserves the right to make technical changes. Liability for consequential damage resulting from the use of Kistler products is excluded.

©2003, Kistler Instrumente AG, PO Box, Eulachstr. 22, CH-8408 Winterthur
Tel +41 52 224 11 11, Fax 224 14 14, info@kistler.com, www.kistler.com

Page 1/6


Technical Data Valid for all Modules

Operating temperature range	°C	0 ... 60
Min./Max. temperature	°C	-10/60
Vibration resistance (20 ... 2000 Hz, duration 16 min, cycle 2 min)	gp	10
Shock resistance (1 ms)	g	200
Sound resistance	dBA	120
Front panel dimensions	mm	128,7 x 35,0
HE	-	3
TE	-	7

The module outputs are available on the interface card Type 5225A1. This interface card is described in data sheet of Type 2853A...

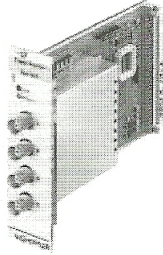
4-Channel Thermocouple Amplifier Type 2207A

Temperature amplifier for the connection of up to 4 thermocouples or temperature sensors Types K and J. The amplifier is equipped with differential amplifier and cold spot compensation.

Technical Data

Channels		4
Thermocouple	Type	J or K
Measuring range I	°C	0 ... 400
Measuring range II	°C	0 ... 200
Error measuring range I	%	<0,5
Error measuring range II	%	<0,2
Zero point error	mV	<10 mV
Frequency range (-3dB)	kHz	0 ... >1
Probe interrupt detection (neg. saturation)	V	-9 ... -10,5
Output voltage	V	0 ... 10
Output current	mA	0 ... 2
Output resistance	Ω	10
Output interference signal (0,1 ... 1 MHz)	mV _{pp}	<10
Thermocouple connection	Type	Phoenix screw terminals
Weight	kg	≈0,28

000-408e-02.03 (DB19.001e)

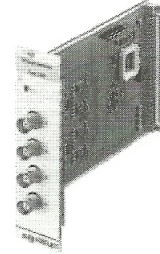


4-Channel Charge Amplifier Type 5063A1

The charge amplifier for piezoelectric sensors is equipped with differential inputs and a common ground. All amplifiers have a common Operate.

Technical Data

Channels		4
Measuring range I	pC	$\pm 5'000 \dots \pm 50'000$
Measuring range I on delivery calibrated to	pC	$\pm 20'000$
Measuring range I/II ratio		4
Error	%	$< \pm 1$
Drift (0 ... 50 °C)	pC/s	$< \pm 0,2$
(25 °C)	pC/s	$< \pm 0,05$
Frequency range (20 V _{pp})	kHz	0 ... >25
Reset/Operate transition	pC	$< \pm 2$
Signal polarity	negative input charge results in pos. output voltage	
Max. voltage between sensor GND and output/supply voltage	V	$< \pm 50$
Suppression of the interference signals between sensor GND and output/supply GND	dB	>70
Output voltage	V	0 ... ± 10
Output current	mA	0 ... ± 2
Output resistance	Ω	10
Output interference signal (0,1 Hz ... 10 MHz)	mV _{pp}	<10
Sensor connections	Type	BNC neg.
Weight	kg	$\approx 0,26$



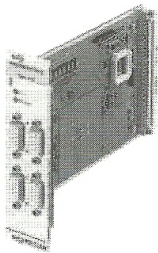
4-Channel Voltage Amplifier Type 5227A1

Voltage amplifier for the connection of up to 4 «voltage sources» with $\pm 10V$. The settings required are made using the software.

Technical Data

Channels		4
Measuring range	V	± 10
Selectable gain		1 / 2 / 5 / 10
Error	%	$< \pm 0,5$
Zero point error	mV	$< \pm 10$
with gain 10	mV	$< \pm 20$
Frequency range (20 V _{pp}) -3dB	kHz	0 ... >50
-5%	kHz	0 ... >30
Max. voltage between sensor GND and output/supply voltage	V	$< \pm 50$
Suppression of the interference signals between sensor GND and output/supply GND	dB	>70
Input resistance	M Ω	>10
Output voltage	V	0 ... ± 10
Output current	mA	0 ... ± 2
Output resistance	Ω	10
Output interference signal (0,1 Hz ... 10 MHz)	mV _{pp}	<10
Sensor connections	Type	BNC neg.
Weight	kg	$\approx 0,21$

000-408e-02.03 (DB19.001e)



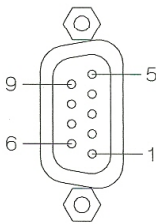
4-Channel Amplifier Interface Type 5613A1/A2

Amplifier interface for connection of up to 4 external amplifiers or transmitters. The module provides a excitation voltage for the external amplifiers of 24 V (5613A1) or ± 15 V (5613A2) respectively as well as Operate and Range signals (for all channels active simultaneously).

Technical Data

	Type 5613A1	Type 5613A2
Channels		4
Measuring range	V	± 10
Gain		1
Error	%	$< \pm 0,1$
Zero point error	mV	$< \pm 2$
Frequency range (20V _{pp})	kHz	0 ... >50
Input resistance	k Ω	>300
Output voltage	V	0 ... ± 10
Output current	mA	0 ... ± 2
Output resistance	Ω	10
Output interference signal (0,1 Hz ... 10 MHz)	mV _{pp}	<10
Power supply for external amplifier (electrically isolated)		
Voltage	VDC	24 ± 15
Current consumption per channel	mA	<45 $< \pm 30$
Sensor connections	Type	Sub D 9 female
Weight	kg	$\approx 0,16$

Pin Allocation Sub D 9-pole



Pin Allocation:

1	(-15 V)
2	+24 V (+15 V)
3	+RANGE II
4	+OPERATE
5	Signal Input
6	Power GND
7	-RANGE II
8	-OPERATE
9	Signal GND

Pin allocation Type 5613A... Operate, Range and excitation voltage for external Amplifier.

000-408e-02.03 (DB19.001e)

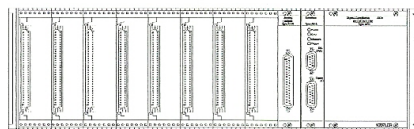
Ordering Code**Signal Conditioning Platform Type 2853A...**

When ordering, please use the form below. Place a cross next to the chassis Type (Chassis Rack or Desktop) as well as the modules required and their positions in the module slots (see data sheet SCP chassis).

- ☐ Chassis Rack (19") Type 2853A11
☐ Desktop Type 2853A12

Interfaces (these SCP modules must be included in the order)

- ☒ 5615 CPU interface
☒ 5225A1 Analog interface



Slot 1	Slot 2	Slot 3	Slot 4	Slot 5	Slot 6	Slot 7	Slot 8	Type	
<input type="checkbox"/>	<input type="checkbox"/>	<input type="checkbox"/>	<input type="checkbox"/>	<input type="checkbox"/>	<input type="checkbox"/>	<input type="checkbox"/>	<input type="checkbox"/>	2207A	4-channel temperature amplifier
<input type="checkbox"/>	<input type="checkbox"/>	<input type="checkbox"/>	<input type="checkbox"/>	<input type="checkbox"/>	<input type="checkbox"/>	<input type="checkbox"/>	<input type="checkbox"/>	5063A1	4-channel charge amplifier
<input type="checkbox"/>	<input type="checkbox"/>	<input type="checkbox"/>	<input type="checkbox"/>	<input type="checkbox"/>	<input type="checkbox"/>	<input type="checkbox"/>	<input type="checkbox"/>	5227A1	4-channel voltage amplifier
<input type="checkbox"/>	<input type="checkbox"/>	<input type="checkbox"/>	<input type="checkbox"/>	<input type="checkbox"/>	<input type="checkbox"/>	<input type="checkbox"/>	<input type="checkbox"/>	5613A1	4-channel amplifier interface
<input type="checkbox"/>	<input type="checkbox"/>	<input type="checkbox"/>	<input type="checkbox"/>	<input type="checkbox"/>	<input type="checkbox"/>	<input type="checkbox"/>	<input type="checkbox"/>	5613A2	4-channel amplifier interface
<input type="checkbox"/>	<input type="checkbox"/>	<input type="checkbox"/>	<input type="checkbox"/>	<input type="checkbox"/>	<input type="checkbox"/>	<input type="checkbox"/>	<input type="checkbox"/>	5700A09	Dummy plate
<input type="checkbox"/>	<input type="checkbox"/>	<input type="checkbox"/>	<input type="checkbox"/>	<input type="checkbox"/>	<input type="checkbox"/>	<input type="checkbox"/>	<input type="checkbox"/>		open

Order form: Please place a cross against the allocation of each slot

Accessories Included

- Software on CD
- CPU interface card
- Analog interface card

Type/Art. No.

7.643.014
 5615
 5225A1

Optional Accessories**Type/Art. No.**

- DataFlow software for process visualization 2805A-02-1
process monitoring and process documentation for Windows 95c, Windows 98SE, NT, 2000, XP with license code on parallel port.
- DataFlow software for process visualization 2805A-02-2
process monitoring and process documentation for Windows 95c, Windows 98SE, NT, 2000, XP with license code on USB port
- A/D card 16-channel PC card 12 bit resolution 2855B1
- A/D card 16-channel PC card 16 bit resolution 2855A5
- A/D card 16-channel PCI card 16 bit resolution 2855A4
- A/D card 64-channel PCI card 16 bit resolution 2855A6
- A/D card 16-channel ISA card 12 bit resolution 2855A3
- A/D card 32-channel ISA card 12 bit resolution 2855A2
- Connecting cable from A/D card Type 2855B1 1200B21 to SCP chassis
- Connecting cable from A/D card Type 2855A5 1200B21 to SCP chassis
- Connecting cable from A/D card Type 2855A4 1200A13 to SCP chassis
- Connecting cable from A/D card Type 2855A6 1200A41 to SCP chassis
- Connecting cable from A/D card Type 2855A3 1200A13 to SCP chassis
- Connecting cable from A/D card Type 2855A2 1200A41 to SCP chassis
- Communication cable, serial 5 m 1200A27
- Grounding cable 5.590.175
- Connecting cable from charge amplifier Type 5039A... to amplifier interface Type 5613A1 1200A5
- Connecting cable from hydraulic pressure transmitter Type 4095A... (4 ... 20 mA) to amplifier interface Type 5613A1 1200A39
- Connecting cable from SmartAmp Type 5049A... 1200A9 to amplifier interface Type 5613A1

000-408e-02.03 (DB19.001e)

This information corresponds to the current state of knowledge. Kistler reserves the right to make technical changes. Liability for consequential damage resulting from the use of Kistler products is excluded.

©2003, Kistler Instrumente AG, PO Box, Eulachstr. 22, CH-8408 Winterthur
 Tel +41 52 224 11 11, Fax 224 14 14, info@kistler.com, www.kistler.com

- Connecting cable from charge amplifier Type 5011 to amplifier interface Type 5613A1 1200A7
- Connecting cable from hydraulic pressure transmitter Type 4095A... (0 ... 10 V) to amplifier interface Type 5613A1 1200A11
- Connecting cable from piezoresistive amplifier Type 4618A0 and 4618A2 to amplifier interface Type 5613A1 1200A29
- Connecting cable from temperature amplifier Type 2809A1 for connection to Interface Type 5613A1 1200A25
- Connecting cable from extrusion sensor Type 4096/97 (0 ... 10 V) to amplifier interface Type 5613A1 1200A33
- Connecting cable from digital amplifier Type 4620A1 to amplifier interface Type 5613A1 1200A35
- Connecting cable from extrusion sensor Type 4096/97 (4 ... 20 mA) to amplifier interface Type 5613A1 1200A37
- Connecting cable to interface card Type 5615 for digital inputs and outputs 1200A15
- Inductive proximity switch for Operate signal; connection to interface card Type 5615 2231

Typical configurations with DataFlow software for process visualization, process monitoring and process documentation. These components must be ordered in addition for the SCP chassis and for the SCP modules.

Version I: Connection to Laptop (16 Channels) Type

- DataFlow software for process visualization, process monitoring and process documentation with license code on USB port 2805A-02-2
- A/D card 16-channel PC card 12 bit resolution 2855B1
- Communication cable, serial 5 m 1200A27
- Connecting cable from A/D card Type 2855B1 to SCP chassis 1200B21
- Inductive proximity switch for Operate and Trigger signals; connection to interface card Type 5615 2231

Version II: Connection to Standard PC (16 Channels)

- DataFlow software for process visualization, process monitoring and process documentation with license code on parallel port 2805A-02-1
- A/D card 16-channel PCI card 16 bit resolution 2855A4
- Connecting cable from A/D card Type 2855B1 to SCP chassis 1200A13
- Communication cable, serial 5 m Inductive proximity switch for Operate signal; connection to interface card Type 5615 1200A27 2231

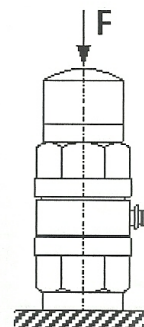
000-408e-02.03 (DB19.001e)

Kalibrierschein KRAFT Calibration Certificate FORCE

Type 9331B

Serial No. 1656892

Kalibriert durch Calibrated by	Datum Date	
K. Ta	07.01.2008	
Referenzgeräte Reference Equipment	Typ Type	Serien-Nr. Serial No.
Gebrauchsnorm Working Standard	Kistler 9331A	523233
Ladungsverstärker Charge Amplifier	Kistler 5017B	1107086
Ladungskalibrator Charge Calibrator	Kistler 5395A	988262
Umgebungstemperatur Ambient Temperature °C	Relative Feuchte Relative Humidity %	
23	43	



Messergebnisse Results of Measurement

Kalibrierter Bereich Calibrated Range kN	Empfindlichkeit Sensitivity pC / N	Linearität Linearity ≤ ± % FSO
0 ... 20	-3,838	0,03
0 ... 0,2	-3,820	0,05
0 ... -20	-3,804	0,21

Messverfahren **Kontinuierliche Kalibrierung, Vergleichsverfahren**
 Measurement Procedure Continuous Calibration, Comparison Method

Bestätigung Confirmation

Die Geräte halten die Herstelltoleranzen gemäss Spezifikationen der Datenblätter ein. Wir bestätigen, dass das oben identifizierte Gerät nach den vorgeschriebenen Verfahren geprüft wurde. Alle Messmittel sind auf nationale Normale rückverfolgbar. Kistler betreibt die SCS (Swiss Calibration Service) Kalibrierstelle Nr. 049, akkreditiert nach ISO 17025. Das Kistler Qualitätsmanagement System ist nach ISO 9001 zertifiziert.

The equipment meets the manufacturing tolerances according to the specification data sheets. We confirm that the device identified above was tested by the prescribed procedures. All measuring devices are traceable to national standards. The SCS (Swiss Calibration Service) Calibration Laboratory No. 049 is operated by Kistler and accredited per ISO 17025. The Kistler Quality Management System is certified per ISO 9001.

Kistler Instrumente AG
 Eulachstrasse 22
 PO Box
 CH-8408 Wintherthur

Tel. +41 52 224 11 11
 Fax +41 52 224 14 14
 info@kistler.com

ZKB Winterthur BC 732
 Swift: ZKBKCHZZ80A
 Account: 1132-0374.628

IBAN: CH67 0070 0113 2003 7462 8
 VAT: 229 713
 ISO 9001 certified

Seite page 1 / 1

www.kistler.com

Kistler Software License Agreement

Important! Please read the License Agreement enclosed herewith or incorporated in the installation set-up carefully before installing the software. By installing the software, you expressly accept the terms of this License Agreement. If you do not accept these terms, please return the data carrier in the original package, together with the user documentation, to the source from which they were purchased and you will receive a credit.

1. Object of contract

- 1.1 Software Products (hereinafter referred to as the "Software Products") comprise the computer software stored on the data carriers, together with the related user documentation, whether in printed or electronic form. The Software Products are the property of Kistler Instrumente AG, Winterthur and are protected both by computer software copyright laws and by international copyright conventions. The Software Products are not sold but licensed.
- 1.2 The Software Products operate basically in accordance with the information provided in the user documentation. Particular attention must be paid to the requirements for installation and operation.

2. Requirements for installation and operation

- 2.1 It is necessary to comply with the minimum technical requirements for the operation of Software Products, as indicated in the sales documentation applying at the time.
- 2.2 The licensee is aware that it is necessary to enter the parameters of the equipment used by the licensee in the specified files in order to use the Software Products and that the accuracy of these data affects the accuracy of the results of the calculations. The data supplied by Kistler is provided simply by way of example.
- 2.3 The licensee may install the Software Products on its computer by itself or may have them installed by Kistler, with a basic introduction to the use of the program being provided at the same time. In this latter case, a supplement is charged. A supplement is also charged if the licensee requires additional utilities.
- 2.4 Kistler offers training for the purpose of ensuring the proper application of its programs. Such training is carried out under a separate agreement and is invoiced separately to the licensee.

3. Rights of use

- 3.1 Kistler hereby grants the licensee a non-exclusive license for its own stipulated use of the Software Products, subject to the following terms and conditions. An individual license is required for each individual workstation. No other rights to Software Products are conveyed hereby.
- 3.2 The license undertakes not to pass the Software Products on to third parties (including its branches and subsidiaries), nor, with the exception of back-up copies, to make copies of them (even for its own purposes) and pass them on to third parties or otherwise dispose of them.
- 3.3 The licensee further undertakes not to make any changes to the Software Products. Such changes have to be carried out by Kistler only. Copyright indications, serial numbers and any other markings serving the purpose of program identification must not be removed or altered in any circumstances, even in program print-outs. The licensee shall ensure that computer material containing Software Products or parts thereof is kept securely and is not accessible to third parties. It is prohibited to decompile, reverse-engineer, disassemble or otherwise reduce the software to a clearly readable form. It is also prohibited to incorporate all or part of the software into secondary products.
- 3.4 Kistler grants the licensee the license to use the Software Products as a long term license. It shall take effect from the date of signature of the license contract and may be terminated by either party upon two years' notice. Kistler shall also have the right to extraordinary termination, particularly if the licensee fails to comply with its obligations under Points 3.1, 3.2 or 3.3 of this contract despite being warned to do so. Upon termination of the license contract, the licensee undertakes to return the Software Products (i.e. all originals and any back-up copies) to Kistler and to remove or to arrange for the removal of any versions stored on other data carriers. This rule applies to all licenses.
- 3.5 The software will be updated from time to time by supplements or new versions. In order to receive these, it is necessary to complete and return the enclosed user registration card.

4. Warranty and liability

- 4.1 As it is impossible, given the present state of technology, to produce programs in such a way that they operate faultlessly in all applications and combinations, Kistler assumes no liability whatsoever for the Software Products being fault-free. However, if, within the warranty period of 12 months from the date of delivery, there should occur a fault which impairs the functioning of a Kistler program to such an extent that it can no longer be used in accordance with the intended purpose, then the program shall be replaced by Kistler, free of charge, within four weeks of the date of the relevant notification by the licensee. If the replacement is defective, the licensee may demand an exchange or a reduction in price. No more extensive claims for replacement are applicable. After the expiry of the warranty period, a defective program will be replaced for an appropriate payment. The other terms and conditions remain in force unaltered.
- 4.2 Kistler gives no guarantee for the function and conformity of dimensioning calculated and designed in accordance with the Software Products.
- 4.3 Kistler's liability for damages due to defect of title and lack of warranted characteristics shall be restricted to three times the (license fee), as well as to such damages as might typically be expected to arise within the framework of a software licensing agreement.
With regard to damage suffered by the licensee, Kistler shall be subject to unlimited liability only for damage caused through intent or gross negligence, including that of its legal representatives and senior personnel. With regard to fault on the part of other vicarious agents, Kistler shall be liable only within the scope of the preceding paragraph.
Any more extensive claim is ruled out.
- 4.4 If any action is brought against Kistler by third parties in connection with the use of the Software Products by the licensee, without Kistler being liable thereby under this contract, the licensee undertakes to hold Kistler harmless if requested to do so.
- 4.5 The licensee's liability to Kistler arising out of or in connection with this contract shall be restricted to three times the (license fee), as well as to such damages as might typically be expected to arise within the framework of a software licensing agreement.
With regard to damage suffered by Kistler, the licensee shall be subject to unlimited liability only for damage caused through intent or gross negligence, including that of its legal representatives and senior personnel. With regard to fault on the part of other vicarious agents, the license shall be liable only within the scope of the preceding paragraph.

5. Final provisions

- 5.1 Subsidiary agreements shall be valid only if in written form. Any amendment of the requirement of written form must also be in writing.
- 5.2 (Kistler's) General Terms and Conditions of Business are also applicable.
- 5.3 The contracting parties are agreed that the substantive law of Switzerland shall apply to all legal relations arising out of this contract.
- 5.4 The legal venue is Winterthur.
- 5.5 Should any provision of the contract be or become invalid after the conclusion of the contract, the other parts of the contract shall remain unaffected. The parties shall make every effort to replace the invalid provision with a valid provision which approximates as closely as possible to the economic intention of the invalid provision. The same shall apply to any loophole in the contract.

Kistler Instrumente AG, PO Box, CH-8408 Winterthur, Switzerland
info@kistler.com

Prüfbescheinigung Test certificate

Type **5063A1** Serial No. **1668787**

Geprüft durch Tested by	Datum Date
C.T. Le	14.03.2008

Referenzgeräte Reference Equipment	Typ Type
DMM	
DMM	Keithley 199
Frequenzgenerator Frequency Generator	Philips PM5138
Ladungskalibrator Charge Calibrator	Kistler 5395A

Umgebungstemperatur Ambient Temperature	Relative Feuchte Relative Humidity
°C	%
24	40

Technische Daten Technical Data

Anzahl Kanäle Number of Channels
4

Spezifikation Specification	Bereich Range	Toleranz Tolerance
Messbereichsfehler Range Error		% < ±1
Nullpunktfehler Zero Point Error		mV < ±10
Ausgangsstörsignal Output Interference Signal	Hz 0,1 ... 10'000'000	mVpp < 10
Drift bei 25°C Drift at 25°C		pC/s < ±0,05

Bestätigung Confirmation

Wir bestätigen, dass das oben identifizierte Gerät nach den vorgeschriebenen Verfahren geprüft wurde. Alle Messmittel sind auf nationale Normale rückverfolgbar. Kistler betreibt die SCS (Swiss Calibration Service) Kalibrierstelle Nr. 049, akkreditiert nach ISO 17025. Das Kistler Qualitätsmanagement System ist nach ISO 9001 zertifiziert.

We confirm that the device identified above was tested by the prescribed procedures. All measuring devices are traceable to national standards, the reference standards through the SCS (Swiss Calibration Service) Calibration Laboratory No. 049, operated by Kistler and accredited per ISO 17025. The Kistler Quality Management System is certified per ISO 9001.

Kistler Instrumente AG
Eulachstrasse 22
PO Box
CH-8408 Winterthur

Tel. +41 52-224 11 11
Fax +41 52-224 14 14
info@kistler.ch

UBS Zürich BC 230
Swift UBSWCHZH80A
Account 230-Q3722854.0
MwSt. 229 713

IBAN: (CH53 0023 0230
Q372 2854 0)
ISO 9001 certified
Quality System

Seite page 1/1

www.kistler.com

- Connecting cable from charge amplifier Type 5011 to amplifier interface Type 5613A1 1200A7
- Connecting cable from hydraulic pressure transmitter Type 4095A... (0 ... 10 V) to amplifier interface Type 5613A1 1200A11
- Connecting cable from piezoresistive amplifier Type 4618A0 and 4618A2 to amplifier interface Type 5613A1 1200A29
- Connecting cable from temperature amplifier Type 2809A1 for connection to Interface Type 5613A1 1200A25
- Connecting cable from extrusion sensor Type 4096/97 (0 ... 10 V) to amplifier interface Type 5613A1 1200A33
- Connecting cable from digital amplifier Type 4620A1 to amplifier interface Type 5613A1 1200A35
- Connecting cable from extrusion sensor Type 4096/97 (4 ... 20 mA) to amplifier interface Type 5613A1 1200A37
- Connecting cable to interface card Type 5615 for digital inputs and outputs 1200A15
- Inductive proximity switch for Operate signal; connection to interface card Type 5615 2231

Typical configurations with DataFlow software for process visualization, process monitoring and process documentation. These components must be ordered in addition for the SCF chassis and for the SCP modules.

Version I: Connection to Laptop (16 Channels) Type

- DataFlow software for process visualization, 2805A-02-2 process monitoring and process documentation with license code on USB port
- A/D card 16-channel PC card 12 bit resolution 2855B1
- Communication cable, serial 5 m 1200A27
- Connecting cable from A/D card Type 2855B1 to SCP chassis 1200B21
- Inductive proximity switch for Operate and Trigger signals; connection to interface card Type 5615 2231

Version II: Connection to Standard PC (16 Channels)

- DataFlow software for process visualization, 2805A-02-1 process monitoring and process documentation with license code on parallel port
- A/D card 16-channel PCI card 16 bit resolution 2855A4
- Connecting cable from A/D card Type 2855B1 to SCP chassis 1200A13
- Communication cable, serial 5 m Inductive proximity switch for Operate signal; connection to interface card Type 5615 1200A27 2231

000-408e-02.03 (DB19,001e)

APPENDIX G
Moldflow's Analysis Log

APPENDIX G.1

Copyright Autodesk, Inc. All rights reserved.
(C)2009

Portions of this software are covered by U.S. Patent Numbers 5,287,408 and 6,096,088.

Cool Analysis

Version: ami2010-main (Build 09034-001)
32-bit build

Analysis running on host: mukhtar-PC
Operating System: Windows Vista
Processor type: GenuineIntel x86 Family 6 Model 15 Stepping 13 ~1995 MHz
Number of Processors: 2
Total Physical Memory: 2037 MBytes

Analysis commenced at Sun Jul 26 11:48:56 2009

Executed: Sun Jul 26 11:48:58 2009

Mesh Type	= 3D Tetrahedra
Number of nodes	= 36979
Number of beam elements	= 214
Number of triangular elements	= 0
Number of tetrahedral elements	= 202348

Reading nodal data...

Reading beam element data...

Reading triangular element data...

Reading tetrahedral element data...

Method of calculating geometrical influence = Ideal

Cool analysis type = Manual

Total number of part elements	= 26
Total number of runner elements	= 26
Total number of shell facets	= 20032
Total number of mold elements	= 536
Total number of circuit elements	= 188

Co-ordinates of part extremity:

	X	Y	Z
Maximum	115.94844 mm	14.99562 mm	60.25000 mm
Minimum	-14.99791 mm	-15.16810 mm	-0.00018 mm
Orientation	246.89479 mm	45.15934 mm	120.50018 mm

** WARNING 701360 ** Beam element 222394 has a very bad length/diameter ratio

** WARNING 701360 ** Beam element 222408 has a very bad length/diameter ratio

** WARNING 701380 ** Warnings were reported in the model.

Mesh quality may be poor.

Co-ordinates of mold extremity:

	X	Y	Z
Center	50.47527 mm	-0.08625 mm	30.12490 mm
Right corner	300.37662 mm	249.81511 mm	280.02626 mm
Left corner	-199.42608 mm	-249.98760 mm	-219.77645 mm

Using mesh aggregation

** WARNING 701360 ** Beam element 222394 has a very bad length/diameter ratio

** WARNING 701360 ** Beam element 222408 has a very bad length/diameter ratio

** WARNING 701380 ** Warnings were reported in the model.

Mesh quality may be poor.

Total Mbytes required for Cool analysis	= 216.78
Total Mbytes available for Cool analysis	= 67952.52

Now beginning the task: Input part model

Current time is: Sun Jul 26 11:49:33 2009

Now beginning the task: Input mold model

Current time is: Sun Jul 26 11:49:33 2009

Performing cooling network analysis

Inlet node	Flowrate in/out (lit/min)	Reynolds No. range	Press. drop over circuit (MPa)	Pumping power over circuit (kW)
57016	3.81	4997.7 - 10000.0	0.0029	1.821e-04
57017	3.81	10000.0 - 11005.7	0.0166	0.001

Now beginning the task: Boundary Integration

Current time is: Sun Jul 26 11:49:33 2009

Now beginning the task: Solution of equilibrium TMP field

Current time is: Sun Jul 26 11:50:06 2009

Calculating 3D fluxes						
+-----+-----+						
Time (s) (%)Frozen						
+-----+-----+						
1.84 28.47						
4.41 60.07						
8.01 91.02						
13.06 100.00						
20.12 100.00						
30.00 100.00						
+-----+-----+						
+-----+-----+-----+-----+-----+-----+						
External Cycle time Avg temp Avg temp Dif temp Dif temp Circ temp						
iteration (s) iteration deviation iteration deviation residual						
+-----+-----+-----+-----+-----+-----+						
1 35.000 9 19.981163 0 0.000000 1.000000						
1 35.000 8 9.011693 0 0.000000 1.000000						
1 35.000 4 5.859069 0 0.000000 1.000000						
1 35.000 3 1.737987 0 0.000000 1.000000						
1 35.000 1 0.000931 0 0.000000 1.000000						
+-----+-----+-----+-----+-----+-----+						
+-----+-----+						
Calculating 3D fluxes						
+-----+-----+						
Time (s) (%)Frozen						
+-----+-----+						
1.84 33.01						
4.41 68.98						
8.01 100.00						
13.06 100.00						
20.12 100.00						
30.00 100.00						
+-----+-----+						
Residual 0.084836						
+-----+-----+-----+-----+-----+-----+						
External Cycle time Avg temp Avg temp Dif temp Dif temp Circ temp						
iteration (s) iteration deviation iteration deviation residual						
+-----+-----+-----+-----+-----+-----+						
1 35.000 0 0.000311 0 0.000000 1.000000						
+-----+-----+-----+-----+-----+-----+						
+-----+-----+-----+-----+-----+-----+						
+-----+-----+						

```

|
|Calculating 3D fluxes|
|
+-----+-----+
|Time (s) |(%)Frozen |
+-----+-----+
| 1.84| 32.87|
| 4.41| 68.90|
| 8.01| 100.00|
| 13.06| 100.00|
| 20.12| 100.00|
| 30.00| 100.00|
+-----+-----+
| Residual | 0.001393|
+-----+-----+
|
|
|External |Cycle time|Avg temp |Avg temp |Dif temp |Dif temp |Circ temp |
|iteration | (s) |iteration |deviation |iteration |deviation |residual |
+-----+-----+
| 2| 35.000| 12| 0.021010| 0| 0.000000| 1.000000|
| 2| 35.000| 3| 0.004897| 0| 0.000000| 1.000000|
| 2| 35.000| 0| 0.001026| 0| 0.000000| 1.000000|
+-----+-----+
+-----+-----+
+-----+-----+
|
|Calculating 3D fluxes|
|
+-----+-----+
|Time (s) |(%)Frozen |
+-----+-----+
| 1.84| 32.87|
| 4.41| 68.89|
| 8.01| 100.00|
| 13.06| 100.00|
| 20.12| 100.00|
| 30.00| 100.00|
+-----+-----+
| Residual | 0.000001|
+-----+-----+
|
|
|External |Cycle time|Avg temp |Avg temp |Dif temp |Dif temp |Circ temp |
|iteration | (s) |iteration |deviation |iteration |deviation |residual |
+-----+-----+
| 3| 35.000| 6| 0.006070| 0| 0.000000| 0.000144|
| 3| 35.000| 0| 0.001062| 0| 0.000000| 0.000144|
| 3| 35.000| 0| 0.000385| 0| 0.000000| 0.000144|
+-----+-----+
+-----+-----+

```

Coolant Temperatures

Inlet node	Coolant temp. range	Coolant temp. rise over circuit
57016	25.0 - 25.1	0.1 C
57017	25.0 - 25.1	0.1 C

Final circuit temperature residual: 4.01341E-08

```

+-----+-----+
|
|Calculating 3D fluxes|
|
+-----+-----+
|Time (s) |(%)Frozen |
+-----+-----+
| 1.84| 32.87|
| 4.41| 68.90|
| 8.01| 100.00|
| 13.06| 100.00|

```

20.12	100.00
30.00	100.00

** WARNING 702560 ** Calculating internal mold temperatures option has been selected,
however the external mold boundaries have not been modeled.
Continuing analysis without calculating the internal mold temperatures.

Summary of Cavity Temperature Results

```

=====
Part surface temperature - maximum      = 30.9823 C
Part surface temperature - minimum      = 25.0000 C
Part surface temperature - average      = 28.8733 C
Cavity surface temperature - maximum    = 29.7373 C
Cavity surface temperature - minimum    = 25.0000 C
Cavity surface temperature - average    = 26.9257 C
Average mold exterior temperature      = 25.1622 C
Cycle time                             = 35.0000 s

```

Execution time

Analysis commenced at Sun Jul 26 11:48:56 2009
 Analysis completed at Sun Jul 26 11:56:50 2009
 CPU time used 432.45 s
 Copyright Autodesk, Inc. All rights reserved.
 (C)2009
 Portions of this software are covered by U.S. Patent Numbers 5,287,408 and 6,096,088.

Coupled 3D Flow Solver.

Version: ami2010-main (Build 09034-001)
 32-bit build

Analysis running on host: mukhtar-PC
 Operating System: Windows Vista
 Processor type: GenuineIntel x86 Family 6 Model 15 Stepping 13 ~1995 MHz
 Number of Processors: 2
 Total Physical Memory: 2037 MBytes

Analysis commenced at Sun Jul 26 11:56:51 2009
 Mesh and boundary conditions file name : design3aa_3d-new_cooling.udm
 Results files core name : design3aa_3d-new_cooling~3

Core shift calculation : ON

Solver Parameters:

=====

Solver setup:

```

-----
Solver                      = Coupled 3D
Solution type                = Stokes
AMG matrix solver selection  = Automatic
Simulate inertia effect      = No
Simulate gravity effect      = No
Gate diameter at cavity injection locations = Automatic

```

Filling parameters:

```

-----
Maximum %volume to fill per time step = 4.000 %
Maximum iterations per time step      = 50
Convergence tolerance (scaling factor) = 1.000

```

Packing parameters:

```

-----
Maximum time step            = 2.000 s
Maximum iterations per time step = 50
Convergence tolerance (scaling factor) = 1.000

```

Intermediate results:

Intermediate results type = Write at constant intervals
Number of intermediate results in filling phase = 5
Number of intermediate results in packing phase = 5
Number of intermediate results in cooling phase = 3

Material Data:

=====

Manufacturer Idemitsu Petrochemical Co Ltd
Trade name HT-50
Family name PS

Specific heat (Cp) = 1340.0000 J/kg-C

Thermal conductivity = 0.1670 W/m-C

Transition temperature = 100.0000 C

PVT Model: 2-domain modified Tait

coefficients: b5 = 376.8100 K

b6 = 3.5250E-07 K/Pa

Liquid phase Solid phase

b1m = 0.0010 b1s = 0.0010 m^3/kg

b2m = 6.0420E-07 b2s = 2.2340E-07 m^3/kg-K

b3m = 1.8592E+08 b3s = 2.6630E+08 Pa

b4m = 0.0049 b4s = 0.0035 1/K

b7 = 0.0000 m^3/kg

b8 = 0.0000 1/K

b9 = 0.0000 1/Pa

Viscosity model: Cross-WLF

coefficients: n = 0.3180

TAUS = 1.7710E+04 Pa

D1 = 2.8265E+10 Pa-s

D2 = 373.1500 K

D3 = 0.0000 K/Pa

A1 = 20.3620

A2T = 51.6000 K

Reading interface file from Cool analysis.

No mesh for the cores was found.

Core shift analysis switched OFF

Model Details:

=====

Mesh Type = 3D Tetrahedra

Laminates across radius of beam elements = 12

Total number of nodes = 36789

Number of 3D nodes = 36762

Number of HS nodes = 25

Number of interface nodes = 2

Total number of injection location nodes = 1

The injection location node numbers are:

46800

Total number of elements = 202374

Number of part elements = 202374

Number of tetrahedral elements = 202348

Number of sprue/runner/gate elements = 26

Total volume = 18.7701 cm^3

Volume of tetrahedral elements = 16.2731 cm^3

Volume of sprue/runner/gate elements = 2.4970 cm^3

Volume filled initially = 0.0000 cm³
 Volume to be filled = 18.7701 cm³
 Part volume to be filled = 16.2731 cm³
 Sprue/runner/gate volume to be filled = 2.4970 cm³
 Parting plane normal (dx) = 0.0000
 (dy) = 0.0000
 (dz) = 1.0000
 Total projected area = 8.0736 cm²

Process Settings:

=====

Machine parameters:

Maximum injection pressure = 1.9300E+02 MPa
 Maximum machine clamp force = 1.2500E+02 tonne
 Maximum machine injection rate = 1.2700E+02 cm³/s
 Machine hydraulic response time = 1.0000E-02 s

Temperature control:

Melt temperature = 200.00 C
 Mold temperature = 26.93 C
 Mold-melt heat transfer coefficients
 Global values. (Superseded by any values set on individual elements.)
 Filling = 5000.0000 W/m²-C
 Packing = 2500.0000 W/m²-C
 Detached = 1250.0000 W/m²-C
 Atmospheric temperature = 25.00 C

Filling Control:

Filling control type = Automatic
 Fill time = 1.73 s
 Stroke volume determination = Automatic

Velocity/pressure switch-over control:

Velocity/pressure switch-over control type = Automatic

Pack/holding control:

Pack/holding control type = %Filling pressure vs time
 Pressure profile:
 duration % filling pressure

 0.00 s 80.00
 10.00 s 80.00

Cooling time:

Cooling time determination = Prior Cool analysis
 Injection + packing + cooling time = 30.00 s

AMG matrix solver = Not used

Filling Phase: Status: V = Velocity control
 ===== V/P = Velocity/pressure switch-over
 P = Pressure control

Time (s)	Fill Vol (%)	Inj Press (MPa)	Clamp F (tonne)	Flow Rate (cm ³ /s)	Frozen Vol (%)	Status
0.027	1.388	3.641e+00	0.00e+00	7.780	0.00	V
0.092	3.886	9.435e+00	0.00e+00	8.584	0.00	V
0.144	7.055	1.263e+01	0.00e+00	9.650	0.00	V
0.217	11.055	1.540e+01	3.76e-02	10.102	0.00	V
0.256	13.292	1.778e+01	1.22e-01	10.150	0.00	V

0.257	13.295	1.835e+01	2.02e-01	7.847	0.00	V
0.259	13.303	1.906e+01	3.03e-01	4.821	0.00	V
0.260	13.304	1.963e+01	3.45e-01	3.617	0.00	V
0.262	13.339	2.106e+01	4.09e-01	3.110	0.00	V
0.268	13.417	2.471e+01	4.99e-01	3.098	0.00	V
0.287	13.738	3.255e+01	6.88e-01	4.507	0.04	V
0.349	15.877	3.857e+01	8.29e-01	7.728	0.12	V
0.400	19.877	4.084e+01	9.05e-01	10.027	0.99	V
0.469	23.877	4.268e+01	9.70e-01	10.460	2.98	V
0.538	27.878	4.388e+01	1.01e+00	10.617	4.89	V
0.607	31.879	4.485e+01	1.04e+00	10.694	6.21	V
0.676	35.880	4.553e+01	1.06e+00	10.736	7.14	V
0.745	39.880	4.595e+01	1.08e+00	10.777	7.79	V
0.814	43.882	4.653e+01	1.11e+00	10.788	8.35	V
0.884	47.884	4.718e+01	1.13e+00	10.778	8.86	V
0.953	51.887	4.756e+01	1.15e+00	10.792	9.33	V
1.022	55.886	4.786e+01	1.17e+00	10.813	9.78	V
1.091	59.888	4.823e+01	1.19e+00	10.816	10.17	V
1.161	63.887	4.876e+01	1.21e+00	10.809	10.58	V
1.230	67.888	4.948e+01	1.24e+00	10.797	11.03	V
1.300	71.885	5.049e+01	1.29e+00	10.782	11.49	V
1.371	75.889	5.129e+01	1.32e+00	10.785	11.95	V
1.441	79.888	5.224e+01	1.37e+00	10.793	12.33	V
1.513	83.884	5.488e+01	1.51e+00	10.751	12.75	V
1.586	87.881	5.819e+01	1.68e+00	10.705	13.28	V
1.659	91.881	6.109e+01	1.84e+00	10.718	13.74	V
1.731	95.880	6.389e+01	2.03e+00	10.746	14.16	V
1.772	97.937	6.675e+01	2.24e+00	10.735	14.35	V

Automatic V/P switch-over point reached. Switching to pressure control.

1.794	98.967	7.015e+01	2.58e+00	10.652	14.44	V/P
1.804	99.420	5.612e+01	2.44e+00	6.947	14.42	P
1.846	99.854	5.612e+01	2.64e+00	3.176	15.28	P
1.889	100.000	5.612e+01	3.08e+00	3.049	16.16	Filled

End of filling phase results summary :

Current time from start of cycle = 1.8888 s
Total mass = 19.0263 g
Part mass = 16.5035 g
Sprue/runner/gate mass = 2.5228 g
Frozen volume = 16.1644 %
Injection pressure = 56.1238 MPa
Volumetric shrinkage - minimum = 0.6233 %
Volumetric shrinkage - maximum = 10.6523 %
Time at velocity/pressure switch-over = 1.7942 s
Injection pressure at velocity/pressure switch-over = 70.1547 MPa
Volume filled at velocity/pressure switch-over = 98.9670 %

End of filling. Packing will now commence.

Pack Analysis

Time (s)	Packing (%)	Inj Press (MPa)	Clamp F (tonne)	Part Mass (g)	Frozen Vol (%)	Status
1.902	0.05	5.612e+01	3.20e+00	1.65e+01	16.34	P
1.926	0.13	5.612e+01	3.25e+00	1.65e+01	16.59	P
2.020	0.47	5.612e+01	3.25e+00	1.65e+01	17.89	P
2.383	1.75	5.612e+01	2.93e+00	1.65e+01	22.40	P
2.715	2.93	5.612e+01	2.59e+00	1.66e+01	27.31	P
3.020	4.01	5.612e+01	2.26e+00	1.66e+01	32.57	P
3.311	5.04	5.612e+01	1.95e+00	1.66e+01	38.11	P
3.573	5.97	5.612e+01	1.77e+00	1.66e+01	44.40	P
3.781	6.71	5.612e+01	1.71e+00	1.66e+01	50.75	P
3.945	7.29	5.612e+01	1.70e+00	1.66e+01	55.11	P
4.133	7.96	5.612e+01	1.71e+00	1.66e+01	58.00	P
4.459	9.11	5.612e+01	1.74e+00	1.66e+01	60.98	P

5.005	11.05	5.612e+01	1.75e+00	1.66e+01	65.90	P
5.560	13.02	5.612e+01	1.73e+00	1.66e+01	71.03	P
6.101	14.94	5.612e+01	1.69e+00	1.66e+01	76.25	P
6.620	16.77	5.612e+01	1.64e+00	1.66e+01	81.77	P
7.090	18.44	5.612e+01	1.60e+00	1.66e+01	86.85	P
7.552	20.08	5.612e+01	1.56e+00	1.66e+01	91.54	P
8.045	21.82	5.612e+01	1.51e+00	1.66e+01	95.92	P
8.607	23.82	5.612e+01	1.48e+00	1.66e+01	99.10	P
9.491	26.95	5.612e+01	1.43e+00	1.66e+01	100.00	P
11.334	33.49	5.612e+01	1.43e+00	1.66e+01	100.00	P
11.794	35.12	5.612e+01	1.38e+00	1.66e+01	100.00	P
11.795	35.12	4.911e+01	1.38e+00	1.66e+01	100.00	P
11.800	35.14	2.105e+01	1.37e+00	1.66e+01	100.00	P
11.804	35.15	0.000e+00	1.37e+00	1.66e+01	100.00	P
11.819	35.21	0.000e+00	1.36e+00	1.66e+01	100.00	P
11.879	35.42	0.000e+00	1.35e+00	1.66e+01	100.00	P
12.119	36.27	0.000e+00	1.32e+00	1.66e+01	100.00	P
13.079	39.67	0.000e+00	1.23e+00	1.66e+01	100.00	P
15.079	46.77	0.000e+00	1.05e+00	1.66e+01	100.00	P
17.079	53.86	0.000e+00	8.99e-01	1.66e+01	100.00	P
19.079	60.95	0.000e+00	7.74e-01	1.66e+01	100.00	P
21.079	68.04	0.000e+00	6.69e-01	1.66e+01	100.00	P
23.079	75.13	0.000e+00	5.81e-01	1.66e+01	100.00	P
25.079	82.22	0.000e+00	5.07e-01	1.66e+01	100.00	P
27.079	89.31	0.000e+00	4.46e-01	1.66e+01	100.00	P
29.079	96.40	0.000e+00	3.95e-01	1.66e+01	100.00	P
30.000	99.66	0.000e+00	3.72e-01	1.66e+01	100.00	P

End of packing phase results summary :

Current time from start of cycle = 30.0000 s
Total mass = 19.2543 g
Part mass = 16.6350 g
Sprue/runner/gate mass = 2.6193 g
Frozen volume = 100.0000 %
Injection pressure = 0.0000 MPa
Volumetric shrinkage - minimum = 0.5739 %
Volumetric shrinkage - maximum = 10.6523 %
Maximum velocity = 1.1887E+04 cm/s
Maximum shear rate = 2.8240E+06 1/s

Execution time

Analysis commenced at Sun Jul 26 11:56:51 2009
Analysis completed at Sun Jul 26 12:20:22 2009
CPU time used 1390.09 s
equivalent to 0 hr, 23 min
Elapsed wall clock time 1411.00 s
equivalent to 0 hr, 23 min

Copyright Autodesk, Inc. All rights reserved.

(C)2009

Portions of this software are covered by U.S. Patent Numbers 5,287,408 and 6,096,088.

Warp Analysis

Version: ami2010-main (Build 09034-001)
32-bit build

Analysis running on host: mukhtar-PC

Operating System: Windows Vista

Processor type: GenuineIntel x86 Family 6 Model 15 Stepping 13 ~1995 MHz

Number of Processors: 2

Total Physical Memory: 2037 MBytes

Analysis commenced at Sun Jul 26 12:20:25 2009

Model file name: design3aa_3d-new_cooling.udm

Reading solver parameters...
Reading mechanical property and shrinkage data...

Read input tetra mesh:
Total number of nodes: 36979 tetras: 202348

** WARNING 201412 ** The mesh aggregation option is used in the analysis. This option is recommended for typical thin-walled parts, but should not be used for chunky parts.

Warp Analysis using a 2-layer aggregated 2nd-order tetrahedral mesh.
Number of vertex nodes: 16224
Number of midside nodes: 95776
Total number of nodes in Warp analysis: 112000
Total number of elements in Warp analysis: 69536
Estimated memory requirement: 440 Mbytes.

Mapping shrinkage and material property data...

Defining anchor plane...
Number of separate cavities = 2

Writing input file for structural analysis program...

Launching structural analysis program...

Reading structural analysis input file...
...finished reading structural analysis input file.

Beginning load incrementation loop...

Setting structure information...

Assembling stiffness matrix...

Solving finite element static equilibrium equations...
Using AMG matrix solver

```
-----  
Kstep Kstra Nref Nite Node lpos Rfac Displacement  
-----  
1 1 1 0 15 1 1.000e+00 -3.225e-01
```

Minimum/maximum displacements at last step (unit: mm):

	Node	Min.	Node	Max.
Trans-X	2907	-1.4995e-01	23398	1.8381e-01
Trans-Y	129295	-1.0142e-01	81421	1.7801e-01
Trans-Z	4907	-7.7542e-03	23108	3.1087e-01

Elapsed wall clock time in structural analysis: 91.86 secs.

Read input tetra mesh:
Total number of nodes: 36979 tetras: 202348
Mapping warpage result...
Writing result file...

Execution time
Analysis commenced at Sun Jul 26 12:21:18 2009
Analysis completed at Sun Jul 26 12:23:01 2009
CPU time used 99.23 s
Elapsed wall clock time 103.00 s
equivalent to 0 hr, 1 min
Warp analysis has completed successfully.

Injection Machine Setup Sheet

General Information

Project Name: design3aa_3d-new_cooling.udm

Version: ami2010

Date: Sun Jul 26 12:20:22 2009

Processing Type: Thermoplastics injection molding

Machine Name: Default injection molding machine #1

Material Name: HT-50 : Idemitsu Petrochemical Co Ltd

Machine Specification:

Maximum pressure: 193.0000 MPa
Screw diameter: 45.0000 mm
Maximum injection speed: 79.8526 mm/s
Screw intensification ratio: 10.0000
Machine maximum clamp force: 125.0000 tonne

Temperature Settings

Mold temperature: 26.9300 C
Melt temperature: 200.0000 C

Part Volume, Stroke and Maximum Clamp Force

Total volume of the part and cold runners: 18.7701 cm³
Maximum clamp force required: 3.2534 tonne

Injection Settings

Filling Control:

Filling control type = Automatic
Fill time = 1.73 s
Stroke volume determination = Automatic
Filling control type = Injection time
Stroke volume determination = Automatic
Filling control type = Flow rate
Stroke volume determination = Automatic

Velocity/pressure switch-over:

Switch-over Time: 1.7942 s
Switch-over Pressure: 70.1547 MPa

Switch-over Volume: 98.9670 %

Packing pressure profile

Duration (s)	Pressure (MPa)
0.0100	56.1238
9.9900	56.1238
0.0100	0.0000
18.1958	0.0000

Cooling time: 20.0000 s

APPENDIX G.2

Copyright Autodesk, Inc. All rights reserved.

(C)2009

Portions of this software are covered by U.S. Patent Numbers 5,287,408 and 6,096,088.

Cool Analysis

Version: ami2010-main (Build 09034-001)

32-bit build

Analysis running on host: mukhtar-PC

Operating System: Windows Vista

Processor type: GenuineIntel x86 Family 6 Model 15 Stepping 13 ~1994 MHz

Number of Processors: 2

Total Physical Memory: 2037 MBytes

Analysis commenced at Tue Jul 28 11:17:37 2009

Executed: Tue Jul 28 11:17:39 2009

Mesh Type	= 3D Tetrahedra
Number of nodes	= 36979
Number of beam elements	= 214
Number of triangular elements	= 0
Number of tetrahedral elements	= 202348

Reading nodal data...

Reading beam element data...

Reading triangular element data...

Reading tetrahedral element data...

Method of calculating geometrical influence = Ideal

Cool analysis type = Manual

Total number of part elements	= 26
Total number of runner elements	= 26
Total number of shell facets	= 20032
Total number of mold elements	= 536
Total number of circuit elements	= 188

Co-ordinates of part extremity:

	X	Y	Z
Maximum	115.94844 mm	14.99562 mm	60.25000 mm
Minimum	-14.99791 mm	-15.16810 mm	-0.00018 mm
Orientation	246.89479 mm	45.15934 mm	120.50018 mm

** WARNING 701360 ** Beam element 222394 has a very bad length/diameter ratio

** WARNING 701360 ** Beam element 222408 has a very bad length/diameter ratio

** WARNING 701380 ** Warnings were reported in the model.

Mesh quality may be poor.

Co-ordinates of mold extremity:

	X	Y	Z
Center	50.47527 mm	-0.08625 mm	30.12490 mm
Right corner	300.37662 mm	249.81511 mm	280.02626 mm
Left corner	-199.42608 mm	-249.98760 mm	-219.77645 mm

Using mesh aggregation

** WARNING 701360 ** Beam element 222394 has a very bad length/diameter ratio

** WARNING 701360 ** Beam element 222408 has a very bad length/diameter ratio

** WARNING 701380 ** Warnings were reported in the model.

Mesh quality may be poor.

Total Mbytes required for Cool analysis	= 216.78
Total Mbytes available for Cool analysis	= 67764.08

Now beginning the task: Input part model

Current time is: Tue Jul 28 11:18:17 2009

Now beginning the task: Input mold model

Current time is: Tue Jul 28 11:18:17 2009

Performing cooling network analysis

Inlet node	Flowrate in/out (lit/min)	Reynolds No. range	Press. drop over circuit (MPa)	Pumping power over circuit (kW)
57016	3.81	4997.7 - 10000.0	0.0029	1.821e-04
57017	3.81	10000.0 - 11005.7	0.0166	0.001

Now beginning the task: Boundary Integration

Current time is: Tue Jul 28 11:18:17 2009

Now beginning the task: Solution of equilibrium TMP field

Current time is: Tue Jul 28 11:18:48 2009

[Calculating 3D fluxes]						
[Time (s) (%)Frozen						
1.84 16.55						
4.41 36.26						
8.01 62.80						
13.06 97.03						
20.12 100.00						
30.00 100.00						

```

+-----+-----+
|                                         |
|Calculating 3D fluxes|
|                                         |
+-----+-----+
|Time (s) |(%)Frozen |
+-----+-----+
|  1.84|  25.29|
|  4.41|  49.65|
|  8.01|  73.06|
| 13.06| 100.00|
| 20.12| 100.00|
| 30.00| 100.00|
+-----+-----+
| Residual | 0.001498|
+-----+-----+
|                                         |
|External |Cycle time|Avg temp |Avg temp |Dif temp |Dif temp |Circ temp |
|iteration | (s)  |iteration |deviation |iteration |deviation |residual  |
+-----+-----+
|      2| 35.000|      1| 0.004328|      0| 0.000000| 1.000000|
|      2| 35.000|      3| 0.004963|      0| 0.000000| 1.000000|
+-----+-----+
+-----+-----+
|                                         |
|Calculating 3D fluxes|
|                                         |
+-----+-----+
|Time (s) |(%)Frozen |
+-----+-----+
|  1.84|  25.30|
|  4.41|  49.66|
|  8.01|  73.07|
| 13.06| 100.00|
| 20.12| 100.00|
| 30.00| 100.00|
+-----+-----+
| Residual | 0.000032|
+-----+-----+
|                                         |
|External |Cycle time|Avg temp |Avg temp |Dif temp |Dif temp |Circ temp |
|iteration | (s)  |iteration |deviation |iteration |deviation |residual  |
+-----+-----+
|      3| 35.000|      7| 0.005759|      0| 0.000000| 0.000208|
|      3| 35.000|      0| 0.001323|      0| 0.000000| 0.000208|
|      3| 35.000|      0| 0.000565|      0| 0.000000| 0.000208|
+-----+-----+
+-----+-----+

```

Coolant Temperatures

Inlet node	Coolant temp. range	Coolant temp. rise over circuit
57016	25.0 - 25.1	0.1 C
57017	25.0 - 25.1	0.1 C

Final circuit temperature residual: 4.05180E-08

```

+-----+-----+
|                                         |
|Calculating 3D fluxes|
|                                         |
+-----+-----+
|Time (s) |(%)Frozen |
+-----+-----+
|  1.84|  25.30|
|  4.41|  49.66|
|  8.01|  73.07|
| 13.06| 100.00|

```

```
| 20.12| 100.00|
| 30.00| 100.00|
+-----+-----+
```

** WARNING 702560 ** Calculating internal mold temperatures option has been selected,
however the external mold boundaries have not been modeled.
Continuing analysis without calculating the internal mold temperatures.

Summary of Cavity Temperature Results

```
=====
Part surface temperature - maximum      = 34.2251 C
Part surface temperature - minimum      = 25.0000 C
Part surface temperature - average      = 31.0761 C
Cavity surface temperature - maximum    = 31.9283 C
Cavity surface temperature - minimum    = 25.0000 C
Cavity surface temperature - average    = 28.1207 C
Average mold exterior temperature      = 25.3038 C
Cycle time                             = 35.0000 s
```

Execution time

```
Analysis commenced at   Tue Jul 28 11:17:37 2009
Analysis completed at   Tue Jul 28 11:25:15 2009
CPU time used           433.71 s
Copyright Autodesk, Inc. All rights reserved.
(C)2009
Portions of this software are covered by U.S. Patent Numbers 5,287,408 and 6,096,088.
```

Coupled 3D Flow Solver.

```
Version: ami2010-main (Build 09034-001)
32-bit build
```

Analysis running on host: mukhtar-PC

Operating System: Windows Vista

Processor type: GenuineIntel x86 Family 6 Model 15 Stepping 13 ~1994 MHz

Number of Processors: 2

Total Physical Memory: 2037 MBytes

Analysis commenced at Tue Jul 28 11:25:16 2009

Mesh and boundary conditions file name : design3aa_3d-new_coolingabs180.udm

Results files core name : design3aa_3d-new_coolingabs180~2

Core shift calculation : ON

Solver Parameters:

```
=====
```

Solver setup:

```
-----
Solver                      = Coupled 3D
Solution type                = Stokes
AMG matrix solver selection  = Automatic
Simulate inertia effect      = No
Simulate gravity effect      = No
Gate diameter at cavity injection locations = Automatic
```

Filling parameters:

```
-----
Maximum %volume to fill per time step = 4.000 %
Maximum iterations per time step      = 50
Convergence tolerance (scaling factor) = 1.000
```

Packing parameters:

```
-----
Maximum time step            = 2.000 s
Maximum iterations per time step = 50
Convergence tolerance (scaling factor) = 1.000
```

Intermediate results:

Intermediate results type = Write at constant intervals
Number of intermediate results in filling phase = 5
Number of intermediate results in packing phase = 5
Number of intermediate results in cooling phase = 3

Material Data:

=====

Manufacturer	Chi Mei Corporation
Trade name	Polylac PA-757
Family name	ABS

Specific heat (Cp) = 2013.0000 J/kg-C

Thermal conductivity = 0.1970 W/m-C

Transition temperature = 94.0000 C

PVT Model: 2-domain modified Tait

coefficients: b5 = 367.2500 K

b6 = 2.0500E-07 K/Pa

Liquid phase Solid phase

b1m = 0.0010 b1s = 0.0010 m³/kg

b2m = 5.0000E-07 b2s = 3.1500E-07 m³/kg-K

b3m = 1.2333E+08 b3s = 1.4501E+08 Pa

b4m = 0.0034 b4s = 0.0044 1/K

b7 = 0.0000 m³/kg

b8 = 0.0000 1/K

b9 = 0.0000 1/Pa

Viscosity model: Cross-WLF

coefficients: n = 0.2237

TAUS = 7.9200E+04 Pa

D1 = 1.3000E+12 Pa-s

D2 = 373.1500 K

D3 = 0.0000 K/Pa

A1 = 27.4520

A2T = 51.6000 K

Reading interface file from Cool analysis.

No mesh for the cores was found.

Core shift analysis switched OFF

Model Details:

=====

Mesh Type	= 3D Tetrahedra
Laminates across radius of beam elements	= 12
Total number of nodes	= 36789
Number of 3D nodes	= 36762
Number of HS nodes	= 25
Number of interface nodes	= 2
Total number of injection location nodes	= 1

The injection location node numbers are:
46800

Total number of elements	= 202374
Number of part elements	= 202374
Number of tetrahedral elements	= 202348
Number of sprue/runner/gate elements	= 26

Total volume	= 18.7701 cm ³
Volume of tetrahedral elements	= 16.2731 cm ³
Volume of sprue/runner/gate elements	= 2.4970 cm ³

Volume filled initially = 0.0000 cm³
 Volume to be filled = 18.7701 cm³
 Part volume to be filled = 16.2731 cm³
 Sprue/runner/gate volume to be filled = 2.4970 cm³
 Parting plane normal (dx) = 0.0000
 (dy) = 0.0000
 (dz) = 1.0000
 Total projected area = 8.0736 cm²

Process Settings:

=====

Machine parameters:

Maximum injection pressure = 1.9300E+02 MPa
 Maximum machine clamp force = 1.2500E+02 tonne
 Maximum machine injection rate = 1.2700E+02 cm³/s
 Machine hydraulic response time = 1.0000E-02 s

Temperature control:

Melt temperature = 210.00 C
 Mold temperature = 28.12 C
 Mold-melt heat transfer coefficients
 Global values. (Superseded by any values set on individual elements.)
 Filling = 5000.0000 W/m²-C
 Packing = 2500.0000 W/m²-C
 Detached = 1250.0000 W/m²-C
 Atmospheric temperature = 25.00 C

Filling Control:

Filling control type = Automatic
 Fill time = 1.50 s
 Stroke volume determination = Automatic

Velocity/pressure switch-over control:

Velocity/pressure switch-over control type = Automatic

Pack/holding control:

Pack/holding control type = %Filling pressure vs time
 Pressure profile:
 duration % filling pressure

 0.00 s 80.00
 10.00 s 80.00

Cooling time:

Cooling time determination = Prior Cool analysis
 Injection + packing + cooling time = 30.00 s

AMG matrix solver = Not used

Filling Phase: Status: V = Velocity control
 =====
 V/P = Velocity/pressure switch-over
 P = Pressure control

Time (s)	Fill Vol (%)	Inj Press (MPa)	Clamp F (tonne)	Flow Rate (cm ³ /s)	Frozen Vol (%)	Status
0.023	0.389	2.222e+00	0.00e+00	0.975	0.00	V
0.157	3.886	1.237e+01	0.00e+00	6.399	0.00	V
0.171	7.055	1.523e+01	0.00e+00	10.226	0.00	V
0.196	9.585	1.679e+01	2.41e-02	9.987	0.00	V
0.246	13.283	2.007e+01	1.28e-01	11.342	0.00	V

0.248	13.295	2.053e+01	1.91e-01	9.257	0.00	V
0.249	13.303	2.095e+01	2.87e-01	6.268	0.00	V
0.250	13.304	2.145e+01	3.22e-01	4.691	0.00	V
0.251	13.343	2.236e+01	3.76e-01	3.827	0.00	V
0.254	13.405	2.405e+01	4.23e-01	3.478	0.00	V
0.262	13.547	2.790e+01	5.13e-01	3.760	0.01	V
0.285	14.083	3.586e+01	7.07e-01	5.737	0.00	V
0.345	16.791	4.103e+01	8.37e-01	9.269	0.01	V
0.389	20.792	4.246e+01	8.77e-01	11.672	0.10	V
0.447	24.794	4.344e+01	9.10e-01	12.187	0.80	V
0.506	28.795	4.420e+01	9.38e-01	12.326	1.94	V
0.565	32.796	4.497e+01	9.65e-01	12.362	2.98	V
0.625	36.794	4.575e+01	9.92e-01	12.368	3.85	V
0.685	40.795	4.649e+01	1.02e+00	12.378	4.54	V
0.744	44.796	4.719e+01	1.05e+00	12.393	5.12	V
0.804	48.798	4.785e+01	1.07e+00	12.406	5.62	V
0.863	52.796	4.839e+01	1.10e+00	12.424	6.05	V
0.922	56.796	4.897e+01	1.12e+00	12.437	6.39	V
0.982	60.799	5.012e+01	1.17e+00	12.403	6.85	V
1.042	64.800	5.147e+01	1.23e+00	12.363	7.24	V
1.103	68.796	5.282e+01	1.28e+00	12.363	7.60	V
1.163	72.799	5.391e+01	1.32e+00	12.389	7.95	V
1.222	76.799	5.455e+01	1.36e+00	12.434	8.24	V
1.282	80.804	5.505e+01	1.39e+00	12.468	8.49	V
1.345	84.795	5.773e+01	1.53e+00	12.404	8.65	V
1.394	87.990	6.024e+01	1.67e+00	12.329	8.87	V
1.456	91.992	6.322e+01	1.82e+00	12.343	9.18	V
1.518	95.989	6.626e+01	1.99e+00	12.370	9.48	V
1.554	97.991	6.915e+01	2.23e+00	12.361	9.61	V

Automatic V/P switch-over point reached. Switching to pressure control.

1.563	98.493	7.008e+01	2.33e+00	12.331	9.61	V/P
1.569	99.073	6.118e+01	2.20e+00	9.568	9.59	P
1.573	99.147	5.606e+01	2.06e+00	5.785	9.64	P
1.598	99.713	5.606e+01	2.09e+00	4.619	9.93	P
1.631	100.000	5.606e+01	2.58e+00	4.482	10.52	Filled

End of filling phase results summary :

Current time from start of cycle = 1.6315 s
Total mass = 18.7494 g
Part mass = 16.2446 g
Sprue/runner/gate mass = 2.5048 g
Frozen volume = 10.5196 %
Injection pressure = 56.0638 MPa
Volumetric shrinkage - minimum = 0.5471 %
Volumetric shrinkage - maximum = 9.5521 %
Time at velocity/pressure switch-over = 1.5630 s
Injection pressure at velocity/pressure switch-over = 70.0798 MPa
Volume filled at velocity/pressure switch-over = 98.4932 %

End of filling. Packing will now commence.

Pack Analysis

Time (s)	Packing (%)	Inj Press (MPa)	Clamp F (tonne)	Part Mass (g)	Frozen Vol (%)	Status
1.644	0.04	5.606e+01	2.76e+00	1.62e+01	10.72	P
1.673	0.15	5.606e+01	2.90e+00	1.63e+01	10.92	P
1.755	0.43	5.606e+01	3.03e+00	1.63e+01	11.55	P
1.979	1.22	5.606e+01	3.07e+00	1.63e+01	13.28	P
2.630	3.51	5.606e+01	2.79e+00	1.64e+01	18.33	P
3.254	5.71	5.606e+01	2.46e+00	1.64e+01	24.51	P
3.759	7.48	5.606e+01	2.21e+00	1.64e+01	30.53	P
4.178	8.96	5.606e+01	2.01e+00	1.64e+01	36.23	P
4.433	9.85	5.606e+01	1.88e+00	1.64e+01	40.36	P
4.614	10.49	5.606e+01	1.81e+00	1.64e+01	44.26	P

4.845	11.30	5.606e+01	1.76e+00	1.64e+01	49.94	P
5.049	12.02	5.606e+01	1.74e+00	1.64e+01	53.85	P
5.309	12.93	5.606e+01	1.73e+00	1.64e+01	56.23	P
5.856	14.86	5.606e+01	1.72e+00	1.64e+01	59.60	P
6.669	17.71	5.606e+01	1.67e+00	1.64e+01	64.79	P
7.451	20.47	5.606e+01	1.63e+00	1.64e+01	70.13	P
8.184	23.04	5.606e+01	1.59e+00	1.64e+01	75.42	P
8.875	25.47	5.606e+01	1.55e+00	1.64e+01	80.67	P
9.534	27.79	5.606e+01	1.52e+00	1.64e+01	86.10	P
10.142	29.93	5.606e+01	1.49e+00	1.64e+01	91.12	P
10.746	32.05	5.606e+01	1.48e+00	1.64e+01	95.60	P
11.563	34.92	5.606e+01	1.46e+00	1.64e+01	99.57	P
11.564	34.93	4.906e+01	1.46e+00	1.64e+01	99.57	P
11.569	34.95	2.103e+01	1.46e+00	1.64e+01	99.58	P
11.573	34.96	0.000e+00	1.46e+00	1.64e+01	99.59	P
11.588	35.01	0.000e+00	1.46e+00	1.64e+01	99.62	P
11.648	35.22	0.000e+00	1.46e+00	1.64e+01	99.74	P
11.888	36.07	0.000e+00	1.41e+00	1.64e+01	99.99	P
12.848	39.44	0.000e+00	1.13e+00	1.64e+01	100.00	P
14.848	46.48	0.000e+00	8.56e-01	1.64e+01	100.00	P
16.848	53.51	0.000e+00	6.87e-01	1.64e+01	100.00	P
18.848	60.54	0.000e+00	5.70e-01	1.64e+01	100.00	P
20.848	67.58	0.000e+00	4.71e-01	1.64e+01	100.00	P
22.848	74.61	0.000e+00	3.89e-01	1.64e+01	100.00	P
24.848	81.64	0.000e+00	3.18e-01	1.64e+01	100.00	P
26.848	88.68	0.000e+00	2.57e-01	1.64e+01	100.00	P
28.848	95.71	0.000e+00	2.05e-01	1.64e+01	100.00	P
30.000	99.76	0.000e+00	1.76e-01	1.64e+01	100.00	P

End of packing phase results summary :

Current time from start of cycle = 30.0000 s
Total mass = 18.9640 g
Part mass = 16.3905 g
Sprue/runner/gate mass = 2.5735 g
Frozen volume = 100.0000 %
Injection pressure = 0.0000 MPa
Volumetric shrinkage - minimum = 0.1724 %
Volumetric shrinkage - maximum = 9.5521 %
Maximum velocity = 5.8042E+04 cm/s
Maximum shear rate = 9.6230E+06 1/s

Execution time

Analysis commenced at Tue Jul 28 11:25:16 2009
Analysis completed at Tue Jul 28 11:48:23 2009
CPU time used 1333.79 s
equivalent to 0 hr, 22 min
Elapsed wall clock time 1387.00 s
equivalent to 0 hr, 23 min

Copyright Autodesk, Inc. All rights reserved.

(C)2009

Portions of this software are covered by U.S. Patent Numbers 5,287,408 and 6,096,088.

Warp Analysis

Version: ami2010-main (Build 09034-001)
32-bit build

Analysis running on host: mukhtar-PC

Operating System: Windows Vista

Processor type: GenuineIntel x86 Family 6 Model 15 Stepping 13 ~1994 MHz

Number of Processors: 2

Total Physical Memory: 2037 MBytes

Analysis commenced at Tue Jul 28 11:48:28 2009

Model file name: design3aa_3d-new_coolingabs180.udm

Reading solver parameters...
Reading mechanical property and shrinkage data...

Read input tetra mesh:
Total number of nodes: 36979 tetras: 202348

** WARNING 201412 ** The mesh aggregation option is used in the analysis. This option is recommended for typical thin-walled parts, but should not be used for chunky parts.

Warp Analysis using a 2-layer aggregated 2nd-order tetrahedral mesh.
Number of vertex nodes: 16224
Number of midside nodes: 95776
Total number of nodes in Warp analysis: 112000
Total number of elements in Warp analysis: 69536
Estimated memory requirement: 440 Mbytes.

Mapping shrinkage and material property data...

Defining anchor plane...
Number of separate cavities = 2

Writing input file for structural analysis program...

Launching structural analysis program...

Reading structural analysis input file...
...finished reading structural analysis input file.

Beginning load incrementation loop...

Setting structure information...

Assembling stiffness matrix...

Solving finite element static equilibrium equations...
Using AMG matrix solver

```
-----  
Kstep Kstra Nref Nite Node Ipos Rfac Displacement  
-----  
1   1   1   0   15   1 1.000e+00 -2.986e-01  
-----
```

Minimum/maximum displacements at last step (unit: mm):

	Node	Min.	Node	Max.
Trans-X	3456	-1.3967e-01	22625	1.7378e-01
Trans-Y	129295	-1.0024e-01	81421	1.6615e-01
Trans-Z	4915	-1.0358e-02	4725	2.9004e-01

Elapsed wall clock time in structural analysis: 101.08 secs.

Read input tetra mesh:
Total number of nodes: 36979 tetras: 202348
Mapping warpage result...
Writing result file...

Execution time
Analysis commenced at Tue Jul 28 11:49:24 2009
Analysis completed at Tue Jul 28 11:51:17 2009
CPU time used 108.14 s
Elapsed wall clock time 113.00 s
equivalent to 0 hr, 1 min
Warp analysis has completed successfully.

Injection Machine Setup Sheet

General Information

Project Name: design3aa_3d-new_coolingabs210.udm

Version: ami2010

Date: Tue Jul 28 14:58:47 2009

Processing Type: Thermoplastics injection molding

Machine Name: Default injection molding machine #1

Material Name: Polylac PA-757 : Chi Mei Corporation

Machine Specification:

Maximum pressure: 193.0000 MPa
Screw diameter: 45.0000 mm
Maximum injection speed: 79.8526 mm/s
Screw intensification ratio: 10.0000
Machine maximum clamp force: 125.0000 tonne

Temperature Settings

Mold temperature: 27.5700 C
Melt temperature: 180.0000 C

Part Volume, Stroke and Maximum Clamp Force

Total volume of the part and cold runners: 18.7701 cm³
Maximum clamp force required: 3.9275 tonne

Injection Settings

Filling Control:

Filling control type = Automatic
Fill time = 1.50 s
Stroke volume determination = Automatic
Filling control type = Injection time
Stroke volume determination = Automatic
Filling control type = Flow rate
Stroke volume determination = Automatic

Velocity/pressure switch-over:

Switch-over Time: 1.5655 s
Switch-over Pressure: 94.9632 MPa

Switch-over Volume: 98.5798 %

Packing pressure profile

Duration (s)	Pressure (MPa)
0.0100	75.9706
9.9900	75.9706
0.0100	0.0000
18.4245	0.0000

Cooling time: 20.0000 s

APPENDIX G.3

Copyright Autodesk, Inc. All rights reserved.

(C)2009

Portions of this software are covered by U.S. Patent Numbers 5,287,408 and 6,096,088.

Cool Analysis

Version: ami2010-main (Build 09034-001)

32-bit build

Analysis running on host: mukhtar-PC

Operating System: Windows Vista

Processor type: GenuineIntel x86 Family 6 Model 15 Stepping 13 ~1995 MHz

Number of Processors: 2

Total Physical Memory: 2037 MBytes

Analysis commenced at Wed Jul 29 13:31:23 2009

Executed: Wed Jul 29 13:31:24 2009

Mesh Type	= 3D Tetrahedra
Number of nodes	= 36979
Number of beam elements	= 214
Number of triangular elements	= 0
Number of tetrahedral elements	= 202348

Reading nodal data...

Reading beam element data...

Reading triangular element data...

Reading tetrahedral element data...

Method of calculating geometrical influence = Ideal

Cool analysis type = Manual

Total number of part elements	= 26
Total number of runner elements	= 26
Total number of shell facets	= 20032
Total number of mold elements	= 536
Total number of circuit elements	= 188

Co-ordinates of part extremity:

	X	Y	Z
Maximum	115.94844 mm	14.99562 mm	60.25000 mm
Minimum	-14.99791 mm	-15.16810 mm	-0.00018 mm
Orientation	246.89479 mm	45.15934 mm	120.50018 mm

** WARNING 701360 ** Beam element 222394 has a very bad length/diameter ratio

** WARNING 701360 ** Beam element 222408 has a very bad length/diameter ratio

** WARNING 701380 ** Warnings were reported in the model.

Mesh quality may be poor.

Co-ordinates of mold extremity:

	X	Y	Z
Center	50.47527 mm	-0.08625 mm	30.12490 mm
Right corner	300.37662 mm	249.81511 mm	280.02626 mm
Left corner	-199.42608 mm	-249.98760 mm	-219.77645 mm

Using mesh aggregation

** WARNING 701360 ** Beam element 222394 has a very bad length/diameter ratio

** WARNING 701360 ** Beam element 222408 has a very bad length/diameter ratio

** WARNING 701380 ** Warnings were reported in the model.

Mesh quality may be poor.

Total Mbytes required for Cool analysis	= 216.78
Total Mbytes available for Cool analysis	= 67372.51

Now beginning the task: Input part model

Current time is: Wed Jul 29 13:31:59 2009

Now beginning the task: Input mold model
Current time is: Wed Jul 29 13:31:59 2009
Performing cooling network analysis

Inlet node	Flowrate in/out (lit/min)	Reynolds No. range	Press. drop over circuit (MPa)	Pumping power over circuit (kW)
57016	3.81	4997.7 - 10000.0	0.0029	1.821e-04
57017	3.81	10000.0 - 11005.7	0.0166	0.001

Now beginning the task: Boundary Integration
Current time is: Wed Jul 29 13:31:59 2009

Now beginning the task: Solution of equilibrium TMP field
Current time is: Wed Jul 29 13:32:28 2009

Time (s)	(%)Frozen
1.84	16.94
4.41	37.21
8.01	63.94
13.06	99.88
20.12	100.00
30.00	100.00

External iteration	Cycle time (s)	Avg temp iteration	Avg temp deviation	Dif temp iteration	Dif temp deviation	Circ temp residual
1	35.000	8	20.000000	0	0.000000	1.000000
1	35.000	9	29.997562	0	0.000000	1.000000
1	35.000	8	22.488306	0	0.000000	1.000000
1	35.000	8	12.430295	0	0.000000	1.000000
1	35.000	4	0.013296	0	0.000000	1.000000

Time (s)	(%)Frozen
1.84	34.23
4.41	66.83
8.01	99.93
13.06	100.00
20.12	100.00
30.00	100.00

Residual
0.259510

External iteration	Cycle time (s)	Avg temp iteration	Avg temp deviation	Dif temp iteration	Dif temp deviation	Circ temp residual
1	35.000	12	0.332396	0	0.000000	1.000000
1	35.000	0	0.001008	0	0.000000	1.000000

```

|
|Calculating 3D fluxes|
|
+-----+
|Time (s) |(%)Frozen |
+-----+
| 1.84| 33.76|
| 4.41| 66.48|
| 8.01| 99.77|
| 13.06| 100.00|
| 20.12| 100.00|
| 30.00| 100.00|
+-----+
| Residual | 0.005026|
+-----+
|
|
|External |Cycle time|Avg temp |Avg temp |Dif temp |Dif temp |Circ temp |
|iteration | (s) |iteration |deviation |iteration |deviation |residual |
+-----+
| 1| 35.000| 0| 0.000744| 0| 0.000000| 1.000000|
+-----+
| 2| 35.000| 12| 0.599026| 0| 0.000000| 1.000000|
| 2| 35.000| 0| 0.002778| 0| 0.000000| 1.000000|
+-----+
+-----+
|
|Calculating 3D fluxes|
|
+-----+
|Time (s) |(%)Frozen |
+-----+
| 1.84| 33.73|
| 4.41| 66.42|
| 8.01| 99.73|
| 13.06| 100.00|
| 20.12| 100.00|
| 30.00| 100.00|
+-----+
| Residual | 0.000045|
+-----+
|
|
|External |Cycle time|Avg temp |Avg temp |Dif temp |Dif temp |Circ temp |
|iteration | (s) |iteration |deviation |iteration |deviation |residual |
+-----+
| 2| 35.000| 0| 0.001718| 0| 0.000000| 1.000000|
+-----+
+-----+
+-----+
|
|Calculating 3D fluxes|
|
+-----+
|Time (s) |(%)Frozen |
+-----+
| 1.84| 33.73|
| 4.41| 66.42|
| 8.01| 99.73|
| 13.06| 100.00|
| 20.12| 100.00|
| 30.00| 100.00|
+-----+
| Residual | 0.000050|
+-----+
|
|
|External |Cycle time|Avg temp |Avg temp |Dif temp |Dif temp |Circ temp |
|iteration | (s) |iteration |deviation |iteration |deviation |residual |
+-----+
| 3| 35.000| 8| 0.010459| 0| 0.000000| 0.000396|
| 3| 35.000| 0| 0.001297| 0| 0.000000| 0.000396|
| 3| 35.000| 0| 0.000701| 0| 0.000000| 0.000396|
+-----+

```

-----+

Coolant Temperatures

Inlet node	Coolant temp. range	Coolant temp. rise over circuit
57016	25.0 - 25.1	0.1 C
57017	25.0 - 25.1	0.1 C

Final circuit temperature residual: 2.30719E-08

```

+-----+
|       |
|       |
|Calculating 3D fluxes|
|       |
+-----+
|Time (s) | (%)Frozen |
+-----+
| 1.84| 33.73|
| 4.41| 66.42|
| 8.01| 99.73|
| 13.06| 100.00|
| 20.12| 100.00|
| 30.00| 100.00|
+-----+

```

** WARNING 702560 ** Calculating internal mold temperatures option has been selected, however the external mold boundaries have not been modeled.
Continuing analysis without calculating the internal mold temperatures.

Summary of Cavity Temperature Results

```

=====
Part surface temperature - maximum      = 40.3667 C
Part surface temperature - minimum      = 25.8067 C
Part surface temperature - average      = 35.2474 C
Cavity surface temperature - maximum    = 36.2482 C
Cavity surface temperature - minimum    = 25.8067 C
Cavity surface temperature - average    = 30.3771 C
Average mold exterior temperature      = 25.5740 C
Cycle time                             = 35.0000 s

```

Execution time

Analysis commenced at Wed Jul 29 13:31:23 2009
Analysis completed at Wed Jul 29 13:39:38 2009
CPU time used 492.65 s

Copyright Autodesk, Inc. All rights reserved.
(C)2009

Portions of this software are covered by U.S. Patent Numbers 5,287,408 and 6,096,088.

Coupled 3D Flow Solver.

Version: ami2010-main (Build 09034-001)
32-bit build

Analysis running on host: mukhtar-PC

Operating System: Windows Vista

Processor type: GenuineIntel x86 Family 6 Model 15 Stepping 13 ~1995 MHz

Number of Processors: 2

Total Physical Memory: 2037 MBytes

Analysis commenced at Wed Jul 29 13:39:40 2009

Mesh and boundary conditions file name : design3aa_3d-new_coolingpa6265.udm

Results files core name : design3aa_3d-new_coolingpa6265~4

Core shift calculation : ON

Solver Parameters:

=====

Solver setup:

Solver = Coupled 3D
Solution type = Stokes
AMG matrix solver selection = Automatic
Simulate inertia effect = No
Simulate gravity effect = No
Gate diameter at cavity injection locations = Automatic

Filling parameters:

Maximum %volume to fill per time step = 4.000 %
Maximum iterations per time step = 50
Convergence tolerance (scaling factor) = 1.000

Packing parameters:

Maximum time step = 2.000 s
Maximum iterations per time step = 50
Convergence tolerance (scaling factor) = 1.000

Intermediate results:

Intermediate results type = Write at constant intervals
Number of intermediate results in filling phase = 5
Number of intermediate results in packing phase = 5
Number of intermediate results in cooling phase = 3

Material Data:

=====

Manufacturer Mitsubishi Group
Trade name Novamid-1010C2
Family name PA6

Specific heat (Cp) = 2600.0000 J/kg-C

Thermal conductivity = 0.2580 W/m-C

Transition temperature = 185.0000 C

PVT Model: 2-domain modified Tait

coefficients: b5 = 498.1500 K

b6 = 5.8000E-08 K/Pa

Liquid phase Solid phase

b1m = 0.0010 b1s = 0.0010 m³/kg

b2m = 6.4700E-07 b2s = 3.6900E-07 m³/kg-K

b3m = 1.4300E+08 b3s = 1.8000E+08 Pa

b4m = 0.0036 b4s = 0.0046 1/K

b7 = 6.8500E-05 m³/kg

b8 = 0.0440 1/K

b9 = 3.5900E-09 1/Pa

Viscosity model:

Cross-WLF

coefficients: n = 0.1453

TAUS = 4.1673E+05 Pa

D1 = 4.7800E+13 Pa-s

D2 = 323.1500 K

D3 = 0.0000 K/Pa

A1 = 33.4000

A2T = 51.6000 K

Reading interface file from Cool analysis.

No mesh for the cores was found.

Core shift analysis switched OFF

Model Details:

=====

Mesh Type	=	3D Tetrahedra
Laminates across radius of beam elements	=	12
Total number of nodes	=	36789
Number of 3D nodes	=	36762
Number of HS nodes	=	25
Number of interface nodes	=	2
Total number of injection location nodes	=	1
The injection location node numbers are: 46800		
Total number of elements	=	202374
Number of part elements	=	202374
Number of tetrahedral elements	=	202348
Number of sprue/runner/gate elements	=	26
Total volume	=	18.7701 cm ³
Volume of tetrahedral elements	=	16.2731 cm ³
Volume of sprue/runner/gate elements	=	2.4970 cm ³
Volume filled initially	=	0.0000 cm ³
Volume to be filled	=	18.7701 cm ³
Part volume to be filled	=	16.2731 cm ³
Sprue/runner/gate volume to be filled	=	2.4970 cm ³
Parting plane normal	(dx) =	0.0000
	(dy) =	0.0000
	(dz) =	1.0000
Total projected area	=	8.0736 cm ²

Process Settings:

=====

Machine parameters:

Maximum injection pressure	=	1.9300E+02 MPa
Maximum machine clamp force	=	1.2500E+02 tonne
Maximum machine injection rate	=	1.2700E+02 cm ³ /s
Machine hydraulic response time	=	1.0000E-02 s

Temperature control:

Melt temperature	=	265.00 C
Mold temperature	=	30.38 C
Mold-melt heat transfer coefficients		
Global values. (Superseded by any values set on individual elements.)		
Filling	=	5000.0000 W/m ² -C
Packing	=	2500.0000 W/m ² -C
Detached	=	1250.0000 W/m ² -C
Atmospheric temperature	=	25.00 C

Filling Control:

Filling control type	=	Automatic
Fill time	=	0.92 s
Stroke volume determination	=	Automatic

Velocity/pressure switch-over control:

Velocity/pressure switch-over control type	=	Automatic
--	---	-----------

Pack/holding control:

Pack/holding control type	=	%Filling pressure vs time
---------------------------	---	---------------------------

Pressure profile:

duration	% filling pressure
----------	--------------------

0.00 s	80.00
--------	-------

10.00 s 80.00

Cooling time:

Cooling time determination = Prior Cool analysis
Injection + packing + cooling time = 30.00 s

AMG matrix solver = Not used

Filling Phase: Status: V = Velocity control
===== V/P = Velocity/pressure switch-over
P = Pressure control

Time (s)	Fill Vol (%)	Inj Press (MPa)	Clamp F (tonne)	Flow Rate (cm ³ /s)	Frozen Vol (%)	Status
0.018	2.000	3.183e+00	0.00e+00	17.614	0.00	V
0.063	5.929	6.450e+00	0.00e+00	18.412	0.00	V
0.070	7.055	6.872e+00	0.00e+00	19.343	0.00	V
0.098	10.004	7.798e+00	7.80e-03	19.672	0.00	V
0.129	13.292	1.012e+01	8.06e-02	19.580	0.00	V
0.131	13.294	1.076e+01	1.33e-01	17.640	0.00	V
0.132	13.308	1.162e+01	2.71e-01	12.034	0.00	V
0.134	13.346	1.348e+01	3.59e-01	6.964	0.00	V
0.138	13.476	1.739e+01	4.62e-01	6.662	0.11	V
0.150	13.990	2.479e+01	6.33e-01	10.321	0.06	V
0.188	17.021	3.032e+01	7.66e-01	15.901	0.05	V
0.218	21.023	3.230e+01	8.26e-01	19.120	0.51	V
0.255	25.022	3.311e+01	8.48e-01	19.857	1.81	V
0.292	29.024	3.503e+01	9.14e-01	19.964	4.09	V
0.331	33.022	3.561e+01	9.25e-01	20.010	5.76	V
0.368	37.025	3.747e+01	9.93e-01	20.043	6.96	V
0.406	41.025	3.762e+01	9.89e-01	20.097	8.08	V
0.443	45.026	3.876e+01	1.03e+00	20.199	8.88	V
0.481	49.025	3.917e+01	1.04e+00	20.175	9.72	V
0.519	53.027	3.908e+01	1.03e+00	20.310	10.51	V
0.556	57.027	3.914e+01	1.04e+00	20.345	11.23	V
0.593	61.027	3.932e+01	1.04e+00	20.321	12.00	V
0.631	65.027	3.949e+01	1.05e+00	20.313	12.65	V
0.669	69.030	3.963e+01	1.05e+00	20.318	13.25	V
0.706	73.029	3.973e+01	1.06e+00	20.324	13.83	V
0.744	77.030	3.984e+01	1.06e+00	20.328	14.37	V
0.782	81.028	3.986e+01	1.06e+00	20.333	14.78	V
0.820	85.025	4.032e+01	1.09e+00	20.318	15.32	V
0.858	89.025	4.066e+01	1.10e+00	20.305	15.98	V
0.897	93.024	4.114e+01	1.13e+00	20.309	16.68	V
0.930	96.514	4.138e+01	1.15e+00	20.315	17.23	V
0.948	98.254	4.215e+01	1.18e+00	20.289	17.48	V
0.957	99.124	4.211e+01	1.19e+00	20.301	17.56	V

Automatic V/P switch-over point reached. Switching to pressure control.

0.962	99.561	4.324e+01	1.28e+00	20.145	17.56	V/P
0.969	100.000	3.703e+01	1.54e+00	19.941	17.62	Filled

End of filling phase results summary :

Current time from start of cycle = 0.9690 s
Total mass = 18.7744 g
Part mass = 16.2749 g
Sprue/runner/gate mass = 2.4995 g
Frozen volume = 17.6159 %
Injection pressure = 37.0292 MPa
Volumetric shrinkage - minimum = 7.1058 %
Volumetric shrinkage - maximum = 17.0133 %
Time at velocity/pressure switch-over = 0.9618 s
Injection pressure at velocity/pressure switch-over = 43.2449 MPa
Volume filled at velocity/pressure switch-over = 99.5610 %

End of filling. Packing will now commence.

Pack Analysis

Time (s)	Packing (%)	Inj Press (MPa)	Clamp F (tonne)	Part Mass (g)	Frozen Vol (%)	Status
0.970	0.00	3.581e+01	1.60e+00	1.63e+01	17.70	P
0.972	0.01	3.460e+01	1.61e+00	1.63e+01	17.72	P
0.977	0.03	3.460e+01	1.70e+00	1.63e+01	17.87	P
0.991	0.08	3.460e+01	1.84e+00	1.63e+01	18.30	P
1.015	0.16	3.460e+01	1.95e+00	1.63e+01	19.00	P
1.068	0.34	3.460e+01	2.02e+00	1.64e+01	20.53	P
1.228	0.89	3.460e+01	1.95e+00	1.64e+01	24.67	P
1.423	1.56	3.460e+01	1.77e+00	1.65e+01	29.37	P
1.629	2.27	3.460e+01	1.56e+00	1.65e+01	34.26	P
1.837	2.99	3.460e+01	1.35e+00	1.66e+01	39.12	P
2.041	3.69	3.460e+01	1.15e+00	1.67e+01	43.79	P
2.257	4.44	3.460e+01	1.14e+00	1.67e+01	48.79	P
2.473	5.18	3.460e+01	1.15e+00	1.67e+01	54.50	P
2.662	5.83	3.460e+01	1.14e+00	1.68e+01	60.36	P
2.823	6.38	3.460e+01	1.14e+00	1.68e+01	64.34	P
3.025	7.08	3.460e+01	1.14e+00	1.68e+01	66.85	P
3.429	8.47	3.460e+01	1.15e+00	1.69e+01	71.04	P
3.911	10.13	3.460e+01	1.15e+00	1.69e+01	75.76	P
4.422	11.89	3.460e+01	1.15e+00	1.69e+01	80.71	P
4.937	13.67	3.460e+01	1.15e+00	1.69e+01	86.30	P
5.399	15.25	3.460e+01	1.15e+00	1.69e+01	92.64	P
5.762	16.51	3.460e+01	1.15e+00	1.69e+01	97.40	P
6.144	17.82	3.460e+01	1.15e+00	1.69e+01	99.82	P
6.934	20.54	3.460e+01	1.14e+00	1.69e+01	100.00	P
8.934	27.43	3.460e+01	1.12e+00	1.69e+01	100.00	P
10.556	33.02	3.460e+01	1.06e+00	1.69e+01	100.00	P
10.962	34.41	3.460e+01	8.95e-01	1.69e+01	100.00	P
10.963	34.42	3.027e+01	8.80e-01	1.69e+01	100.00	P
10.968	34.43	1.297e+01	8.74e-01	1.69e+01	100.00	P
10.972	34.45	0.000e+00	8.70e-01	1.69e+01	100.00	P
10.987	34.50	0.000e+00	8.56e-01	1.69e+01	100.00	P
11.047	34.71	0.000e+00	8.03e-01	1.69e+01	100.00	P
11.287	35.53	0.000e+00	6.70e-01	1.69e+01	100.00	P
12.247	38.84	0.000e+00	3.66e-01	1.69e+01	100.00	P
13.955	44.72	0.000e+00	0.00e+00	1.69e+01	100.00	P
15.774	50.99	0.000e+00	0.00e+00	1.69e+01	100.00	P
17.774	57.87	0.000e+00	0.00e+00	1.69e+01	100.00	P
19.774	64.76	0.000e+00	0.00e+00	1.69e+01	100.00	P
21.774	71.65	0.000e+00	0.00e+00	1.69e+01	100.00	P
23.774	78.54	0.000e+00	0.00e+00	1.69e+01	100.00	P
25.774	85.42	0.000e+00	0.00e+00	1.69e+01	100.00	P
27.774	92.31	0.000e+00	0.00e+00	1.69e+01	100.00	P
29.555	98.44	0.000e+00	0.00e+00	1.69e+01	100.00	P
30.000	100.00	0.000e+00	0.00e+00	1.69e+01	100.00	P

End of packing phase results summary :

Current time from start of cycle = 30.0000 s
Total mass = 19.6426 g
Part mass = 16.8737 g
Sprue/runner/gate mass = 2.7688 g
Frozen volume = 100.0000 %
Injection pressure = 0.0000 MPa
Volumetric shrinkage - minimum = 6.2956 %
Volumetric shrinkage - maximum = 17.0133 %
Maximum velocity = 2.3205E+05 cm/s
Maximum shear rate = 1.0000E+07 1/s

Execution time

Analysis commenced at Wed Jul 29 13:39:40 2009
Analysis completed at Wed Jul 29 14:02:30 2009

CPU time used 1363.76 s
equivalent to 0 hr, 22 min
Elapsed wall clock time 1370.00 s
equivalent to 0 hr, 22 min
Copyright Autodesk, Inc. All rights reserved.
(C)2009
Portions of this software are covered by U.S. Patent Numbers 5,287,408 and 6,096,088.

Warp Analysis

Version: ami2010-main (Build 09034-001)
32-bit build

Analysis running on host: mukhtar-PC
Operating System: Windows Vista
Processor type: GenuineIntel x86 Family 6 Model 15 Stepping 13 ~1995 MHz
Number of Processors: 2
Total Physical Memory: 2037 MBytes

Analysis commenced at Wed Jul 29 14:02:34 2009

Model file name: design3aa_3d-new_coolingpa6265.udm

Reading solver parameters...
Reading mechanical property and shrinkage data...

Read input tetra mesh:
Total number of nodes: 36979 tetras: 202348

**** WARNING 201412 **** The mesh aggregation option is used in the analysis. This option is recommended for typical thin-walled parts, but should not be used for chunky parts.

Warp Analysis using a 2-layer aggregated 2nd-order tetrahedral mesh.
Number of vertex nodes: 16224
Number of midside nodes: 95776
Total number of nodes in Warp analysis: 112000
Total number of elements in Warp analysis: 69536
Estimated memory requirement: 440 Mbytes.

Mapping shrinkage and material property data...

Defining anchor plane...
Number of separate cavities = 2

Writing input file for structural analysis program...

Launching structural analysis program...

Reading structural analysis input file...
...finished reading structural analysis input file.

Beginning load incrementation loop...

Setting structure information...

Assembling stiffness matrix...

Solving finite element static equilibrium equations...
Using AMG matrix solver

```
-----
Kstep Kstra Nref Nite Node lpos Rfac Displacement
-----
1 1 1 0 15 1 1.000e+00 -9.769e-01
```

Minimum/maximum displacements at last step (unit: mm):

	Node	Min.	Node	Max.
Trans-X	5003	-4.5476e-01	23394	5.8506e-01
Trans-Y	132864	-3.1161e-01	84735	5.2953e-01
Trans-Z	4915	-8.6506e-03	23108	9.3029e-01

Elapsed wall clock time in structural analysis: 90.49 secs.

Read input tetra mesh:
 Total number of nodes: 36979 tetras: 202348
 Mapping warpage result...
 Writing result file...

Execution time
 Analysis commenced at Wed Jul 29 14:03:27 2009
 Analysis completed at Wed Jul 29 14:05:07 2009
 CPU time used 100.53 s
 Elapsed wall clock time 100.00 s
 equivalent to 0 hr, 1 min
 Warp analysis has completed successfully.

Injection Machine Setup Sheet

General Information

Project Name: design3aa_3d-new_coolingpa6265.udm

Version: ami2010

Date: Wed Jul 29 14:02:30 2009

Processing Type: Thermoplastics injection molding

Machine Name: Default injection molding machine #1

Material Name: Novamid-1010C2 : Mitsubishi Group

Machine Specification:

Maximum pressure: 193.0000 MPa
Screw diameter: 45.0000 mm
Maximum injection speed: 79.8526 mm/s
Screw intensification ratio: 10.0000
Machine maximum clamp force: 125.0000 tonne

Temperature Settings

Mold temperature: 30.3800 C
Melt temperature: 265.0000 C

Part Volume, Stroke and Maximum Clamp Force

Total volume of the part and cold runners: 18.7701 cm³
Maximum clamp force required: 2.0226 tonne

Injection Settings

Filling Control:

Filling control type = Automatic
Fill time = 0.92 s
Stroke volume determination = Automatic
Filling control type = Injection time
Stroke volume determination = Automatic
Filling control type = Flow rate
Stroke volume determination = Automatic

Velocity/pressure switch-over:

Switch-over Time: 0.9618 s
Switch-over Pressure: 43.2449 MPa

Switch-over Volume: 99.5610 %

Packing pressure profile

Duration (s)	Pressure (MPa)
0.0100	34.5959
9.9900	34.5959
0.0100	0.0000
19.0282	0.0000

Cooling time: 20.0000 s

APPENDIX H

Moldflow Analysis Results

APPENDIX H.1

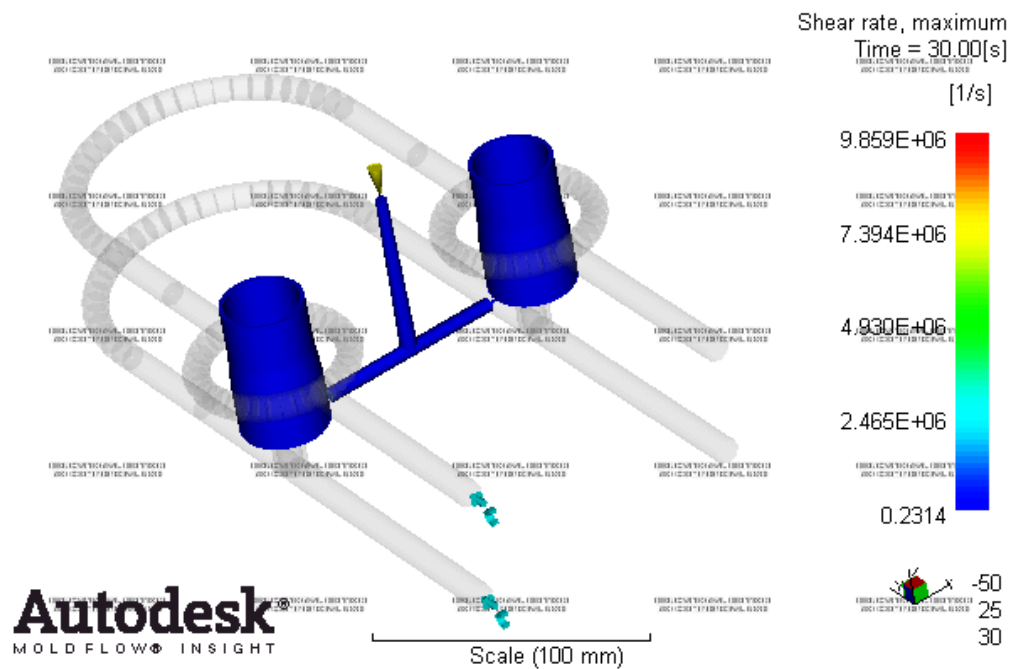


Figure H.1.1: Maximum Shear Rate For HIPS

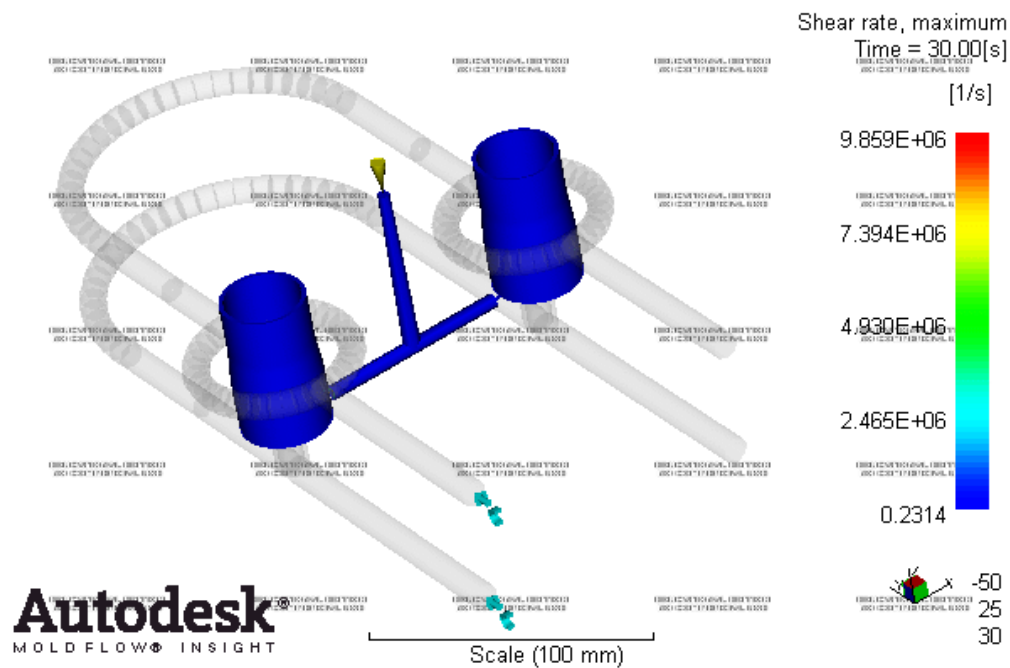


Figure H.1.2: Maximum Shear Rate For ABS

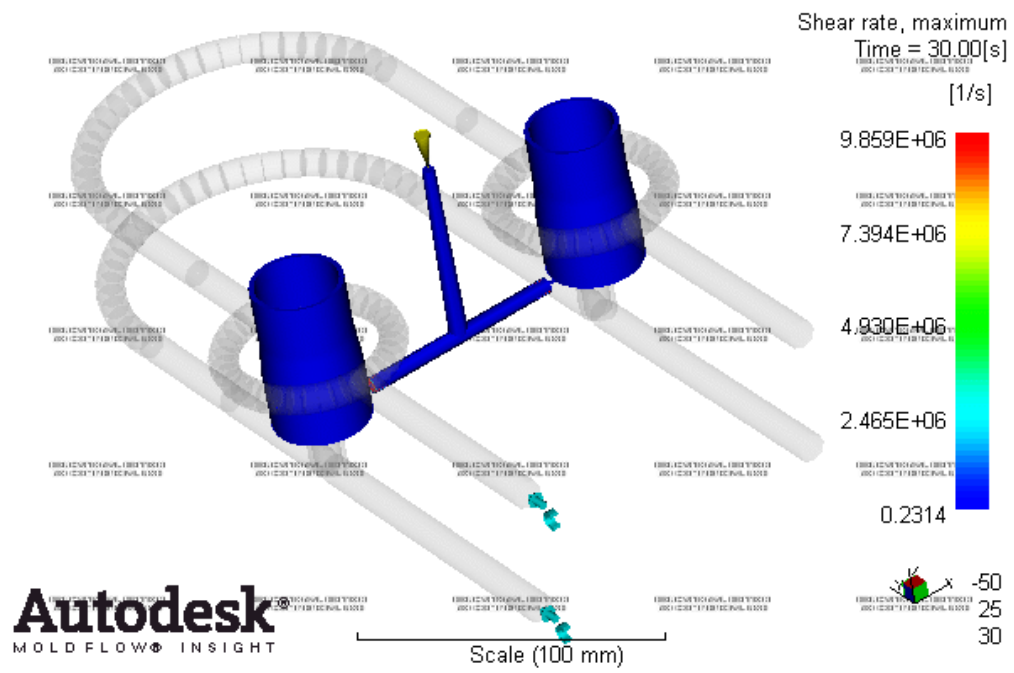


Figure H.1.3: Maximum Shear Rate For PA6

APPENDIX H.2

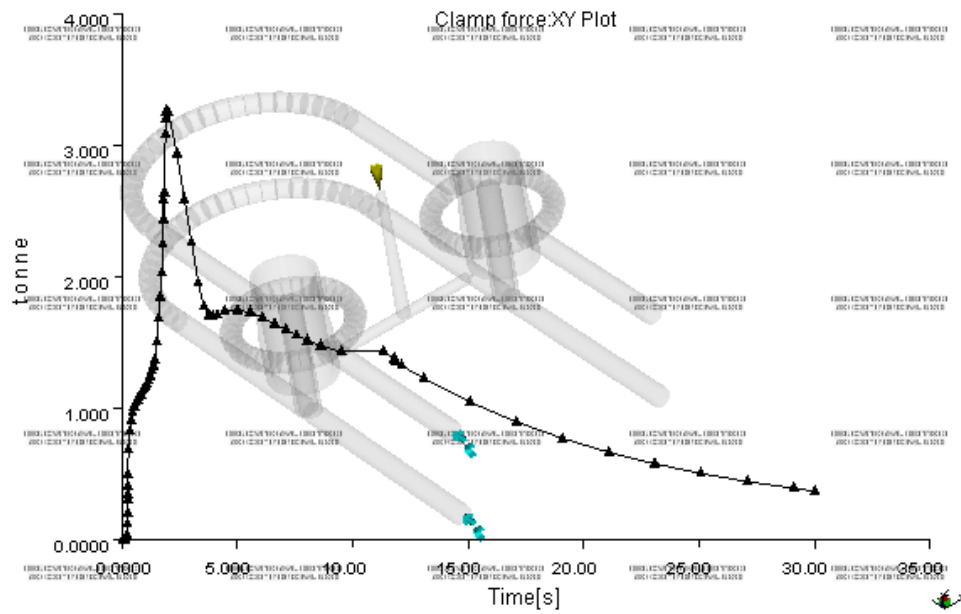


Figure H.2.1: Clamp Force: XY Plot For HIPS

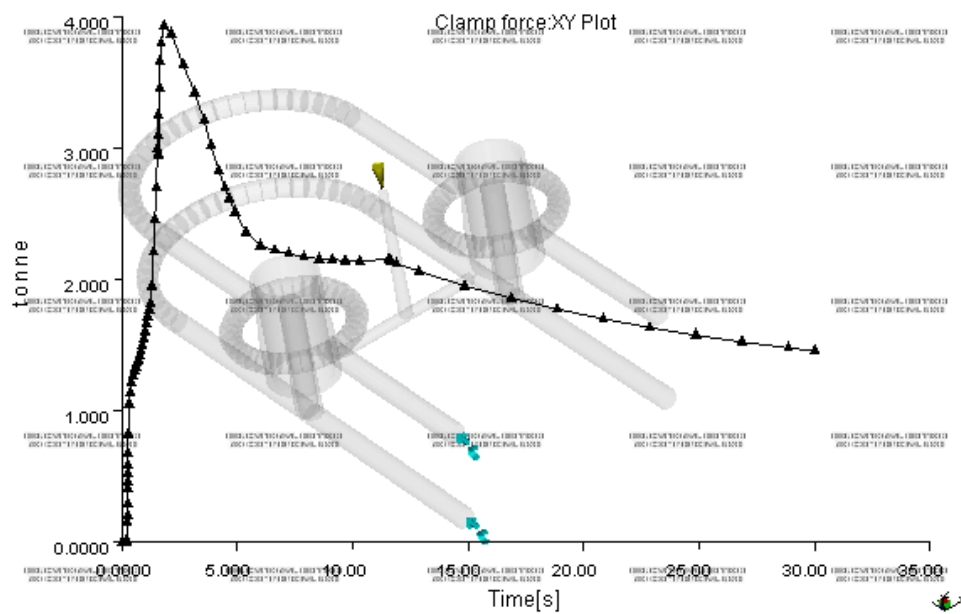


Figure H.2.2: Clamp Force: XY Plot For ABS

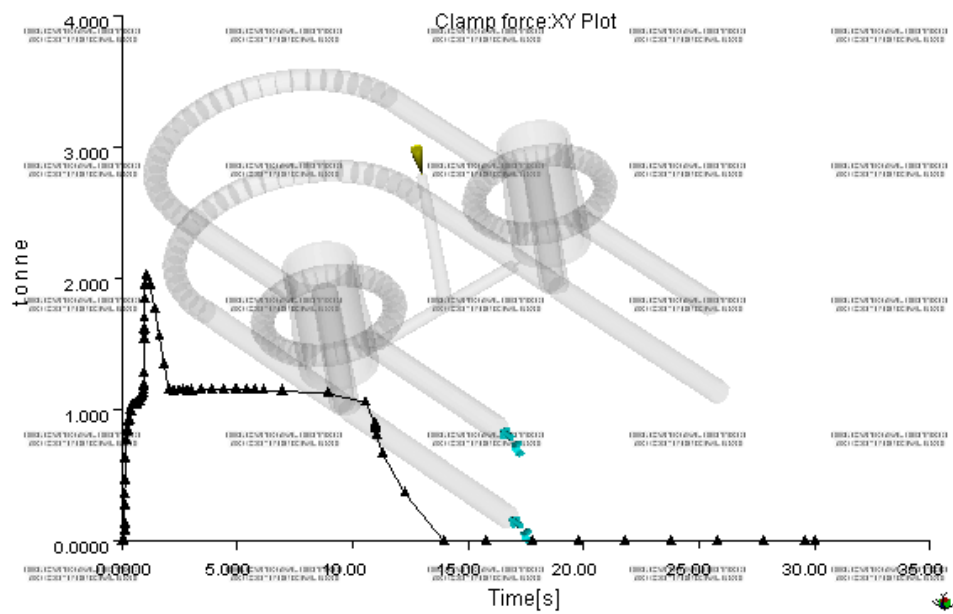


Figure H.2.3: Clamp Force: XY Plot For PA6

APPENDIX H.3

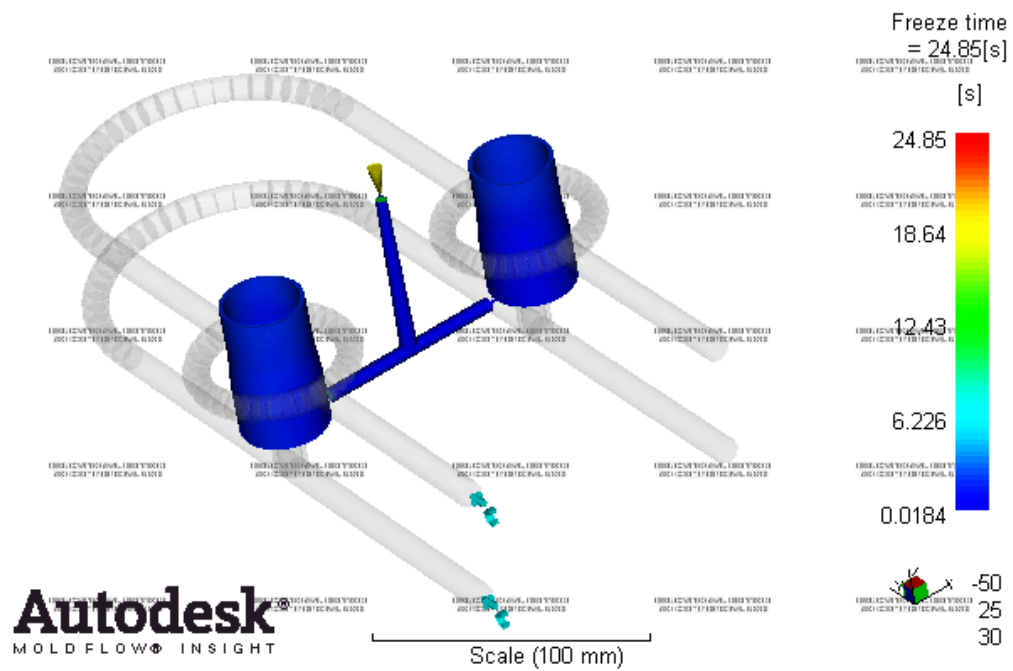


Figure H.3.1: Freeze Time For HIPS

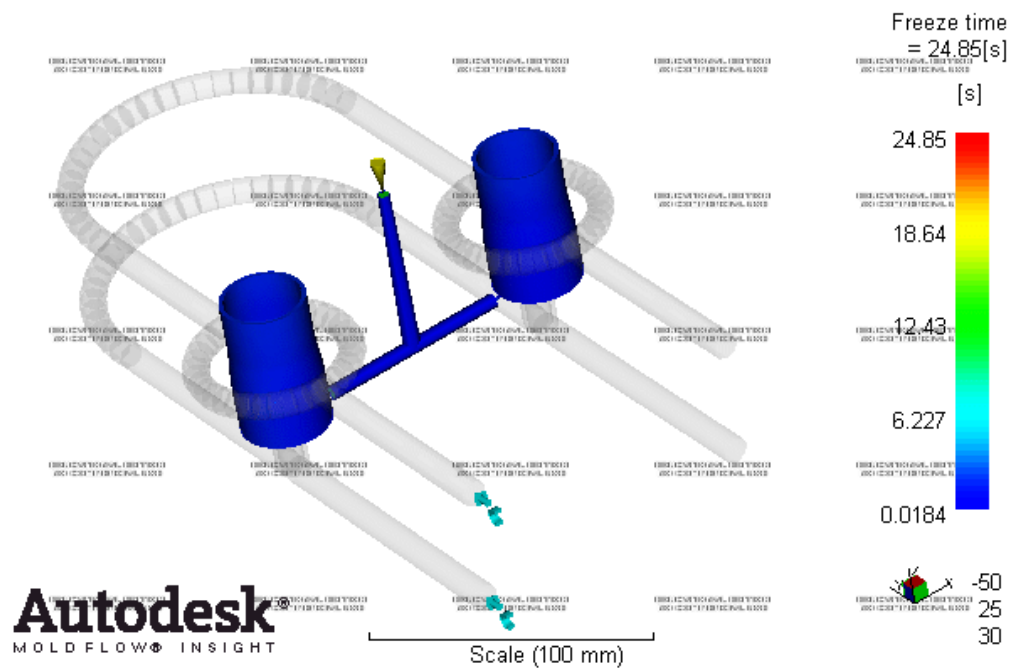


Figure H.3.2: Freeze Time For ABS

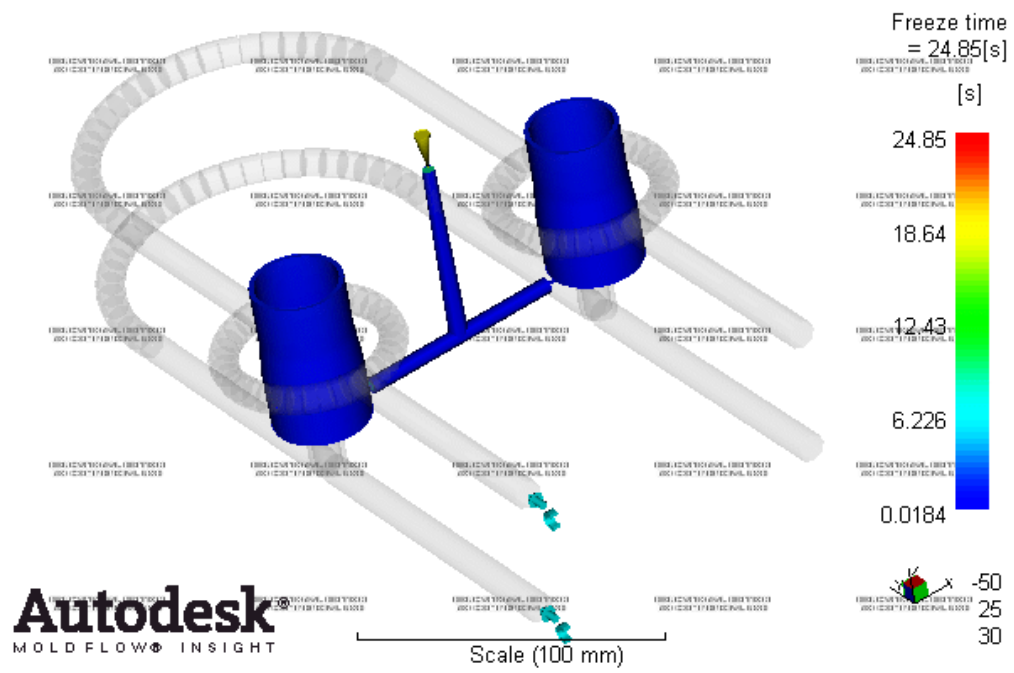
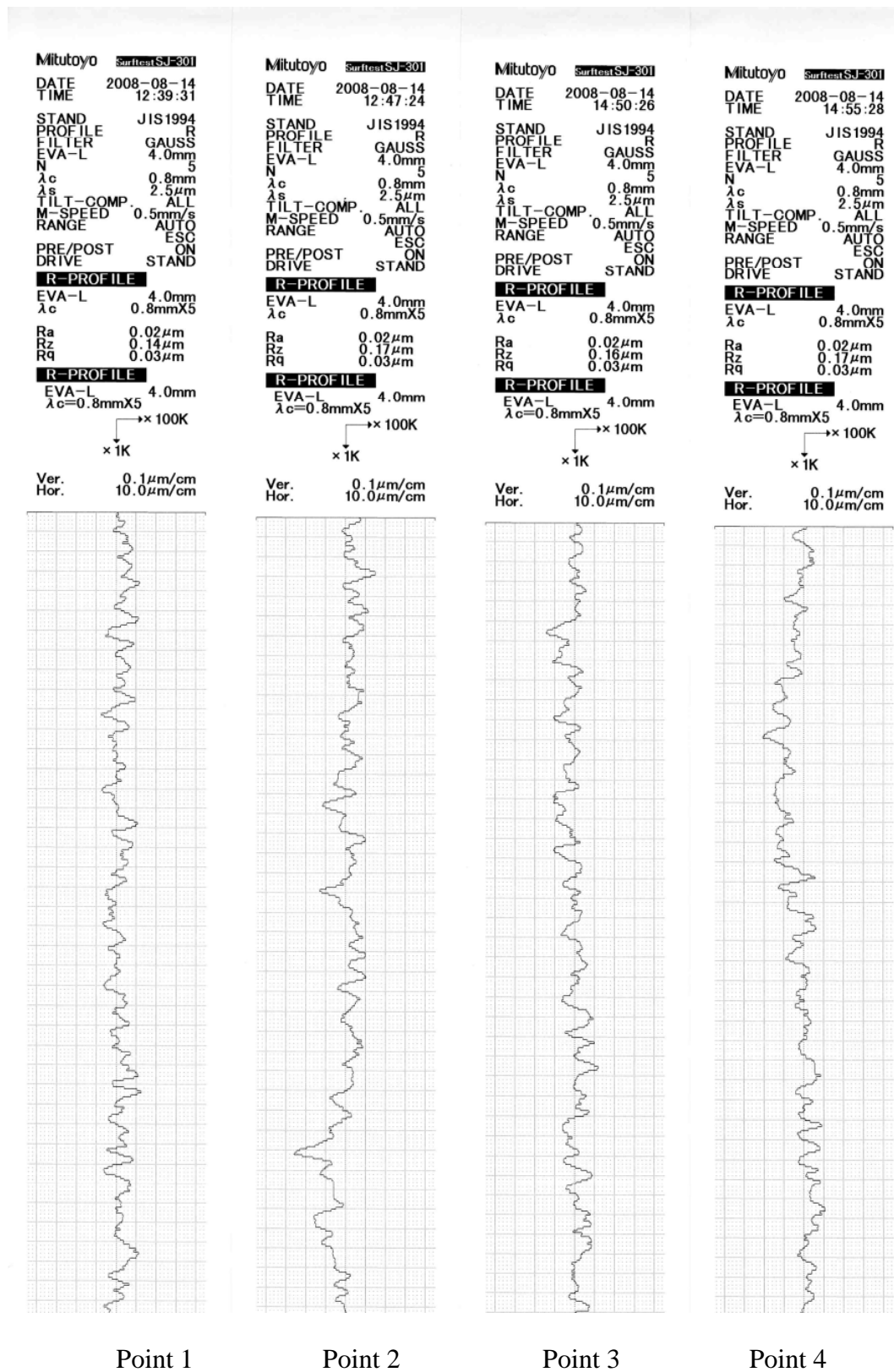


Figure H.3.3: Freeze Time For PA6

APPENDIX I
Surface Roughness Value

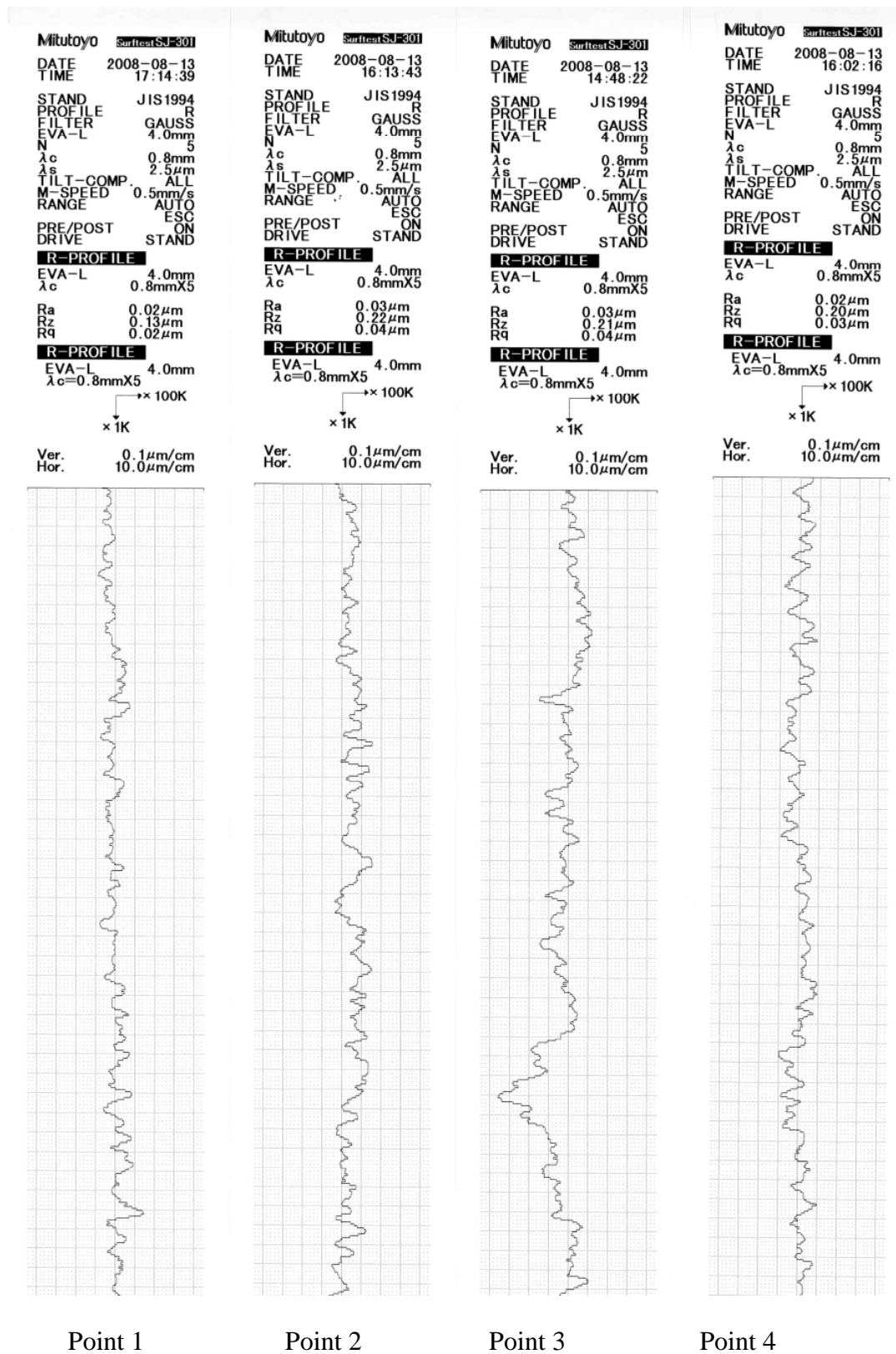
APPENDIX I.1

Polished Surface Core Insert 1



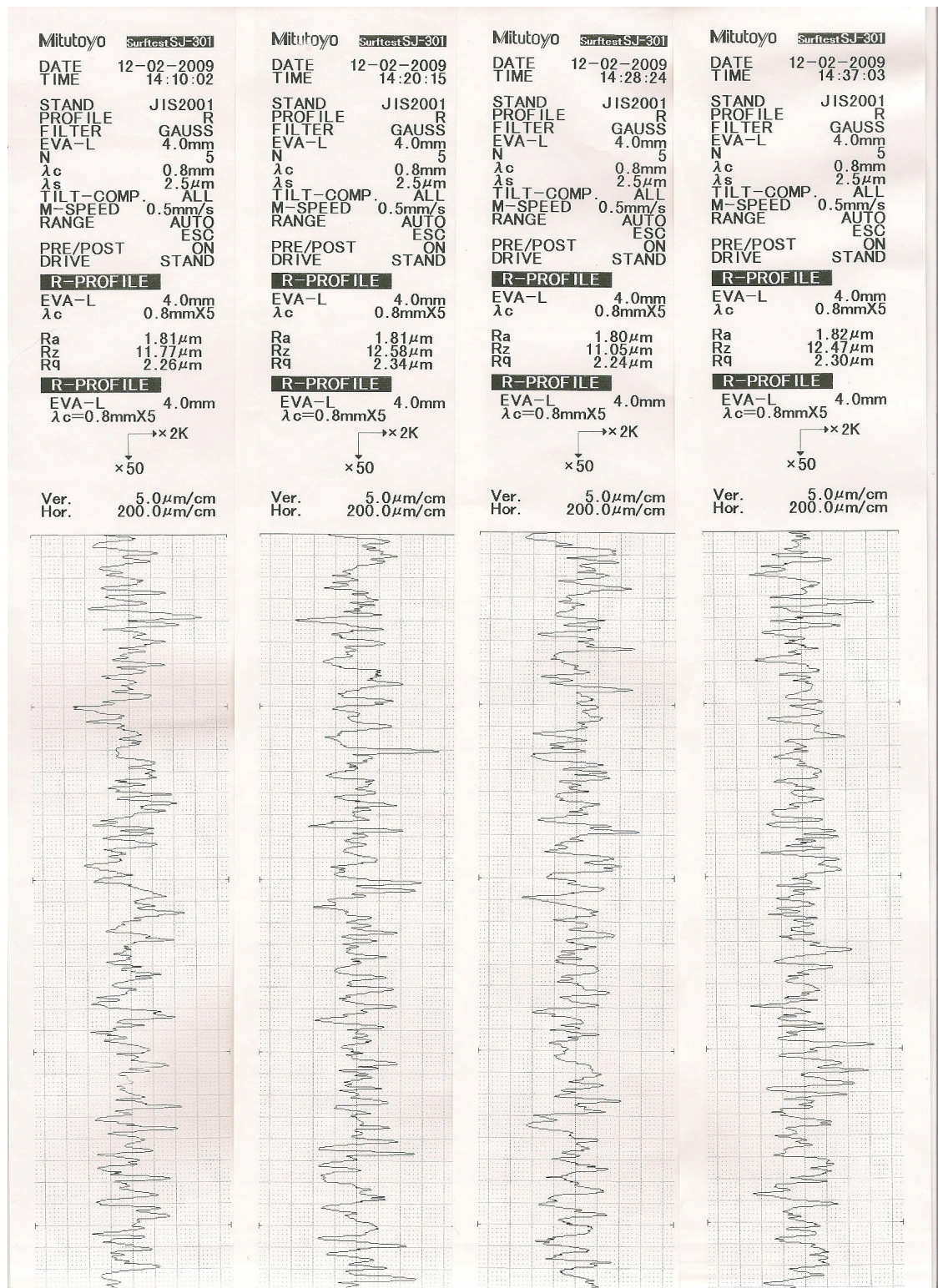
APPENDIX I.2

Polished Surface Core Insert 2



APPENDIX I.3

Sparked Surface Core Insert 1



Point 1

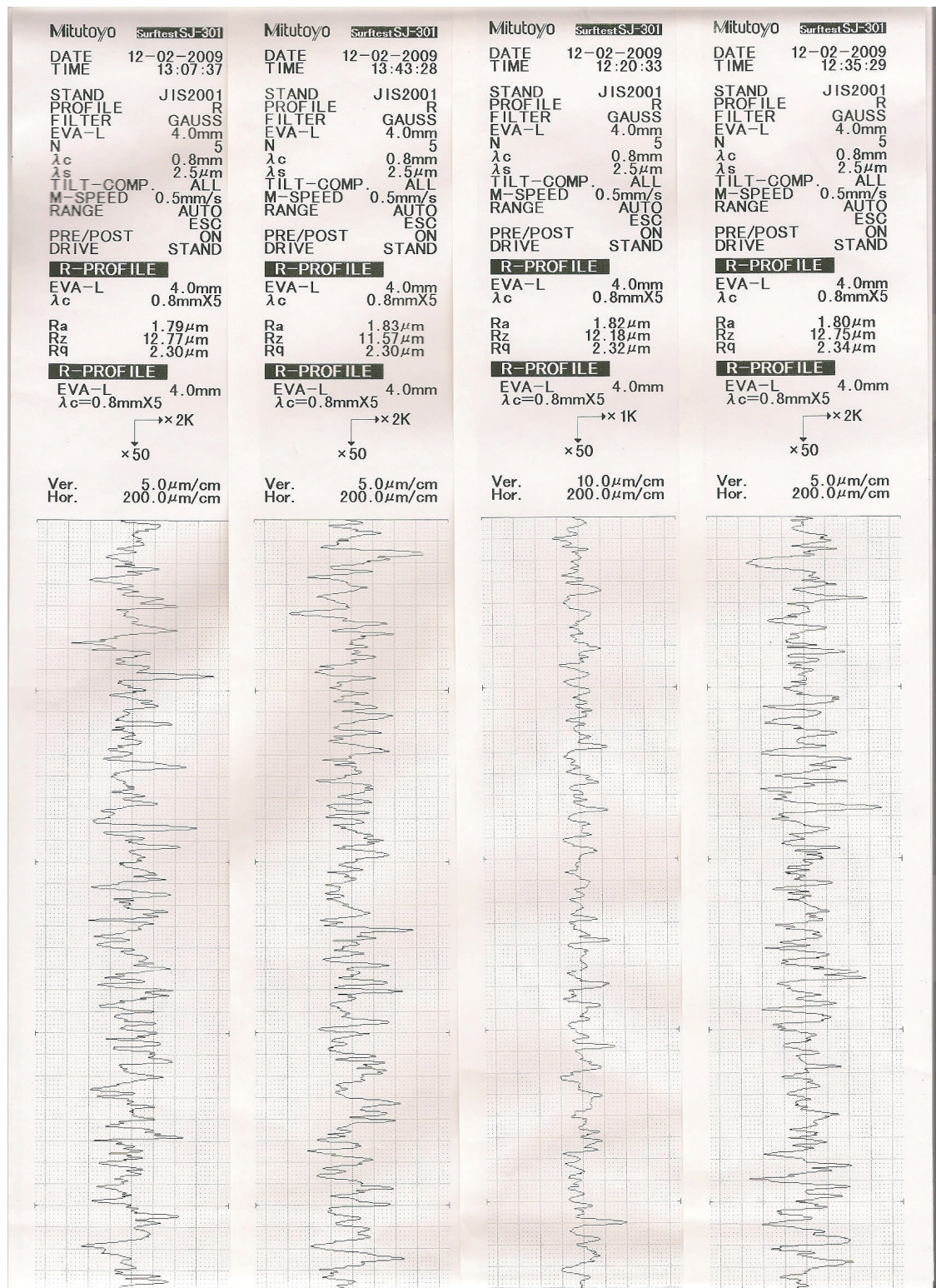
Point 2

Point 3

Point 4

APPENDIX I.4

Sparked Surface Core Insert 2



Point 1

Point 2

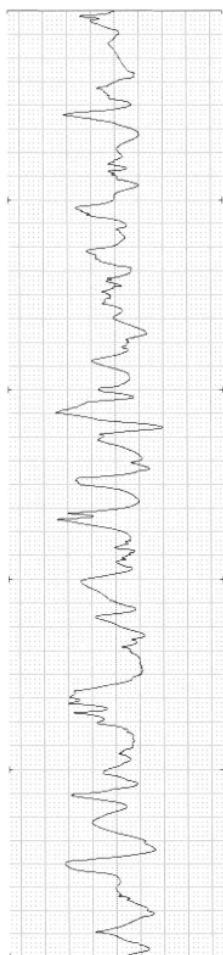
Point 3

Point 4

APPENDIX I.5

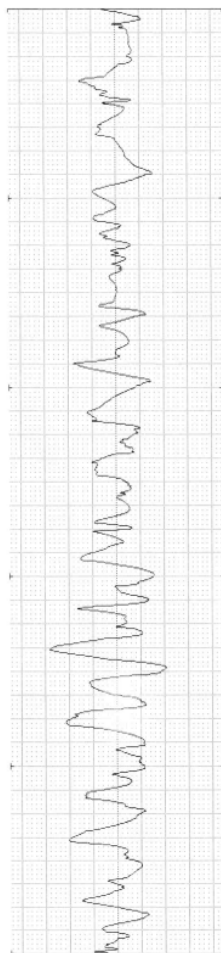
Sparked Surface Core Insert 1

Mitutoyo **SurfTest SJ-301**
 DATE 2008-08-12
 TIME 16:35:28
 STAND JIS1994
 PROFILE R
 FILTER GAUSS
 EVA-L 4.0mm
 N 5
 λ_c 0.8mm
 λ_s 2.5 μ m
 TILT-COMP. ALL
 M-SPEED 0.5mm/s
 RANGE AUTO
 PRE/POST ESC
 DRIVE ON
 STAND
R-PROFILE
 EVA-L 4.0mm
 λ_c 0.8mmX5
 Ra 3.23 μ m
 Rz #11.48 μ m
 Rq 3.99 μ m
R-PROFILE
 EVA-L 4.0mm
 λ_c 0.8mmX5
 Ver. 10.0 μ m/cm
 Hor. 200.0 μ m/cm



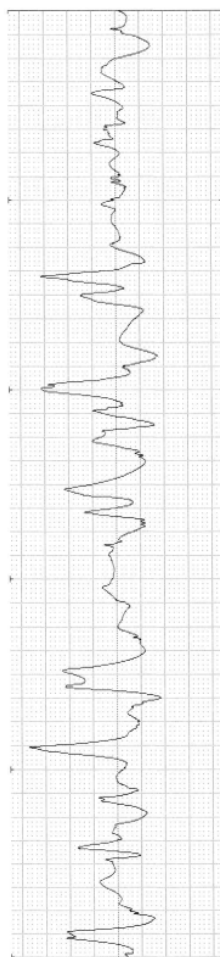
Point 1

Mitutoyo **SurfTest SJ-301**
 DATE 2008-08-13
 TIME 10:52:17
 STAND JIS1994
 PROFILE R
 FILTER GAUSS
 EVA-L 4.0mm
 N 5
 λ_c 0.8mm
 λ_s 2.5 μ m
 TILT-COMP. ALL
 M-SPEED 0.5mm/s
 RANGE AUTO
 PRE/POST ESC
 DRIVE ON
 STAND
R-PROFILE
 EVA-L 4.0mm
 λ_c 0.8mmX5
 Ra 3.21 μ m
 Rz #11.44 μ m
 Rq 3.91 μ m
R-PROFILE
 EVA-L 4.0mm
 λ_c 0.8mmX5
 Ver. 10.0 μ m/cm
 Hor. 200.0 μ m/cm



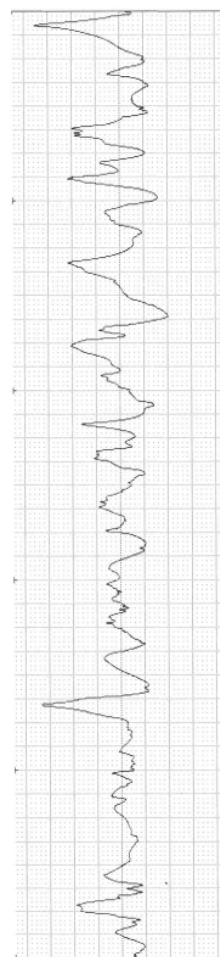
Point 2

Mitutoyo **SurfTest SJ-301**
 DATE 2008-08-12
 TIME 15:36:36
 STAND JIS1994
 PROFILE R
 FILTER GAUSS
 EVA-L 4.0mm
 N 5
 λ_c 0.8mm
 λ_s 2.5 μ m
 TILT-COMP. ALL
 M-SPEED 0.5mm/s
 RANGE AUTO
 PRE/POST ESC
 DRIVE ON
 STAND
R-PROFILE
 EVA-L 4.0mm
 λ_c 0.8mmX5
 Ra 3.21 μ m
 Rz #13.94 μ m
 Rq 4.31 μ m
R-PROFILE
 EVA-L 4.0mm
 λ_c 0.8mmX5
 Ver. 10.0 μ m/cm
 Hor. 200.0 μ m/cm



Point 3

Mitutoyo **SurfTest SJ-301**
 DATE 2008-08-12
 TIME 16:13:45
 STAND JIS1994
 PROFILE R
 FILTER GAUSS
 EVA-L 4.0mm
 N 5
 λ_c 0.8mm
 λ_s 2.5 μ m
 TILT-COMP. ALL
 M-SPEED 0.5mm/s
 RANGE AUTO
 PRE/POST ESC
 DRIVE ON
 STAND
R-PROFILE
 EVA-L 4.0mm
 λ_c 0.8mmX5
 Ra 3.21 μ m
 Rz #11.79 μ m
 Rq 4.14 μ m
R-PROFILE
 EVA-L 4.0mm
 λ_c 0.8mmX5
 Ver. 10.0 μ m/cm
 Hor. 200.0 μ m/cm

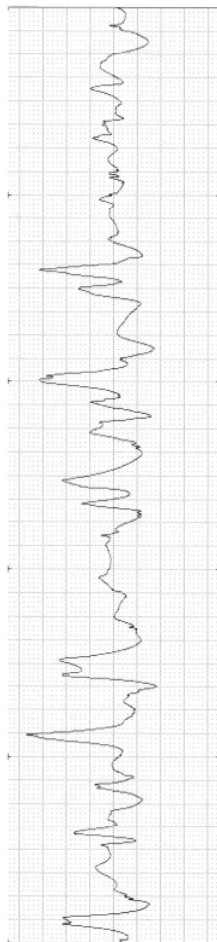


Point 4

APPENDIX I.6

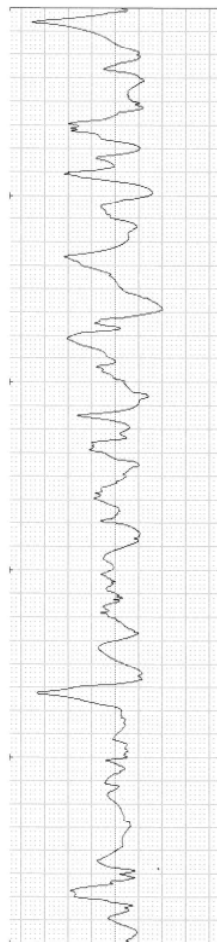
Sparked Surface Core Insert 2

Mitutoyo Surftest SJ-301
 DATE 2008-08-12
 TIME 15:36:36
 STAND JIS1994
 PROFILE R
 FILTER GAUSS
 EVA-L 4.0mm
 N 5
 λ_c 0.8mm
 λ_s 2.5 μ m
 TILT-COMP. ALL
 M-SPEED 0.5mm/s
 RANGE AUTO
 PRE/POST ESC
 DRIVE ON
 STAND
R-PROFILE
 EVA-L 4.0mm
 λ_c 0.8mmX5
 Ra 3.21 μ m
 Rz #13.94 μ m
 Rq 4.31 μ m
R-PROFILE
 EVA-L 4.0mm
 λ_c 0.8mmX5
 x1K
 x50
 Ver. 10.0 μ m/cm
 Hor. 200.0 μ m/cm



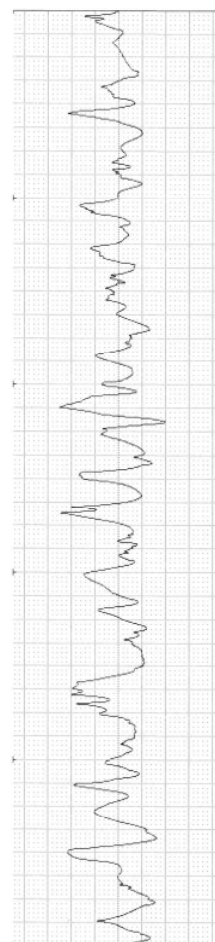
Point 1

Mitutoyo Surftest SJ-301
 DATE 2008-08-12
 TIME 16:13:45
 STAND JIS1994
 PROFILE R
 FILTER GAUSS
 EVA-L 4.0mm
 N 5
 λ_c 0.8mm
 λ_s 2.5 μ m
 TILT-COMP. ALL
 M-SPEED 0.5mm/s
 RANGE AUTO
 PRE/POST ESC
 DRIVE ON
 STAND
R-PROFILE
 EVA-L 4.0mm
 λ_c 0.8mmX5
 Ra 3.21 μ m
 Rz #11.79 μ m
 Rq 4.14 μ m
R-PROFILE
 EVA-L 4.0mm
 λ_c 0.8mmX5
 x1K
 x50
 Ver. 10.0 μ m/cm
 Hor. 200.0 μ m/cm



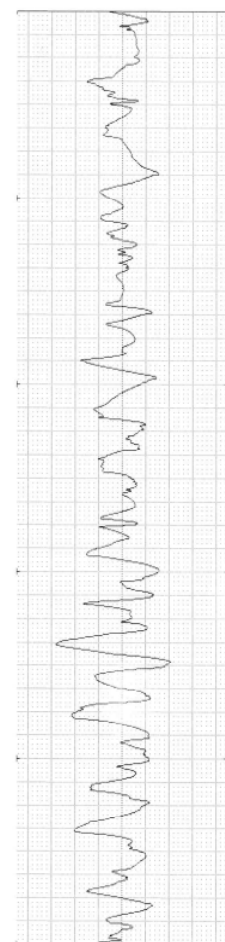
Point 2

Mitutoyo Surftest SJ-301
 DATE 2008-08-12
 TIME 16:35:28
 STAND JIS1994
 PROFILE R
 FILTER GAUSS
 EVA-L 4.0mm
 N 5
 λ_c 0.8mm
 λ_s 2.5 μ m
 TILT-COMP. ALL
 M-SPEED 0.5mm/s
 RANGE AUTO
 PRE/POST ESC
 DRIVE ON
 STAND
R-PROFILE
 EVA-L 4.0mm
 λ_c 0.8mmX5
 Ra 3.23 μ m
 Rz #11.48 μ m
 Rq 3.99 μ m
R-PROFILE
 EVA-L 4.0mm
 λ_c 0.8mmX5
 x1K
 x50
 Ver. 10.0 μ m/cm
 Hor. 200.0 μ m/cm



Point 3

Mitutoyo Surftest SJ-301
 DATE 2008-08-13
 TIME 10:52:17
 STAND JIS1994
 PROFILE R
 FILTER GAUSS
 EVA-L 4.0mm
 N 5
 λ_c 0.8mm
 λ_s 2.5 μ m
 TILT-COMP. ALL
 M-SPEED 0.5mm/s
 RANGE AUTO
 PRE/POST ESC
 DRIVE ON
 STAND
R-PROFILE
 EVA-L 4.0mm
 λ_c 0.8mmX5
 Ra 3.21 μ m
 Rz #11.44 μ m
 Rq 3.91 μ m
R-PROFILE
 EVA-L 4.0mm
 λ_c 0.8mmX5
 x1K
 x50
 Ver. 10.0 μ m/cm
 Hor. 200.0 μ m/cm



Point 4

APPENDIX I.7

Measurement the surface roughness of the core inserts



Figure I.7.1: Set-up equipment for measuring the surface roughness

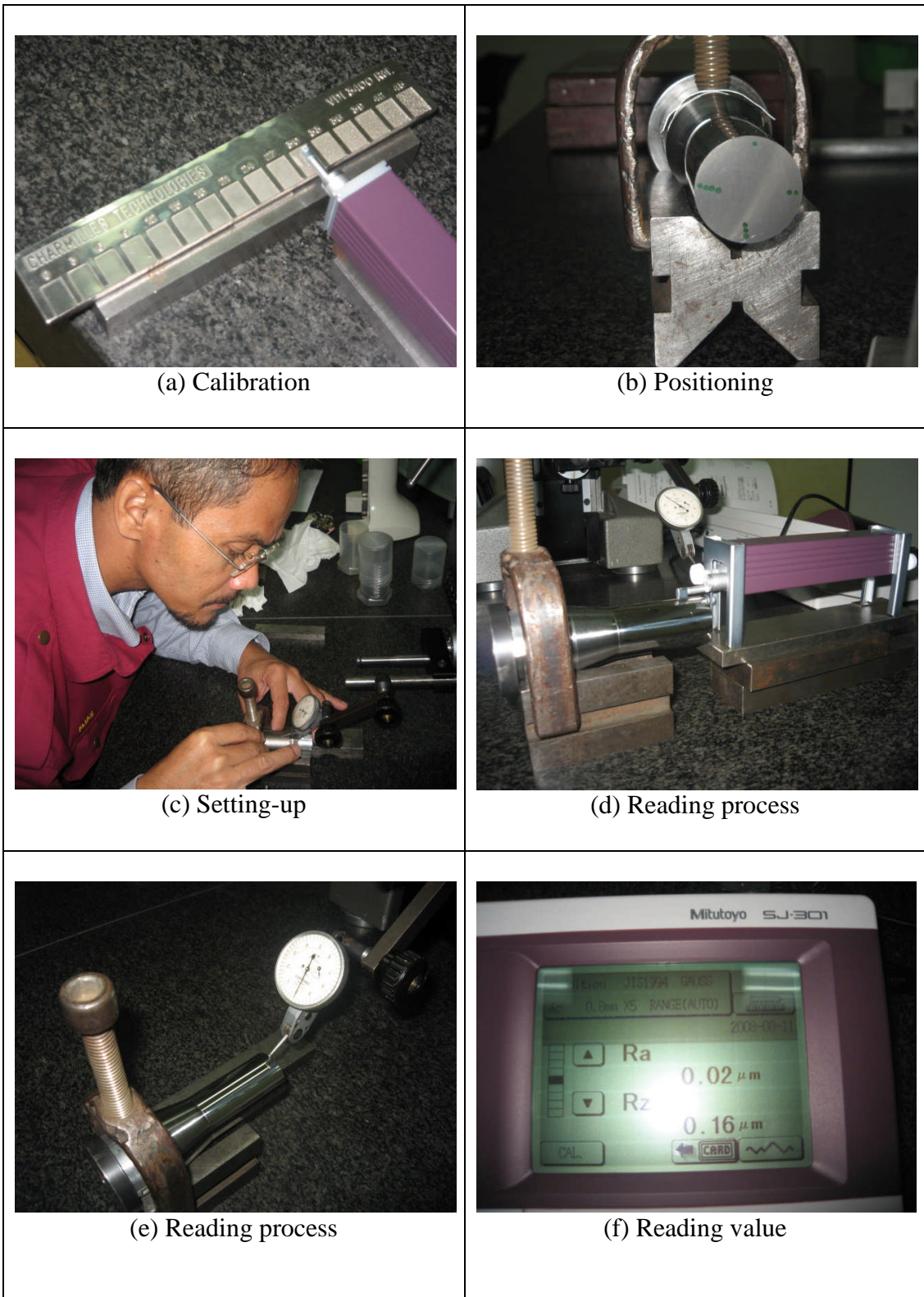


Figure I.7.2: Process for measuring the surface roughness

APPENDIX J

Sample Graph for Ejection Force

Dry-run and with Moulding

APPENDIX J.1

y(t) Graph

Act: Ejection Force

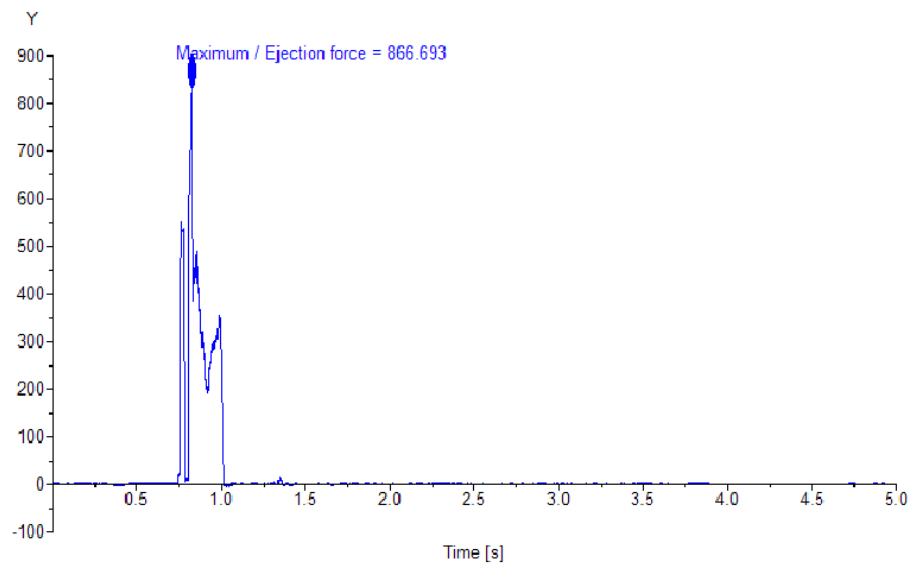


Figure J.1: Dry run (without molding)

y(t) Graph

Act: Ejection Force

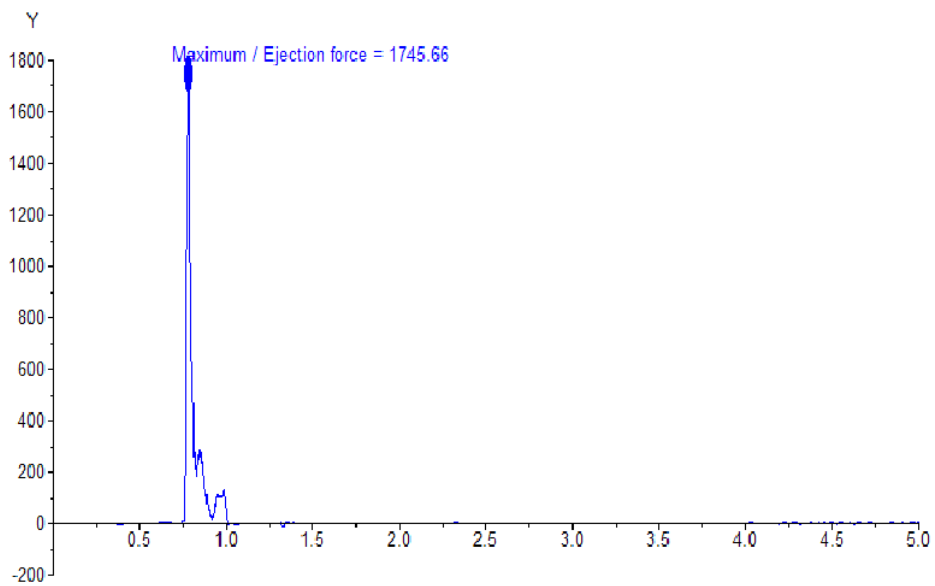


Figure J.2: Ejection force (with molding)

APPENDIX K

Tabulated Data for L_{81} Orthogonal Array

APPENDIX K.1

Table K.1: L81 Array for HIPS

Surface	Expt No.	A	B	C	D	E	F	Ejection force for PS	S/N ratio for smaller-the-better	cavity 1			cavity 2			Melt Temperature			Injection Pressure			Packing Pressure			Cooling Time		
		X1	X2	X3	X4	X5	X6			A1	A2	A3	B1	B2	B3	C1	C2	C3	D1	D2	D3	E1	E2	E3	F1	F2	F3
S1	1	1	1	1	1	1	1	333955.7	-110.47	-110.474			-110.474			-110.474			-110.474			-110.474			-110.474		
	2	1	1	1	2	2	2	292138.7	-109.31	-109.312			-109.312			-109.312		-109.312			-109.312			-109.312			
	3	1	1	1	3	3	3	254834.4	-108.13	-108.125			-108.125			-108.125			-108.125			-108.125			-108.125		
	4	1	1	2	1	2	3	336354.6	-110.54	-110.536			-110.536			-110.536			-110.536			-110.536			-110.536		
	5	1	1	2	2	3	1	329753	-110.36	-110.364			-110.364			-110.364		-110.364			-110.364			-110.364			
	6	1	1	2	3	1	2	336825.6	-110.55	-110.548			-110.548			-110.548			-110.548			-110.548			-110.548		
	7	1	1	3	1	3	2	275475.6	-108.80	-108.802			-108.802		-108.802		-108.802			-108.802			-108.802			-108.802	
	8	1	1	3	2	1	3	288241.5	-109.20	-109.195			-109.195		-109.195		-109.195			-109.195			-109.195			-109.195	
	9	1	1	3	3	2	1	326621.2	-110.28	-110.281			-110.281			-110.281			-110.281			-110.281			-110.281		
S2	10	1	2	1	1	1	1	158897.7	-104.02	-104.022			-104.022			-104.022		-104.022			-104.022			-104.022			
	11	1	2	1	2	2	2	163011.9	-104.24	-104.244			-104.244			-104.244		-104.244			-104.244			-104.244			
	12	1	2	1	3	3	3	164672.6	-104.33	-104.332			-104.332			-104.332			-104.332			-104.332			-104.332		
	13	1	2	2	1	2	3	193096.4	-105.72	-105.715			-105.715		-105.715		-105.715			-105.715			-105.715			-105.715	
	14	1	2	2	2	3	1	212358.6	-106.54	-106.541			-106.541			-106.541		-106.541			-106.541			-106.541			
	15	1	2	2	3	1	2	253447.3	-108.08	-108.078			-108.078		-108.078		-108.078			-108.078			-108.078			-108.078	
	16	1	2	3	1	3	2	209939.4	-106.44	-106.442			-106.442		-106.442		-106.442			-106.442			-106.442			-106.442	
	17	1	2	3	2	1	3	230581.6	-107.26	-107.256			-107.256		-107.256		-107.256			-107.256			-107.256			-107.256	
	18	1	2	3	3	2	1	239157.3	-107.57	-107.574			-107.574			-107.574			-107.574			-107.574			-107.574		
S3	19	1	3	1	1	1	1	124774.2	-101.92	-101.922			-101.922			-101.922		-101.922			-101.922			-101.922			
	20	1	3	1	2	2	2	131631.9	-102.39	-102.387			-102.387			-102.387		-102.387			-102.387			-102.387			
	21	1	3	1	3	3	3	150416.4	-103.55	-103.546			-103.546			-103.546			-103.546			-103.546			-103.546		
	22	1	3	2	1	2	3	111199	-100.92	-100.922			-100.922		-100.922		-100.922			-100.922			-100.922			-100.922	
	23	1	3	2	2	3	1	113553.8	-101.10	-101.104			-101.104		-101.104		-101.104			-101.104			-101.104			-101.104	
	24	1	3	2	3	1	2	113879	-101.13	-101.129			-101.129		-101.129		-101.129			-101.129			-101.129			-101.129	
	25	1	3	3	1	3	2	136403.4	-102.70	-102.697			-102.697		-102.697		-102.697			-102.697			-102.697			-102.697	
	26	1	3	3	2	1	3	127985.4	-102.14	-102.143			-102.143		-102.143		-102.143			-102.143			-102.143			-102.143	
	27	1	3	3	3	2	1	102033.5	-100.17	-100.175			-100.175			-100.175			-100.175			-100.175			-100.175		
S4	28	2	1	1	1	1	1	198270.4	-105.95	-105.945			-105.945			-105.945		-105.945			-105.945			-105.945			
	29	2	1	1	2	2	2	189540.7	-105.55	-105.554			-105.554			-105.554		-105.554			-105.554			-105.554			
	30	2	1	1	3	3	3	187706.9	-105.47	-105.47			-105.47			-105.47		-105.47			-105.47			-105.47			
	31	2	1	2	1	2	3	246591.3	-107.84	-107.84			-107.84		-107.84		-107.84			-107.84			-107.84			-107.84	
	32	2	1	2	2	3	1	235053.5	-107.42	-107.423			-107.423		-107.423		-107.423			-107.423			-107.423			-107.423	
	33	2	1	2	3	1	2	220097.7	-106.85	-106.852			-106.852		-106.852		-106.852			-106.852			-106.852			-106.852	
	34	2	1	3	1	3	2	256835.4	-108.19	-108.193			-108.193		-108.193		-108.193			-108.193			-108.193			-108.193	
	35	2	1	3	2	1	3	237939.2	-107.53	-107.529			-107.529		-107.529		-107.529			-107.529			-107.529			-107.529	
	36	2	1	3	3	2	1	225446.8	-107.06	-107.061			-107.061			-107.061			-107.061			-107.061			-107.061		
S5	37	2	2	1	1	1	1	183941.5	-105.29	-105.294			-105.294			-105.294		-105.294			-105.294			-105.294			
	38	2	2	1	2	2	2	176515.4	-104.94	-104.936			-104.936			-104.936		-104.936			-104.936			-104.936			
	39	2	2	1	3	3	3	162407.1	-104.21	-104.212			-104.212			-104.212		-104.212			-104.212			-104.212			
	40	2	2	2	1	2	3	214390.2	-106.62	-106.624			-106.624			-106.624			-106.624			-106.624			-106.624		
	41	2	2	2	2	3	1	199557.6	-106.00	-106.001			-106.001		-106.001		-106.001			-106.001			-106.001			-106.001	
	42	2	2	2	3	1	2	188267.8	-105.50	-105.496			-105.496		-105.496		-105.496			-105.496			-105.496			-105.496	
	43	2	2	3	1	3	2	217278.5	-106.74	-106.74			-106.74		-106.74		-106.74			-106.74			-106.74			-106.74	
	44	2	2	3	2	1	3	224044.5	-107.01	-107.007			-107.007		-107.007		-107.007			-107.007			-107.007			-107.007	
	45	2	2	3	3	2	1	211503.9	-106.51	-106.506			-106.506		-106.506		-106.506			-106.506			-106.506			-106.506	

APPENDIX K.2

Table K.2: L81 Array for ABS

Surface	Expt No.	A	B	C	D	E	F	Ejection force for ABS	for smaller-the-better	cavity 1			cavity 2			Melt Temperature			Injection Pressure			Packing Pressure			Cooling Time		
		X	X	X	X	X	X			A1	A2	A3	B1	B2	B3	C1	C2	C3	D1	D2	D3	E1	E2	E3	F1	F2	F3
		1	2	5	14	23	32																				
S1	1	1	1	1	1	1	1	262352.5	-108.38	-108.378			-108.378			-108.378			-108.378			-108.378			-108.378		
	2	1	1	1	2	2	2	267433.5	-108.54	-108.544			-108.544			-108.544			-108.544			-108.544			-108.544		
	3	1	1	1	3	3	3	246012.3	-107.82	-107.819			-107.819			-107.819			-107.819			-107.819			-107.819		
	4	1	1	2	1	2	3	241876.4	-107.67	-107.672			-107.672			-107.672			-107.672			-107.672			-107.672		
	5	1	1	2	2	3	1	276288.1	-108.83	-108.827			-108.827			-108.827			-108.827			-108.827			-108.827		
	6	1	1	2	3	1	2	249873.2	-107.95	-107.954			-107.954			-107.954			-107.954			-107.954			-107.954		
	7	1	1	3	1	3	2	294598.7	-109.38	-109.385			-109.385			-109.385			-109.385			-109.385			-109.385		
	8	1	1	3	2	1	3	277913.8	-108.88	-108.878			-108.878			-108.878			-108.878			-108.878			-108.878		
	9	1	1	3	3	2	1	265682	-108.49	-108.487			-108.487			-108.487			-108.487			-108.487			-108.487		
S2	10	1	2	1	1	1	1	183376.7	-105.27	-105.267			-105.267			-105.267			-105.267			-105.267			-105.267		
	11	1	2	1	2	2	2	193428.3	-105.73	-105.73			-105.73			-105.73			-105.73			-105.73			-105.73		
	12	1	2	1	3	3	3	209613	-106.43	-106.428			-106.428			-106.428			-106.428			-106.428			-106.428		
	13	1	2	2	1	2	3	183748.1	-105.28	-105.284			-105.284			-105.284			-105.284			-105.284			-105.284		
	14	1	2	2	2	3	1	191222.3	-105.63	-105.631			-105.631			-105.631			-105.631			-105.631			-105.631		
	15	1	2	2	3	1	2	188675.5	-105.51	-105.514			-105.514			-105.514			-105.514			-105.514			-105.514		
	16	1	2	3	1	3	2	169870.8	-104.60	-104.602			-104.602			-104.602			-104.602			-104.602			-104.602		
	17	1	2	3	2	1	3	154806.3	-103.80	-103.796			-103.796			-103.796			-103.796			-103.796			-103.796		
	18	1	2	3	3	2	1	166713.6	-104.44	-104.439			-104.439			-104.439			-104.439			-104.439			-104.439		
S3	19	1	3	1	1	1	1	136465.6	-102.70	-102.7			-102.7			-102.7			-102.7			-102.7			-102.7		
	20	1	3	1	2	2	2	103035.7	-100.26	-100.26			-100.26			-100.26			-100.26			-100.26			-100.26		
	21	1	3	1	3	3	3	108716.3	-100.73	-100.726			-100.726			-100.726			-100.726			-100.726			-100.726		
	22	1	3	2	1	2	3	141284.3	-103.00	-103.002			-103.002			-103.002			-103.002			-103.002			-103.002		
	23	1	3	2	2	3	1	111495	-100.95	-100.945			-100.945			-100.945			-100.945			-100.945			-100.945		
	24	1	3	2	3	1	2	117828.5	-101.43	-101.425			-101.425			-101.425			-101.425			-101.425			-101.425		
	25	1	3	3	1	3	2	149133.7	-103.47	-103.472			-103.472			-103.472			-103.472			-103.472			-103.472		
	26	1	3	3	2	1	3	118245.6	-101.46	-101.456			-101.456			-101.456			-101.456			-101.456			-101.456		
	27	1	3	3	3	2	1	115754.5	-101.27	-101.271			-101.271			-101.271			-101.271			-101.271			-101.271		
S4	28	2	1	1	1	1	1	197466.1	-105.91	-105.91			-105.91			-105.91			-105.91			-105.91			-105.91		
	29	2	1	1	2	2	2	202361.1	-106.12	-106.123			-106.123			-106.123			-106.123			-106.123			-106.123		
	30	2	1	1	3	3	3	202323.6	-106.12	-106.121			-106.121			-106.121			-106.121			-106.121			-106.121		
	31	2	1	2	1	2	3	195808.2	-105.84	-105.837			-105.837			-105.837			-105.837			-105.837			-105.837		
	32	2	1	2	2	3	1	205379.7	-106.25	-106.251			-106.251			-106.251			-106.251			-106.251			-106.251		
	33	2	1	2	3	1	2	215220.5	-106.66	-106.658			-106.658			-106.658			-106.658			-106.658			-106.658		
	34	2	1	3	1	3	2	179755.3	-105.09	-105.094			-105.094			-105.094			-105.094			-105.094			-105.094		
	35	2	1	3	2	1	3	183987.8	-105.30	-105.296			-105.296			-105.296			-105.296			-105.296			-105.296		
	36	2	1	3	3	2	1	190458.4	-105.60	-105.596			-105.596			-105.596			-105.596			-105.596			-105.596		
S5	37	2	2	1	1	1	1	167913.3	-104.50	-104.502			-104.502			-104.502			-104.502			-104.502			-104.502		
	38	2	2	1	2	2	2	152364.9	-103.66	-103.658			-103.658			-103.658			-103.658			-103.658			-103.658		
	39	2	2	1	3	3	3	141430.7	-103.01	-103.011			-103.011			-103.011			-103.011			-103.011			-103.011		
	40	2	2	2	1	2	3	166525.7	-104.43	-104.43			-104.43			-104.43			-104.43			-104.43			-104.43		
	41	2	2	2	2	3	1	163597.1	-104.28	-104.276			-104.276			-104.276			-104.276			-104.276			-104.276		
	42	2	2	2	3	1	2	173247.4	-104.77	-104.773			-104.773			-104.773			-104.773			-104.773			-104.773		
	43	2	2	3	1	3	2	170353.6	-104.63	-104.627			-104.627			-104.627			-104.627			-104.627			-104.627		
	44	2	2	3	2	1	3	172986.7	-104.76	-104.76			-104.76			-104.76			-104.76			-104.76			-104.76		
	45	2	2	3	3	2	1	174322.8	-104.83	-104.827			-104.827			-104.827			-104.827			-104.827			-104.827		

[illegible]

APPENDIX K.3

Table K.3: L81 Array for PA6

Surface	Expt No.	A	B	C	D	E	F	Ejection force for PA6	for smaller-the-better	cavity 1			cavity 2			Melt Temperature			Injection Pressure			Packing Pressure			Cooling Time		
		1	2	3	4	5	6			A1	A2	A3	B1	B2	B3	C1	C2	C3	D1	D2	D3	E1	E2	E3	F1	F2	F3
S1	1	1	1	1	1	1	1	127616.8	-102.12	-102.118			-102.118			-102.118			-102.118			-102.118			-102.118		
	2	1	1	1	2	2	2	114033.7	-101.14	-101.141			-101.141			-101.141				-101.141				-101.141			
	3	1	1	1	3	3	3	98471	-99.87	-99.8662			-99.8662			-99.8662				-99.8662			-99.8662			-99.8662	
	4	1	1	2	1	2	3	105959.3	-100.50	-100.503			-100.503			-100.503			-100.503			-100.503				-100.503	
	5	1	1	2	2	3	1	103546.2	-100.30	-100.303			-100.303			-100.303			-100.303			-100.303			-100.303		
	6	1	1	2	3	1	2	99047	-99.92	-99.9168			-99.9168			-99.9168			-99.9168			-99.9168			-99.9168		
	7	1	1	3	1	3	2	94740.2	-99.53	-99.5307			-99.5307			-99.5307			-99.5307			-99.5307			-99.5307		
	8	1	1	3	2	1	3	101270.2	-100.11	-100.11			-100.11			-100.11			-100.11			-100.11				-100.11	
	9	1	1	3	3	2	1	76713	-97.70	-97.6974			-97.6974			-97.6974			-97.6974			-97.6974			-97.6974		
S2	10	1	2	1	1	1	1	95690.7	-99.62	-99.6174			-99.6174			-99.6174			-99.6174			-99.6174			-99.6174		
	11	1	2	1	2	2	2	76432.4	-97.67	-97.6655			-97.6655			-97.6655			-97.6655			-97.6655			-97.6655		
	12	1	2	1	3	3	3	57459.7	-95.19	-95.1873			-95.1873			-95.1873			-95.1873			-95.1873			-95.1873		
	13	1	2	2	1	2	3	114081.3	-101.14	-101.144			-101.144			-101.144			-101.144			-101.144			-101.144		
	14	1	2	2	2	3	1	101047	-100.09	-100.09			-100.09			-100.09			-100.09			-100.09			-100.09		
	15	1	2	2	3	1	2	89151.2	-99.00	-99.0025			-99.0025			-99.0025			-99.0025			-99.0025			-99.0025		
	16	1	2	3	1	3	2	154891.5	-103.80	-103.801			-103.801			-103.801			-103.801			-103.801			-103.801		
	17	1	2	3	2	1	3	144944.7	-103.22	-103.224			-103.224			-103.224			-103.224			-103.224			-103.224		
	18	1	2	3	3	2	1	114548.5	-101.18	-101.18			-101.18			-101.18			-101.18			-101.18			-101.18		
S3	19	1	3	1	1	1	1	62142.3	-95.87	-95.8677			-95.8677			-95.8677			-95.8677			-95.8677			-95.8677		
	20	1	3	1	2	2	2	38312.7	-91.67	-91.6669			-91.6669			-91.6669			-91.6669			-91.6669			-91.6669		
	21	1	3	1	3	3	3	32480.2	-90.23	-90.2324			-90.2324			-90.2324			-90.2324			-90.2324			-90.2324		
	22	1	3	2	1	2	3	95468.1	-99.60	-99.5972			-99.5972			-99.5972			-99.5972			-99.5972			-99.5972		
	23	1	3	2	2	3	1	46570.7	-93.36	-93.3623			-93.3623			-93.3623			-93.3623			-93.3623			-93.3623		
	24	1	3	2	3	1	2	47065.8	-93.45	-93.4541			-93.4541			-93.4541			-93.4541			-93.4541			-93.4541		
	25	1	3	3	1	3	2	111555.3	-100.95	-100.95			-100.95			-100.95			-100.95			-100.95			-100.95		
	26	1	3	3	2	1	3	97772.2	-99.80	-99.8043			-99.8043			-99.8043			-99.8043			-99.8043			-99.8043		
	27	1	3	3	3	2	1	73566	-97.33	-97.3335			-97.3335			-97.3335			-97.3335			-97.3335			-97.3335		
S4	28	2	1	1	1	1	1	97922.4	-99.82	-99.8176			-99.8176			-99.8176			-99.8176			-99.8176			-99.8176		
	29	2	1	1	2	2	2	83894.7	-98.47	-98.4747			-98.4747			-98.4747			-98.4747			-98.4747			-98.4747		
	30	2	1	1	3	3	3	76943	-97.72	-97.7234			-97.7234			-97.7234			-97.7234			-97.7234			-97.7234		
	31	2	1	2	1	2	3	129962.8	-102.28	-102.276			-102.276			-102.276			-102.276			-102.276			-102.276		
	32	2	1	2	2	3	1	91240.9	-99.20	-99.2038			-99.2038			-99.2038			-99.2038			-99.2038			-99.2038		
	33	2	1	2	3	1	2	80471.9	-98.11	-98.1129			-98.1129			-98.1129			-98.1129			-98.1129			-98.1129		
	34	2	1	3	1	3	2	154641.4	-103.79	-103.787			-103.787			-103.787			-103.787			-103.787			-103.787		
	35	2	1	3	2	1	3	137062.6	-102.74	-102.738			-102.738			-102.738			-102.738			-102.738			-102.738		
	36	2	1	3	3	2	1	112955.1	-101.06	-101.058			-101.058			-101.058			-101.058			-101.058			-101.058		
S5	37	2	2	1	1	1	1	132875.1	-102.47	-102.469			-102.469			-102.469			-102.469			-102.469			-102.469		
	38	2	2	1	2	2	2	116395.8	-101.32	-101.319			-101.319			-101.319			-101.319			-101.319			-101.319		
	39	2	2	1	3	3	3	62907	-95.97	-95.974			-95.974			-95.974			-95.974			-95.974			-95.974		
	40	2	2	2	1	2	3	165884.4	-104.40	-104.396			-104.396			-104.396			-104.396			-104.396			-104.396		
	41	2	2	2	2	3	1	175658	-104.89	-104.893			-104.893			-104.893			-104.893			-104.893			-104.893		
	42	2	2	2	3	1	2	157919	-103.97	-103.969			-103.969			-103.969			-103.969			-103.969			-103.969		
	43	2	2	3	1	3	2	151819.7	-103.63	-103.627			-103.627			-103.627			-103.627			-103.627			-103.627		
	44	2	2	3	2	1	3	135908.5	-102.66	-102.665			-102.665			-102.665			-102.665			-102.665			-102.665		
	45	2	2	3	3	2	1	78014.6	-97.84	-97.8435			-97.8435			-97.8435			-97.8435			-97.8435			-97.8435		

[illegible]

LIST OF PUBLICATIONS

Journal

1. Mohd A, C Hindle, WAY Yusoff, Mould Filling and Pressure Distribution for Polymer Resins, *Advanced Materials Research* Vols. 264-265 (2011), pp. 771-776

Proceedings

1. Mohd A, C. Hindle, “Analyze the Surface Roughness and the Ejection Force for Amorphous Resins”, International Conference on Advanced Manufacturing (ICAM 2011), ITC, Kemaman, Terengganu, MALAYSIA, 23 – 24 May 2011
2. Mohd A, C. Hindle, S. Zainal Ariffin, U. M. Zulkifli, “Simulation Studies on Mould Filling and Pressure For Polymers Resins”, International Conference on Advanced Manufacturing (ICAM 2011), ITC, Kemaman, Terengganu, MALAYSIA, 23 – 24 May 2011
3. Mohd A, C. Hindle, “A Study on the Effect of Surface Roughness on the Ejection of Molding”, ANTEC 2011, Hynes Convention Center & Boston Marriot Copley Center Hotel, Boston, Massachusetts, USA, 01 – 05 May 2011
4. Mohd A, C. Hindle, WAY Yusoff, “Simulation Studies of Mould Filling and Pressure Distribution”, The International Conference on Advances in Materials and Processing Technologies (AMPT 2009), Legend Hotel, Kuala Lumpur, MALAYSIA, 26 – 29 Oct 2009